UNIVERSITÉ DE LORRAINE | BIBLIOTHÈQUES UNIVERSITAIRES

AVERTISSEMENT

Ce document est le fruit d'un long travail approuvé par le jury de soutenance et mis à disposition de l'ensemble de la communauté universitaire élargie.

Il est soumis à la propriété intellectuelle de l'auteur. Ceci implique une obligation de citation et de référencement lors de l'utilisation de ce document.

D'autre part, toute contrefaçon, plagiat, reproduction illicite encourt une poursuite pénale.

Contact bibliothèque : ddoc-theses-contact@univ-lorraine.fr
*(Cette adresse ne permet pas de contacter les auteurs)*

LIENS

Code de la Propriété Intellectuelle. articles L 122. 4
Code de la Propriété Intellectuelle. articles L 335.2- L 335.10
http://www.cfcopies.com/V2/leg/leg_droi.php
http://www.culture.gouv.fr/culture/infos-pratiques/droits/protection.htm

# PhD Thesis

Presented and publicly defended to obtain the title of

## DOCTOR OF THE UNIVERSITY OF LORRAINE

**Discipline**: GEOSCIENCES

**By:** Abdoul Fattah KIEMDE

**Directed by:** Alexandre CHAGNES

# Development of direct boron extraction process from the salar de Hombre Muerto (Argentina) brines within the framework of battery-grade lithium carbonate ($Li_2CO_3$) production

**On 15th October 2024**

**Jury Members:**

| | | |
|---|---|---|
| **PhD supervisor** | **Prof. Alexandre CHAGNES** | **Université de Lorraine, Nancy** |
| **Reviewers** | **Prof. Micheline DRAYE** | **Université de Savoie Mont Blanc** |
| | **Dr. Juliette Sirieix PLENET** | **Sorbonne Université, Paris** |
| **Examiners** | **Prof. Marc HEBRANT** | **Université de Lorraine, Nancy (President of the jury)** |
| | **Prof. Victoria FLEXER** | **CONICET, University of Jujuy (Argentina)** |
| **Guest member** | **Dr. Jérôme MARIN** | **CNRS-Université de Lorraine, Nancy** |

# Acknowledgements

This PhD work was carried out at GeoRessources laboratory (Université de Lorraine) in France and CIDMEJu laboratory in Argentina from October 2021 to October 2024. I would like to thank my director Professor Alexandre CHAGNES for giving me the opportunity to learn and improve my skills in hydrometallurgy. Thanks to Jérôme MARIN and Frédéric DIOT for the technical support I received at GeoRessources. My gratitude also goes to Sébastien LECLERC, Younes BOUIZI, Renaud GLAY and Marie-Noelle PONS for their assistance in nuclear magnetic resonance (NMR), X-ray diffraction (XRD) and total organic carbon (TOC) analyses.

I would like to express my gratitude to LabEx RESSOURCES21 for funding my research. I must also express my deepest gratitude to Lorraine University of Excellence, the French embassy in Argentina and ECOS-Sud for financially supported my mobility in Argentina.

I would like to convey my sincere gratitude to my supervisor Professor Victoria FLEXER for hosting me in her laboratory in Argentina. This journey enabled me to learn more about electrodialysis operations and discover a new research environment. By the way, I would like to thank César Diaz NIETO, and Maria Laura VERA for their availability and kindness during my research at CIDMEJu.

My sincere gratitude to the jury members of my thesis for the effort and time they devoted to reviewing this work.

My heartiest thanks go to my colleagues Allen, Pierric, Alexandra, Théo, Nicolas, Abdoulaye, Camilo, Patricio, Ana, Luciana, Cecilia, Walter, Yasmine and Paola.

Finally, special thanks to my parents who supported and encouraged me along these three years.

Thank you all for your encouragement and support!

# Abstract

Continental brines as those of the salar de Hombre Muerto in the northwest Argentina are important resources of dissolved salts which could potentially be extracted economically for industrial purposes, particularly in the production of lithium-ion batteries. However, the extraction of lithium salts from brines is accompanied by the production of huge amounts of solid waste including mixed salts of sodium, calcium, magnesium, potassium, chlorides and boron. In the current facilities, lithium is processed from brines concentrated by solar evaporation without significant co-valorization of these salts. In some facilities, boron is extracted by highly soluble alcohols within the brines with co-extraction of lithium. When it is not co-valorized, boron is stored as well as sodium, calcium, magnesium and potassium in stockpiles with potential environmental concerns. Hence, development of new processes is mandatory to bypass solar evaporation and reduce industrial waste. Furthermore, it can be even envisaged to co-valorize some of these salts such as boron that can be used in agriculture, nuclear, detergent, pharmaceutical, glass and ceramic industries. In this context, this research delves into the development of direct boron and lithium extraction from the salar de Hombre Muerto brines by combining solvent extraction and electrodialysis process in order to valorize boron and produce high-grade lithium carbonate for lithium-ion batteries.

Extraction solvent composed of 2 mol $L^{-1}$ 2-butyloctan-1-ol in kerosene was employed to selectively extract 94.2% boron from a native brine of the salar de Hombre Muerto in four mixers-settlers at pH=7.5, phase volume ratio O/A=4 and 25 °C. Then, the boron-loaded extraction solvent was fully stripped by 0.1 mol $L^{-1}$ sodium hydroxide at phase volume ratio O/A=4 and 25 °C. This highly selective and efficient extractant allowed to crystallize boron as borax ($Na_2B_4O_7 \cdot 2H_2O$, purity=99%). Solvent extraction of boron was successfully implemented in a three-stage process combining electrodialysis and precipitation operations leading to the production of high-grade borax, high-grade lithium carbonate, magnesium hydroxide and sodium carbonate. Each of three stages was composed of three compartments in which water was reduced in the cathodic compartment and oxidized in the anodic compartment. By combining electrodialysis and precipitation *via* the hydroxide anions ($OH^-$) produced in the cathodic compartment, stage I enabled magnesium production as magnesium hydroxide ($Mg(OH)_2$). Stages II and III combined electrodialysis and precipitation employing carbon dioxide ($CO_2$). Therefore, sodium and lithium were produced as sodium carbonate ($Na_2CO_3$) and lithium carbonate ($Li_2CO_3$). Magnesium hydroxide ($Mg(OH)_2$), sodium carbonate ($Na_2CO_3$) and lithium carbonate ($Li_2CO_3$) were successively produced along the

process with purities of 71.2%, 99.99% and 99.9%, respectively. Most importantly, combining solvent extraction of boron and electrodialysis contributed to reduce the energy consumption by 32%. At the end of the process, the total dissolved solid (TDS) of the brine was decreased by 99.8%. This brine depleted of salts can be recycled in the process.

This research reveals the importance of direct boron and lithium extraction as well as the co-valorization of the other brine components such as magnesium and sodium in the next generation of lithium production plants. This is an avenue for sustainable battery-grade lithium carbonate production since this process leads to near-zero waste production and avoids water loss which reduces drastically environmental impact. Furthermore, unlike traditional methods relying on the use of sodium carbonate to precipitate lithium, the present process uses $CO_2$ to produce lithium carbonate and contributes, therefore, to $CO_2$ storage.

# Résumé

Les saumures continentales comme celles du salar de Hombre Muerto dans le Nord-Ouest de l'Argentine sont des ressources importantes en sels minéraux dissous qui pourraient être extraits pour des applications industrielles, particulièrement dans la production des batteries lithium-ion. Cependant, l'extraction des sels de lithium à partir des saumures s'accompagne de la production d'énormes quantités de déchets solides tels que des sels mixtes de sodium, de calcium, de magnésium et de potassium, mais aussi des sels de bore. Dans les installations industrielles actuelles, le lithium est extrait à partir des saumures concentrées par évaporation solaire sans nécessairement co-valoriser ces sels. Dans certaines installations industrielles, le bore est extrait par des alcools très solubles dans les saumures avec une co-extraction du lithium. Lorsqu'il n'est pas co-valorisé, le bore est stocké avec les sels de sodium, de calcium, de magnésium et de potassium dans des décharges, ce qui peut poser des problèmes environnementaux. Le développement de nouveaux procédés d'extraction de lithium est donc nécessaire pour éviter l'évaporation solaire et réduire la quantité de déchets générés. En outre, la co-valorisation de certains sels est envisageable, comme le bore, qui peut être utilisé dans l'agriculture, le nucléaire, les détergents, les produits pharmaceutiques et dans les industries de production de verre et de céramique. Dans ce contexte, cette recherche se penche sur le développement d'un procédé d'extraction directe du bore et du lithium à partir des saumures du salar de Hombre Muerto en combinant un procédé d'extraction liquide-liquide et un procédé d'électrodialyse afin de valoriser le bore et de produire du carbonate de lithium de haute qualité pour la fabrication des batteries lithium-ion.

Un solvant d'extraction composé de 2 mol $L^{-1}$ de 2-butyloctan-1-ol dilué dans du kérosène a été utilisé pour extraire sélectivement 94,2% de bore d'une saumure native du salar de Hombre Muerto. Pour cela, il est nécessaire d'utiliser quatre mélangeurs-décanteurs avec un rapport des volumes des phases organique et aqueuse O/A=4 sans ajuster le pH de la saumure (pH=7.5). Le bore peut ensuite être entièrement désextrait du solvant d'extraction chargé en bore en une étape à l'aide d'une solution de désextraction constituée d'hydroxyde de sodium à 0,1 mol $L^{-1}$ avec un rapport des volumes des phases O/A=4. Suite à l'extraction extrêmement sélective du bore et à la désextraction, le bore peut être cristallisé sous forme de borax ($Na_2B_4O_7•2H_2O$, pureté=99%). La combinaison d'une opération d'extraction liquide-liquide du bore avec des opérations d'électrodialyse et de précipitation ont permis de produire du borax de haute qualité, du carbonate de lithium de qualité batterie, de l'hydroxyde de magnésium et du carbonate de sodium. Les opérations d'électrodialyse ont été réalisées dans des cellules à

trois compartiments. La réduction de l'eau dans l'électrodialyseur génère des ions hydroxydes qui réagissent avec le magnésium dans l'étape I pour former un hydroxyde de magnésium ($Mg(OH)_2$). Les étapes II et III combinent une opération d'électrodialyse et une opération de précipitation en présence de dioxyde de carbone ($CO_2$) pour produire du carbonate de sodium ($Na_2CO_3$) et du carbonate de lithium ($Li_2CO_3$). L'hydroxyde de magnésium ($Mg(OH)_2$), le carbonate de sodium ($Na_2CO_3$) et le carbonate de lithium ($Li_2CO_3$) ont été successivement produits par ce procédé avec des puretés respectives de 71,20 %, 99,99 % et 99,90 %. Plus important encore, la combinaison de l'extraction liquide-liquide du bore et de l'électrodialyse a contribué à réduire la consommation énergétique des opérations d'électrodialyse de 32%. À la fin du procédé, la charge totale dissoute (CTD) de la saumure a été réduite de 99,8 %. Cette saumure appauvrie en sels peut être recyclée dans le procédé.

Cette recherche montre l'importance de l'extraction directe du bore et du lithium ainsi que la co-valorisation des autres constituants de la saumure telles que le magnésium et le sodium dans les prochaines générations des usines de production de lithium. Il s'agit d'une voie pour la production durable de carbonate de lithium de qualité batterie, car ce procédé génère moins de déchet et évite les pertes en eau, ce qui réduit considérablement son impact environnemental. En outre, contrairement aux méthodes traditionnelles qui reposent sur l'utilisation de carbonate de sodium pour précipiter le lithium, ce procédé utilise le $CO_2$ pour produire du carbonate de lithium et contribue donc au stockage du $CO_2$.

# Table of contents

Acknowledgements ..... 1
Abstract ..... 2
Résumé ..... 4
Table of contents ..... 6
List of figures ..... 10
List of tables ..... 16
Nomenclature ..... 21
General introduction ..... 23
References ..... 25
1 Chapter 1: Literature review on boron and lithium ..... 28
1.1 Introduction ..... 29
1.2 Literature review on boron ..... 30
1.2.1 Boron sources, resources and production ..... 30
1.2.2 Boron applications in industry ..... 32
1.2.3 Boron processing ..... 33
1.2.3.1 Boron extraction from ores ..... 33
1.2.3.2 Boron extraction from brines ..... 35
1.2.3.3 Solvent extraction ..... 35
1.2.3.3.1 Principle of solvent extraction ..... 35
1.2.3.3.2 Solvent extraction conditions ..... 40
1.2.3.4 Boron extraction by alcohols ..... 44
1.2.3.4.1 Boron extraction by mono alcohols ..... 44
1.2.3.4.2 Boron extraction by diols ..... 52
1.2.3.4.3 Boron extraction by alcohol-based deep eutectic solvents ..... 59
1.2.3.5 Boron extraction by alcohols in industry ..... 60

1.3 Literature review on lithium ..... 65
1.3.1 Lithium sources, resources and geographic distribution ..... 65
1.3.2 Lithium market and applications in industry ..... 67
1.3.3 Lithium processing ..... 69
1.3.3.1 Lithium processing from ores ..... 69
1.3.3.2 Lithium processing from brines ..... 71
1.3.3.2.1 Conventional processes ..... 72
1.3.3.2.2 New processes based on Direct Lithium Extraction ..... 77
1.4 Conclusion ..... 82
References ..... 84
2 Chapter 2: Boron extraction from the salar de Hombre Muerto brines by alcohols ..... 96
2.1 Introduction ..... 97
2.2 Material and methods ..... 98
2.2.1 Materials ..... 98
2.2.2 Methods ..... 101
2.2.2.1 Solvent extraction and stripping ..... 101
2.2.2.2 Analyses ..... 102
2.3 Results and discussions ..... 105
2.3.1 Boron speciation calculations ..... 105
2.3.2 Boron extraction by conventional solvents and DESs ..... 109
2.3.2.1 Influence of the diluent on boron extraction ..... 110
2.3.2.2 Influence of the extractant ..... 112
2.3.2.3 Influence of the pH ..... 115
2.3.2.4 Boron stripping ..... 121
2.3.3 Optimization of boron extraction and stripping conditions in the presence of 2-butyloctan-1-ol as extractant ..... 124
2.3.3.1 Boron extraction and impurities co-extraction ..... 124

2.3.3.2 Boron stripping....127
2.3.4 Nature of the extracted complex....129
2.3.5 Boron crystallization....132
2.3.6 Flowsheet for boron extraction and valorization as borax....134
2.4 Conclusion....139
References....141
3 Chapter 3: Production of high-grade borax and lithium carbonate by combining solvent extraction, precipitation and electrodialysis operations....146
3.1 Introduction....147
3.2 Materials and methods....147
3.2.1 Boron extraction and stripping....147
3.2.2 Brine processing by electrodialysis....148
3.2.2.1 Electrodialysis cells....148
3.2.2.2 Data analysis....152
3.2.3 Analyses....153
3.2.4 Speciation calculations....154
3.3 Results and discussion....154
3.3.1 Boron extraction....154
3.3.2 Stage I of the electrodialysis....155
3.3.2.1 Magnesium and calcium removal....155
3.3.2.2 Magnesium hydroxide production....161
3.3.3 Stage II of the electrodialysis....163
3.3.3.1 Sodium recovery....163
3.3.3.2 Sodium carbonate production....166
3.3.4 Stage III of the electrodialysis....171
3.3.4.1 Lithium recovery....171
3.3.4.2 Lithium carbonate production....172

3.3.5 Flowsheet of the overall process ..... 175
3.4 Conclusion ..... 177
References ..... 179
General conclusion ..... 183
References ..... 186
Summary of the thesis in French ..... 186
Appendices ..... 201
Appendix A ..... 201
Development of elemental analysis method ..... 201
References ..... 206
Appendix B ..... 214

# List of figures

Figure 1. 1: Flowsheet for boron extraction from ulexite ores in the Lerma Valley near Salta (Argentina) [26]. ....34
Figure 1. 2: General flowsheet for solvent extraction (SX). ....37
Figure 1. 3: Scheme of mixers-settlers configuration from Kislik. [51]. ....38
Figure 1. 4: Flowsheet implemented to extract glaserite and boron from the Searles lake brine in U.S. (adapted from Garrett) [26]. ....64
Figure 1. 5: Lithium occurrence. ....65
Figure 1. 6: Lithium-based commercial products [79]. ....68
Figure 1. 7: Lithium demand from 2020 to 2034 according to Statista in 2024 [87]. ....69
Figure 1. 8: General flowsheet of lithium carbonate production from ores. ....71
Figure 1. 9: General flowsheet for lithium carbonate production from brines. Flowsheet adapted from those reported by Chagnes [88], Meng el al. [79], Swain [78] and Choubey et al. [89]. ....74
Figure 1. 10: Flowsheet of lithium carbonate production from salar de Atacama (Chile) by the company Chemetall in 1984 [76]. ....76
Figure 1. 11: Flowsheet of Eramet's process for lithium carbonate production from salar de Centenario (Argentina). ....78
Figure 1. 12: Electrodialysis process for lithium carbonate production from brines [106]. ....80

Figure 2. 1: Comparison of boron speciation in pure water (a) calculated by using the Phreeqc software with the Pitzer and Minteq.V4 databases and (b) reported in literature [9], [Boron] = 0.1 mol $kg^{-1}$) . ....107
Figure 2. 2: Distribution of boron species as a function of pH for (a) 0.15 mol $L^{-1}$ boron and (b) 1.5 mol $L^{-1}$ boron in pure water. Speciation calculation performed by using the Phreeqc software with the Pitzer and Minteq.V4 databases. ....107
Figure 2. 3: Boron speciation vs. pH in (a) the synthetic brine or the native brine 1 and (b) the native brine 2. ....108
Figure 2. 4: Influence of O/A volume ratio on the extraction efficiencies of boron by 1 mol $L^{-1}$ (a) mono alcohols diluted in kerosene and (b) diols diluted in kerosene modified with toluene at pH=1 and 35 °C. ....114
Figure 2. 5: Influence of O/A volume ratio on the extraction efficiencies of boron by diols-based DESs (Men:TMPD and Men:MPD) at pH=5.5 and 25 °C. ....114

Figure 2. 6: Influence of the initial pH on boron extraction from the synthetic brine by (a) the mono alcohols BOc, EH and Oc diluted in kerosene (O/A=4) and (b) the diols EHD, BEPD and MPD diluted in kerosene modified with 60% (wt) toluene (O/A=2). Alcohol concentration=1 mol $L^{-1}$; 35 °C. No co-extraction of K, Li, Mg, Ca and Na was observed with mono alcohols. ..... 117

Figure 2. 7: Influence of the initial pH on boron extraction from the synthetic brine by diols-based DESs (Men:TMPD and Men:MPD) at O/A=0.5 and 25 °C. No co-extraction of K, Li, Mg, Ca and Na was observed. ..... 118

Figure 2. 8: Boron speciation in the synthetic brine as a function of initial pH (only the extractable boron species and the non-extractable species $NaH_2BO_3$ are reported)..... 118

Figure 2. 9: Influence of the initial pH of the synthetic brine on the extraction of boron and other elements (K, Li, Mg, Ca and Na) by (a) EHD, (b) BEPD and (c) MPD diluted in kerosene modified with toluene ([alcohol]=1 mol $L^{-1}$, O/A=2 and 35 °C)..... 119

Figure 2. 10: Boron stripping at 35 °C from an organic phase composed of 1 mol $L^{-1}$ (a) mono alcohols in kerosene and (b) diols in kerosene and 60% (wt.) toluene. Stripping solutions: 0.2 mol $L^{-1}$ NaOH, 0.2 mol $L^{-1}$ HCl or deionized water at 35 °C. The loaded organic phase was obtained by contacting the synthetic brine with the fresh organic phase at (a) O/A=4 and (b) O/A=2. ..... 123

Figure 2. 11: Boron stripping at 25 °C from an organic phase composed of diol-based DESs (Men:TMPD and Men:MPD). Stripping solutions: 0.2 mol $L^{-1}$ NaOH, 0.2 mol $L^{-1}$ HCl or deionized water at 25 °C. The loaded organic phase was obtained by contacting the synthetic brine with the fresh organic phase at O/A=1. ..... 124

Figure 2. 12: Influence of (a) 2-butyloctan-1-ol concentration in kerosene (O/A=4, pH=1, 25 °C), (b) pH (O/A=4, extraction solvent: 2 mol $L^{-1}$ 2-butyloctan-1-ol, 25 °C) and (c) O/A (pH=1, extraction solvent: 2 mol $L^{-1}$ 2-butyloctan-1-ol in kerosene, 25 °C) on boron extraction efficiency from the synthetic brine (SB). ..... 125

Figure 2. 13: Extraction of boron from the synthetic brine (SB) and the native brines (NB1 and NB2) at different phase volume ratios O/A (extraction solvent: 2 mol $L^{-1}$ 2-butyloctan-1-ol in kerosene, pH=5.5 for SB, pH=6.9 for NB1, pH=7.5 for NB2, 25 °C ). ..... 126

Figure 2. 14: Boron stripping efficiency when 0.2 mol $L^{-1}$ NaOH, 0.2 mol $L^{-1}$ HCl and deionized water are used as stripping solutions (O/A=4, 25 °C). The organic phase was previously loaded by contacting the extraction solvent (2 mol $L^{-1}$ 2-butyloctan-1-ol diluted in kerosene) with the synthetic brine (SB) at O/A=4, pH=5.5 and 25 °C. ..... 128

Figure 2. 15: Influence of sodium hydroxyde concentration on boron stripping efficiency (O/A=4, 25 °C). The organic phase was previously loaded by contacting the extraction solvent (2 mol $L^{-1}$ 2-butyloctan-1-ol diluted in kerosene) with the synthetic brine (SB) at O/A=4, pH=5.5 and 25 °C. .....128
Figure 2. 16: Stacked $^{1}H$ NMR spectrum of the organic phase before extraction (blue spectrum) and after extraction (red spectrum). .....131
Figure 2. 17: log of the distribution ratio of boron as a function of log of the concentration of 2-butyloctan-1-ol in the organic phase after extraction ([2-butyloctan-1-ol]=0.5−3 mol $L^{-1}$, O/A=4, pH=1 and 25 °C).....132
Figure 2. 18: X-ray diffraction (XRD) pattern of the crystallized solid (in black) and teepleite [35] (in red). .....133
Figure 2. 19: X-ray diffraction (XRD) patterns of the crystallized solid (in black), borax (in red) and Tincalconite (in blue). The phases were identified by using the database of the X-ray diffractometer (EVA software). .....134
Figure 2. 20: McCabe-Thiele diagrams for boron extraction from (a) the synthetic brine (SB) with O/A=4, (b) the native brine 1 (NB1) for O/A=7 and (c) the native brine 2 (NB2) with O/A=4 ($C_{B,org}$ and $C_{B,aq}$ are boron concentration in the organic phase and in the aquous phase, respectively). .....135
Figure 2. 21: Simulation model for countercurrent extraction of boron from synthetic (SB) and native brine 2 (NB2) using 2 mol $L^{-1}$ 2-butyloctan-1-ol diluted in kerosene (O/A=4; pH=5.5 and 7.5). LO: Loaded organic phase, A: Aqueous phase. .....136
Figure 2. 22: Flowsheet for boron extraction from brine and valorization as borax. .....138

Figure 3. 1: (a) Stage I, (b) Stage II and (c) Stage III implemented during the electrodialysis experiments. .....150
Figure 3. 2: pH of the non-pretreated brine and the boron-depleted brine as a function of the electrodialysis time (dpt denotes depleted). .....156
Figure 3. 3: (a) Magnesium and (b) calcium concentrations in the brines as a function of the pH during the electrodialysis (dpt denotes depleted). .....157
Figure 3. 4: Magnesium speciation vs pH in the non-pretreated brine and brine depleted of boron. Only $MgOH^{+}$, $MgH_2BO_3^{+}$ and $MgB(OH)_4^{+}$ species were reported in these Figures (dpt denotes depleted). .....158

Figure 3. 5: Ca speciation vs pH in the non-pretreated brine and the brine depleted of boron. Only $CaOH^+$, $CaH_2BO_3^+$ and $CaB(OH)_4^+$ species were reported in these Figures. dpt denotes depleted. ..... 160
Figure 3. 6: XRD pattern of the solid obtained after magnesium and calcium removal (in black). Reference XRD patterns of NaCl (in red) and $Mg(OH)_2$ (in blue). ..... 162
Figure 3. 7: XRD pattern of the solid obtained after washing (in black). Reference patterns of $Mg(OH)_2$ (in red) and NaCl (in blue). ..... 163
Figure 3. 8: Normalized concentrations of (a) sodium, and (b) lithium and potassium in the middle compartment as a function of the circulated charge per liter of brine for the non-pretreated brine and the boron-depleted brine depleted (dpt denotes depleted). ..... 165
Figure 3. 9: Carbonate speciation in pure water as a function of pH. 0.1 mol $L^{-1}$ carbonate was used for speciation calculations. ..... 168
Figure 3. 10: Sodium, lithium, potassium and carbonate anions ($CO_3^{2-}$) concentrations in the catholyte during $CO_2$ bubbling as a function of pH. ..... 169
Figure 3. 11: Carbonate speciation as a function of pH (a) before $CO_2$ bubbling and (b) at the maximum concentration of carbonate (69.5 g $L^{-1}$) obtained during $CO_2$ bubbling. ..... 170
Figure 3. 12: XRD pattern of the solid after washing (in black). Reference XRD patterns of sodium carbonate in red. The solid was obtained by precipitation of the catholyte in stage II. ..... 171
Figure 3. 13: XRD pattern of the crystallized solid from the catholyte of stage III (in black), and reference XRD patterns of lithium carbonate (in red) and sodium carbonate (in blue). ..... 174
Figure 3. 14: XRD pattern of the washed solid (in black) and reference XRD patterns of lithium carbonate (in red). The solid was obtained by crystallization of the catholyte in stage III. ..... 174
Figure 3. 15: Flowsheet of the overall process for borax, magnesium hydroxide, sodium carbonate and battery-grade lithium carbonate production from the salar de Hombre brine (dpt denotes depleted. ) ..... 176

Figure A. 1: Extraction efficiency of boron from the synthetic brine (SB) as a function of time at different phase volume ratios. Extraction solvent: 1 mol $L^{-1}$ BOc in kerosene; pH=1; temperature=35 °C (no co-extraction of K, Li, Mg, Na and Ca was observed). ..... 207

Figure A. 2: Extraction efficiency of boron from the synthetic brine (SB) as a function of time at different pH of the synthetic solution. Extraction solvent: 1 mol $L^{-1}$ BOc in kerosene; O/A=1; temperature=35 °C (no co-extraction of K, Li, Mg, Na and Ca was observed). .....207
Figure A. 3: Influence of time on the stripping efficiency of boron from an extraction solvent containing 1 mol $L^{-1}$ BOc in kerosene previously loaded with 0.25 g $L^{-1}$ boron by contacting the extraction solvent with the synthetic brine (SB) at O/A=4 (temperature=35 °C and pH=5.5). Stripping solutions: 0.2 mol $L^{-1}$ NaOH, 0.2 mol $L^{-1}$ HCl or deionized water; O/A=4; temperature=35 °C.....208
Figure A. 4: Extraction efficiency of boron from the synthetic brine (SB) as a function of time for different DES (no co-extraction of K, Li, Mg, Na and Ca was observed). Extraction conditions: O/A=1, pH=5.5 and 25 °C. .....208
Figure A. 5: Calcium speciation in the synthetic brine vs. pH. .....209
Figure A. 6: Potassium speciation in the synthetic brine vs. pH. .....210
Figure A. 7: Lithium speciation in the synthetic brine vs. pH.....210
Figure A. 8: Magnesium speciation in the synthetic brine vs. pH.....211
Figure A. 9: Sodium speciation in the synthetic brine vs. pH. .....211
Figure A. 10: McCabe-Thiele diagrams for boron removal from (a) the synthetic brine (SB) at O/A=6, (b) the native brine 1 (NB1) at O/A=9 and (c) the native brine 2 (NB2) at O/A=6 ($C_{B,org}$ and $C_{B,aq}$ are boron concentration in the organic phase and in the aquous phase, respectively).....213

Figure B. 1: Setup of experiments (a) before boron extraction, (b) during boron extraction and (c) during boron stripping.....214
Figure B. 2: Calcium and magnesium concentrations vs. pH during electrodialysis in (a) the non-pretreated brine and (b) the boron-depleted brine. .....217
Figure B. 3: Speciation of (a) magnesium and (b) calcium vs. pH in the non-pretreated brine before stage I of the electrodialysis process. .....218
Figure B. 4: Speciation of (a) magnesium and (b) calcium vs pH in the boron-depleted brine before stage I of the electrodialysis process. .....219
Figure B. 5: Speciation of (a) sodium, (b) lithium and (c) potassium vs pH in the non-pretreated brine before stage II of the electrodialysis process.....221

Figure B. 6: Speciation of (a) sodium, (b) lithium and (c) potassium vs pH in the boron-depleted brine before stage II of the electrodialysis process. ..... 222

# List of tables

Table 1. 1: Commercial boron minerals and their $B_2O_3$ content. .....30
Table 1. 2: Distribution of boron resources across countries reported by Etimaden (2023) [6]. .....31
Table 1. 3: Boron brines deposits, their estimated reserves in 1998 and boron concentration. .....31
Table 1. 4: Main extractants used in SX from Chagnes.[52]. .....43
Table 1. 5: Literature review on boron extraction by alcohols from different aqueous solution. .....47
Table 1. 6: Composition, pH and density of (1) East Taijinaier salt lake brine (northwest China) depleted of potassium, (2) acidified West Taijinaier salt Lake brine and (3) East Taijinaier salt lake brine concentrated by evaporation. .....49
Table 1. 7: Thermodynamic properties of boron extraction by mono alcohols from (1) East Taijinaier salt lake brine (northwest China) depleted of potassium, (2) acidified West Taijinaier salt Lake brine and (3) East Taijinaier salt lake brine concentrated. SK: sulfonated kerosene. .....50
Table 1. 8: Composition, pH and density of (1) the Jinaier salt lake brine (Qinghai province, China), (2) underground brine from Dazhou (China) and concentrated by evaporation, and (3) brine concentrated by evaporation. .....53
Table 1. 9: Distribution ratios and extraction efficiencies of boron for extraction solvents containing diols. Ionic strength I=0.5 mol $L^{-1}$; extraction conditions: pH=2, O/A=1 and 25 °C. .....56
Table 1. 10: Boron extraction efficiencies and losses of 0.5 mol $L^{-1}$ diols diluted in chloroform. Aqueous solution containing: 0.01 mol $L^{-1}$ boric acid, 0.49 mol $L^{-1}$ NaCl and 0.01 mol $L^{-1}$ HCl, Ionic strength I=0.5 mol $L^{-1}$; extraction conditions: pH=2; O/A=1, 25 °C. .....58
Table 1. 11: (a) Extraction and (b) stripping conditions of boron in the processes developed by (1) Chemetall company in 1998, (2) Minsal company in 2002, and (3) Anon et al. in 1996 ($E_B$: boron extraction efficiency in %, $SE_B$: boron stripping efficiency in %). .....61
Table 1. 12: Composition of the concentrated brine from salar de Atacama (1) before boron extraction and (2) after boron extraction under the operating conditions reported in Table 1. 13 for the Chemetall company. .....61
Table 1. 13: Mineral composition of the Searles lake brine. .....63
Table 1. 14: World lithium resources in 2024 [77]. .....67

Table 1. 15: Typical composition of spodumene deposits (minerals concentration in %wt) [76]. .....70
Table 1. 16: Average composition of lithium-containing brines with commercial value [76]. .....72
Table 1. 17: Several direct lithium extraction (DLE) processes. .....77

Table 2. 1: Structures and dynamic viscosities of the selected alcohols at 25 °C (η=dynamic viscosity of pure alcohol). .....99
Table 2. 2: Composition, pH, ionic strength (I) and density at room temperature (25±0.5 °C) of native brine 1 (NB1), native brine 2 (NB2) and synthetic brine (SB). The ionic strength was determined by considering the speciation calculated with the Phreeqc software (databases: Pitzer, Core10, Amm and Minteq.V4). .....100
Table 2. 3: Chemical reactions and thermodynamic constants used for speciation calculations of boron with Phreeqc (databases: Pitzer and Minteq.V4). .....106
Table 2. 4: Effect of diluents on boron extraction efficiency ($E_B$), dynamic viscosity (η) and water solubility in the organic phase ($w_{H2O}$) after boron extraction by the extractant 1 mol $L^{-1}$ alcohol. Extraction conditions: O/A=1, pH=1 and 35 °C. ns: not soluble, *i.e.* solubility<1 mol $L^{-1}$. .....112
Table 2. 5: Effect of HBA on boron extraction efficiency ($E_B$), dynamic viscosity (η) and water solubility in the organic phase ($w_{H2O}$) after boron extraction by DESs. Extraction conditions: O/A=1, pH=5.5 and 25 °C. .....112
Table 2. 6: Extraction efficiencies of boron ($E_B$) by mono alcohols in kerosene and diols in the mixture of kerosene and toluene, dynamic viscosities (η) and water solubility ($w_{H2O}$) in the loaded organic phase, and solubility of the alcohols ($S_{alc}$) in the synthetic brine under the optimal extraction conditions. .....120
Table 2. 7: Extraction efficiencies of boron ($E_B$) by diol-based DESs (Men:TMPD and Men:MPD), dynamic viscosities after extraction (η) and water solubility ($w_{H2O}$) in the loaded organic phase, and solubility of DES ($S_{DES}$) in the synthetic brine under the optimal extraction conditions (O/A=0.5, and 25 °C). .....120
Table 2. 8: Boron extraction efficiency in each stage of four-stage continuous countercurrent extraction for the synthetic brine (SB) and the native brine 2 (NB2) (Extractant=2 mol $L^{-1}$ 2-butyloctan-1-ol, Diluent=kerosene, O/A=4, 25 °C). .....137

Table 2. 9: Composition, pH and density of the synthetic brine (SB) before extraction and after extraction (Extractant=2 mol $L^{-1}$ 2-butyloctan-1-ol, Diluent=kerosene, O/A=4, 25 °C). .....138

Table 3. 1: Composition, total dissolved solid (TDS) and pH of the brine from the salar de Hombre Muerto.....148

Table 3. 2: Composition and pH of the brine of the salar de Hombre Muerto (1) before and (2) after boron extraction.....154

Table 3. 3: Solubility at 25 °C or 20 °C of salts that could precipitate in the cathodic compartment (* solubility at 20 °C) [16].....156

Table 3. 4: Composition and pH of (1) non-pretreated brine, (2) non-pretreated brine in the cathodic compartment after magnesium and calcium removal, (3) boron-depleted brine, and (4) boron-depleted brine in the cathodic compartment after magnesium and calcium removal. .....161

Table 3. 5: Composition and pH of (1) the non-pretreated brine before stage II, (2) the non-pretreated brine in the middle compartment after stage II, (3) the boron-depleted brine before stage II, and (4) the boron-depleted brine in the middle compartment after stage II. .....164

Table 3. 6: Separation coefficients of $K^+$, $Na^+$ and $Li^+$ as a function of the circulated charge per liter of brine (a) for the non-pretreated brine and (b) the boron-depleted brine. .....166

Table 3. 7: Solubility of the salts at 25 °C in pure water [16]. .....168

Table 3. 8: Evolution of pH in the three compartments of stage III, voltage, current and, concentrations of lithium, sodium and potassium in the middle compartment as a function of the electrodialysis extent. .....172

Table 3. 9: Composition of catholyte (1) before evaporation, (2) when the volume of catholyte was reduced by 2 and (3) when the volume of the catholyte was reduced by 4.....173

Table A. 1: Sodium, sulfate and chloride concentrations in the standards used to plot the standardization curves for sodium analysis. .....202

Table A. 2: Volumes of sodium standard (1,000 mg $L^{-1}$), hydrochloric acid (purity=37%), sulfuric acid (purity=96%) and nitric acid (purity=65%) used to prepare each standard in 100mL volumetric flask.....202

Table A. 3: Sodium, sulfate, chloride, boron, potassium, magnesium and lithium concentrations in the standards used to plot the standardization curves for boron, potassium, magnesium and lithium analyses.....203
Table A. 4: Volume of 26 g $L^{-1}$ NaCl, HCl (purity=37%), $H_2SO_4$ (purity=96%), $HNO_3$ (purity=65%), K, Mg, B and Li standards (1,000 mg $L^{-1}$) used to prepare each standard in 100mL volumetric flask.....203
Table A. 5: Sodium, sulfate, chloride and calcium concentrations in the standards used to plot the standardization curves for calcium analysis.....204
Table A. 6: Volume of 26 g $L^{-1}$ NaCl, HCl (purity=37%), $H_2SO_4$ (purity=96%), $HNO_3$ (purity=65%) and calcium standard (1,000 mg $L^{-1}$) used to prepare each standard in 100mL volumetric flask. .....204
Table A. 7: Volume of sample, 262.7 g $L^{-1}$ NaCl, HCl (purity=37%) and $H_2SO_4$ (purity=96%) used to obtain the concentrations of sodium, chloride and sulfate in the matrices for each type of stripping solution. .....205
Table A. 8: Concentrations of B, K, Li, Mg, Na and Ca for 10 analyses of the synthetic brine, the standard deviations and the analytical error.....206
Table A. 9: Influence of the temperature on the extraction efficiency of boron (extraction solvent: 2 mol $L^{-1}$ 2-butyloctan-1-ol, O/A=4, pH=5.5). .....209

Table B. 1: Concentration of boron as a function of time in the brine after extraction and in the stripping solution after stripping. Extraction conditions: 2 mol $L^{-1}$ 2-butyloctan-1-ol in kerosene, pH=7.5, O/A=4 and 25 °C. Stripping conditions: 0.1 mol $L^{-1}$ NaOH, O/A=4 and 25 °C. .....214
Table B. 2: Technical specifications of ion exchange membranes. Data provided by the manufacturer (Membranes International Inc., https://ionexchangemembranes.com/). ..215
Table B. 3: Boron extraction efficiencies from the salar de Hombre Muerto brine as a function of the extraction step. Extraction conditions: 2 mol $L^{-1}$ 2-butyloctan-1-ol in kerosene, pH=7.5, O/A=4 and 25 °C. .....215
Table B. 4: Evolution of pH, current, voltage, and concentrations of boron, calcium and magnesium in the non-pretreated brine in the cathodic compartment during the electrodialysis in stage I.....216

Table B. 5: Evolution of pH, current, voltage, and concentrations of boron, calcium and magnesium in the boron-depleted brine in the cathodic compartment during the electrodialysis in stage I. ..... 216
Table B. 6: Composition of the solid obtained for (1) the non-pretreated brine and (2) the boron-depleted brine after magnesium and calcium precipitations in stage I of the electrodialysis process ..... 220
Table B. 7: pH in the three compartments, current, voltage, and concentrations of sodium, lithium and potassium in the middle compartment at the end of each electrodialysis experiment in stage II for the non-pretreated brine. ..... 220
Table B. 8: Values of pH in the three compartments, current, voltage, and concentrations of sodium, lithium and potassium in the middle compartment at the end of each electrodialysis experiment in stage II for the boron-depleted brine. ..... 220

# Nomenclature

## List of abbreviation

| | |
|---|---|
| BOc | 2-butyloctan-1-ol |
| EH | 2-ethylhexan-1-ol |
| Oc | octan-1-ol |
| EHD | 2-ethylhexane-1,3-diol |
| MPD | 2-methylpentane-2,4-diol |
| BEPD | 2-butyl-2-ethylpropane-1,3-diol |
| TMPD | 2,2,4-trimethylpentane-1,3-diol |
| DESs | deep eutectic solvents |
| Men | menthol |
| Thy | thymol |
| HBD | hydrogen bond donor |
| HBA | hydrogen bond acceptor |
| SB | synthetic brine |
| NB1 | native brine 1 |
| NB2 | native brine 2 |
| TOC | total organic carbon |
| ED | electrodialysis |
| AEM | anion exchange membrane |
| CEM | cation exchange membrane |
| SPM | suspended particle matter |
| XRD | X-ray diffraction |
| dpt | depleted |
| TDS | total dissolved solid |

# List of symbols

Bar symbols in equations refer to organic phase and symbols without bar refer to aqueous phase

All pH without mention of equilibrium pH refer to initial pH

| | |
|---|---|
| $\eta$ | dynamic viscosity |
| $D_e$ | distribution ratio of the element e |
| $E_e$ (%) | extraction efficiency of the element e |
| $Se_{1}/_{e_2}$ | selectivity coefficient of the element $e_1$ towards the element $e_2$ |
| $SE_B$ | stripping efficiency of boron |
| $S_{alc}$ | solubility of alcohol |
| $S_{DES}$ | solubility of DES |
| O/A | organic to aqueous phase volume ratio |
| E | electrical energy consumption |
| $C/C_0$ | the normalized concentration |
| $E_{source}$ | voltage drop |
| $F_{M_1-M_2}$ | separation coefficient |

# General introduction

Presently, minerals demand is still increasing due to the development of new technologies for the energy transition. Most of minerals are extracted from ores. However, lithium minerals are extracted from both brines and ores, making brines an alternative resource to ensure huge production of lithium for industry applications in long term. Brines contain various minerals depending on the deposit. They can be divided into two groups such as underground brines (oilfields and geothermal brines) and continental brines (salt lake and salar brines). Salar brines are mainly located in South America, *i.e.* Argentina, Chile and Bolivia, at high altitude in extremely low rainfall regions.

The salar de Hombre Muerto brine, in northwest Argentina, is rich in lithium, potassium, calcium, sodium, magnesium, boron, chloride and sulfate. Lithium recovery process from that brine is challenging due to the high concentration of impurities. Currently, lithium extraction processes are based on solar evaporation and chemical precipitation steps [1]. It occurs between one and two years from the evaporation operations to lithium extraction. Furthermore, these conventional processes are responsible of huge amount of water loss during evaporation and consume huge chemicals for impurities precipitation without their co-valorization. In fact, the impurities removed from brines as salts are stored in landfills with potential environment impact. For circular economy perspective, that technology is not enough efficient and sustainable for huge lithium production in long term. New lithium extraction technologies relying on liquid-liquid extraction, solid-liquid extraction or membrane technologies are investigated to extract lithium in an efficient and sustainable manner. Among these technologies, electrodialysis is reported in literature as an interesting technology [2]. Recently, Diaz Nieto et al. ([3], [4], [5]), worked on the development of a process combining electrodialysis and successive precipitation stages enabling the separation of magnesium, calcium, sodium and lithium as magnesium hydroxide, calcium hydroxide, sodium carbonate and low-battery grade lithium carbonate (purity=97.5%), respectively. Such a purity of lithium carbonate is however too low since battery-grade lithium carbonate must reach 99.5% purity [6]. Among the impurities, the removal of boron is particularly important. Its presence can cause filtration issues after the precipitation stage and significantly reduce the purity of lithium carbonate, thus preventing its use in the production of lithium-ion batteries since less than 25 mg $L^{-1}$ boron in brines is mandatory to produce battery-grade lithium salts [7]. In addition, the use of this technology may enable boron co-valorization, and therefore, may contribute to meet demand for the most boron-intensive industries (glass, ceramic, agriculture and detergent

industries) [8] and other industries such as nuclear [9], steel [10], pharmaceutical [11], catalysis [12], textile [13], hydrogen storage [14], concrete [15] and military [16].

Many technologies such as adsorption [17], chemical precipitation [18], electrodialysis [19], ions exchange [20], solvent extraction ([21], [22], [23], [24]) and reverse osmosis [25] were tested to recover boron from brines or even other aqueous solutions. Solvent extraction is a mature unit operation implemented in hydrometallurgical processes ([26], [27]). In lithium production plants, alcohol is commonly used as extractant for solvent extraction of boron from brines after solar evaporation, despite the typically high solubility of alcohol molecules in brines [28]. The high solubility of alcohol in brine is therefore responsible for high extractant losses, which result in important operating costs and potential environmental issues.

This PhD work is devoted to developing a process for the direct extraction of boron from the native brines of salar de Hombre Muerto with the aim of co-valorizing boron as pure boric acid or borax, as well as producing high-grade lithium carbonate. To achieve this objective, a combination of solvent extraction, electrodialysis, and precipitation stages was employed to recover boron, separate impurities from lithium, and produce lithium carbonate. The novelty of this work lies in its innovative approach to boron and lithium extraction from brines. Unlike traditional methods, which rely on brine concentration through solar evaporation before mineral extraction, this research focuses on direct extraction of boron and lithium from native brines. This approach anticipates the evolution of lithium production plants, which will likely bypass solar evaporation, underscoring the necessity of directly extracting boron from brines a facet seldom explored in previous studies.

To accomplish these objectives, Chapter 1 presents a thorough literature review on boron and lithium, covering their sources, reserves or resources, production, demand, processing, and industrial applications. Chapter 2 focuses on investigating boron extraction from brines using deep eutectic solvents and six alcohols, namely 2-butyloctan-1-ol (BOc), 2-ethylhexan-1-ol (EH), octan-1-ol (Oc), 2-ethylhexane-1,3-diol (EHD), 2-methylpentane-2,4-diol (MPD), and 2-butyl-2-ethylpropane-1,3-diol (BEPD), diluted in kerosene, sulfonated kerosene, and a mixture of kerosene and toluene or m-xylene. These investigations focus on understanding the influence of factors such as the nature of the diluent, alcohol concentration, organic to aqueous phase volume ratios, pH, and temperature on boron extraction efficiency, selectivity towards calcium, magnesium, sodium, lithium, and potassium, alcohol solubility in brines, water solubility in organic phases, and the recyclability of the aforementioned alcohols. Subsequently, efficient boron extraction conditions are utilized to develop a continuous

countercurrent extraction process. Finally, Chapter 3 integrates solvent extraction of boron in a three-stage electrodialysis process to produce lithium carbonate, co-valorize boron and discard calcium, magnesium, and sodium.

# References


[1] F. Meng, J. McNeice, S. S. Zadeh, and A. Ghahreman, "Review of Lithium Production and Recovery from Minerals, Brines, and Lithium-Ion Batteries," *Mineral Processing and Extractive Metallurgy Review*, vol. 42, no. 2, pp. 123–141, Feb. 2021, doi: 10.1080/08827508.2019.1668387.

[2] S. Gmar and A. Chagnes, "Recent advances on electrodialysis for the recovery of lithium from primary and secondary resources," *Hydrometallurgy*, vol. 189, p. 105124, Nov. 2019, doi: 10.1016/j.hydromet.2019.105124.

[3] C. H. Díaz Nieto, K. Rabaey, and V. Flexer, "Membrane electrolysis for the removal of Na+ from brines for the subsequent recovery of lithium salts," *Separation and Purification Technology*, vol. 252, p. 117410, Dec. 2020, doi: 10.1016/j.seppur.2020.117410.

[4] C. H. Díaz Nieto, N. A. Palacios, K. Verbeeck, A. Prévoteau, K. Rabaey, and V. Flexer, "Membrane electrolysis for the removal of Mg2+ and Ca2+ from lithium rich brines," *Water Research*, vol. 154, pp. 117–124, May 2019, doi: 10.1016/j.watres.2019.01.050.

[5] W. R. Torres, C. H. Díaz Nieto, A. Prévoteau, K. Rabaey, and V. Flexer, "Lithium carbonate recovery from brines using membrane electrolysis," *Journal of Membrane Science*, vol. 615, p. 118416, Dec. 2020, doi: 10.1016/j.memsci.2020.118416.

[6] V. T. Luong, D. J. Kang, J. W. An, M. J. Kim, and T. Tran, "Factors affecting the extraction of lithium from lepidolite," *Hydrometallurgy*, vol. 134–135, pp. 54–61, Mar. 2013, doi: 10.1016/j.hydromet.2013.01.015.

[7] J. Guo, Y. Yang, X. Gao, and J. Yu, "Boron extraction from lithium-rich brine using mixed alcohols," *Hydrometallurgy*, vol. 197, p. 105477, Nov. 2020, doi: 10.1016/j.hydromet.2020.105477.

[8] T. Turkbay, J. Bongono, T. Alix, B. Laratte, and B. Elevli, "Prior knowledge of the data on the production capacity of boron facilities in Turkey," *Cleaner Engineering and Technology*, vol. 10, p. 100539, Oct. 2022, doi: 10.1016/j.clet.2022.100539.

[9] M. M. Nasseri, "Comparison of HfB2 and ZrB2 behaviors for using in nuclear industry," *Annals of Nuclear Energy*, vol. 114, pp. 603–606, Apr. 2018, doi: 10.1016/j.anucene.2017.12.060.

[10] J. Eichler and C. Lesniak, “Boron nitride (BN) and BN composites for high-temperature applications,” *Journal of the European Ceramic Society*, vol. 28, no. 5, pp. 1105–1109, Jan. 2008, doi: 10.1016/j.jeurceramsoc.2007.09.005.

[11] F. Ali, N. S Hosmane, and Y. Zhu, “Boron Chemistry for Medical Applications,” *Molecules*, vol. 25, no. 4, Art. no. 4, Jan. 2020, doi: 10.3390/molecules25040828.

[12] “Borophene and Boron-Based Nanosheets: Recent Advances in Synthesis Strategies and Applications in the Field of Environment and Energy - Chand - 2021 - Advanced Materials Interfaces - Wiley Online Library.” Accessed: Jan. 25, 2023. [Online]. Available: https://onlinelibrary-wiley-com.bases-doc.univ-lorraine.fr/doi/full/10.1002/admi.202100045

[13] A. Mergen, M. H. Demirhan, and M. Bilen, “Processing of boric acid from borax by a wet chemical method,” *Advanced Powder Technology*, vol. 14, no. 3, pp. 279–293, Jan. 2003, doi: 10.1163/15685520360685947.

[14] G. Moussa, R. Moury, U. B. Demirci, T. Şener, and P. Miele, “Boron-based hydrides for chemical hydrogen storage,” *International Journal of Energy Research*, vol. 37, no. 8, pp. 825–842, 2013, doi: 10.1002/er.3027.

[15] M. H. Kharita, S. Yousef, and M. AlNassar, “Review on the addition of boron compounds to radiation shielding concrete,” *Progress in Nuclear Energy*, vol. 53, no. 2, pp. 207–211, Mar. 2011, doi: 10.1016/j.pnucene.2010.09.012.

[16] M. M. Harussani, S. M. Sapuan, G. Nadeem, T. Rafin, and W. Kirubaanand, “Recent applications of carbon-based composites in defence industry: A review,” *Defence Technology*, vol. 18, no. 8, pp. 1281–1300, Aug. 2022, doi: 10.1016/j.dt.2022.03.006.

[17] Z. Guan, J. Lv, P. Bai, and X. Guo, “Boron removal from aqueous solutions by adsorption — A review,” *Desalination*, vol. 383, pp. 29–37, Apr. 2016, doi: 10.1016/j.desal.2015.12.026.

[18] Y.-J. Shih, C.-H. Liu, W.-C. Lan, and Y.-H. Huang, “A novel chemical oxo-precipitation (COP) process for efficient remediation of boron wastewater at room temperature,” *Chemosphere*, vol. 111, pp. 232–237, Sep. 2014, doi: 10.1016/j.chemosphere.2014.03.121.

[19] L. Melnik, O. Vysotskaja, and B. Kornilovich, “Boron behavior during desalination of sea and underground water by electrodialysis,” *Desalination*, vol. 124, no. 1, pp. 125–130, Nov. 1999, doi: 10.1016/S0011-9164(99)00096-X.

[20] M. Gazi and N. Bicak, “Selective boron extraction by polymer supported 2-hydroxylethylamino propylene glycol functions,” *Reactive and Functional Polymers*, vol. 67, no. 10, pp. 936–942, Oct. 2007, doi: 10.1016/j.reactfunctpolym.2007.05.019.

[21] N. Bicak, M. Gazi, and B. F. Senkal, “Polymer supported amino bis-(cis-propan 2,3 diol) functions for removal of trace boron from water,” *Reactive and Functional Polymers*, vol. 65, no. 1, pp. 143–148, Nov. 2005, doi: 10.1016/j.reactfunctpolym.2005.01.010.

[22] M. D. Joshi, G. Chalumot, Y. Kim, and J. L. Anderson, “Synthesis of glucaminium-based ionic liquids and their application in the removal of boron from water,” *Chem. Commun.*, vol. 48, no. 10, pp. 1410–1412, Jan. 2012, doi: 10.1039/C1CC14327A.

[23] M. Karakaplan, S. Tural, B. Tural, Y. Turgut, and H. Hoşgören, “The Solvent Extraction of Boron with Synthesized Aliphatic 1,3-Diols: Stripping and Extraction Behavior of Boron by 2,2,5-Trimethyl-1,3-hexanediol,” *Solvent Extraction and Ion Exchange*, vol. 22, no. 6, pp. 897–911, Dec. 2004, doi: 10.1081/SEI-200037400.

[24] W. L. A. Brooks, C. C. Deng, and B. S. Sumerlin, “Structure–Reactivity Relationships in Boronic Acid–Diol Complexation,” *ACS Omega*, vol. 3, no. 12, pp. 17863–17870, Dec. 2018, doi: 10.1021/acsomega.8b02999.

[25] A. Farhat, F. Ahmad, N. Hilal, and H. A. Arafat, “Boron removal in new generation reverse osmosis (RO) membranes using two-pass RO without pH adjustment,” *Desalination*, vol. 310, pp. 50–59, Feb. 2013, doi: 10.1016/j.desal.2012.10.003.

[26] G. M. Ritcey, “Solvent extraction in hydrometallurgy: Present and future,” *Tsinghua Science and Technology*, vol. 11, no. 2, pp. 137–152, Apr. 2006, doi: 10.1016/S1007-0214(06)70168-7.

[27] A. Chagnes, Ed., *Advances in Hydrometallurgy*. MDPI - Multidisciplinary Digital Publishing Institute, 2020. doi: 10.3390/books978-3-03928-940-0.

[28] D. E. Garrett, “Part 1 - Lithium,” in *Handbook of Lithium and Natural Calcium Chloride*, D. E. Garrett, Ed., Oxford: Academic Press, 2004, pp. 1–235. doi: 10.1016/B978-012276152-2/50037-2.

# 1 Chapter 1: Literature review on boron and lithium


1.1 Introduction ..... 29
1.2 Literature review on boron ..... 30
1.2.1 Boron sources, resources and production ..... 30
1.2.2 Boron applications in industry ..... 32
1.2.3 Boron processing ..... 33
1.2.3.1 Boron extraction from ores ..... 33
1.2.3.2 Boron extraction from brines ..... 35
1.2.3.3 Solvent extraction ..... 35
1.2.3.3.1 Principle of solvent extraction ..... 35
1.2.3.3.2 Solvent extraction conditions ..... 40
1.2.3.4 Boron extraction by alcohols ..... 44
1.2.3.4.1 Boron extraction by mono alcohols ..... 44
1.2.3.4.2 Boron extraction by diols ..... 52
1.2.3.4.3 Boron extraction by alcohol-based deep eutectic solvents ..... 59
1.2.3.5 Boron extraction by alcohols in industry ..... 60
1.3 Literature review on lithium ..... 65
1.3.1 Lithium sources, resources and geographic distribution ..... 65
1.3.2 Lithium market and applications in industry ..... 67
1.3.3 Lithium processing ..... 69
1.3.3.1 Lithium processing from ores ..... 69
1.3.3.2 Lithium processing from brines ..... 71
1.3.3.2.1 Conventional processes ..... 72
1.3.3.2.2 New processes based on Direct Lithium Extraction ..... 77
1.4 Conclusion ..... 82
References ..... 84

## 1.1 Introduction

Boron (B) is a metalloid with a melting point of about 2,075 °C and a boiling point of 4,000 °C. It has two stable isotopes: $^{10}B$ and $^{11}B$. The $^{10}B$ has a high capacity for neutron capture, making it useful for various nuclear applications. In earth crust, boron content typically ranges from 5 mg $kg^{-1}$ to 100 mg $kg^{-1}$ [1]. However, there is significant variation in boron content in water depending on its source. For instance, boron concentration ranges from 15−300 mg $L^{-1}$ ([2], [3]) in waste water from industries which employed boron as raw material, and can reach up to 8,000 mg $L^{-1}$ in brines [4]. In drinking water, boron concentration is recommended to be no more than 2.4 mg $L^{-1}$ by the World Health Organization (WHO) [5]. Boron is also essential micronutrient for animals, plants and humans. On the other hand, lithium (Li) with a molar weight of 6.94 g $mol^{-1}$, is the lightest metal in the periodic table and it is used in specific industries such as ceramic, glass, greases, lubricants, catalysts and electronic and lithium-ion batteries.

Boron and lithium have long served as crucial raw materials in industrial applications. In recent years, their demand has surged alongside the development of new sustainable materials for the energy transition. Extracting boron and lithium from ores may be more costly and resource-intensive than from brines due to the energy and chemical-intensive processes involved in mineral beneficiation and leaching. The increasing production of lithium from brines is expected to drive a corresponding rise in boron extraction. This is because lithium-rich continental brines, such as those found in salars, often contain high levels of boron. Currently, boron in brine is typically regarded as a by-product, but there is growing recognition of its potential value. Developing sustainable processes capable of co-valorizing boron with lithium is of significant importance. This could open avenues for their combined use in industries such as glass, ceramics, agriculture, and detergents, contributing to both economic efficiency and environmental sustainability.

In current lithium production plants utilizing solar evaporation, boron is typically extracted from brines without being valorized. Only few lithium production plants engaged in co-valorization of boron. When boron is not co-valorized, it is stored in stockpiles, posing potential environmental hazards. Presently, several industrial programs are planning to implement direct lithium extraction methods (DLE) as an alternative to solar evaporation. This shift aims to reduce environmental impacts such as water loss through evaporation, which can lead to water

table issues, and to drastically decrease lithium loss occurring during precipitation along solar evaporation processes.

The processing steps for boron and lithium are heavily influenced by the composition of brines. Thus, a thorough understanding of the elements' nature and concentrations within the brines is essential before embarking on any investigation into boron and lithium extraction. This chapter aims to provide a comprehensive review of boron and lithium sources, as well as their resources, reserves, production, demand, processing methods, and applications across various industries.

## 1.2 Literature review on boron

### 1.2.1 Boron sources, resources and production

Worldwide boron resources are estimated to be around 400 million tons in ores and brines deposits [6]. Table 1. 1 gathers the well-known boron minerals among about 230 identified boron minerals [7].

**Table 1. 1:** Commercial boron minerals and their $B_2O_3$ content.

| Mineral | Chemical Formula | $B_2O_3$ (%wt) |
|---|---|---|
| Boric acid | $H_3BO_3$ or $B(OH)_3$ | 56.4 |
| Tincal (Borax) | $Na_2B_4O_7 \cdot 10H_2O$ | 36.5 |
| Tincalconite | $Na_2B_4O_7 \cdot 5H_2O$ | 48.8 |
| Kernite | $Na_2B_4O_7 \cdot 4H_2O$ | 51.0 |
| Ulexite | $NaCaB_5O_9 \cdot 8H_2O$ | 43.0 |
| Colémanite | $Ca_2B_6O_{11} \cdot 5H_2O$ | 50.8 |

Turkey holds the world's largest boron resource, accounting for approximately 73% followed by Russia with 7.7%, U.S. with 6.1%, Chile with 3.2% and China with 2.8% (see boron resources repartition by country in Table 1. 2). According to the U.S. geological survey, boron reserves from ores were estimated to be more than 1.4 million tons in 2022. Unlike boron reserve from traditional mineral sources, information on boron worldwide reserves from brines, including sea water, continental and underground brines is not available. This is due to the irregular distribution in such sources and the limited research conducted in this field.

**Table 1. 2:** Distribution of boron resources across countries reported by Etimaden (2023) [6].

| Country | Distribution of boron resources (%) |
|---|---|
| Turkey | 73.4 |
| Russia | 7.7 |
| U.S. | 6.2 |
| Chile | 3.2 |
| China | 2.8 |
| Peru | 1.7 |
| Serbia | 1.6 |
| Bolivia | 1.5 |
| Kazakhstan | 1.2 |
| Argentina | 0.7 |

Table 1. 3 gathers estimated amount of boron and boron concentration in different brines deposits in 1998 according to Garrett [8]. Searles lake (20.5 million tons of boron) is the greatest boron deposit, followed by salar de Uyuni, Bolivia (3.2 million tons of boron), and salar de Atacama, Chile (3.1 million tons of boron).

**Table 1. 3:** Boron brines deposits, their estimated reserves in 1998 and boron concentration.

| Brine origin | Deposit, Country | B amount (million tons) | B (%wt) |
|---|---|---|---|
| Salar | Salar de Hombre Muerto, Argentina | 0.34 | - |
| | Salar de Uyuni, Bolivia | 3.2 | - |
| | Salar de Atacama, Chile | 3.1 | - |
| Salt lake | Xiao Qaidam lake, China | 0.06 | - |
| | Nei Mongol Plateau, China | 0.16 | - |
| | Inder Lake, Russia | - | 0.07 |
| | Hachinhama lake, USA | - | 1.86 |
| | Owens lake, USA | 0.06 | - |
| | Searles lake, USA | 20.5 | - |
| Geothermal | Salton sea geothermal brine and Cerro Prieto, Mexico | 2 | - |

Nowadays, boron is mainly produced as boric acid, borax and elemental nanoboron from four boron minerals which are commercially important including tincal ($Na_2B_4O_7{\cdot}10H_2O$), ulexite ($NaCaB_5O_9{\bullet}8H_2O$), kernite ($Na_2B_4O_7{\bullet}4H_2O$) and Colemanite ($Ca_2B_6O_{11}{\cdot}5H_2O$). Around 12 million tons of boron minerals were produced from mining in 2016 [9] whereas a huge amount of boron could be potentially extracted from brines. The most expensive boron products is elemental nanoboron ($1.7 million per ton) followed by boric acid ($800 per ton for 99% purity) and borax ($500 per ton).

## 1.2.2 Boron applications in industry

Nowadays, boron is widely present in many human activities. Boric acid and borax are employed in the most boron-intensive industries including agriculture ([10], [11]), glass, ceramic ([12], [13]), and detergent, which represent 86% of boron worldwide consumption [9]. Beside these industries, boron is used in nuclear [14], steel [15], pharmaceutical [16], catalyst [17], hydrogen storage [18], concrete [19], textile [20], and military sectors [21]. Therefore, boron is classified as a strategic commodity in many countries, including U.S. and EU.

Indeed, boron is an essential nutrient for plant growth. It is used as fertilizer in agriculture at various concentrations depending on the variety of the plants. Hence, there are three categories of plants such as sensitive, semi-tolerant and tolerant plants which require 1 ppm, 4 ppm and 10 ppm of boron concentration in soils, respectively [22]. For instance, the sensitive plants include bean, cucumber, garlic, peanut, sesame, sugar cane, sunflower and wheat. The semi-tolerant plants are barley, cabbage, oats, mustard, cauliflower, tobacco and tomato, and the tolerant plants are cotton, asparagus and sorghum.

Boron's high hardness on the Mohs' scale and its high melting point provide good resistance to high temperatures, toughness, chemical resistance, and durability for a variety of materials including glasses, ceramics, metal alloys, concrete, and military materials. For instance, borosilicate glasses with 1−34 %wt of $B_2O_3$ are used in insulation, optical glasses in pharmaceutic, laboratory and kitchen materials as Pyrex. Boron-based plastics, aluminum and titanium are used in aircrafts, submarine and tanks. Boron carbide ($B_4C$) ceramics are employed in engines, mechanical seals, bearings, cutting tools, wheel dressing tools and blast nozzles [23]. Boron is also used to increase the shielding properties of concreates [19]. Boron nitride (BN) composite is used in steel production as a side-dam material for thin-strip casting as well as a break ring for horizontal continuous casting [15].

Borax is employed for detergent production because it allows to emulsify oil and greases, and reduces the surface tension of water, which favors loosening dirty particles [22]. Boric acid and sodium borates have a bactericidal action that inhibit gram-negative bacteria. Boric acid has been used for long as an eye wash as collyrium in pharmaceutical industry. Boron neutron capture therapy is employed in medicine for cancer treatment. Indeed, compounds such as the icosahedral anion ($^{10}B_{12}H_{11}SH)^{2-}$, which contain high $^{10}B$ content capable of attaching to tumorous tissue, are injected into cancer patients and subsequently exposed at a high-neutron source [16]. In addition, $^{10}B$ isotope is used as boric acid or zirconium diboride ($ZrB_2$) and

hafnium diboride ($HfB_2$) thin films in nuclear reactors to absorb thermal neutrons [14]. Boric acid is a buffer during the dyeing of nylon carpet in textile sector. Boron nitride nanotubes may potentially be used as hydrogen storage material [24]. Borophene can be used as electrocatalyst for carbon dioxide reduction [17].

The international boron symposium Boron 2022, held in Istanbul between 5−7 October 2022, highlighted the importance of boron in military industry, *i.e.* bulletproof vest, optical and laser systems production, catalysts, electronics, *i.e.* superconductor and MR imaging system production, for hydrogen storage and to manufacturing lightweight building materials.

### 1.2.3 Boron processing

Boron recovery process strongly depends on factors such as the source, concentration and composition of the minerals. Boron brines are the most economical source for extracting boron, as boron is already dissolved in water, eliminating the need for energy-intensive crushing and grinding steps, as well as large quantities of chemicals required for leaching as in the case with boron extraction from ores [25].

#### 1.2.3.1 Boron extraction from ores

The need for high-efficiency boron recovery, production of high-purity boron products, and cost-effective processes has led to the implementation of various technologies in the industry for processing boron specific for each deposit. In general, boron recovery from ores follows two steps: (i) mineral processing to produce a concentrate (crushing, grinding, washing, magnetic separation, electrostatic separation, calcination, centrifugation, flotation), and (ii) refining (leaching, filtration, crystallization and drying).

In 1994, boron processing plant was built in the Lerma Valley near Salta (Argentina) to produce boric acid from ulexite ores ($NaCa[B_5O_6(OH)_6]•5\ H_2O$) [26]. As shown in Figure 1. 1, the flowsheet of this plant involved crushing, grinding, washing, screening, leaching, decantation, filtration, crystallization, centrifugation and drying. First, the ore containing 22-25 %wt $B_2O_3$, 4−15 %wt Chloride, 1−6 %wt sulfate and 9−34 %wt insoluble acid, was first crushed, milled and washed.

Thereafter, the mineral was concentrated by hydrocyclone separation. Then, the concentrate containing 36−40 %wt $B_2O_3$, 0.2−0.9 %wt chloride, 0.4−0.7 %wt sulfate and 4−16% insoluble acid was batch leached with sulfuric acid at 60−80 °C. After dissolution, the liquid was separated from the residual slurry in a settler. Then, the residual slurry fed a steam-heated

settler, and the clear liquid was withdrawn. The solid was removed from the settler, filtered, washed, repulped and sent to a tailings pond. The liquid from the settlers and the filtrates fed agitated batch crystallizers where cooling water circulated through internal cooling coils. After crystallization, the liquid was removed by centrifugation and partially recycled to the leach tank. The boric acid crystals were then repulped, washed, and dried in a parallel flow hot-air rotary dryer. The product was kept below 95 °C to prevent dehydration to metaboric acid ($HBO_2$). The bleed steam from the end liquid allowed removing $Na_2SO_4$ formed during leaching, along with NaCl and $Na_2SO_4$ present in the ore. The extraction efficiency reached 78−87% $B_2O_3$ and 500 tons per month of boric acid were produced.

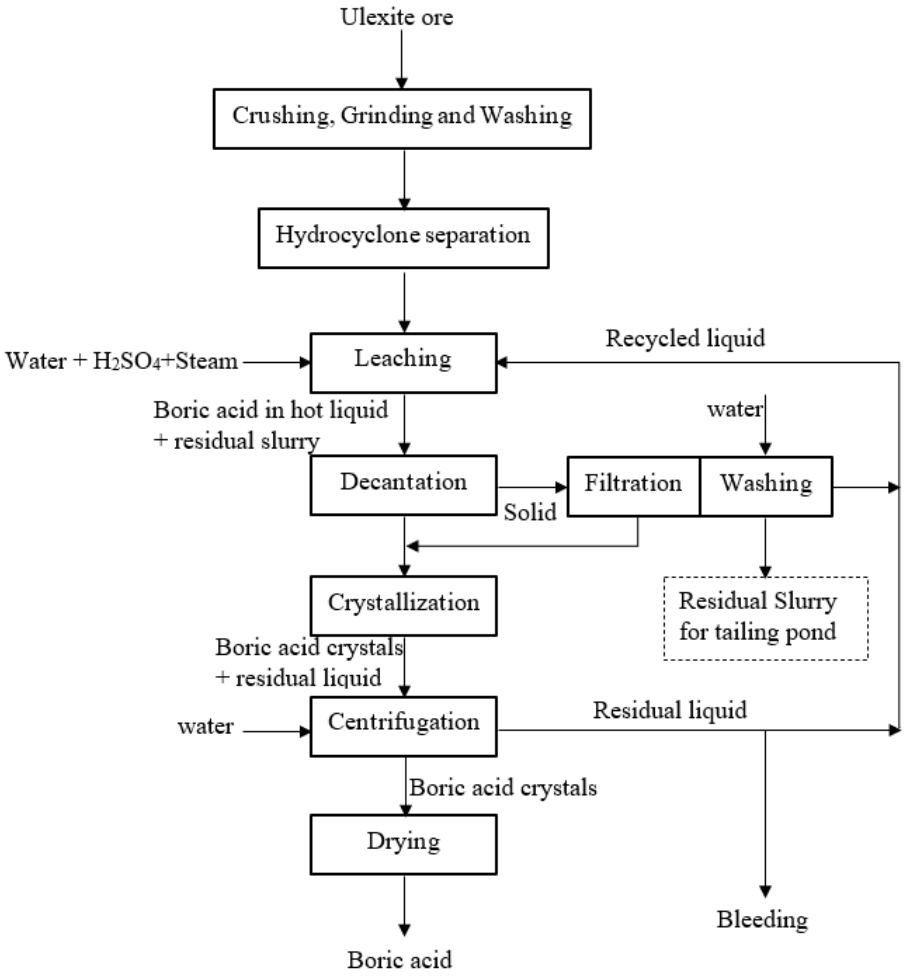



**Figure 1. 1:** Flowsheet for boron extraction from ulexite ores in the Lerma Valley near Salta (Argentina) [26].

### 1.2.3.2 Boron extraction from brines

As for ores, flowsheets to extract boron from brines depend on the composition and the concentration of the species in the brines. Several unit operations were implemented for boron recovery from salar, salt lake and geothermal brines including evaporation, carbonation, ion exchange, and solvent extraction but also crystallization, filtration, centrifugation, dehydration, calcination and drying [26].

Many papers investigated adsorption ([27], [28], [29], [30], [31], [32]), ion exchange ([33], [34], [35], [36]), electrodialysis ([37], [38]), reverse osmosis ([39], [40]), chemical precipitation ([41], [42], [43]) and solvent extraction [44] to recover boron from low or high concentrated brines. Each technology shows limits depending on the nature of the brine. For instance, electrodialysis, ion exchange and chemical precipitation are not highly selective towards boron ([45], [46]) when brines contain many impurities. Adsorption requires many stages and consumes an important amount of fresh water [47]. Reverse osmosis is an expensive technology that suffers from membrane ageing, especially when highly saline brines are processed. Solvent extraction suffers from extraction solvent loss when boron is processed from very low saline water. In addition, extraction solvent with good stability, affordability, safety, and easy of regeneration are needed for eco-efficient and selective extraction.

Nowadays, solvent extraction is a mature operation used for the extraction of several metals including zinc, cobalt, zirconium, molybdenum, nickel, vanadium, platinum, tungsten, copper, and rhenium. It is also employed for non-metal extraction such as boron.

### 1.2.3.3 Solvent extraction

#### 1.2.3.3.1 Principle of solvent extraction

The extraction technique designed by the International Union of Pure and Applied Chemistry (IUPAC) as liquid-liquid extraction (LLE) [48], more commonly called solvent extraction (SX), is a mature technology used in hydrometallurgy ([49], [50], [51]) to recover many valuable metals including boron from aqueous solutions. SX refers to a distribution of a solute between an immiscible organic phase, which is the extraction solvent, and an aqueous phase after mixing. In the case of mineral recovery from ores, solvent extraction occurs after mineral beneficiation and leaching, unlike in brines.

As illustrated in Figure 1. 2, solvent extraction involves three main steps. These include extraction of the solute from the aqueous phase, scrubbing of the organic phase in order to remove co-extracted impurities, and stripping of the solute from the loaded extraction solvent.

This allows for the recovery of the target solute for further post-treatments such as precipitation, crystallization or electrometallurgy. In solvent extraction, the extraction solvent is reused for further extraction after stripping and the solute-depleted aqueous phase can be reinjected somewhere in the hydrometallurgical process to save water. The configuration of SX flowsheet depends mainly on the physicochemistry of the aqueous phase. Sometimes, scrubbing and regeneration of the extraction solvent are not performed. Nevertheless, all these steps cover most of solvent extraction processes.

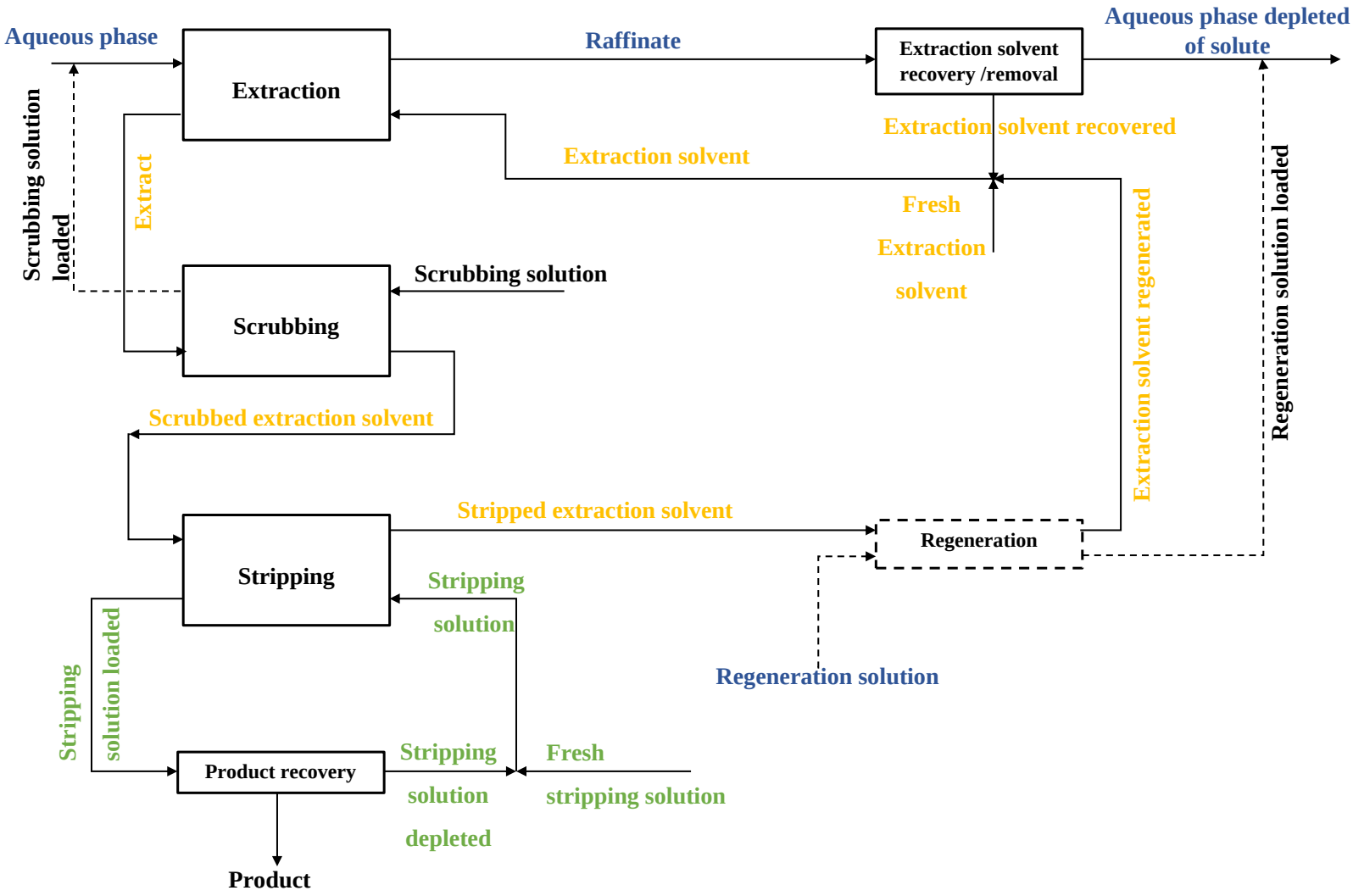



**Figure 1. 2:** General flowsheet for solvent extraction (SX).

In industry, solvent extraction (SX) is a continuous process performed in equipment such as mixers-settlers, centrifuge extractors or gravitational columns. In most cases, mixers-settlers are used since it is efficient, easy to perform and control. Figure 1. 3 shows configuration of 2 mixers-settlers.

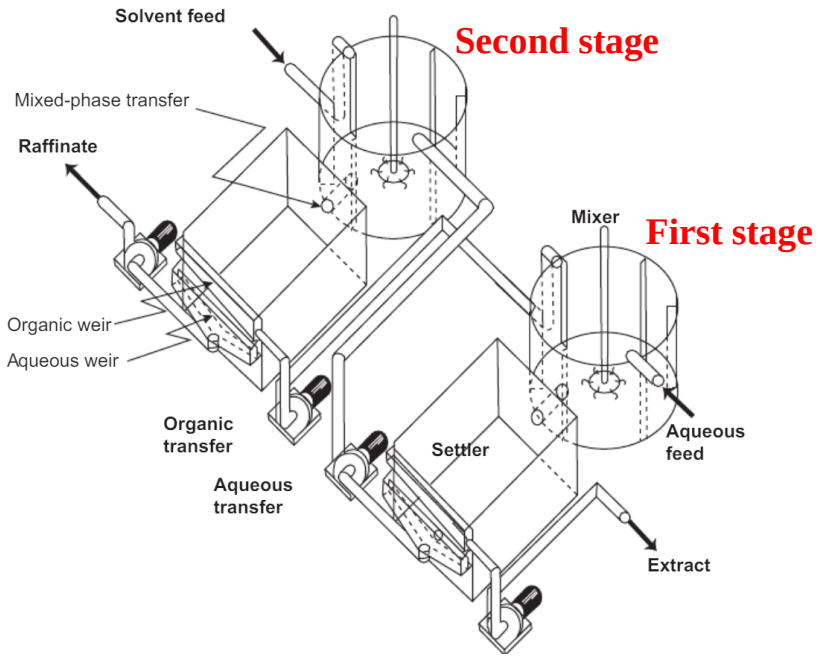



**Figure 1. 3:** Scheme of mixers-settlers configuration from Kislik. [51].

First, the extraction solvent and the aqueous phase containing the valuable solute feed the mixers in countercurrent where the two phases are mixed with propellers or impellers in tanks. The fresh aqueous phase feeds the first stage, where it is mixed with partially loaded extraction solvent from the second stage. Then, the mixed phases are separated in the settler under gravity. They feed gently the settler which is a relatively large and shallow tank. The heavy phase, *i.e.* the aqueous phase, remains at the bottom while the light phase, *i.e.* the organic phase, is at the top of the tank. The fully loaded extraction solvent overflows an upper weir and passes to scrubbing and stripping stages. The raffinate from the first-stage underflows a lower weir and is pumped to the second stage, where it is mixed with the fresh extraction solvent. In most cases, several stages are needed to remove the solute from the aqueous phase and strip the solute from the loaded extraction solvent.

The chemical potentials of a solute S in an aqueous phase and an organic phase is defined as:

$$\mu_S = \mu_S^0 + RT\ln(a_S) \qquad (1.\ 1)$$

$$\mu_S^0 + RT\ln(a_S) = \mu_{\bar{S}}^0 + RT\ln(a_{\bar{S}}) \quad (1.\ 2)$$

where and $\mu_s^0$is the standard chemical potential of S, $a_S$ and $a_{\bar{S}}$ are the activities of the solute S in the aqueous and the organic phase, respectively, R is the gas constant, and T is the temperature.

After mixing the two immiscible phases (organic and aqueous phase) and after settling, the chemical potentials defined in Equations (1. 1) and (1. 2) are equal at the equilibrium and the following equation can be deduced:

$$K_{D,S}^0 = \frac{a_{\bar{S}}}{a_S} = e^{\left(\frac{\Delta\mu^0}{RT}\right)} \quad (1.\ 3)$$

where $\Delta\mu^0 = \mu_S^0 - \mu_{\bar{S}}^0$

Therefore, the activity ratio of the solute between the organic and the aqueous phase remains constant at constant temperature. However, this constant is not easily calculated since such calculations need to calculate the activity coefficients of the solute in the organic phase and in the aqueous phase. There are several models to calculate activity coefficients in aqueous phases but only a few in organic phases.

Instead of using the thermodynamic constant $K_{D,S}^0$ , hydrometallurgists determine the distribution ratio of a solute S defined as:

$$D_S = \frac{\overline{[S_t]}}{[S_t]} \quad (1.\ 4)$$

where $\overline{[S_t]}$ and $[S_t]$ are the total concentrations of the solute in the organic phase and in the aqueous phase at equilibrium, respectively (the subscript t denotes total).

Another important definition in solvent extraction is the extraction efficiency. The extraction efficiency of the solute S ($E_s$ (%)) is calculated as follows:

$$E_S(\%) = \frac{\overline{[S_t]} \times \bar{F}}{[S_t] \times F + \overline{\overline{[S_t]}} \times \bar{F}} \times 100 \quad (1.\ 5)$$

where $\overline{[S_t]}$ and $[S_t]$ are the total concentrations of the solute S in the organic phase and in the aqueous phase at equilibrium, respectively. $\bar{F}$ and F denote the volume flowrates of the organic and the aqueous phases (or the volume of the organic and the aqueous phases), respectively.

By combining Equation 1. 4 and 1. 5, the extraction efficiency of the solute S can be rewritten as follows.

$$E_S(\%) = \frac{D_S \times \nu}{1 + D_S \times \nu} \times 100 \quad (1.6)$$

where $\nu = \bar{F}/F$ is the ratio between the organic phase volume flowrate and the aqueous phase volume flowrate. In batch processes $\nu = O/A$ is used with O and A stand for the organic and the aqueous phase volumes, respectively.

The selectivity coefficient ($S_{S_1/S_2}$) for solute $S_1$ towards solute $S_2$ is calculated as follows:

$$S_{S_1/S_2} = \frac{D_{S_1}}{D_{S_2}} \quad (1.7)$$

where $D_{S_1}$ and $D_{S_2}$ are the distribution ratios of solute 1 and solute 2, respectively.

The stripping efficiency of solute S ($SE_S$) is calculated as:

$$SE_S(\%) = \frac{[S]' \times F'}{\overline{[S]}' \times \bar{F}' + [S]' \times F'} \times 100 \quad (1.8)$$

$[S]'$ and $\overline{[S]}'$ are the solute concentrations in the stripping solution and in the organic phase at equilibrium during the stripping step. $\bar{F}'$ and $F'$represent the volume flowrates of the organic phase and the stripping solution, respectively.

#### 1.2.3.3.2 Solvent extraction conditions

The performance of an extraction solvent depends on the nature of the extractant and the diluent, as well as on the speciation of the metals and impurities in the aqueous phase, which depends on pH, redox and the composition of the aqueous phase. Furthermore, the ionic strength can change the extraction solvent performance since ionic strength acts on the activity coefficients of the species in solution.

Whatever the configuration of the contactor, *i.e.* the equipment in which extraction or stripping are performed, it is recommended that the aqueous phase be the dispersed phase and the organic phase be the continuous phase to improve the mass transfer. Therefore, good mixing of the two phases must provide better emulsion and enough interfacial tension (4−5 mN $m^{-1}$) to keep the aqueous phase well dispersed in order to avoid changes along the operation [51]. The extraction solvent contains the extractant, *i.e.* the molecule which extracts the solute, and the diluent, *i.e.* the organic phase in which the extractant is diluted by solvation.

The diluent should be able to reduce the viscosity of the extractant and must display a good thermal stability, *i.e.* high boiling point, low vapor pressure and high flash point. The diluent can be benzene, toluene, xylene, kerosene, sulfonated kerosene or chloroform. However, long

chains aliphatic diluents are preferred for safety reasons. Diluents with low dipole moment and low permittivity provide low solubility of the extraction solvent in water and low water solubility in the extraction solvent.

The extractant must display low solubility in the aqueous phase, high hydrophobic property and extraction efficiency, and most importantly a better selectivity for the target solute. In some cases, a co-extractant is used to improve the extraction efficiency. The co-extractant also improves the affinity between the extractant and the diluent. Sometimes, phase modifier is needed to prevent three phases formation, improve the separation and the solubility of the solute in the extraction solvent. The nature of the extractant employed is related on the nature of the target solute (anionic, cationic or neutral species). Chagnes. [52] reported four varieties of extractants including solvating and chelating extractants, and anionic and cationic exchangers, which are gathered in Table 1. 4. The first category of extractants, *i.e.* the solvating extractants, includes carbon-oxygen compounds (amides, ethers, ketones and alcohols), phosphorus-oxygen compounds (tri-*n*-butylphosphate (TBP)) and phosphine oxides (tri-*n*-octylphosphine oxide (TOPO)). They extract neutral solute by solvation. For instance, TBP is used for uranium (VI) or zirconium (IV) extraction in nitric acid medium as follows:

$$UO_2^{2+} + 2NO_3^- + 2\,\overline{TBP} \;\rightleftarrows\; \overline{UO_2(NO_3)_2(TBP)_2} \qquad (1.\,9)$$

where $\overline{TBP}$ and $\overline{UO_2(NO_3)_2(TBP)_2}$ are TBP in the organic phase and the uranium-TBP adduct extracted in the organic phase, respectively.

The chelating extractants contain hydroxyl and oxime groups. They are organic compounds containing a nitrogen atom linked to a carbon atom by a double bond, and to a hydroxyl function. LIX (hydroxyoxime compounds) and Accorga (oxime compounds) are used for copper extraction. For instance, LIX 64 N extracts copper as follows:

$$Cu^{2+} + 2\,\overline{(LIX\,64N)} \;\rightleftarrows\; \overline{Cu(LIX\,64N)_2} + 2\,H^+ \qquad (1.\,10)$$

where $\overline{(LIX\,64N)}$ and $\overline{Cu(LIX\,64N)_2}$ are LIX 64N in the organic phase and the complex copper-LIX 64N extracted in the organic phase, respectively.

Anionic exchangers are primary, secondary, and tertiary aliphatic amines which extract anionic species. They include all classes of alkylammonium salts and quaternary ammonium salts. Alamine 336 is used for uranium (VI) extraction from sulfuric acid medium as follows:

$$UO_2(SO_4)_3^{4-} + 2\,\overline{((R_3NH)_2SO_4)} \;\rightleftarrows\; \overline{UO_2(SO_4)_3(R_3NH)_4} + 2SO_4^{2-} \qquad (1.\,11)$$

where $\overline{((R_3NH)_2SO_4)}$ and $\overline{UO_2(SO_4)_3(R_3NH)_4}$ are Alamine 336 in the organic phase and the ion-pair uranium-Alamine extracted in the organic phase, respectively.

The last category, *i.e.* the cationic exchangers, are protons donors organic acids. They include di(ethyl-2-hexyl) phosphoric acid (HDEHP), bis (2,2,4-trimethylpentyl) phosphinic acid (Cyanex 272), carboxylic acids, sulfonic acids and phosphoric acids. Zinc is extracted by HDEHP in sulfuric acid medium as follows:

$$Zn^{2+} + 2\,\overline{HDEHP} \;\rightleftarrows\; \overline{Zn(DEHP)_2} + 2H^{+} \qquad (1.\,12)$$

where $\overline{HDEHP}$ and $\overline{Zn(DEHP)_2}$are HDEHP in the organic phase and the complex zinc-HDEHP extracted in the organic phase, respectively.

Finally, the specifications for an extraction solvent are:

- High extraction efficiency and selectivity toward the target solute
- High extraction and diffusion kinetics
- High stability
- High regeneration capacity
- Low toxicity and low corrosivity
- Low solubility in the aqueous phase and in the stripping solution to avoid extraction solvent losses and eventual environment issues if no effluent treatment is implemented
- Moderate dynamic viscosity (2−3 mPa s) for easy phase separation.

**Table 1. 4:** Main extractants used in SX from Chagnes.[52].

| Extractant category | Commercial name | Chemical formulae | Aqueous phase medium | Species extracted |
|---|---|---|---|---|
| Solvating | TBP | tri(*n*-butyl)phosphate | $HNO_3$ | U, rare earths |
| | 2-ethyl-1-hexanol | 2-ethylhexan-1-ol | HCl, $H_2SO_4$ | B |
| solvating + cationic | TOPO + HDEHP | tri(*n*-octyl) phosphine oxide + HDEHP | $H_2SO_4$ | U |
| Chelating | LIX 64 N (LIX 63 + LIX 65 N) | hydroxyoxime + oxime de nonyl-5-hydroxyl-2 benzophenone oxime | $H_2SO_4$ – $NH_4OH$ | Cu |
| | KELEX 100 | hydroxyquinoleine | $NaAlO_2$ | Ga |
| Anionic exchanger | Alamine 336 – Adogen 364 – Hostarex | RN with R radical carbon | $H_2SO_4$ | U, V, Mo, W, Pt |
| | LA 1 or LA 2 | amberlite RNH | HCl | Ni, Co, U |
| | TOA | trioctylamine | $H_2SO_4$ | Mo, Re, W |
| | Adogen 381 | tri(isooctyl)amine | HCl | Co |
| Cationic exchanger | HDEHP | di(ethylhexyl) phosphoric acid | $H_2SO_4$ | U, Zn, Mo, V, Co, Ni |
| | HDEHP | di(ethylhexyl) phosphoric acid | HCl | Rare earths |
| | VERSATIC 911 or 10 | Carboxylic acid | $H_2SO_4$ | Co, Ni |

The nature of the stripping solution is depending on the type of solute and the nature of the extracted complex. The stripping solution can be sodium hydroxide, hydrochloric acid or deionized water. The stripping solution must exhibit high stripping efficiency for the target solute and contain less impurities since impurity in the stripping solution may reduce drastically the purity of the final product. Both extraction and stripping operations may be influenced by temperature and pH.

Besides the physicochemical parameters, implementing SX also involves investigations on the thermodynamic, kinetic, mass transfer, and the chemical equilibrium for better understanding of the whole process. In the past, a large range of extractants including ionic

liquids ([53], [54], [55], [56]), amine compounds ([57], [58]) and alcohols ([59], [60]) were tested to recover boron from aqueous solutions including brines. However, alcohols have shown better extraction efficiency due to their good affinity for boron species. Alcohols compounds are categorized as aliphatic alcohols such as mono alcohols and di-hydroxy alcohols (diols), and cyclic alcohols such as phenols [61].

### 1.2.3.4 Boron extraction by alcohols

Table 1. 5 gathers the main alcohols-based extraction solvents reported in the literature for boron extraction from various brines including synthetic brines and native brines concentrated by evaporation. The nature of the aqueous and organic phases, the extraction conditions and results are detailed in the following sections.

#### 1.2.3.4.1 Boron extraction by mono alcohols

Zhang et al. [62] investigated the use of 2-ethylhexan-1-ol (EH) diluted in sulfonated kerosene to extract boron from East Taijinaier salt lake brine (northwest China) depleted of potassium (see brine composition in Table 1. 6). The extraction and stripping stages were conducted with separating funnels for 5 min shaking, and the organic-aqueous phase mixtures were settled for 30 min. Three-stage countercurrent extraction and stripping were simulated at pH=2.38, 25 °C, volume ratio between the organic phase and the aqueous phase O/A=1 with 50% (vol.) 2-ethylhexan-1-ol in sulfonated kerosene, and deionized water, respectively. The initial concentration of boron in the brine was 2.48 g $L^{-1}$. The results showed high extraction efficiency of 99.5%, stripping efficiency of 97.8% and relative high purity of boron in the organic phase after extraction, *i.e.* purity=95.5%. The purity of boron in the organic phase was improved to 99.5% by scrubbing with water. However, 50% boron was lost during the scrubbing step.

It was reported that boron is extracted as boric acid from the aqueous phase by EH following Equation 1. 13.

$$H_3BO_3 + n\overline{ROH} \rightleftarrows \overline{H_3BO_3.nROH} \qquad (1.\ 13)$$

where ROH is the mono alcohol (EH) and n is the number of alcohol molecules.

To determine the number of alcohol molecules (n) involved in boron extraction, the following equations were used:

$$K = \frac{\overline{[H_3BO_3.nROH]}}{[H_3BO_3]\,\overline{[ROH]}^n} \quad (1.\ 14)$$

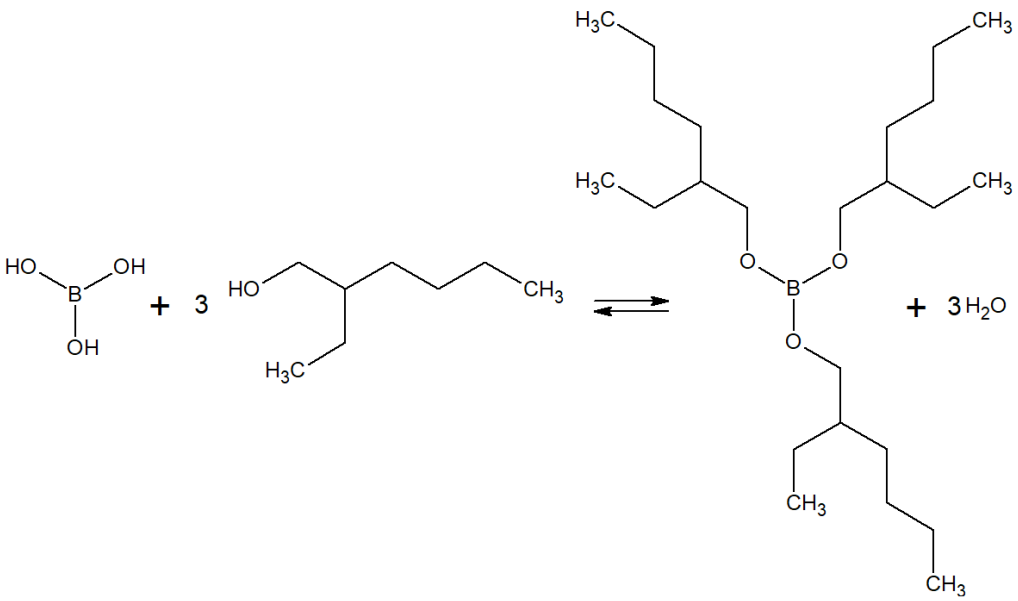
$$D = \frac{\overline{[H_3BO_3.nROH]}}{[H_3BO_3]} \quad (1.\ 15)$$

$$K = \frac{D}{\overline{[ROH]}^n} \quad (1.\ 16)$$

$$\log D = n \log\overline{[ROH]} + \log K \quad (1.\ 17)$$

First, as shown in Equation 1. 14, the equilibrium constant (K) was calculated as the ratio between the concentration of boron in the organic phase $\overline{[H_3BO_3.nROH]}$ at equilibrium and the concentration of boric acid in the aqueous phase $[H_3BO_3]$ at equilibrium multiplied by the concentration of alcohol in the organic phase ($\overline{[ROH]}$) at equilibrium. Second, the distribution ratio of boron (D) reported in Equation 1. 15 was calculated as the concentration of boron in the organic phase ($\overline{[H_3BO_3.nROH]}$) at equilibrium divided by the concentration of boron ($[H_3BO_3]$) in the aqueous phase at equilibrium. Third, the relationship between K and D was established as shown in Equation 1. 16. It is then possible to deduce a linear relationship between logD and $\log\overline{[ROH]}$ (Equation 1. 17).

The association constant between boric acid and 2-ethylhexanol (n=0.7) was determined experimentally by the slope analysis method, which consists in plotting the logarithm of the distribution ratio as a function of the logarithm of the concentration of free EH ($\overline{[ROH]}$) in the organic phase at equilibrium. In this study, the authors considered that their experimental condition allows to assume EH concentration at the equilibrium equal to EH concentration before extraction. Then, the equilibrium constant can be determined from the intercept. Due to the low value of the association constant (n=0.7), it was reported that boron is mainly extracted by solvation through hydrogen bonding and molecular interactions rather than esterification since esterification would have involved 3 equivalents of 2-ethylhexan-1-ol (n=3):




(1. 18)

It was reported that esterification may also occur but it was inferred that the kinetics is low.

In contrast, using the same extractant, *i.e.* 2-ethylhexan-1-ol, Guo et al. [63] found that boron is extracted as boric acid by esterification. The ester complex was identified by FTIR (Fourier Transform Infrared Spectroscopy) analysis and DFT (Density Functional Theory) calculations confirmed that esterification may occur from a thermodynamic perspective. The difference in the nature of the extracted complex (solvate or ester) may be attributed to the difference in brine composition, and more especially boron concentration. Zhang et al. [62] performed extraction from brine containing initially 2.48 g $L^{-1}$ boron while Guo et al. [63] worked with a brine containing 4.7 g $L^{-1}$ boron. Therefore, it can be inferred that boron extraction may be controlled by solvation in lower boron concentrated brines as reported by Zhang et al. [62].

**Table 1. 5:** Literature review on boron extraction by alcohols from different aqueous solution.

| Article | Boron sources and type of contactor | Extractant | Diluent | Co-extractant | Extraction mechanism ; volume Ratio (O/A) | Extraction efficiency (%), pH, and stage number | Stripping solution, efficiency (%) and stage |
|---|---|---|---|---|---|---|---|
| 1/Ran Zhang et al. 2016 [62] | Pretreated East Taijinaier Salt lake brine; Continuous extraction simulated with separation funnels | 2-ethylhexanol | Sulfonated kerosene | - | Solvation and esterification; 1/1 | 99.5; pH=2.38; 3 stages | $H_2O$; 97.8; 3 stages |
| 2/ Jie Guo et al. 2020 [63] | Brine concentrated by evaporation; Glass reactor | 2,2,4-trimethylpentane-1,3-diol (TMPD) | sulfonated kerosene | 2-ethylhexanol | Esterification ; 1/ 1 | 99.95; pH=1.55; 2 stages | NaOH; 99.99; 2 stages |
| 3/ Xiaowu Peng et al. 2018 [64] | Acidified west Taijinaier salt lake brine; Continuous extraction simulated with separation funnels | 2-butyloctan-1-ol | Sulfonated kerosene | - | Esterification; 1/1 | 99.35; pH=1.3; 3 stages | $H_2O$; 99.63; 3 stages |
| 4/Adam Balinski. 2021 [25] | Synthetic boric acid solution; Batch extraction in centrifuge tubes | n-octanol, 2-ethylhexan-1-ol, 2-butyloctan-1-ol, octan-2-ol and 3,7-dimethyloctan-3-ol | Sulfonated kerosene | - | Solvation and esterification; 2/1 | 7.4-41.2; pH=1.9-2.1; 1 stage | - |

| | | | | | | | |
|---|---|---|---|---|---|---|---|
| 5/ Xu el al. 2021 [45] | East Taijinaier Salt Lake brine concentrated by evaporation; Batch extraction in beakers | Isodecanol | Sulfonated kerosene | - | Esterification; 1/1 | 99.07; pH=3.5; 3 stage | $H_2O$; 98.71; 3 stages |
| 6/ Xuebing Fan et al. 2018 [65] | Underground brine concentrated by evaporation ; Continuous centrifugal extractor | 2-ethylhexane-1,3-diol(EHD) | sulfonated kerosene | - | Esterification; 1/1 | 98.46; pH=2-3; 5 stages | NaOH; 97; 5 stages |
| 7/ Mehmet Karakaplan et al.2004 [66] | Low salinity Synthetic brine; Jacketed glass tube | 2,2,5-trimethylhexane-1,3-diol | chloroform | - | Esterification; 1/1 | 96.8; pH=2; 1 stage | NaOH; 96.7; 1 stage |
| 8/ H. Hosgoren , Mehmet Karakaplan et al.1997 [60] | Low salinity Synthetic brine; Jacketed glass tube | 1,2-dihydroxy-4-oxadodecane (DHD) | - | n-amyl alcohol | Esterification; 1/1 | 87; pH=12.23; 1 stage | $H_2SO_4$ ; 79.2; 1 stage |
| 9/ Bilsen TURAL et al.2007 [67] | Low salinity Synthetic brine; Jacketed glass tube | 2,2,6-trimethylheptane-1,3-diol | kerosene | - | Esterification; 1/1 | 95.1; pH=2; 1 stage | NaOH; 97; 1stage |
| 10/ Ghaiath Almustafa et al. 2020 [68] | Synthetic boron solution; Centrifuge tubes | 1/ menthol + 2-methylpentane-2,4-diol (MPD) 2/ Thymol + MPD | - | - | Esterification; 1/1 mass ratio | 1/ 83.2; pH=5; 1 stage 2/ 90.1; pH=5;1 stage | 1/ NaOH;100 ; 1 stage 2/ NaOH; 95 ; 1 stage |

| | | | | | | | |
|---|---|---|---|---|---|---|---|
| 11/ Ghaiath Almustafa et al. 2021 [69] | Synthetic boron solution; Centrifuge tubes | Thymol +TMPD | - | - | Esterification; 1/1 mass ratio | 98; pH=2; 1 stage | NaOH; 100; 1 stage |
| 12/ P. AYERS et al.1981[59] | Wastewater/industrial effluents; Mixer-Settler | 2-ethylhexane-1,3-diol (EHD) and 2-chloro-4-(1,1,3,3-tetramethylbutyl)-6-methylol-phenol (CTMP) | - | - | Esterification; 1/1 | 95; pH=11; 1 stage | - |
| 13/ Michiaki Matsumoto and Kazuo Kondo.1997 [70] | Synthetized boron solution; Mixer-Settler (100 hrs operation) | 2-butyl-2-ethylpropane-l,3-diol (BEPD) | 2-ethylhexanol | - | Esterification; 1/1 | Depended on reaction time and extractant concentration; 2 stages | NaOH; 2 stages |

**Table 1. 6:** Composition, pH and density of (1) East Taijinaier salt lake brine (northwest China) depleted of potassium, (2) acidified West Taijinaier salt Lake brine and (3) East Taijinaier salt lake brine concentrated by evaporation.

| Brine | pH | Density (g $cm^{-3}$) | Concentration (g $L^{-1}$) | | | | | | | | | Reference |
|---|---|---|---|---|---|---|---|---|---|---|---|---|
| | | | Li | Ca | Mg | B | Na | K | Fe | $Cl^-$ | $SO_4^{2-}$ | |
| (1) | 2.38 | 1.3 | 6.7 | 0.06 | 93.9 | 2.48 | 1.44 | 0.68 | 0.097 | 300 | - | Zhang et al. [62] |
| (2) | 1.3 | 1.36 | 1.96 | - | 113.76 | 2.59 | 1.46 | - | - | 330.03 | 30.89 | Peng et al. [64] |
| (3) | 4.5 | 1.3 | 5.16 | - | 102.31 | 7.32 | 1.45 | - | - | 298.03 | 35.12 | Xu et al. [45] |

The thermodynamic properties, *i.e.* the change of Gibbs energy ($\Delta G$), enthalpy ($\Delta H$) and entropy ($\Delta S$), of boron extraction by EH in sulfonated kerosene reported in Table 1. 7 were determined by using the Van't Hoff equation:

$$\frac{d\,\ln K}{d\,\frac{1}{T}} = -\frac{\Delta H}{R} \qquad (1.\ 19)$$

where K is the equilibrium constant, T is the temperature, R is the universal gas constant and $\Delta H$ is the change of enthalpy.

From Equations 1. 17 and 1. 19, the relationship between the distribution ratio (D) and the change of enthalpy is as follows:

$$\log D = -\frac{\Delta H}{2.303\ RT} + n.\log[\overline{ROH}] \qquad (1.\ 20)$$

At constant concentration of EH ($[\overline{ROH}]$), the linear relationship logD vs. 1/T allows to determine the change in enthalpy of extraction ($\Delta H = -9.37\ kJ\ mol^{-1}$) from the slope. Therefore, boron extraction by EH is an exothermic reaction. The change of Gibbs energy ($\Delta G = -3.47\ kJ\ mol^{-1}K^{-1}$) and entropy ($\Delta S = -19.8\ J\ mol^{-1}$) were calculated as follows:

$$\Delta G = -RT\ \ln K \qquad (1.\ 21)$$

$$\Delta S = \frac{\Delta H - \Delta G}{T} \qquad (1.\ 22)$$

**Table 1. 7:** Thermodynamic properties of boron extraction by mono alcohols from (1) East Taijinaier salt lake brine (northwest China) depleted of potassium, (2) acidified West Taijinaier salt Lake brine and (3) East Taijinaier salt lake brine concentrated. SK: sulfonated kerosene.

| Brine | Alcohol | Diluent | Thermodynamic properties | | | Reference |
|---|---|---|---|---|---|---|
| | | | **$\Delta G$ (kJ mol$^{-1}$ K$^{-1}$)** | **$\Delta H$ (kJ mol$^{-1}$)** | **$\Delta S$ (J mol$^{-1}$)** | |
| (1) | EH | SK | −3.47 | −9.37 | −19.8 | Zhang et al. [62] |
| (2) | BOc | SK | −2.83 | −24.9 | −74 | Peng et al. [64] |
| (3) | Isodecanol | SK | −0.126 | −9.248 | −31.133 | Xu et al. [45] |

Peng et al. [64] investigated boron recovery from acidified West Taijinaier salt Lake brine (see brine composition in Table 1. 6) by using 2-butyloctan-1-ol dissolved in sulfonated kerosene. The initial concentration of boron in the brine was 2.59 g $L^{-1}$. Three-stage continuous countercurrent extraction and stripping simulated with separation funnels were performed. The organic and the aqueous phases were shaken in the separation funnels at 300 rpm for 15 min and settled for 30 min. Under these condition, the extraction and stripping efficiencies of boron reached 99.35% at 20 °C, pH=1.3 and O/A=1 by using 2 mol $L^{-1}$ 2-butyl-1-n-octanol, and 99.63% at 20 °C and O/A=1 by using deionized water, respectively. Finally, the purity of the stripping solution was relatively high (98% boron purity). The extracted complex was identified as an ester between 2-butyl-1-n-octanol and boric acid molecules by FTIR analysis. From Van't Hoff equation, the change of Gibbs energy ($\Delta G$), enthalpy ($\Delta H$) and entropy ($\Delta S$) were determined as $-2.83$ kJ $mol^{-1}K^{-1}$, $-24.9$ kJ $mol^{-1}$ and $-74$ J $mol^{-1}$, respectively.

Hejda and Jedináková ([71], [72]) addressed the extraction of boron as boric acid from synthetic radioactive wastes by solvent extraction using several neat aliphatic alcohols including *n*-octanol, *n*-hexanol, 2-octanol, 2-ethylhexanol and *n*-decanol. The ionic strength of the aqueous phase was 0.5 mol $kg^{-1}$. The extraction experiments were performed by contacting the organic phase and the aqueous phase during 5 min (aqueous phase: 0.2 mol $L^{-1}$ boric acid at pH 4.5, temperature: 25 °C). The highest distribution ratio of boron was obtained by using 2-ethylhexanol (distribution ratios were 0.224 for *n*-hexanol, 0.168 for *n*-octanol, 0.096 for 2-octanol, 0.367 for 2-ethylhexanol and 0.155 for *n*-decanol).

Recently, Balinski et al. [25] determined the extraction performances of boron by five mono alcohols, *i.e.* *n*-octanol, 2-ethylhexan-1-ol, 2-butyloctan-1-ol, 2-octanol and 3,7-dimethyl-3-octanol. They discussed the effect of the chemical structures of the alohols on the distribution ratios. All the extractants were diluted in kerosene so that the volume fraction of the alcohols in the extraction solvent ranged between 10% (vol.) and 100% (vol.). The experiments were performed in centrifuge tubes at pH=1.9−2.1 and 20 °C, and the aqueous phase contained initially 185 mmol $L^{-1}$ boric acid. The organic and the aqueous phases were contacted at phase volume ratio O/A=2, for two hours under stirring rate of 60 rpm. This study showed that the distribution ratio increases with increasing the volume fraction of the alcohols in the extraction solvent. In addition, 2-ethylhexan-1-ol exhibited the highest distribution ratio of boron (0.35) whereas alcohols with a steric hindrance around the hydroxyl groups such as 2-octanol and 3,7-dimethyl-3-octanol, exhibited the lowest distribution ratios (0.09 and 0.04, respectively). It was found that the extraction equilibrium involves the formation of species

which the ratio between boric acid and alcohol (ROH:$H_3BO_3$) is 1:2, as shown in Equation 1. 23.

$$2H_3BO_3 + \overline{ROH} \rightleftarrows 2\overline{H_3BO_3.ROH} \quad (1.\ 23)$$

where ROH is the mono alcohol and $2H_3BO_3.ROH$ is the extracted complex.

From the extraction equilibrium, the authors stated that solvation and esterification could occur between boric acid and the alcohol molecules. They also studied the effect of the ionic strength on the distribution ratio of boron between the organic phase containing 70% (vol.) 2-ethylhexan-1-ol diluted in kerosene (equivalent to 4.46 mol $L^{-1}$ alcohol) and aqueous phase containing NaCl, $MgCl_2$, $Na_2SO_4$, $LiNO_3$ and LiCl at various concentrations at pH=1.9−2.1. It was found that the distribution ratio of boron increases with increasing the salts concentration. Furthermore, $MgCl_2$ led to the highest distribution ratio (6.2). Therefore, boron extraction was also depending on the salting-out effect. This may also be explained by the formation of magnesium borates species which are extractable complexes[73].

Xu et al.[45] investigated boron extraction from East Taijinaier salt lake brine concentrated by evaporation (see brine composition in Table 1. 6) by several mono alcohols (*n*-octanol, 6-methylheptanol, 2-ethylhexanol, 2-octanol, 3,5,5-trimethyl-1-hexanol, *n*-decanol, isodecanol, 2-propyl-1-heptanol and isotridecanol) . The brine containing 7.32 g $L^{-1}$ boron was contacted with 3 mol $L^{-1}$ of alcohol diluted in sulfonated kerosene. The extraction was carried out with beaker for 15 min stirring at O/A=2, 20 °C and pH=2. Isodecanol exhibited the highest extraction efficiency of boron (84.46%). Thus, isodecanol was selected to simulate continuous extraction and stripping experiments. At phase volume ratio O/A=1, 20 °C and pH=3.5, 2.5 mol $L^{-1}$ isodecanol extracted 99.07% boron and deionized water stripped 98.71% boron from the loaded organic phase in three-stage countercurrent extraction and stripping, respectively. FTIR spectra showed that the extracted species was an ester compounds. Van't Hoff equation was used to calculate the change of Gibbs energy of extraction $\Delta G = -0.126$ kJ $mol^{-1}K^{-1}$, the enthalpy of extraction $\Delta H = -9.248$ kJ $mol^{-1}$ and the entropy of extraction $\Delta S = -31.133$ J $mol^{-1}$ (Table 1. 7).

#### 1.2.3.4.2 Boron extraction by diols

Lü et al. [74] studied the kinetic of extraction of boric acid from Jinaier salt lake brine (see brine composition in Table 1. 8) in Qinghai province (China) using extraction solvent containing 2-ethylhexane-1,3-diol (EHD) diluted in toluene and a method called "single drop

technique" which consists in the extraction of solute from an aqueous phase contained in a glass vessel by adding the extraction solvent drop by drop (see more details of the extraction setup in the article of Lü et al. [74]).

**Table 1. 8:** Composition, pH and density of (1) the Jinaier salt lake brine (Qinghai province, China), (2) underground brine from Dazhou (China) and concentrated by evaporation, and (3) brine concentrated by evaporation.

| Brine | pH | Density (g $cm^{-3}$) | Concentration (g $L^{-1}$) | | | | | | | | | Reference |
|---|---|---|---|---|---|---|---|---|---|---|---|---|
| | | | Li | Ca | Mg | B | Na | K | Br | $Cl^-$ | $SO_4^{2-}$ | |
| (1) | - | 1.28 | - | - | 88.06 | 1.89 | - | - | - | 277.84 | 6.35 | Lü et al. [74] |
| (2) | - | - | 0.68 | 3.58 | 22.44 | 2.71 | 63.91 | 55.66 | 3.20 | 225.76 | 2.53 | Fan et al. [65] |
| (3) | 1.55 | 1.25 | 64.36 | - | 12.22 | 4.74 | 1.74 | 5.19 | - | 359.93 | - | Guo et al. [63] |

The extraction kinetic ($r$) at constant temperature was determined by using Equation 1. 24:

$$r = \frac{Vd\overline{[H_3BO_3]}}{Sdt} \quad (1.\ 24)$$

where $\overline{[H_3BO_3]}$ is boric acid concentration in the organic phase and $t$ is the extraction time. $V$ and $S$ are the volume of the organic phase drop and its surface area, respectively.

Extraction kinetic of 1253.3 mol $m^{-2}$ $s^{-1}$ was observed when 0.1748 mol $L^{-1}$ boric acid was contacted with the organic phase containing 0.9205 mol $L^{-1}$ EHD (pH=1, 45 °C).

The following extraction kinetics ($r$) can be expressed by using the extraction equilibrium reported in Equation 1. 26 :

$$r = k\,[H_3BO_3]^a\overline{[R(OH)_2]}^b \quad (1.\ 25)$$

$$aH_3BO_3 + b\overline{R(OH)_2} \rightleftarrows \overline{aH_3BO_3.bR(OH)_2} \quad (1.\ 26)$$

where($\overline{[R(OH)_2]}$) is EHD concentration in the organic phase, $a$ and $b$ are the reaction orders with respect to boric acid concentration ($[H_3BO_3]$) and alcohol concentration ($\overline{[R(OH)_2]}$). $k$ is the kinetic constant.

The extraction kinetic increased with increasing boric acid concentration, EHD concentration and temperature as depicted in Equation 1. 25. The influence of the temperature on the extraction kinetic is shown by the Arrhenius equation:

$$k = A\, e^{\frac{-E_a}{R\,T}} \quad (1.\ 27)$$

Equation 1. 27 can be rewritten as follows:

$$ln\ k = ln\ A - \frac{E_a}{\mathrm{R\,T}} \quad (1.\ 28)$$

where *k* is the kinetic constant and *A* is a constant. R and T are the universal gas constant and temperature, respectively. $E_a$ is the activation energy.

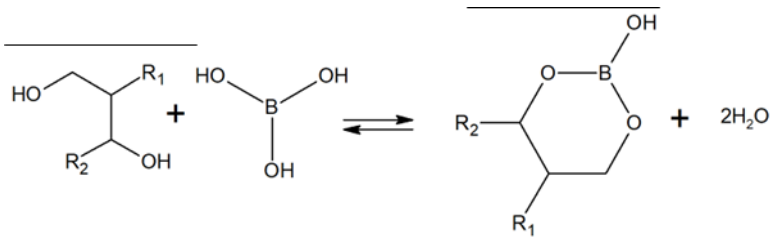
Equation 1. 25 can be rewritten as follows:

$$\log r = a\ log[\mathrm{H_3BO_3}] + \log\left(k\overline{[\mathrm{R(OH)_2}]}^{b}\right) \quad (1.\ 29)$$

*a* was determined experimentally by plotting log *r* as a function of $\log([\mathrm{H_3BO_3}])$ at constant $\overline{[\mathrm{R(OH)_2}]}$ and *b* was determined by plotting log *r* as a function of $\log \overline{[\mathrm{R(OH)_2}]}$ at constant $[\mathrm{H_3BO_3}]$. Then, *k* was be determined from Equation 1. 25 using *a* and *b.*

At 45 °C, *k*, *a* and *b* were determined as $9.085\times 10^{-3}$ $L^2$ $mol^{-1}$ $m^{-2}$ $s^{-1}$, 1.106 and 0.995, respectively. Therefore, the extraction is first-order with respect to EHD and boric acid, *i.e.* the extraction involves one equivalent molecule of boric acid and EHD.

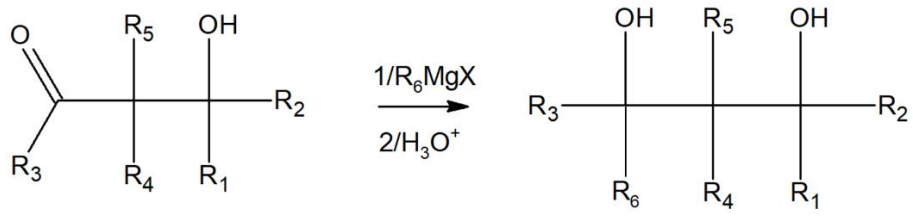
More recently, Fan et al. [65] carried out boron extraction by 2-ethylhexane-1,3-diol (EHD) diluted in sulfonated kerosene from an underground brine, *i.e.* brine from Dazhou (China) concentrated by evaporation. The solvent extraction experiments were performed in a continuous centrifugal extractor. The initial boron concentration was 2.71 g $L^{-1}$ (see concentration of the other brine constituents in Table 1. 8). A five-stage extraction was needed with 30% (vol.) EHD +70% (vol.) sulfonated kerosene at O/A=0.5 and pH=2-3 to extract 98.46% boron. Moreover, five stages were necessary to strip 97% boron from the loaded organic phase with 1 mol $L^{-1}$ NaOH at O/A=1. FTIR spectra showed that boron was extracted by esterification involving one molecule of EHD and one molecule of boric acid as follows:




(1. 30)

where $R_1$ and $R_2$ are ethyl and propyl groups, respectively.

Karakaplan et al. [75] conducted the first studies on boron extraction by using primary, secondary and tertiary diols. The following Grignard reaction was implemented to synthetize the alcohols (see the first nine alcohols gathered in Table 1. 9):




(1. 31)

where $R_1$, $R_2$, $R_3$, $R_4$ and $R_5$ are $CH_3$ or H. $R_6MgX$ is the Grignard reagent with $R_6$ refers to octyl or benzyl group, and X is halogen.

The authors reported that boron was extracted from the aqueous phase as boric acid by esterification. The extraction tests were performed with a jacketed glass tube at 25±0.1 °C by contacting a synthetic aqueous solution at pH=2 containing 0.01 mol $L^{-1}$ boric acid, 0.49 mol $L^{-1}$ sodium chloride and 0.01 mol $L^{-1}$ hydrochloric acid (ionic strength I=0.5 mol $L^{-1}$). The extraction solvents contained 0.5 mol $L^{-1}$ diols diluted in chloroform. The volume ratio between the organic phase and the aqueous phase (O/A) was 1 and the mixtures were stirred at 1300 rpm for 15 min and separated by gravity for 30 min. The distribution ratios and the extraction efficiencies of boron for all alcohols are reported in Table 1. 9. Among the first nine alcohols, the highest extraction efficiency of boron (95.35%) was obtained by 2-methyl-3-benzylbutane-1,3-diol. Alcohols in the class of 3°−3° had the lowest extraction efficiency, *i.e.* extraction efficiencies between 26.49% and 30.93%, due to the high steric hindrance of the alkyl groups at the vicinity of the hydroxyl groups which prevent boric acid extraction. Therefore, the chemical structure of diols strongly influenced boron extraction. It was found that diols with low steric hindrance promoted boron extraction by stabilizing the boric acid-alcohol complex as illustrated in Equation 1. 30.

In order to improve aliphatic diols extraction efficiencies, Karakaplan et al. [66] led a second investigation with new diols synthetized with Grignard reagents containing small alkyl groups such as iso-propyl, iso-butyl and iso-pentyl (the new diols synthetized are the last nine alcohols gathered in Table 1. 9). The composition of the synthetic brine as well as the extraction conditions were similar to the first investigations conducted by Karakaplan et al. [75]. Diols in the classes of 1°–2°,1°–3° and 2°–3° at 0.5 mol $L^{-1}$ diluted in chloroform were used. It was found that alcohols with iso-butyl and iso-propyl alkyl groups in classes of 1°–2° and 1°–3° were the best extractants.

**Table 1. 9:** Distribution ratios and extraction efficiencies of boron for extraction solvents containing diols. Ionic strength I=0.5 mol $L^{-1}$; extraction conditions: pH=2, O/A=1 and 25 °C.

| N° | Diol | Alcohol class | Distribution ratio | Extraction efficiency (%) |
|---|---|---|---|---|
| 1 | 2-Benzylpentane-2,4-diol | 3°–3° | 0.448 | 30.93 |
| 2 | 2,4-Dimethyldodecane-2,4-diol | 3°–3° | 0.360 | 26.49 |
| 3 | 2-Benzylpentane-2,4-diol | 3°–2° | 4.807 | 82.78 |
| 4 | 1-Benzylbutane-1,3-diol | 2°–2° | 7.591 | 88.36 |
| 5 | Dodecane-2,4-diol | 2°–2° | 0.507 | 33.65 |
| 6 | 2-Methyl-3-benzylbutane-1,3-diol | 1°–3° | 20.50 | 95.35 |
| 7 | 2,2-Dimethyl-1-benzylpropane-1,3-diol | 1°–2° | 14.70 | 93.61 |
| 8 | 2,2-Dimethylundecane-1,3-diol | 1°–2° | 2.13 | 68.07 |
| 9 | Undecane-1,3-diol | 1°–2° | 2.68 | 72.82 |
| 10 | 4,5-Dimethylhexane-2,4-diol | 2°–3° | 6.1 | 85.9 |
| 11 | 4,6-Dimethylheptane-2,4-diol | 2°–3° | 2.48 | 71.2 |
| 12 | 4,7-Dimethyloctane-2,4-diol | 2°–3° | 2.2 | 68.8 |
| 13 | 2,2,4-Trimethylpentane-1,3-diol | 1°–2° | 31.7 | 96.9 |
| 14 | 2,2,5-Trimethylhexane-1,3-diol | 1°–2° | 30.3 | 96.8 |
| 15 | 2,2,6-Trimethylheptane-1,3-diol | 1°–2° | 10.7 | 91.4 |
| 16 | 2,3,4-Trimethylpentane-1,3-diol | 1°–3° | 25.7 | 96.3 |
| 17 | 2,3,5-Trimethylhexane-1,3-diol | 1°–3° | 25.6 | 96.2 |
| 18 | 2,3,6-Trimethylheptane-1,3-diol | 1°–3° | 18.2 | 94.8 |

These alcohols structures and classes created a neutral and stable ester complex with boric acid through the methyl and two germinal methyl groups at the 2-position of diols. Among the diols investigated, 2,2,4-trimethylpentane-1,3-diol (TMPD) and 2,2,5-trimethyhexane-1,3-diol (TMhD) displayed the highest extraction efficiencies, *i.e.* 96.9% and 96.8%, respectively. Because of the high carbon number of TMhD, TMhD-based extraction solvent was selected to investigate the effect of the diluents including toluene, chlorobenzene, 2-octanol and *n*-Amyl alcohol on boron extraction. TMhD in toluene exhibited the highest extraction efficiency

(92.1%) while the other diluents implied extraction efficiencies lower than 90%. However, chloroform still provided a better extraction efficiency (96.8%). The authors reported that chloroform can participate to the extraction by forming hydrogen bonds with TMhD as well as boric acid and the complex boric acid-TMhD.

Sodium hydroxide was used to strip boron from the loaded organic phase. Stripping efficiency of 96.7% was reached using 0.1 mol $L^{-1}$ sodium hydroxide. It was suggested that diols with carbon number between 8 and 10, and short alkyl groups provide highest extraction efficiency.

In order to reduce the operating cost of SX processes, it is of great importance to investigate the solubility of the alcohols into the aqueous phase. Indeed, the solubility must be as low as possible. Tural et al. [67] determined the solubility of diols in synthetic brine containing 0.01 mol $L^{-1}$ boric acid, 0.49 mol $L^{-1}$ sodium chloride and 0.01 mol $L^{-1}$ hydrochloric acid with ionic strength I=0.5 mol $L^{-1}$. The extraction conditions, *i.e.* pH, O/A and temperature, were similar to the first and second studies conducted prior by Karakaplan et al ([75], [66]). Table 1. 10 gathers the investigated alcohols, the extraction efficiencies of boron and the alcohols losses which increases when the solubility increases. The alcohol loss, $Alc_{loss}$ (%wt), is calculated as follows:

$$Alc_{loss}(\%) = \frac{S_{alc} \times V_{aq}}{\overline{M_{alc}}} \times 100 \quad (1.\ 32)$$

where $S_{alc}$ and $\overline{M_{alc}}$ are the solubility of alcohol in the aqueous phase and the initial mass of alcohol in the organic phase, respectively. $V_{aq}$ is the volume of the aqueous phase.

**Table 1. 10:** Boron extraction efficiencies and losses of 0.5 mol $L^{-1}$ diols diluted in chloroform. Aqueous solution containing: 0.01 mol $L^{-1}$ boric acid, 0.49 mol $L^{-1}$ NaCl and 0.01 mol $L^{-1}$ HCl, Ionic strength I=0.5 mol $L^{-1}$; extraction conditions: pH=2; O/A=1, 25 °C.

| Alcohol | Alcohol loss (%wt) | Boron extraction efficiency (%) |
|---|---|---|
| 2,2,4-trimethylpentane-1,3-diol | 3 | 96.9 |
| 2,3,4-trimethylpentane-1,3-diol | 3.2 | 96.3 |
| 2,2,5-trimethylhexane-1,3-diol | 0.55 | 96.8 |
| 2,3,5-trimethylhexane-1,3-diol | 0.77 | 96.2 |
| 2,2,6-trimethylheptane-1,3-diol | 0.33 | 91.4 |
| 2,3,6-trimethylheptane-1,3-diol | 0.45 | 94.8 |
| 1-benzyl-2,2-dimethylpropane-1,3-diol | 0.22 | 63.9 |
| 1-benzyl-1-methylpropane-1,3-diol | 0.66 | 75.5 |
| 2-ethylhexane-1,3-diol (EHD) | 4.18 | 96.2 |

Extraction solvent containing 2-ethylhexane-1,3-diol (EHD) exhibited the highest solubility since 4.18 %wt was lost in the aqueous phase while the lowest alcohol loss (0.22 %wt) was obtained by 1-benzyl-2,2-dimethylpropane-1,3-diol. However, 1-benzyl-2,2-dimethylpropane-1,3-diol exhibited the lowest extraction efficiency (63.9%). Among the studied diols, 2,2,6-trimethylheptane-1,3-diol (TMHD) showed relatively high extraction efficiency (91.4%) and low alcohol loss (0.33%). Thus, TMHD was used diluted in kerosene to investigate its ability to extract boron from the aqueous phase. The results showed that 95.1% boron was extracted by 0.5 mol $L^{-1}$ TMHD at O/A=1, pH=2 and 25 °C. The stripping efficiency reached 97% when 0.05 mol $L^{-1}$ NaOH was used at O/A=1.

Instead of single alcohol, Guo et al. [63] suggested a mixture of 2,2,4-trimethylpentane-1,3-diol (TMPD) and 2-ethylhexan-1-ol to enhance boron extraction efficiency. Therefore, 2-ethylhexan-1-ol was used as co-extractant. Boron extraction was carried out from brine concentrated by evaporation in two-stage countercurrent extraction with glass reactors for two hours stirring at 500 rpm. The extraction efficiency reached 99.95% at O/A=1, pH=1.55 and 25 °C when 0.68 mol $L^{-1}$ TMPD in 30% (vol.) 2-ethylhexanol and 70% (vol.) sulfonated kerosene were used as extraction solvent. Boron was stripped from the loaded organic phase by 0.2 mol $L^{-1}$ NaOH at O/A=0.5. The stripping efficiency reached 99.99% by implementing two stages. These results showed that alcohols mixtures are efficient for boron extraction from brines.

#### 1.2.3.4.3 Boron extraction by alcohol-based deep eutectic solvents

Despite their relative high viscosity, extraction solvents constituted by hydrogen bond acceptor (HBA) and hydrogen bond donor (HBD) compounds, called deep eutectic solvents (DES) could be an alternative to the classical extraction solvent composed of alcohols and aliphatic diluents. DES are prepared by heating two organic compounds (HBA and HBD) initially immiscible at room temperature. Then, the mixture HBA and HBD is cooled down at room temperature to get a miscible organic phase. Generally, HBA compounds used are thymol (Thy) or Menthol (Men) and HBD are aliphatic mono alcohols or diols. Hence, deep eutectic solvents have been used to assess the extraction capacity for boron from aqueous solutions.

Almustafa et al. [68] investigated the extraction of boron from synthetic solution by four DES, *i.e.* thymol (Thy) and Menthol (Men) as HBA, and 1-decanol (Dec) and 2-methylpentane-2,4-diol (MPD) as HBD [68]. First, the DES were synthetized, and their physical properties, *i.e.* density, viscosity and water content, chemical properties, *i.e.* eutectic composition, hydrophobicity, and thermal properties (melting point and decomposition temperature), were evaluated. Then, boron extraction was carried out using 2:1 molar ratio of Thy:MPD, Thy:Dec, Men:MPD and Men:Dec. The aqueous solution contained 100 mg $L^{-1}$ boron obtained by dissolution of boric acid in deionized water. The extraction experiments were studied by shaking the mixture for 15 min at 250 rpm with mechanical incubator shaker in centrifuge tubes containing equal mass of the organic and aqueous phases O/A (wt)=1. At pH=5 and 25 °C, the results showed that the highest boron extraction efficiency (90.1%) was obtained by Thy:MPD. The authors reported that extraction efficiency of boron increased with increasing $Na^+$ and $Cl^-$ ions concentration within the aqueous solution. FTIR spectra showed that boron may be extracted by esterification. Finally, boron was stripped from the loaded Thy:MPD by 0.2 mol $L^{-1}$ sodium hydroxide, 0.2 mol $L^{-1}$ hydrochloric acid and deionized water at 25 °C and O/A (wt)=1. Boron was totally stripped by sodium hydroxide while both deionized water and hydrochloric acid exhibited solely 20% of stripping efficiencies. Additionally, 0.1 mol $L^{-1}$ NaOH achieved relative high stripping efficiency (95%). All these results showed DES can extract boron efficiently. Therefore, the authors decided to study the influence of the chemical structure of the alcohol in the DES on boron extraction. In their recent study, Almustafa et al. [69] used 2,2,4-trimethylpentane-1,3-diol (TMPD) as HBD while keeping the same HBA. After preliminary experiments, Thy:TMPD-based DES at molar ratio 2:1 was selected for boron extraction from a synthetic solution containing 100 mg $L^{-1}$ boron. The extraction was conducted for two hours, at 300 rpm shaking, O/A(wt)=1 and 25 °C. The

influence of pH on the extraction efficiency was studied for pH ranging between 2 and 12. It was found that the extraction efficiency did not depend on pH and reached 98% at pH=2−8. The extracted complex was identified as ester compound by using FTIR and $^{1}H$ NMR spectra. However, the authors reported that boron extraction by TMPD-based DES may involve hydrogen bonding and molecular interactions.

#### 1.2.3.5 Boron extraction by alcohols in industry

Alcohols have been used in industries mainly for boron extraction from brines concentrated by solar evaporation. A significant co-extraction of impurities and extraction solvent loss can occur during boron extraction from these brines. Table 1. 11 gathers the extraction and stripping conditions of boron processing from brines concentrated by solar evaporation in three companies.

In 1998, the company Chemetall performed boron extraction from concentrated brine of the salar de Atacama (Chile) in lithium production plant [76]. Four mixers-settlers were implemented to extract boron at pH 2 by using 20% (vol.) isooctanol or 2-ethylhexan-1-ol diluted in kerosene. The pH of the brine was adjusted by adding hydrochloric acid and the volume ratio between the organic phase (O) and the aqueous phase (A) was O/A=4. Boron extraction efficiency reached 99% and the residual boron concentration was less than 2 mg $L^{-1}$, although 5−10% lithium was lost during boron extraction (see the brine composition before and after boron extraction in Table 1. 12). Thereafter, boron was stripped from the loaded extraction solvent with water or diluted sodium hydroxide by means of four mixers–settlers. However, the solubility of the extraction solvent in the brine and in the stripping solution were not mentioned.

**Table 1. 11:** (a) Extraction and (b) stripping conditions of boron in the processes developed by (1) Chemetall company in 1998, (2) Minsal company in 2002, and (3) Anon et al. in 1996 ($E_B$: boron extraction efficiency in %, $SE_B$: boron stripping efficiency in %).

(a)

| Process | Extractant | Diluent | T (°C) | O/A | $E_B$ (%) | pH | Stage | Brine | Li lost (%) |
|---|---|---|---|---|---|---|---|---|---|
| (1) Chemetall | Isooctanol or 2-ethylhexan-1-ol, 20% (vol) | Kerosene | - | 4 | 99.0 | 2 | 4 | Salar de Atacama concentrated | 5-10 |
| (2) Minsall | Isooctanol, 50% (vol) | Kerosene | 25 | 1 | 99.9 | 2 | 4 | Salar de Atacama concentrated | 10 |
| (3) Anon et al. | 2-chloro-4 (1,1,3,3)-tetramethylbutyl-6-methylol-phenol, 25% (vol) | Kerosene | 34 | 1.6 | 99.4 | 10 | 2 | Searles lake | - |

(b)

| Process | Stripping solution | T (°C) | O/A | $SE_B$ (%) | Stage |
|---|---|---|---|---|---|
| (1) Chemetall | Water | - | - | 100 | 4 |
| (2) Minsall | 0.02 mol $L^{-1}$ NaOH or water | - | 6 | 100 | 3 |
| (3) Anon et al. | 0.5 mol $L^{-1}$ $H_2SO_4$ | 38 | 1 | 100 | 5 |

**Table 1. 12:** Composition of the concentrated brine from salar de Atacama (1) before boron extraction and (2) after boron extraction under the operating conditions reported in Table 1. 13 for the Chemetall company.

| | Concentration (g $L^{-1}$) | | | | | | | |
|---|---|---|---|---|---|---|---|---|
| | **Li** | **Ca** | **Mg** | **B** | **Na** | **K** | **$Cl^-$** | **$SO_4^{2-}$** |
| (1) | 63 | 0.53 | 12.9 | 7.3 | 0.8 | 0.19 | 358.6 | 0.16 |
| (2) | 60.3 | 0.51 | 12.9 | 0.001 | 0.73 | 0.18 | 344.6 | 0.19 |

In 2002, boron was also extracted from concentrated brine containing 8 g $L^{-1}$ boron from the salar de Atacama (Chile) by the Minsal company [76]. The extraction was performed with 50% (vol.) isooctanol in kerosene at O/A=1 and 25 °C. The extraction efficiency of boron reached 99.9% by implementing four mixers-settlers but 10% lithium was lost [76]. The extraction solvent was regenerated in three stages with water or 0.02 mol $L^{-1}$ sodium hydroxide (NaOH) at phase volume ratio O/A=6. The solubility of the extraction solvent in the brine and in the stripping solution were 200 mg $L^{-1}$ and 2,000 mg $L^{-1}$, respectively.

In the flowsheet reported in Figure 1. 4, boron was recovered and valorized as boric acid from the Searles lake brine (California, USA, composition reported in Table 1. 13). The boron extraction plant was designed in 1996 to produce 150 tons per day of boric acid [26]. Boron processing started with boron extraction in two stages at 34 °C and O/A=1.6. The extraction efficiency of boron reached 99.4% by contacting the extraction solvent containing 25% (vol.) 2-chloro-4-(1,1,3,3)tetramethylbutyl-6-methylol-phenol diluted in kerosene (flowrate of the extraction solvent=12,100 L $min^{-1}$, flowrate of the native brine=7,380 L $min^{-1}$).

After extraction, the organic-aqueous phase mixture was sent to three lines of settlers where the two phases were separated. The solubility of the extraction solvent in the brine was 100 mg $L^{-1}$ (pH=8.9). The boron-depleted brine was sent to three parallel lines at 2,460 L $min^{-1}$ each, where the extraction solvent was removed as a froth or vapor in order to reduce the solvent solubility below 17 mg $L^{-1}$ as recommended by the government [26], before returning the boron-depleted brine to the lake. The extraction solvent recovered from the brine was collected and reused.

After extraction, 0.5 mol $L^{-1}$ sulfuric acid was used to strip boron at O/A=1 and 38 °C by using five mixers-settlers in countercurrent. After stripping, the extraction solvent was washed with water so that it could be reused. The plant consumed about 75,700 L per day of concentrated sulfuric acid. Furthermore, 15,100 L of alcohol and 22,700 L of kerosene were needed each week to makeup the extraction solvent.

The boron-loaded stripping solution contained 6.1%wt $H_3BO_3$, 2.8%wt $Na_2SO_4$, 5.2%wt $K_2SO_4$ as well as 10−15 mg $L^{-1}$ extraction solvent due to solubility losses. The stripping solution was first sent through an adsorption column, filled with activated carbon, to remove the extraction solvent.

The activated carbon was regenerated in six-tray furnace at 650−760 °C. The boron-loaded stripping solution without extraction solvent was sent to two hemispherically-domed evaporator-crystallizers where it was joined by recycle sulfuric acid solution and circulated through titanium heat-exchanger tubes at 72,000 L $min^{-1}$. Water was evaporated at 65 °C, and salt cake and glaserite ($K_3Na(SO_4)_2$) were crystallized. They were removed, settled, and dewatered in solid bowl centrifuge. After the first stage of evaporation-crystallization, the overflow was then cooled at 35 °C in the second crystallization stage (flowrate=83,300 L $min^{-1}$). Boric acid was crystallized, and the slurry withdrawn, settled, and dewatered in a four-stage pusher centrifuge. The solid was washed in two stages, and the overflow stripping solution

depleted of boron was returned to the circuit. The boric acid cake was dried in a gas-fired rotary dryer and pneumatically transported to a storage silo. The purity of boric acid was 99.9% and contained only 0.05% $SO_3$ and 0.029% Na.

**Table 1. 13:** Mineral composition of the Searles lake brine.

| Mineral | Content (%wt) |
|---|---|
| KCl | 3.5 |
| $Na_2CO_3$ | 6.5 |
| $Na_2B_4O_7$ | 1.55 |
| $Na_2B_2O_4$ | 0.75 |
| $Na_2SO_4$ | 6 |
| $Na_2S$ | 0.3 |
| $Na_3AsO_4$ | 0.05 |
| $Na_3PO_4$ | 0.1 |
| NaCl | 15.5 |
| $H_2O$ | 65.72 |
| $WO_3$ | 0.005 |
| Br | 0.071 |
| $Li_2O$ | 0.009 |
| I | 0.002 |
| F | 0.001 |

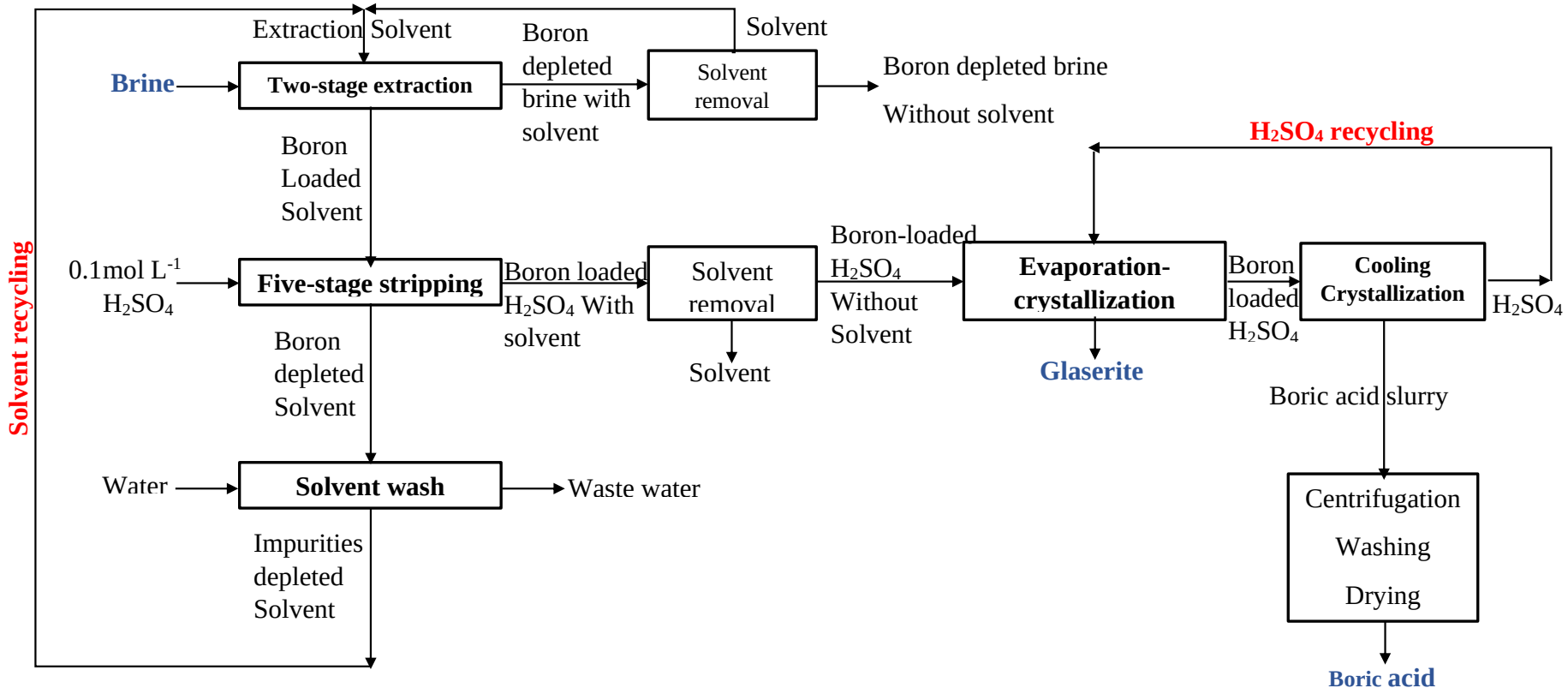



**Figure 1. 4:** Flowsheet implemented to extract glaserite and boron from the Searles lake brine in U.S. (adapted from Garrett) [26].

## 1.3 Literature review on lithium

### 1.3.1 Lithium sources, resources and geographic distribution

Lithium is rarely present as a native element in nature. It is always combined with other species that makes its recovery of critical importance. The two natural sources of lithium, *i.e.* ores and brines, show an irregular geological repartition that makes difficult to assess accurately the global lithium resources. According to the U.S. Geological Survey 2024 (USGS), the worldwide lithium resources are about 105 million tons [77]. As shown in Figure 1. 5, 25% of lithium comes from minerals ores and 75% of lithium is in brines [78]. The lithium resources are located in the five continents. Table 1. 14 shows that the richest lithium countries are Bolivia, Argentina, Chile, U.S., Australia and China, which have more than 6 million tons lithium resources.

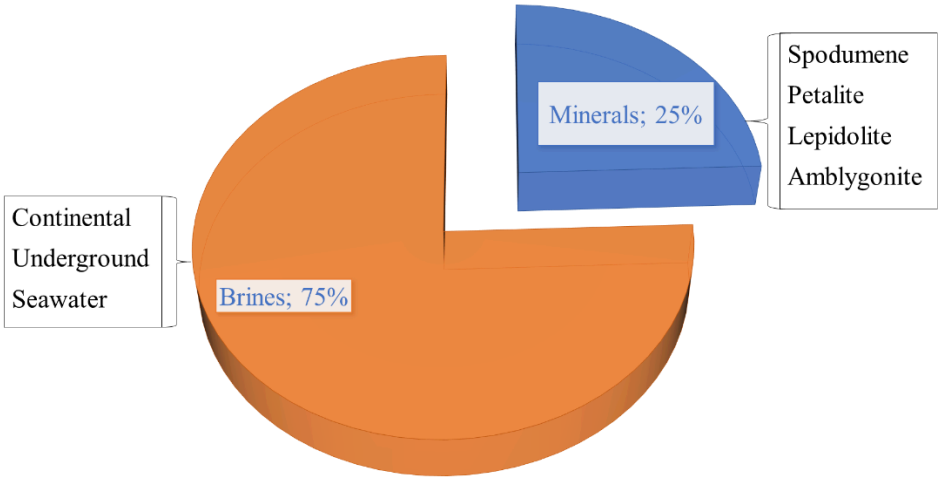



**Figure 1. 5:** Lithium occurrence.

Lithium content in earth's crust is estimated to be less than 100 ppm [79]. Several ores deposits called pegmatites contain lithium but not all are of interest from the commercial perspective because of their low lithium content. Lithium is found in spodumene, lepidolite, petalite and amblygonite minerals (Figure 1. 5) [78]. Spodumene is a stable lithium aluminum silicate ($LiAlSi_2O_6$), Lepidolite a lithium mica compound ($K(Li,Al)_3(Si,Al)_4O_{10}(F,OH)_3$), petalite a monoclinic lithium aluminum silicate ($LiAlSi_4O_{10}$) and amblygonite a fluorophosphate mineral ($LiAlPO_4(F,OH)$). Spodumene is the most important commercial minerals since about 80% of lithium is produced from this mineral [80].

In the other hand, brine is the most important resource of lithium. The brines deposits that contain lithium are classified in three groups: continental brine, underground brine including

geothermal and oil field brine, and seawater. Continental brine is the largest worldwide resource of lithium which represent approximately 59% of global resources. Salar and salt lake brines are categorized in continental brines. They are found in very dry regions at 1,300−4,300 m elevation in saline aquifer and their depth ranges between 15 and 1,400 m. Lithium concentration can reach up to 4,000 mg $L^{-1}$. Lithium in geothermal or oilfield can be extracted between 500 and 4,800 m under the sea where the lithium concentration ranges between 100 and 400 ppm. It is interesting to keep in mind that temperature in geothermal brines is quite higher than in continental or oilfield brines as the temperature can reach 100−400 °C [76]. Garrett et al. reported that seawater only contains about 0.17 mg $L^{-1}$ lithium [4].

According to Kesler et al., 70% of global lithium resources from brines are located in four countries: Argentina, Bolivia, Chile and China ([81], [82]). Argentina, Bolivia and Chile constitute the “Lithium Triangle” that produces about half of the global lithium supply. In China, lithium deposits are located in the lakes of Qinghai Province and the Tibet autonomous region in southwestern China.

**Table 1. 14:** World lithium resources in 2024 [77].

| Country | Resource (tons) |
|---|---|
| Bolivia | 23,000,000 |
| Argentina | 22,000,000 |
| US | 14,000,000 |
| Chile | 11,000,000 |
| Australia | 8,700,000 |
| China | 6,800,000 |
| Germany | 3,800,000 |
| Congo (kinshasa) | 3,000,000 |
| Canada | 3,000,000 |
| Mexico | 1,700,000 |
| Czechia | 1,300,000 |
| Serbia | 1,200,000 |
| Peru | 1,000,000 |
| Russia | 1,000,000 |
| Mali | 890,000 |
| Brazil | 800,000 |
| Zimbabwe | 690,000 |
| Spain | 320,000 |
| Portugal | 270,000 |
| Namibia | 230,000 |
| Ghana | 200,000 |
| Finland | 68,000 |
| Austria | 60,000 |
| Kazakhstan | 50,000 |
| **Total resources** | **105,000,000** |

### 1.3.2 Lithium market and applications in industry

Despite the heterogeneous distribution of lithium on earth, the global lithium resource is sufficient for industrial applications in the next decades. Lithium demand increases year after year with the development of new techniques for decarbonation. Lithium-based commercial products are mainly lithium carbonate, lithium hydroxide, lithium chloride and lithium metal as depicted in Figure 1. 6. Lithium carbonate ($Li_2CO_3$) is the largest lithium compound commercially produced, followed by lithium hydroxide (LiOH) since their global production reach 60% and 23%, respectively [79]. Lithium is extracted from brines and spodumene ores as lithium chloride and lithium sulfate, respectively. These lithium salts are then converted into

lithium carbonate or lithium hydroxide for various applications, and more especially lithium-ion batteries.

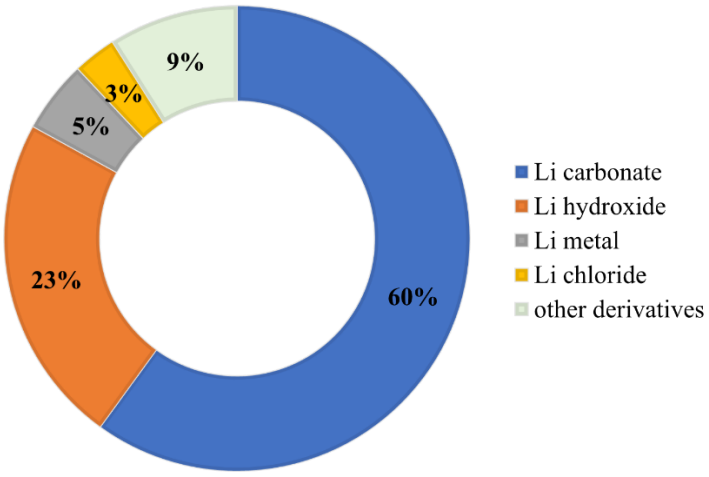



**Figure 1. 6:** Lithium-based commercial products [79].

These lithium products are used for several applications such as the industries of ceramic, glass, greases, lubricants, catalysts, and electronic industries. Lithium demand in electronic industry grows considerably with the increase demand of batteries for portable electronic devices, electric tools, electric vehicles (EVs) and grid storage applications. Indeed, it is known that electricity can be stored in underground surface facilities in the shape of compressed air or hydrogen ([83], [84]). However, these technologies are not suitable for small energy consumption while electricity storage in batteries is the most appropriate solution. Batteries require appropriate metals including lithium for high storage capacity since the energy density of lithium-ion batteries can reach 400 Wh $kg^{-1}$ [85]. Gruber et al. [86] reported that EVs production will climb to 50 million in 2050, which makes battery industries the first user of lithium given that 87% of lithium products are used for batteries production [77]. Batteries industry requires high purity lithium products. For instance, $Li_2CO_3$ with a purity of 99.5−99.95% is needed for lithium-ion batteries production.

Lithium price varies continuously depending on lithium supply and demand. According to the U.S. Geological Survey 2024 (USGS), lithium carbonate prices in China decreased from $76,000 per ton in January 2023 to about $23,000 per ton in November 2023; and lithium hydroxide prices decreased from $81,500 per ton in January 2023 to about $22,500 per ton in November 2023 due to the decrease in lithium demand [77]. Currently, *i.e.* July 2024, lithium carbonate price is about $12,600 per ton.

Global lithium consumption in 2023 was estimated to be 180,000 tons, a 27% increase from the consumption in 2022 [77]. According to Statista 2024 [87], global lithium demand increases gradually with an average of 19% per year (Figure 1. 7). In 2034, it is expected to reach 3.47 million tons of LCE (LCE stands for Lithium Carbonate Equivalent; 1 Li= 5.323 LCE [79]).

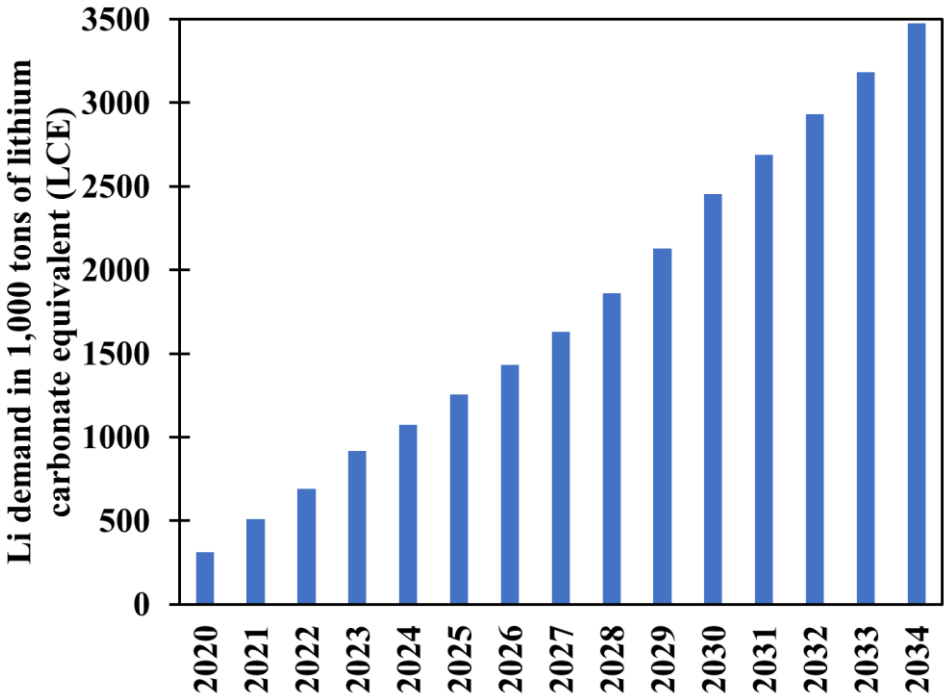



**Figure 1. 7:** Lithium demand from 2020 to 2034 according to Statista in 2024 [87].

## 1.3.3 Lithium processing

Lithium is mainly extracted from primary sources such as brines and ores. Currently, batteries recycling is becoming a new path to producing lithium. Various technologies are developed to recover lithium from these primary sources and the final lithium-based products obtained depend on both techniques and lithium containing source.

### 1.3.3.1 Lithium processing from ores

The composition of lithium ores depends on the origin of the spodumene deposits as shown in Table 1. 15. Many authors proposed general flowsheets for lithium ores extraction, assigned to industrial applications ([76], [88]). As shown in Figure 1. 8, after mineral processing of ores materials, the concentrate is processed by combining hydrometallurgy and pyrometallurgy routes. The pyrometallurgical process relies on minerals calcination or roasting while the hydrometallurgical process starts by minerals leaching with chemicals. Meng et al. [79] reported three processes relying on acid, alkaline and chlorination treatments. Usually, these

processes allows to extracting above 90% lithium ([89], [90]). The concentrated mineral is leached with sulfuric acid ($H_2SO_4$), and limestone or soda ash for acid and alkaline processes, respectively. Chlorination process uses hydrochloric acid, sodium chloride, calcium chloride, or chlorine gas. Among these leaching operations, only acid and alkaline leaching are implemented in industry. After leaching, the impurities can be removed by precipitation using lime as it was performed in 1940 by the company Lithium Corporation of America (Carolina, U.S.) [76]. Membranes technologies can be used to concentrate lithium before product recovery. Afterwards, lithium hydroxide (LiOH) or lithium chloride (LiCl) can be crystallized or processed by carbonation depending on their concentration in the aqueous phase. High concentrations of LiOH or LiCl avoid carbonation treatments.

**Table 1. 15:** Typical composition of spodumene deposits (minerals concentration in %wt) [76].

| **Deposit** | Greenbushes | Tanco | Wekesto |
|---|---|---|---|
| **Country** | Australia | Canada | Manitoba |
| **$Li_2O$** | **2.53** | **7.28** | **6.60** |
| **$K_2O$** | 1.50 | 0.15 | 1.50 |
| **$Na_2O$** | 2.57 | 0.15 | 0.27 |
| **$Al_2O_3$** | 13.94 | 26.00 | 26.70 |
| **$Fe_2O_3$** | 0.94 | 0.045 | 1.29 |
| **$SiO_2$** | 73.74 | - | 64.60 |
| **MgO** | 0.16 | - | 0.07 |
| **CaO** | 0.45 | - | 0.02 |
| **MnO** | - | 0.03 | 0.14 |
| **$Rb_2O$** | 0.32 | - | 0.24 |
| **$Cs_2O$** | 0.04 | - | 0.04 |
| **F** | - | 0.015 | 0.23 |
| **$P_2O_5$** | 0.20 | 0.20 | - |
| **$As_2O_3$** | 0.0079 | - | - |

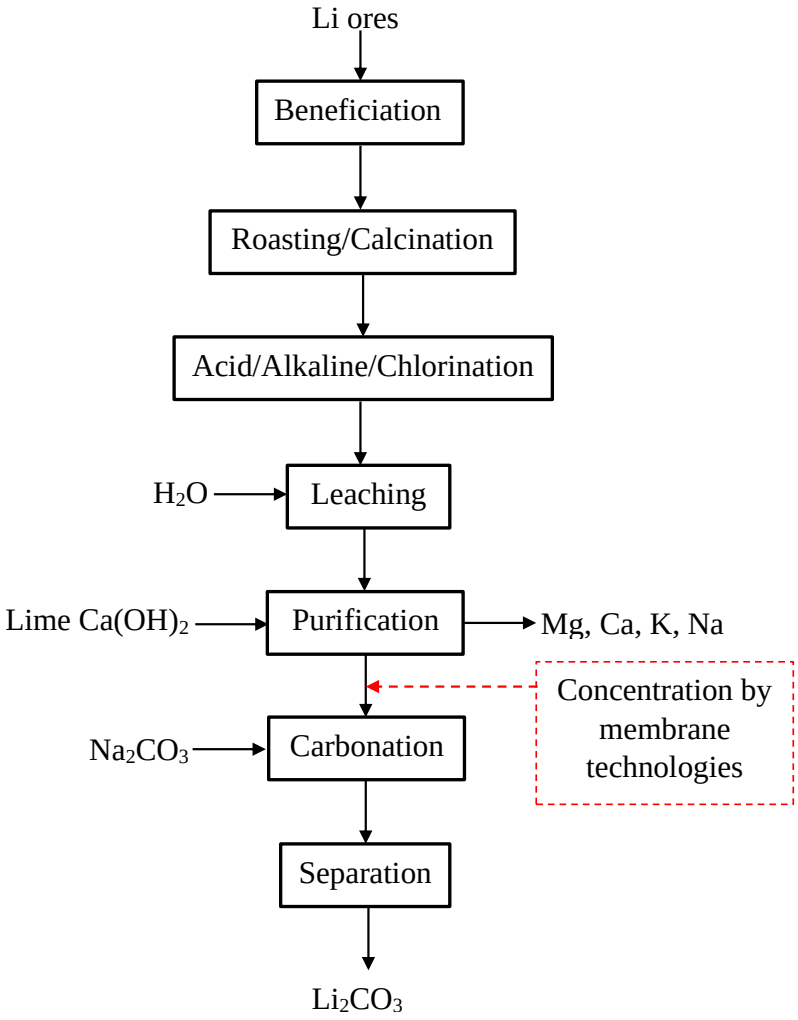



**Figure 1. 8:** General flowsheet of lithium carbonate production from ores.

### 1.3.3.2 Lithium processing from brines

Brines are highly saline aqueous solutions as they contain about 170-330 g of salts per liter [91]. Among brines, continental brines are the largest lithium resources with concentration up to 4,000 mg $L^{-1}$ [76]. In the past, many techniques were investigated to recover lithium from brines including precipitation [92], crystallization [93], solvent extraction ([94], [95], [96], [97], [98]), evaporation [99] and membrane technologies ([100], [101], [102], [103], [104], [105]). Nowadays, solar evaporation is the major technique implemented in the current lithium extraction plants. This process relying on water evaporation in large open air shallow ponds allows concentrating lithium and precipitating the impurities within the brines. It is sluggish and time consuming process since it requires between one year and two years [91]. Moreover,

500 $m^3$ of water per ton of lithium carbonate is lost by evaporation [106]. The majority of continental brine deposits are located in desert regions with low water resources. Therefore, the conventional processes of lithium extraction from brines based on solar evaporation must be changed by new suitable processes reducing the environment impact particularly water consumption and the processing time.

Irrespective of the process, *i.e.* conventional solar evaporation or new processes, lithium recovery from brines is challenging due to the high concentration of impurities. Indeed, lithium-rich continental brines contain sodium, calcium, magnesium, potassium, chloride, carbonate, sulfate, bicarbonate and boron at various concentrations as shown in Table 1. 16.

**Table 1. 16:** Average composition of lithium-containing brines with commercial value [76].

| Brine | Country | Composition (g $L^{-1}$) | | | | | | | | |
|---|---|---|---|---|---|---|---|---|---|---|
| | | Na | K | Mg | **Li** | Ca | Cl | $SO_4$ | **B** | $HCO_3$ |
| Salar de Atacama | Chile | 91.0 | 23.6 | 9.65 | **1.57** | 0.45 | 189.5 | 15.9 | **0.44** | 0.23 |
| Salar de Hombre Muerto | Argentina | 103.0 | 9.7 | 1.41 | **0.90** | 1.21 | 168.0 | 11.4 | **0.54** | 0 |
| Salar de Coipasa | Bolivia | 75.1 | 11.0 | 13.6 | **0.35** | 0.156 | 151.0 | 24.6 | **0.79** | 0.747 |
| Salar de Rincon | Argentina | 97.9 | 6.6 | 3.00 | **0.30** | 0.6 | 158.0 | 0 | **0.40** | 0 |
| Da Qaidam salt lake | China | 56.3 | 4.4 | 20.20 | **0.31** | 0.2 | 134.2 | 34.1 | **0** | 0.6 |

#### 1.3.3.2.1 Conventional processes

In the "Lithium Triangle" also known as Puna Plateau, four lithium facilities are implemented: two in the salar de Atacama (Chile), one in the salar de Hombre Muerto (Argentina) and one in the salar de Olaroz (Argentina). In China, brines from Zabayu lake and Dongtai salt lake are processed by two facilities while in USA one facility operates in Clayton valley (Nevada) ([107], [108]). These seven facilities use conventional processes mainly based on evaporative technology. The conventional processes are called lime soda evaporation processes since they involve several solar evaporation steps, and the use of lime and soda ash to precipitate impurities.

In the conventional process reported in Figure 1. 9, the brine is firstly concentrated in ponds by solar evaporation. Water evaporation is responsible for salt precipitation throughout the time according to the following order: halite (NaCl), sylvite (KCl) and sylvinite (NaCl•KCl). In brines containing high amount of magnesium such as those in salars de Atacama and Uyuni, carnallite ($KCl•MgCl_2•6H_2O$), lithium carnallite ($LiCl•MgCl_2•6H_2O$) or

bishoffite ($MgCl_2 \bullet 6H_2O$) precipitate when 40 g $L^{-1}$ lithium is reached ([109], [110]). As water evaporates and salts precipitate, lithium concentration reaches 60 g $L^{-1}$ within the brine. Lithium can then be precipitated as a solid containing impurities such as magnesium, calcium and boron as well as residual potassium and sodium. These impurities must be removed to produce high-grade lithium salts (99.5−99.99%), *i.e.* lithium carbonate, lithium hydroxide or lithium chloride.

Cations impurities can be recovered by precipitation, crystallization or carbonation using lime (CaO or $Ca(OH)_2$) and soda ash ($Na_2CO_3$). Moreover, lime is used for anions removal. Lime precipitates magnesium and sulfate as magnesium hydroxide ($Mg(OH)_2$) and gypsum ( $CaSO_4 \bullet 2H_2O$), respectively ([109], [111]):

$$MgCl_2 + Ca(OH)_2 \rightarrow Mg(OH)_{2\,(solid)} + CaCl_{2\,(aq)} \quad (1.\ 33)$$

$$Na_2SO_4 + Ca(OH)_2 + 2H_2O \rightarrow CaSO_4 \bullet 2H_2O_{(solid)} + 2NaOH_{\,(aq)} \quad (1.\ 34)$$

Then, boron is removed by solvent extraction after adjusting the pH of the brine with hydrochloric acid. Sodium carbonate is added to precipitate calcium and lithium at the end of the process as calcium carbonate and lithium carbonate, respectively:

$$CaCl_2 + Na_2CO_3 \rightarrow CaCO_{3\,(solid)} + 2NaCl_{(aq)} \quad (1.\ 35)$$

$$2LiCl + Na_2CO_3 \rightarrow Li_2CO_{3\,(solid)} + 2NaCl_{(aq)} \quad (1.\ 36)$$

Ion exchange resin, adsorption and membrane technologies such as electrodialysis can be implemented to reduce drastically impurity concentration and to concentrate lithium before carbonation [88]. After carbonation, the lithium-depleted brine is recycled. The general flowsheet of lithium carbonate production from brine is depicted in Figure 1. 9. The steps in this conventional process could change depending on the composition of the brine but still involves solar evaporation steps, and the use of lime and soda ash.

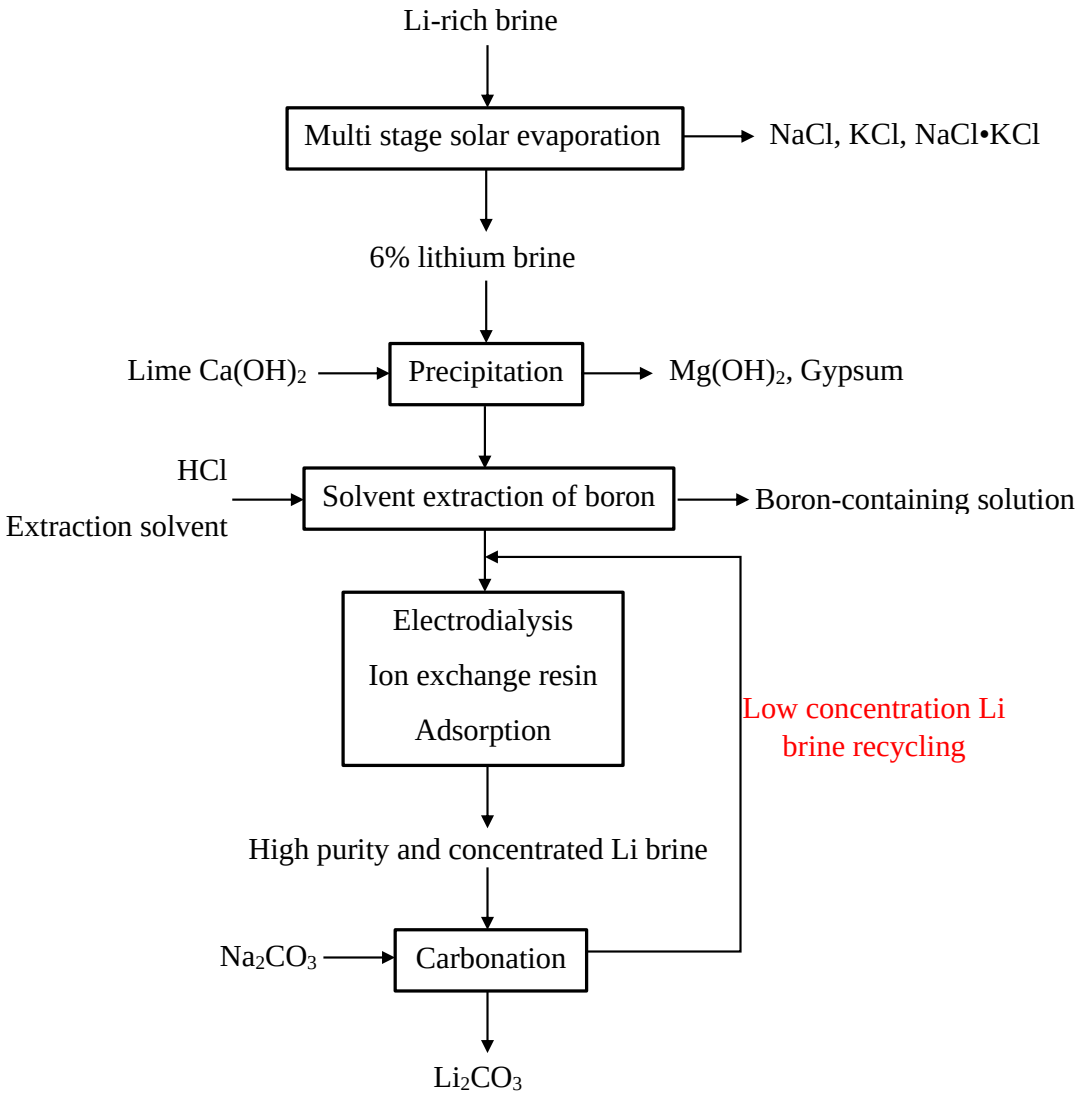



**Figure 1. 9:** General flowsheet for lithium carbonate production from brines. Flowsheet adapted from those reported by Chagnes [88], Meng el al. [79], Swain [78] and Choubey et al. [89].

Chemetall and Minsal companies process lithium from the salar de Atacama (Chile) brines using conventional processes. In 1984, the company Chemetall plant was built to produce 6,350 tons of lithium carbonate equivalent (LCE) per year by processing the brine whose composition is reported in Table 1. 16 [76]. The flowsheet in Figure 1. 10 shows the operations involved in this process. The process started by pumping the brine from underground reservoirs to open air ponds. Then, sodium, boron and sulfate were precipitated by calcium chloride as halite, boron salts and gypsum, respectively. These salts were harvested and placed in stockpiles. The brine was then concentrated by solar evaporation continuously in ponds. The solar evaporation system was constituted of 12 ponds expanded on 150 ha area. The brine was maintained at 25−40 cm depth in the ponds. The evaporation rate of water, the rainfall and the relative humidity were 3,000−3,300 mm per year, 10−25 mm per year and 10%, respectively, with a

moderate wind. Water evaporates and salts crystallized separately following this order: sylvinite, halite-carnallite and halite-bishoffite. Precipitation of sulfate was responsible for large recovery of these by-products. When lithium concentration reached 40 g $L^{-1}$, bischoffite and lithium carnallite precipitated together. Lithium could be recovered from that mixture by leaching, removing the impurities and crystallization or precipitation. At the end of the evaporation process, the brine depleted, magnesium, sodium, potassium and sulfate contained up to 40 g $L^{-1}$ lithium as saturated lithium chloride. It was stored in 0.7 ha floating cover reservoir to prevent further evaporation.

After evaporation, boron with concentration about 8,000 mg $L^{-1}$ was removed by solvent extraction. The brine was first acidified with hydrochloric acid to pH 2 and then contacted with 20% (vol) 2-ethylhexan-1-ol diluted in kerosene. Residual boron concentration of 5 mg $L^{-1}$ was obtained in the brine by performing four stages continuous countercurrent extraction with organic to aqueous phase volume ratio (O/A) 4. However, 5−10% lithium was lost. For the next extraction operations, the organic phase was recovered from the boron-loaded organic phase in four mixers-settlers with water as stripping solution.

Thereafter, the brine depleted of boron was treated with lime to precipitate more magnesium and sulfate. Then, the remaining magnesium and calcium were precipitated by sodium carbonate. The precipitates were recovered by settling and filtration. The brine concentrated in lithium was mixed with sodium carbonate to precipitate lithium as lithium carbonate. The slurry was settled and the lithium salt recovered by filtration. The solid was then dried at 130 °C−160 °C. Lithium carbonate with purity of 99.2−99.99% was obtained.

In 1996, the company Minsal processed lithium in their plant located at the salar de Carmen using the same process developed by the company Chemetall. The brine was processed from salar de Atacama and boron was co-valorized as boric acid. The plant produced 28,000 tons of LCE (purity=99.5%), 650,000 ton of potassium chloride (purity=95%) and 16,000 ton of boric acid per year.

In 2022, the two facilities in the salar de Atacama implemented by both Chemetall and Minsal produced together 121,190 tons of LCE. The Chemetall company also produced 6,000 tons of LCE in the Clayton Valley plant. In the salar de Hombre Muerto and the salar de Olaroz, 26,000 tons and 11,406 tons of LCE, respectively, were produced in 2022 [107].

In the current lithium plants, impurities precipitation requires a large amount of chemicals particularly lime and soda ash, which generates a lot of salts that are not valorized with

environment concern. Furthermore, 90% of the original water in the brines is lost by evaporation [107]. Fresh water is needed to dissolve lime and soda ash, and for extraction solvents recovery. Therefore, conventional processes need improvement to achieve sustainable lithium production.

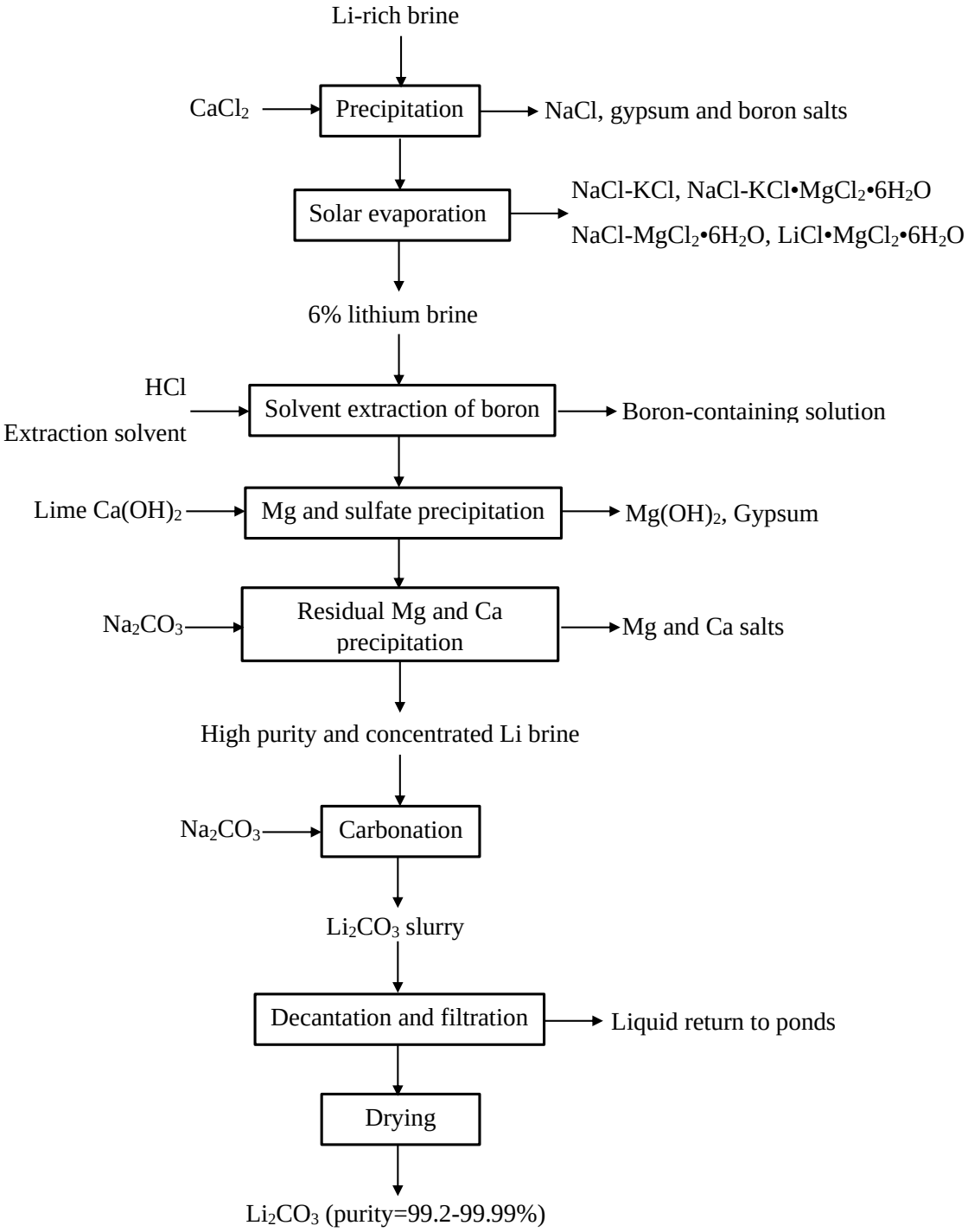



**Figure 1. 10:** Flowsheet of lithium carbonate production from salar de Atacama (Chile) by the company Chemetall in 1984 [76].

#### 1.3.3.2.2 New processes based on Direct Lithium Extraction

Conventional processes for lithium production consume too much water and impact dramatically the hydrogeology of the regions where the plants are located since around 500 $m^3$ of water is evaporated to produce one ton of lithium carbonate. Therefore, new processes have been recently developed to reduce impacts on water table and water consumption during lithium extraction and purification. These new processes bypass evaporative technology and rely on direct lithium extraction (DLE) using ion exchange resins and sorption materials but also implement solvent extraction and (electro)-membrane processes. A smart combination of these technologies makes faster the lithium recovery from brines than the conventional technologies. Some of these technologies are already at the demonstration stage as it is the case for those developed by the companies Eramet, Adionics, and Solvay-Tenova among others (Table 1. 17).

**Table 1. 17:** Several direct lithium extraction (DLE) processes.

| Company | Operations | Li extraction efficiency (%) | Lithium product and purity |
|---|---|---|---|
| Eramet | Adsorption, membrane technologies, evaporation and precipitation | 90 | $Li_2CO_3$ |
| Adionics | Solvent extraction | 98 | Concentrated LiCl solution (99%) |
| Solvay-Tenova | Solvent extraction | - | Lithium salts |

Eramet has developed a process for lithium extraction from the salar de Centenario in Salta province (Argentina) which has 10 million tons reserves of LCE. A 15,000 $m^2$ plant with a capacity of 24,000 tons LCE per year is building in Centenario to processing that brine. As shown in Figure 1. 11, the process involves several operations for direction lithium extraction. First, the brine feeds an adsorption column filled with a patented material very selective towards lithium [112]. The material extracts very selectively lithium with small amount of impurities. The brine depleted of lithium is returned in the salar while lithium is removed from the column with fresh water. Then, calcium, magnesium and sulfate impurities in the lithium-rich liquor are removed by nanofiltration. The brine is concentrated and lithium is concentrated by removing water by means of reverse osmosis and forced evaporation. Residual magnesium, calcium are removed by using ion-exchange resins and boron is extracted by solvent extraction Thereafter, lithium is precipitated as lithium carbonate (battery-grade) using sodium carbonate. That process allows to extract 90% of lithium from brine and to recycle 60% of water.

The technologies developed by Adionics and Solvay-Tenova rely on liquid-liquid extraction using Flionex® and CYANEX® 936, respectively. The very high selectivity of these extractants allows producing battery-grade lithium salts. The Adionics process allows extracting 98% lithium from 50 mg $L^{-1}$–50 g $L^{-1}$ lithium concentrated brines. In 2023, the plant successfully completed 1,500 hours of DLE tests from brines in the salar de Atacama.

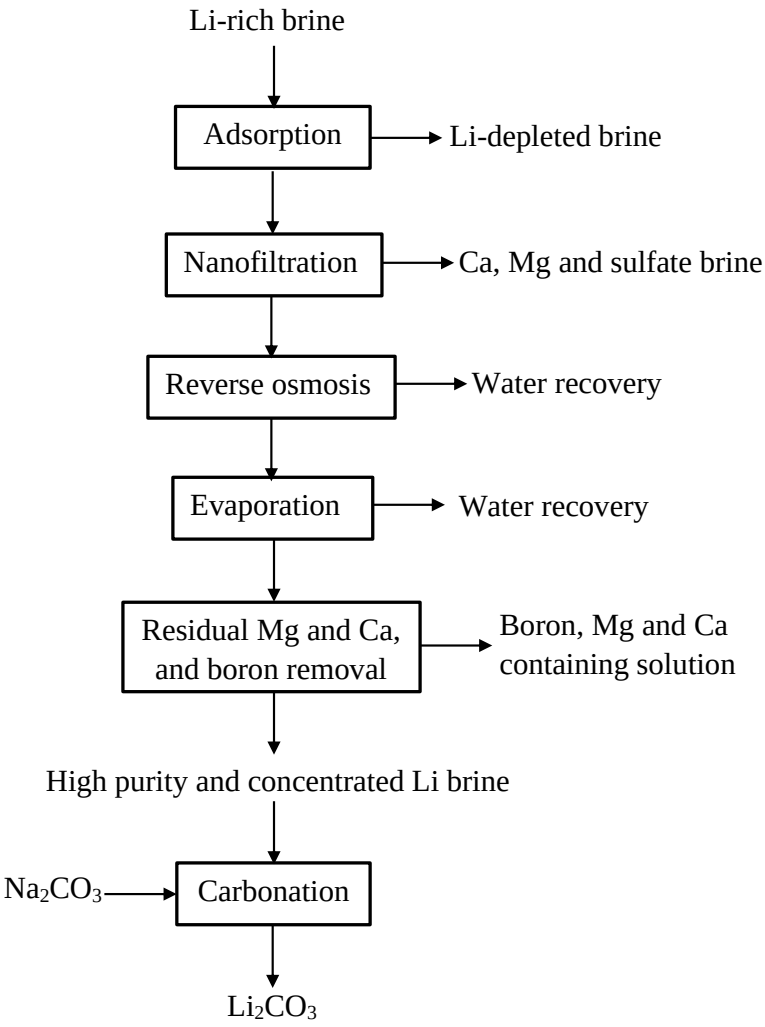



**Figure 1. 11:** Flowsheet of Eramet's process for lithium carbonate production from salar de Centenario (Argentina).

New lithium extraction processes expect to improve the extraction efficiency and the selectivity while reducing the water consumption and lowering the impact on the water table. However, there are still challenges to improve the processes so that their CAPEX, OPEX and their impact on the environment could be decreased. Many other DLE technologies are only developed at the lab scale such as the electrochemical lithium insertion process ([113], [114], [115]), adsorption ([116], [117], [118]), ion exchange ([119], [120], [121]), electrodialysis

([122], [123]), membrane processes ([104], [105]), and solvent extraction ([94], [95], [96], [97], [98], [124]). Electrodialysis process could be more attractive than adsorption, ion exchange and solvent extraction. Indeed, adsorption and ion exchange methods need a huge amount of eluent, usually fresh water, to regenerate the supports. Solvent extraction may suffer from extraction solvent loss which increases the OPEX since it would require makeup of the extraction solvent and the treatment of the aqueous solutions containing extraction solvent.

The demonstration plants previously described do not co-valorized the other minerals with lithium. For economic viewpoint magnesium, calcium, sodium, potassium and boron should be extracted for their valorization in industries. Indeed, magnesium hydroxide ($Mg(OH)_2$), borax or boric acid, and potassium chloride (KCl) are used as fertilizers. $Mg(OH)_2$ is also employed as an acidic waste neutralizer and in flame-retardant composite materials. Sodium carbonate ($Na_2CO_3$) is used for manufacturing soda-lime glasses, fiber glasses, papers and detergents. Calcium carbonate ($CaCO_3$) is a raw material used in glass and ceramic industries. Therefore, lithium extraction from brines sources is an opportunity to concomitant producing magnesium, calcium, sodium, potassium and boron salts.

In this context, Nieto et al. [125], [126]) and Torres et al. [106] proposed a membrane electrolysis process to remove simultaneously from native brines magnesium and calcium in a first stage, sodium in a second stage and lithium in the last stage of the electrodialysis process. Figure 1. 12 shows the steps for magnesium, calcium and sodium impurities valorization, and lithium carbonate production using the electrodialysis process.

Fistly, a sacrificial electrolyzer, at the top left, is constituted by three compartments, *i.e.* anodic, cathodic and middle compartments. The anodic and cathodic compartments are separated by cation and anion exchange membranes, respectively. The anode used was titanium (Ti) mesh electrode coated with an iridium-based mixed metal oxide ($IrO_2/TiO_2$; 65/35%). A stainless steel is used as cathode. The sacrificial electrolyzer is used to precipitating solids and producing alkaline brine (pH=13). Indeed, water electrolysis is operated in the cathodic compartment to produce hydroxide ions which increases the pH of the brine and precipitates magnesium and calcium as $Mg(OH)_2$ and $Ca(OH)_2$, respectively. The solid is recovered and then the alkaline brine feeds a second electrolyzer below the sacrificial electrolyser for increasing the brine pH to 14. That super alkaline brine is used in an external precipitation tank to precipitate magnesium and calcium from the native brine avoiding solid formation in the second electrolyzer.

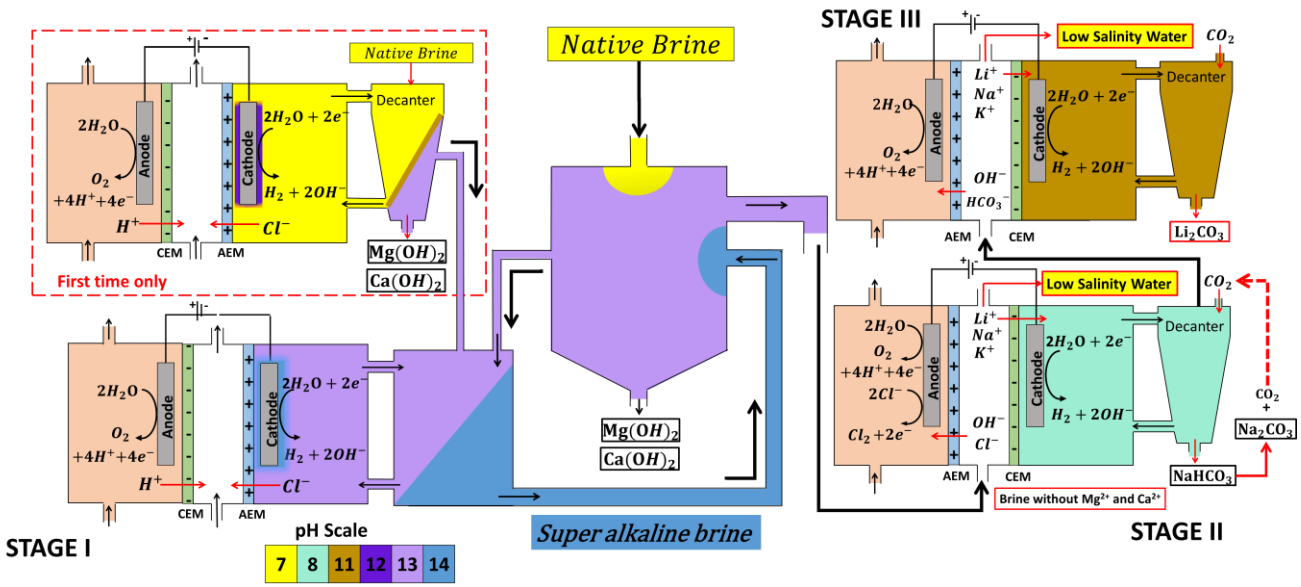



**Figure 1. 12:** Electrodialysis process for lithium carbonate production from brines [106].

This combining electrodialysis and precipitation processes show an excellent extraction efficiency of 99.99% for both magnesium and calcium from the brines located in the salar of Hombre Muerto. The investigations were performed at current density of 223 A $m^{-2}$ for brine containing 3,090 mg $L^{-1}$ magnesium and 685 mg $L^{-1}$ calcium. This first stage requests 62 kWh to process $1m^3$ of brine. Most importantly, lithium is not co-precipitated with $Mg(OH)_2$ and $Ca(OH)_2$, and it remains in solution for further treatments.

Secondly, after magnesium and calcium elimination from brine, Nieto et al. [125] removed monovalent ions, *i.e.* $Na^+$ and $K^+$, in three compartments electrolyzer with configuration similar to those in the first stage but membranes were inversed in the compartments. Because the chemistry of $Li^+$, $Na^+$ and $K^+$ are similar, the removal of sodium and potassium is challenging. The brine feeds the second stage through the intermediate compartment where cations migrate to the cathodic and anions to the anodic compartments as shown in Figure 1. 12. As in the first stage, water electrolysis is processed in the cathodic compartment. At current density of 10 $Am^{-2}$, the ions migrates following this order: $Na^+ > K^+ > Li^+$. Then, as reported in Equation 1. 38, sodium is recovered as sodium bicarbonate ($NaHCO_3$) by reaction with bicarbonate ($HCO_3^-$) which is obtained via reaction between carbon dioxide ($CO_2$) and hydroxide ions (Equation 1. 37) without lithium loss. $NaHCO_3$ is later transformed into sodium carbonate ($Na_2CO_3$) by heating at 100 °C. The purity of $Na_2CO_3$ was 99.5% with energy consumption of 331.3 kWh per 1 $m^3$ of treated brine.

$$CO_2 + OH^- \rightleftarrows HCO_3^- \qquad (1.\ 37)$$

$$HCO_3^- + Na^+ \rightleftarrows NaHCO_3 \quad (1.38)$$

Finally, in the last stage, Torres et al. [106] proposed lithium precipitation using an electrolyzer which has a configuration as that in the second stage. Lithium is extracted from the middle compartment to the cathodic compartment and then precipitated with $CO_2$ as lithium carbonate ($Li_2CO_3$) with purity of 97.5%. The energy consumption is estimated to be 70.6 kWh to treat $1m^3$ of brine. That electrodialysis-based DLE process allows recovering 90% of water with low salinity by decreasing the total dissolved solid (TDS) by 99.7%.

As previously described, the overall process developed and tested in lab scale involves association of electrochemistry operations and precipitation to producing high purity lithium carbonate and by-products, recovering water and $CO_2$ sequestration. Hence, the advanced electrodialysis process is economically more beneficial, low environmental impact, and faster than current conventional solar evaporation processes. Particularly, that DLE technology allows producing raw materials from the brine impurities reducing industrial waste. In this context, it could be implemented in the current lithium facilities.

## 1.4 Conclusion

Nowadays, lithium is one of the critical metals need for energy transition given that it is used for energy storage mainly in electric mobility through the manufacturing of lithium-ion batteries. Large amount of lithium resources is present in brines located in three countries of South America called “Lithium Triangle” which gathers Argentina, Bolivia and Chile. Currently, lithium is produced as salts from brines concentrated by solar evaporation processes as those reported by Garrett et al. [76]. However, lithium recovery from brines is a challenging process due to the high salinity of brines and the presence of many impurities such as boron, magnesium, calcium, potassium and sodium. The impurities within the brines are removed before lithium extraction in order to ensure high-purity lithium products. Particularly, boron concentration in brines must be less than 25 mg $L^{-1}$ to produce battery-grade lithium salts [127]. Therefore, boron extraction from lithium-rich brines is beneficial for its valorization in glass, ceramic, fertilizer and detergent industries. However, few lithium plants reliant on conventional solar evaporation technologies extract and valorize boron. In case boron is not valorized, it is stored in stockpiles with potential environment concern [107]. Moreover, conventional lithium brines processes take much time and require large portion of land to implement solar evaporation ponds. In addition, they are responsible for 90% of water loss in the salars through solar evaporation and require huge chemicals, *i.e.* lime and soda ash, for impurities precipitation which generates significant quantities of waste. Huge fresh water is also required to dissolve the precipitant and wash the lithium products in order to increase the purity. Hence, the conventional lithium processes are not enough eco-efficient and environment friendly for lithium production in the next decades.

New lithium extraction processes based on direct lithium extraction (DLE) from brines have been developed to overcome the conventional processes issues by decreasing the environment impact and chemicals used while producing high-purity lithium salts. However, most of the new processes in demonstration stage such as those developed by Adionics and Solvay-Tenova suffer from impurities co-valorization particularly boron. The advanced electrodialysis process developed by Nieto et al. ([125], [126]) and Torres et al. [106] is a potential route to valorize magnesium, calcium and sodium with lithium. However, boron is still not valorized and precipitates with magnesium and calcium as magnesium and calcium borates, respectively, which decreases the purity of $Mg(OH)_2$ and $Ca(OH)_2$ produced. Thus, boron extraction from lithium-rich continental brines as those of the salar de Hombre Muerto has to be performed. This research is devoted to extract boron by solvent extraction (SX) from

the salar de Hombre Muerto brines and valorize it as boric acid or borax. In this work, combination of SX of boron and the electrodialysis operation is addressed to produce battery-grade lithium carbonate.

Boron extraction from brines by alcohols is a mature technique and extraction properties of several alcohols were tested in the past. Deep eutectic solvents (DES) and aliphatic alcohols such as diols and mono alcohols showed an excellent performance to extract boron from brines. In the next chapter, alcohols are used to study the physiochemistry of boron extraction and propose a suitable flowsheet to extract boron efficiently and selectively.

# References


[1] L.-T. Yang *et al.*, "Citrus Physiological and Molecular Response to Boron Stresses," *Plants*, vol. 11, no. 1, Art. no. 1, Jan. 2022, doi: 10.3390/plants11010040.

[2] M. F. Chong, K. P. Lee, H. J. Chieng, and I. I. Syazwani Binti Ramli, "Removal of boron from ceramic industry wastewater by adsorption–flocculation mechanism using palm oil mill boiler (POMB) bottom ash and polymer," *Water Res.*, vol. 43, no. 13, pp. 3326–3334, Jul. 2009, doi: 10.1016/j.watres.2009.04.044.

[3] L. Kentjono, J. C. Liu, W. C. Chang, and C. Irawan, "Removal of boron and iodine from optoelectronic wastewater using Mg–Al (NO3) layered double hydroxide," *Desalination*, vol. 262, no. 1, pp. 280–283, Nov. 2010, doi: 10.1016/j.desal.2010.06.015.

[4] D. E. Garrett, *Handbook of Lithium and Natural Calcium Chloride*. Elsevier, 2004.

[5] "Guidelines for drinking-water quality, 4th edition, incorporating the 1st addendum." Accessed: Feb. 01, 2022. [Online]. Available: https://www.who.int/publications-detail-redirect/9789241549950

[6] "Boron in the world," Etimaden. Accessed: Mar. 18, 2024. [Online]. Available: https://www.etimaden.gov.tr

[7] D. E. Garrett, "Chapter 1 - Borate Minerals and the Origin of Borate Deposits," in *Borates*, D. E. Garrett, Ed., San Diego: Academic Press, 1998, pp. 1–50. doi: 10.1016/B978-012276060-0/50002-4.

[8] D. E. Garrett, "Chapter 5 - Lake or Brine Deposits," in *Borates*, D. E. Garrett, Ed., San Diego: Academic Press, 1998, pp. 227–253. doi: 10.1016/B978-012276060-0/50006-1.

[9] T. Turkbay, J. Bongono, T. Alix, B. Laratte, and B. Elevli, "Prior knowledge of the data on the production capacity of boron facilities in Turkey," *Clean. Eng. Technol.*, vol. 10, p. 100539, Oct. 2022, doi: 10.1016/j.clet.2022.100539.

[10] R. D. Graham and R. M. Welch, "Plant food micronutrient composition and human nutrition," *Commun. Soil Sci. Plant Anal.*, vol. 31, no. 11–14, pp. 1627–1640, Jun. 2000, doi: 10.1080/00103620009370529.

[11] U. C. Gupta, *Boron and Its Role in Crop Production*. CRC Press, 1993.

[12] Y. Ding, A. Osaka, and Y. Miura, "Enhanced Surface Crystallization of β-Barium Borate on Glass Due to Ultrasonic Treatment," *J. Am. Ceram. Soc.*, vol. 77, no. 3, pp. 749–752, 1994, doi: 10.1111/j.1151-2916.1994.tb05360.x.

[13] L. D. Pye, V. D. Fréchette, and N. J. Kreidl, *Borate Glasses: Structure, Properties, Applications*. Springer Science & Business Media, 2012.

[14] M. M. Nasseri, “Comparison of HfB2 and ZrB2 behaviors for using in nuclear industry,” *Ann. Nucl. Energy*, vol. 114, pp. 603–606, Apr. 2018, doi: 10.1016/j.anucene.2017.12.060.

[15] J. Eichler and C. Lesniak, “Boron nitride (BN) and BN composites for high-temperature applications,” *J. Eur. Ceram. Soc.*, vol. 28, no. 5, pp. 1105–1109, Jan. 2008, doi: 10.1016/j.jeurceramsoc.2007.09.005.

[16] F. Ali, N. S Hosmane, and Y. Zhu, “Boron Chemistry for Medical Applications,” *Molecules*, vol. 25, no. 4, Art. no. 4, Jan. 2020, doi: 10.3390/molecules25040828.

[17] “Borophene and Boron-Based Nanosheets: Recent Advances in Synthesis Strategies and Applications in the Field of Environment and Energy - Chand - 2021 - Advanced Materials Interfaces - Wiley Online Library.” Accessed: Jan. 25, 2023. [Online]. Available: https://onlinelibrary-wiley-com.bases-doc.univ-lorraine.fr/doi/full/10.1002/admi.202100045

[18] G. Moussa, R. Moury, U. B. Demirci, T. Şener, and P. Miele, “Boron-based hydrides for chemical hydrogen storage,” *Int. J. Energy Res.*, vol. 37, no. 8, pp. 825–842, 2013, doi: 10.1002/er.3027.

[19] M. H. Kharita, S. Yousef, and M. AlNassar, “Review on the addition of boron compounds to radiation shielding concrete,” *Prog. Nucl. Energy*, vol. 53, no. 2, pp. 207–211, Mar. 2011, doi: 10.1016/j.pnucene.2010.09.012.

[20] A. Mergen, M. H. Demirhan, and M. Bilen, “Processing of boric acid from borax by a wet chemical method,” *Adv. Powder Technol.*, vol. 14, no. 3, pp. 279–293, Jan. 2003, doi: 10.1163/15685520360685947.

[21] M. M. Harussani, S. M. Sapuan, G. Nadeem, T. Rafin, and W. Kirubaanand, “Recent applications of carbon-based composites in defence industry: A review,” *Def. Technol.*, vol. 18, no. 8, pp. 1281–1300, Aug. 2022, doi: 10.1016/j.dt.2022.03.006.

[22] D. E. Garrett, *Borates: Handbook of Deposits, Processing, Properties, and Use*. Elsevier, 1998.

[23] W. Zhang, “A review of tribological properties for boron carbide ceramics,” *Prog. Mater. Sci.*, vol. 116, p. 100718, Feb. 2021, doi: 10.1016/j.pmatsci.2020.100718.

[24] P. Panigrahi, A. Kumar, H. Bae, H. Lee, R. Ahuja, and T. Hussain, “Capacity enhancement of polylithiated functionalized boron nitride nanotubes: an efficient hydrogen storage medium,” *Phys. Chem. Chem. Phys.*, vol. 22, no. 27, pp. 15675–15682, Jul. 2020, doi: 10.1039/D0CP01237H.

[25] A. Balinski, V. Recksiek, and N. Kelly, “Solvent Extraction of Boric Acid: Comparison of Five Different Monohydric Alcohols and Equilibrium Modeling with Numerical Methods,” *Processes*, vol. 9, no. 2, Art. no. 2, Feb. 2021, doi: 10.3390/pr9020398.

[26] D. E. Garrett, “Chapter 8 - Processing,” in *Borates*, D. E. Garrett, Ed., San Diego: Academic Press, 1998, pp. 333–400. doi: 10.1016/B978-012276060-0/50009-7.

[27] Z. Guan, J. Lv, P. Bai, and X. Guo, “Boron removal from aqueous solutions by adsorption — A review,” *Desalination*, vol. 383, pp. 29–37, Apr. 2016, doi: 10.1016/j.desal.2015.12.026.

[28] S. Nishihama, Y. Sumiyoshi, T. Ookubo, and K. Yoshizuka, “Adsorption of boron using glucamine-based chelate adsorbents,” *Desalination*, vol. 310, pp. 81–86, Feb. 2013, doi: 10.1016/j.desal.2012.06.021.

[29] K. Ooi, H. Kanoh, A. Sonoda, and T. Hirotsu, “Screening of Adsorbents for Boron in Brine,” *J. Ion Exch.*, vol. 7, no. 3, pp. 166–173, 1996, doi: 10.5182/jaie.7.166.

[30] C.-Y. Yan and W.-T. Yi, “Preparation, characterization, and boron adsorption behavior of gluconate-intercalated hydrotalcite,” *Environ. Prog. Sustain. Energy*, vol. 29, no. 4, pp. 450–456, 2010, doi: 10.1002/ep.10433.

[31] N. Hilal, G. J. Kim, and C. Somerfield, “Boron removal from saline water: A comprehensive review,” *Desalination*, vol. 273, no. 1, pp. 23–35, Jun. 2011, doi: 10.1016/j.desal.2010.05.012.

[32] E. Güler, C. Kaya, N. Kabay, and M. Arda, “Boron removal from seawater: State-of-the-art review,” *Desalination*, vol. 356, pp. 85–93, Jan. 2015, doi: 10.1016/j.desal.2014.10.009.

[33] A. Alharati, Y. Swesi, K. Fiaty, and C. Charcosset, “Boron removal in water using a hybrid membrane process of ion exchange resin and microfiltration without continuous resin addition,” *J. Water Process Eng.*, vol. 17, pp. 32–39, Jun. 2017, doi: 10.1016/j.jwpe.2017.03.002.

[34] N. Öztürk and T. E. Köse, “Boron removal from aqueous solutions by ion-exchange resin: Batch studies,” *Desalination*, vol. 227, no. 1, pp. 233–240, Jul. 2008, doi: 10.1016/j.desal.2007.06.028.

[35] C. Yan, W. Yi, P. Ma, X. Deng, and F. Li, “Removal of boron from refined brine by using selective ion exchange resins,” *J. Hazard. Mater.*, vol. 154, no. 1, pp. 564–571, Jun. 2008, doi: 10.1016/j.jhazmat.2007.10.067.

[36] T. E. Köse and N. Öztürk, “Boron removal from aqueous solutions by ion-exchange resin: Column sorption–elution studies,” *J. Hazard. Mater.*, vol. 152, no. 2, pp. 744–749, Apr. 2008, doi: 10.1016/j.jhazmat.2007.07.041.

[37] L. Melnik, O. Vysotskaja, and B. Kornilovich, “Boron behavior during desalination of sea and underground water by electrodialysis,” *Desalination*, vol. 124, no. 1, pp. 125–130, Nov. 1999, doi: 10.1016/S0011-9164(99)00096-X.

[38] P. Dydo, “The effect of process parameters on boric acid transport during the electrodialytic desalination of aqueous solutions containing selected salts,” *Desalination*, vol. 310, pp. 43–49, Feb. 2013, doi: 10.1016/j.desal.2012.04.007.

[39] A. Farhat, F. Ahmad, N. Hilal, and H. A. Arafat, “Boron removal in new generation reverse osmosis (RO) membranes using two-pass RO without pH adjustment,” *Desalination*, vol. 310, pp. 50–59, Feb. 2013, doi: 10.1016/j.desal.2012.10.003.

[40] K. L. Tu, L. D. Nghiem, and A. R. Chivas, “Boron removal by reverse osmosis membranes in seawater desalination applications,” *Sep. Purif. Technol.*, vol. 75, no. 2, pp. 87–101, Oct. 2010, doi: 10.1016/j.seppur.2010.07.021.

[41] T. Itakura, R. Sasai, and H. Itoh, “Precipitation recovery of boron from wastewater by hydrothermal mineralization,” *Water Res.*, vol. 39, no. 12, pp. 2543–2548, Jul. 2005, doi: 10.1016/j.watres.2005.04.035.

[42] Y.-J. Shih, C.-H. Liu, W.-C. Lan, and Y.-H. Huang, “A novel chemical oxo-precipitation (COP) process for efficient remediation of boron wastewater at room temperature,” *Chemosphere*, vol. 111, pp. 232–237, Sep. 2014, doi: 10.1016/j.chemosphere.2014.03.121.

[43] F. Widhiastuti, J.-Y. Lin, Y.-J. Shih, and Y.-H. Huang, “Electrocoagulation of boron by electrochemically co-precipitated spinel ferrites,” *Chem. Eng. J.*, vol. 350, pp. 893–901, Oct. 2018, doi: 10.1016/j.cej.2018.06.041.

[44] F. Folkestad, K. Loiten, G. Mejdell, and A. Torvund, “Method of removing boric acid and boric acid salts from aqueous magnesium chloride solutions,” US3855392A, Dec. 17, 1974 Accessed: Feb. 02, 2022. [Online]. Available: https://patents.google.com/patent/US3855392A/en

[45] Z. Xu *et al.*, “Recovery of boron from brines with high magnesium content by solvent extraction using aliphatic alcohol,” *RSC Adv.*, vol. 11, no. 26, pp. 16096–16105, Apr. 2021, doi: 10.1039/D1RA01906F.

[46] X. Peng, D. Shi, Y. Zhang, L. Zhang, L. Ji, and L. Li, “Recovery of boron from unacidified salt lake brine by solvent extraction with 2,2,4-trimethyl-1,3-pentanediol,” *J. Mol. Liq.*, vol. 326, p. 115301, Mar. 2021, doi: 10.1016/j.molliq.2021.115301.

[47] L. Bonin, D. Deduytsche, M. Wolthers, V. Flexer, and K. Rabaey, “Boron extraction using selective ion exchange resins enables effective magnesium recovery from lithium rich brines with minimal lithium loss,” *Sep. Purif. Technol.*, vol. 275, p. 119177, Nov. 2021, doi: 10.1016/j.seppur.2021.119177.

[48] D. S. Flett, “Principles and practices of solvent extraction. Second Edition, Revised and Expanded. Edited by J Rydberg, M Cox, C Musikas and GR Choppin. Marcel Dekker, New York, 2004. 760 pp, ISBN 0 8247 5053 2,” *J. Chem. Technol. Biotechnol.*, vol. 80, no. 3, pp. 359–360, 2005, doi: 10.1002/jctb.1219.

[49] G. M. Ritcey, “Solvent extraction in hydrometallurgy: Present and future,” *Tsinghua Sci. Technol.*, vol. 11, no. 2, pp. 137–152, Apr. 2006, doi: 10.1016/S1007-0214(06)70168-7.

[50] *Advances in Hydrometallurgy*. MDPI, 2020. doi: 10.3390/books978-3-03928-940-0.

[51] V. S. Kislik, *Solvent Extraction: Classical and Novel Approaches*. Elsevier, 2011.

[52] A. Chagnes, “Métallurgie extractive - Hydrométallurgie,” *Élabor. Recycl. Métaux*, Jun. 2022, doi: 10.51257/a-v4-m2235.

[53] W. Xiang, S. Liang, Z. Zhou, W. Qin, and W. Fei, “Extraction of lithium from salt lake brine containing borate anion and high concentration of magnesium,” *Hydrometallurgy*, vol. 166, pp. 9–15, Dec. 2016, doi: 10.1016/j.hydromet.2016.08.005.

[54] M. D. Joshi, G. Chalumot, Y. Kim, and J. L. Anderson, “Synthesis of glucaminium-based ionic liquids and their application in the removal of boron from water,” *Chem. Commun.*, vol. 48, no. 10, pp. 1410–1412, Jan. 2012, doi: 10.1039/C1CC14327A.

[55] M. T. Coll, A. Fortuny, and A. M. Sastre, “Boron reduction by supported liquid membranes using ALiCY and ALiDEC ionic liquids as carriers,” *Chem. Eng. Res. Des.*, vol. 92, no. 4, pp. 758–763, Apr. 2014, doi: 10.1016/j.cherd.2013.11.010.

[56] A. Fortuny, M. T. Coll, and A. M. Sastre, “Use of methyltrioctyl/decylammonium bis 2,4,4-(trimethylpentyl)phosphinate ionic liquid (ALiCY IL) on the boron extraction in chloride media,” *Sep. Purif. Technol.*, vol. 97, pp. 137–141, Sep. 2012, doi: 10.1016/j.seppur.2012.02.037.

[57] N. Bicak, M. Gazi, and B. F. Senkal, “Polymer supported amino bis-(cis-propan 2,3 diol) functions for removal of trace boron from water,” *React. Funct. Polym.*, vol. 65, no. 1, pp. 143–148, Nov. 2005, doi: 10.1016/j.reactfunctpolym.2005.01.010.

[58] M. Gazi and N. Bicak, “Selective boron extraction by polymer supported 2-hydroxylethylamino propylene glycol functions,” *React. Funct. Polym.*, vol. 67, no. 10, pp. 936–942, Oct. 2007, doi: 10.1016/j.reactfunctpolym.2007.05.019.

[59] P. Ayers, A. W. L. Dudeney, and F. Kahraman, “Solvent extraction of boron with 2-ethyl-1,3-hexanediol and 2-chloro-4-(1,1,3,3-tetramethylbutyl)-6-methylol-phenol,” *J. Inorg. Nucl. Chem.*, vol. 43, no. 9, pp. 2097–2100, 1981, doi: 10.1016/0022-1902(81)80556-8.

[60] H. Hoşgoren, S. Tural, F. Kahraman, M. Toğrul, and M. Karakaplan, “Solvent extraction of boron with l,2-dihydroxy-4-oxadodecane (DHD) in n-amyl alcohol,” *Solvent Extr. Ion Exch.*, vol. 15, no. 2, pp. 249–257, Mar. 1997, doi: 10.1080/07366299708934477.

[61] W. L. A. Brooks, C. C. Deng, and B. S. Sumerlin, “Structure–Reactivity Relationships in Boronic Acid–Diol Complexation,” *ACS Omega*, vol. 3, no. 12, pp. 17863–17870, Dec. 2018, doi: 10.1021/acsomega.8b02999.

[62] R. Zhang *et al.*, “Extraction of boron from salt lake brine using 2-ethylhexanol,” *Hydrometallurgy*, vol. 160, pp. 129–136, Mar. 2016, doi: 10.1016/j.hydromet.2016.01.001.

[63] J. Guo, Y. Yang, X. Gao, and J. Yu, “Boron extraction from lithium-rich brine using mixed alcohols,” *Hydrometallurgy*, vol. 197, p. 105477, Nov. 2020, doi: 10.1016/j.hydromet.2020.105477.

[64] X. Peng *et al.*, “Recovery of boric acid from salt lake brines by solvent extraction with 2-butyl-1-n-octanol,” *Hydrometallurgy*, vol. 177, pp. 161–167, May 2018, doi: 10.1016/j.hydromet.2018.03.013.

[65] X. Fan, X. Yu, Y. Guo, and T. Deng, “Recovery of Boron from Underground Brine by Continuous Centrifugal Extraction with 2-Ethyl-1,3-hexanediol (EHD) and Its Mechanism,” *J. Chem.*, vol. 2018, p. e7530837, Oct. 2018, doi: 10.1155/2018/7530837.

[66] M. Karakaplan, S. Tural, B. Tural, Y. Turgut, and H. Hoşgören, “The Solvent Extraction of Boron with Synthesized Aliphatic 1,3-Diols: Stripping and Extraction Behavior of Boron by 2,2,5-Trimethyl-1,3-hexanediol,” *Solvent Extr. Ion Exch.*, vol. 22, no. 6, pp. 897–911, Dec. 2004, doi: 10.1081/SEI-200037400.

[67] B. Tural, S. Tural, and H. Hoşgören, “Investigation of Some 1,3-Diols for the Requirements of Solvent Extraction of Boron: 2,2,6-Trimethyl-1,3 Heptanediol as a Potential Boron Extractant,” *Turk. J. Chem.*, vol. 31, no. 2, pp. 163–170, May 2007.

[68] G. Almustafa, R. Sulaiman, M. Kumar, I. Adeyemi, H. A. Arafat, and I. AlNashef, "Boron extraction from aqueous medium using novel hydrophobic deep eutectic solvents," *Chem. Eng. J.*, vol. 395, p. 125173, Sep. 2020, doi: 10.1016/j.cej.2020.125173.

[69] G. Almustafa *et al.*, "Liquification of 2,2,4-trimethyl-1,3-pentanediol into hydrophobic eutectic mixtures: A multi-criteria design for eco-efficient boron recovery," *Chem. Eng. J.*, vol. 426, p. 131342, Dec. 2021, doi: 10.1016/j.cej.2021.131342.

[70] M. Matsumoto, K. Kondo, M. Hirata, S. Kokubu, T. Hano, and T. Takada, "Recovery of Boric Acid from Wastewater by Solvent Extraction," *Sep. Sci. Technol.*, vol. 32, no. 5, pp. 983–991, Mar. 1997, doi: 10.1080/01496399708000940.

[71] J. Hejda and V. Jedináková, "Physical and chemical aspects of extraction separation of boric acid from the products of nuclear fission," *J. Radioanal. Nucl. Chem.*, vol. 121, no. 2, pp. 441–446, Apr. 1988, doi: 10.1007/BF02041431.

[72] J. Hejda and V. Jedináková, "Separation of boric acid from radioactive wastes by liquid-liquid extraction," *J. Radioanal. Chem.*, vol. 80, no. 1, pp. 23–29, Mar. 1983, doi: 10.1007/BF02517643.

[73] A. F. Kiemde, J. Marin, V. Flexer, and A. Chagnes, "Boron extraction by aliphatic mono- and di-hydroxy alcohols from a representative continental brine," *Hydrometallurgy*, vol. 225, p. 106280, Apr. 2024, doi: 10.1016/j.hydromet.2024.106280.

[74] J. Lü, J. Liu, Y. Sun, and C. Li, "Kinetics of Forward Extraction of Boric Acid from Salt Lake Brine by 2-Ethyl-1,3-hexanediol in Toluene Using Single Drop Technique," *Chin. J. Chem. Eng.*, vol. 22, no. 5, pp. 496–502, May 2014, doi: 10.1016/S1004-9541(14)60059-8.

[75] M. Karakaplan, S. Tural, M. Sunkür, and H. Hoşgören*, "Effect of 1,3-Diol Structure on the Distribution of Boron Between CHCl3 and Aqueous Phase," *Sep. Sci. Technol.*, vol. 38, no. 8, pp. 1721–1732, Jan. 2003, doi: 10.1081/SS-120019405.

[76] D. E. Garrett, "Part 1 - Lithium," in *Handbook of Lithium and Natural Calcium Chloride*, D. E. Garrett, Ed., Oxford: Academic Press, 2004, pp. 1–235. doi: 10.1016/B978-012276152-2/50037-2.

[77] "Mineral commodity summaries 2024," 2024. doi: 10.3133/mcs2024.

[78] B. Swain, "Recovery and recycling of lithium: A review," *Sep. Purif. Technol.*, vol. 172, pp. 388–403, Jan. 2017, doi: 10.1016/j.seppur.2016.08.031.

[79] F. Meng, J. McNeice, S. S. Zadeh, and A. Ghahreman, "Review of Lithium Production and Recovery from Minerals, Brines, and Lithium-Ion Batteries," *Miner. Process. Extr.*

*Metall. Rev.*, vol. 42, no. 2, pp. 123–141, Feb. 2021, doi: 10.1080/08827508.2019.1668387.

[80] H. Guo, G. Kuang, H. Wang, H. Yu, and X. Zhao, "Investigation of Enhanced Leaching of Lithium from α-Spodumene Using Hydrofluoric and Sulfuric Acid," *Minerals*, vol. 7, no. 11, Art. no. 11, Nov. 2017, doi: 10.3390/min7110205.

[81] S. E. Kesler, P. W. Gruber, P. A. Medina, G. A. Keoleian, M. P. Everson, and T. J. Wallington, "Global lithium resources: Relative importance of pegmatite, brine and other deposits," *Ore Geol. Rev.*, vol. 48, pp. 55–69, Oct. 2012, doi: 10.1016/j.oregeorev.2012.05.006.

[82] T. P. Narins, "The battery business: Lithium availability and the growth of the global electric car industry," *Extr. Ind. Soc.*, vol. 4, no. 2, pp. 321–328, Apr. 2017, doi: 10.1016/j.exis.2017.01.013.

[83] A. B. Gallo, J. R. Simões-Moreira, H. K. M. Costa, M. M. Santos, and E. Moutinho dos Santos, "Energy storage in the energy transition context: A technology review," *Renew. Sustain. Energy Rev.*, vol. 65, pp. 800–822, Nov. 2016, doi: 10.1016/j.rser.2016.07.028.

[84] A. F. Kiemde, N. Ferrando, J.-C. de Hemptinne, Y. L. Gallo, A. Reveillère, and J. S. R. Pinto, "Hydrogen and air storage in salt caverns: a thermodynamic model for phase equilibrium calculations," *Sci. Technol. Energy Transit.*, vol. 78, p. 10, 2023, doi: 10.2516/stet/2023004.

[85] J. Xu *et al.*, "High-Energy Lithium-Ion Batteries: Recent Progress and a Promising Future in Applications," *ENERGY Environ. Mater.*, vol. 6, no. 5, p. e12450, 2023, doi: 10.1002/eem2.12450.

[86] P. W. Gruber, P. A. Medina, G. A. Keoleian, S. E. Kesler, M. P. Everson, and T. J. Wallington, "Global Lithium Availability," *J. Ind. Ecol.*, vol. 15, no. 5, pp. 760–775, 2011, doi: 10.1111/j.1530-9290.2011.00359.x.

[87] "Lithium global demand forecast 2035," Statista. Accessed: Mar. 24, 2024. [Online]. Available: https://www.statista.com/statistics/452025/projected-total-demand-for-lithium-globally/

[88] A. Chagnes, *Lithium Process Chemistry : Resources, Extraction, Batteries, and Recycling*. Elsevier Science, 2015. Accessed: Jan. 25, 2022. [Online]. Available: http://univ.scholarvox.com.bases-doc.univ-lorraine.fr/catalog/book/docid/88829473

[89] P. K. Choubey, M. Kim, R. R. Srivastava, J. Lee, and J.-Y. Lee, "Advance review on the exploitation of the prominent energy-storage element: Lithium. Part I: From mineral

and brine resources," *Miner. Eng.*, vol. 89, pp. 119–137, Apr. 2016, doi: 10.1016/j.mineng.2016.01.010.

[90] N. Vieceli, C. A. Nogueira, M. F. C. Pereira, F. O. Durão, C. Guimarães, and F. Margarido, "Optimization of Lithium Extraction from Lepidolite by Roasting Using Sodium and Calcium Sulfates," *Miner. Process. Extr. Metall. Rev.*, vol. 38, no. 1, pp. 62–72, Jan. 2017, doi: 10.1080/08827508.2016.1262858.

[91] V. Flexer, C. F. Baspineiro, and C. I. Galli, "Lithium recovery from brines: A vital raw material for green energies with a potential environmental impact in its mining and processing," *Sci. Total Environ.*, vol. 639, pp. 1188–1204, Oct. 2018, doi: 10.1016/j.scitotenv.2018.05.223.

[92] J. W. An, D. J. Kang, K. T. Tran, M. J. Kim, T. Lim, and T. Tran, "Recovery of lithium from Uyuni salar brine," *Hydrometallurgy*, vol. 117–118, pp. 64–70, Apr. 2012, doi: 10.1016/j.hydromet.2012.02.008.

[93] C. A. Quist-Jensen, A. Ali, S. Mondal, F. Macedonio, and E. Drioli, "A study of membrane distillation and crystallization for lithium recovery from high-concentrated aqueous solutions," *J. Membr. Sci.*, vol. 505, pp. 167–173, May 2016, doi: 10.1016/j.memsci.2016.01.033.

[94] H. Bukowsky and E. Uhlemann, "Selective Extraction of Lithium Chloride from Brines," *Sep. Sci. Technol.*, vol. 28, no. 6, pp. 1357–1360, Apr. 1993, doi: 10.1080/01496399308018042.

[95] Z. Zhou, W. Qin, and W. Fei, "Extraction Equilibria of Lithium with Tributyl Phosphate in Three Diluents," *J. Chem. Eng. Data*, vol. 56, no. 9, pp. 3518–3522, Sep. 2011, doi: 10.1021/je200246x.

[96] D. Gao *et al.*, "Extraction of lithium from salt lake brine with triisobutyl phosphate in ionic liquid and kerosene," *Chem. Res. Chin. Univ.*, vol. 31, no. 4, pp. 621–626, Aug. 2015, doi: 10.1007/s40242-015-4376-z.

[97] D. Gao, Y. Guo, X. Yu, S. Wang, and T. Deng, "Extracting Lithium from the High Concentration Ratio of Magnesium and Lithium Brine Using Imidazolium-Based Ionic Liquids with Varying Alkyl Chain Lengths," *J. Chem. Eng. Jpn.*, vol. 49, no. 2, pp. 104–110, 2016, doi: 10.1252/jcej.15we046.

[98] C. Shi, Y. Jing, and Y. Jia, "Solvent extraction of lithium ions by tri-n-butyl phosphate using a room temperature ionic liquid," *J. Mol. Liq.*, vol. 215, pp. 640–646, Mar. 2016, doi: 10.1016/j.molliq.2016.01.025.

[99] C. F. Baspineiro, J. Franco, and V. Flexer, “Potential water recovery during lithium mining from high salinity brines,” *Sci. Total Environ.*, vol. 720, p. 137523, Jun. 2020, doi: 10.1016/j.scitotenv.2020.137523.

[100] H. Bukowsky, E. Uhlemann, and D. Steinborn, “The recovery of pure lithium chloride from ‘brines’ containing higher contents of calcium chloride and magnesium chloride,” *Hydrometallurgy*, vol. 27, no. 3, pp. 317–325, Dec. 1991, doi: 10.1016/0304-386X(91)90056-R.

[101] C. Jiang, Y. Wang, Q. Wang, H. Feng, and T. Xu, “Production of Lithium Hydroxide from Lake Brines through Electro–Electrodialysis with Bipolar Membranes (EEDBM),” *Ind. Eng. Chem. Res.*, vol. 53, no. 14, pp. 6103–6112, Apr. 2014, doi: 10.1021/ie404334s.

[102] X. Liu, X. Chen, L. He, and Z. Zhao, “Study on extraction of lithium from salt lake brine by membrane electrolysis,” *Desalination*, vol. 376, pp. 35–40, Nov. 2015, doi: 10.1016/j.desal.2015.08.013.

[103] J. Jagur-Grodzinski and E. Schori, “Solvent-Polymeric Membranes for Separation of Li+ From Other Alkali Metal and Alkaline Earth Ions,” *Isr. J. Chem.*, vol. 26, no. 1, pp. 65–70, 1985, doi: 10.1002/ijch.198500070.

[104] S.-Y. Sun, L.-J. Cai, X.-Y. Nie, X. Song, and J.-G. Yu, “Separation of magnesium and lithium from brine using a Desal nanofiltration membrane,” *J. Water Process Eng.*, vol. 7, pp. 210–217, Sep. 2015, doi: 10.1016/j.jwpe.2015.06.012.

[105] A. Somrani, A. H. Hamzaoui, and M. Pontie, “Study on lithium separation from salt lake brines by nanofiltration (NF) and low pressure reverse osmosis (LPRO),” *Desalination*, vol. 317, pp. 184–192, May 2013, doi: 10.1016/j.desal.2013.03.009.

[106] W. R. Torres, C. H. Díaz Nieto, A. Prévoteau, K. Rabaey, and V. Flexer, “Lithium carbonate recovery from brines using membrane electrolysis,” *J. Membr. Sci.*, vol. 615, p. 118416, Dec. 2020, doi: 10.1016/j.memsci.2020.118416.

[107] M. L. Vera, W. R. Torres, C. I. Galli, A. Chagnes, and V. Flexer, “Environmental impact of direct lithium extraction from brines,” *Nat. Rev. Earth Environ.*, vol. 4, no. 3, Art. no. 3, Mar. 2023, doi: 10.1038/s43017-022-00387-5.

[108] “Mineral commodity summaries 2021 | U.S. Geological Survey.” Accessed: Mar. 14, 2024. [Online]. Available: https://www.usgs.gov/publications/mineral-commodity-summaries-2021

[109] I. Wilkomirsky, “Production of lithium carbonate from brines,” US5993759A, Nov. 30, 1999 Accessed: Jan. 26, 2022. [Online]. Available: https://patents.google.com/patent/US5993759/en

[110] H. Atashi, M. Sarkari, M. Zeinali, and H. Aliabadi, “Recovery of Magnesium Chloride from Resulting Potash Unit Concentrate Case Study: Iran Great Desert Brine,” 2010. Accessed: Feb. 14, 2024. [Online]. Available: https://www.semanticscholar.org/paper/Recovery-of-Magnesium-Chloride-from-Resulting-Unit-Atashi-Sarkari/9c7321f9033310d8039bbee01651ac6238a79f10

[111] P. M. Brown and S. J. Beckerman, “Production of lithium metal grade lithium chloride from lithium-containing brine,” US4980136A, Dec. 25, 1990 Accessed: Jan. 26, 2022. [Online].Available:https://patents.google.com/patent/US4980136/en?oq=production+of+lithium+metal+grade+lithium+chloride+from+lithium+containing+brine

[112] M. Boualleg, F. A. P. Burdet, and R. C. J. R. Soulairol, “Procede de preparation d’un materiau absorbant en l’absence de liant comprenant une etape de traitement hydrothermal et pocede d’extraction de lithium a partir de solutions salines utilisant ledit materiau,” FR3020284A1, Oct. 30, 2015 Accessed: Apr. 07, 2024. [Online]. Available: https://patents.google.com/patent/FR3020284A1/en?q=(direct+lithium+extraction+process)&assignee=eramet&oq=eramet+direct+lithium+extraction+process

[113] X. Liu, X. Chen, Z. Zhao, and X. Liang, “Effect of Na+ on Li extraction from brine using LiFePO4/FePO4 electrodes,” *Hydrometallurgy*, vol. 146, pp. 24–28, May 2014, doi: 10.1016/j.hydromet.2014.03.010.

[114] J. Lee, S.-H. Yu, C. Kim, Y.-E. Sung, and J. Yoon, “Highly selective lithium recovery from brine using a λ-MnO2–Ag battery,” *Phys. Chem. Chem. Phys.*, vol. 15, no. 20, pp. 7690–7695, May 2013, doi: 10.1039/C3CP50919B.

[115] Z. Zhao, X. Si, X. Liu, L. He, and X. Liang, “Li extraction from high Mg/Li ratio brine with LiFePO4/FePO4 as electrode materials,” *Hydrometallurgy*, vol. 133, pp. 75–83, Feb. 2013, doi: 10.1016/j.hydromet.2012.11.013.

[116] M. J. Park *et al.*, “Recyclable composite nanofiber adsorbent for Li+ recovery from seawater desalination retentate,” *Chem. Eng. J.*, vol. 254, pp. 73–81, Oct. 2014, doi: 10.1016/j.cej.2014.05.095.

[117] R. Chitrakar, Y. Makita, K. Ooi, and A. Sonoda, “Magnesium-Doped Manganese Oxide with Lithium Ion-Sieve Property: Lithium Adsorption from Salt Lake Brine,” *Bull. Chem. Soc. Jpn.*, vol. 86, no. 7, pp. 850–855, Jul. 2013, doi: 10.1246/bcsj.20130019.

[118] H. Dong, F. K. Hussain, and E. Chang, “Project Track and Trace Methodology in the Environment of Digital Ecosystem,” in *2007 Inaugural IEEE-IES Digital EcoSystems and Technologies Conference*, Feb. 2007, pp. 357–360. doi: 10.1109/DEST.2007.371998.

[119] R. Chitrakar, Y. Makita, K. Ooi, and A. Sonoda, “Lithium recovery from salt lake brine by H2TiO3,” *Dalton Trans.*, vol. 43, no. 23, pp. 8933–8939, May 2014, doi: 10.1039/C4DT00467A.

[120] S. Nishihama, K. Onishi, and K. Yoshizuka, “Selective Recovery Process of Lithium from Seawater Using Integrated Ion Exchange Methods,” *Solvent Extr. Ion Exch.*, vol. 29, no. 3, pp. 421–431, May 2011, doi: 10.1080/07366299.2011.573435.

[121] H. Bukowsky, E. Uhlemann, and D. Steinborn, “The recovery of pure lithium chloride from ‘brines’ containing higher contents of calcium chloride and magnesium chloride,” *Hydrometallurgy*, vol. 27, no. 3, pp. 317–325, Dec. 1991, doi: 10.1016/0304-386X(91)90056-R.

[122] S. Gmar and A. Chagnes, “Recent advances on electrodialysis for the recovery of lithium from primary and secondary resources,” *Hydrometallurgy*, vol. 189, p. 105124, Nov. 2019, doi: 10.1016/j.hydromet.2019.105124.

[123] W. R. Torres, N. C. Zeballos, and V. Flexer, “Effect of [Na+]/[Li+] concentration ratios in brines on lithium carbonate production through membrane electrolysis,” *Faraday Discuss.*, vol. 247, no. 0, pp. 101–124, Oct. 2023, doi: 10.1039/D3FD00051F.

[124] G. A. Marinkina, A. S. Zanina, S. I. Shergina, I. E. Sokolov, and I. L. Kotlyarevskii, “Effective extractants for the extraction of lithium from aqueous solutions containing sodium and potassium compounds,” *Bull. Russ. Acad. Sci. Div. Chem. Sci.*, vol. 41, no. 6, pp. 1015–1020, Jun. 1992, doi: 10.1007/BF00866576.

[125] C. H. Díaz Nieto, K. Rabaey, and V. Flexer, “Membrane electrolysis for the removal of Na+ from brines for the subsequent recovery of lithium salts,” *Sep. Purif. Technol.*, vol. 252, p. 117410, Dec. 2020, doi: 10.1016/j.seppur.2020.117410.

[126] C. H. Díaz Nieto, N. A. Palacios, K. Verbeeck, A. Prévoteau, K. Rabaey, and V. Flexer, “Membrane electrolysis for the removal of Mg2+ and Ca2+ from lithium rich brines,” *Water Res.*, vol. 154, pp. 117–124, May 2019, doi: 10.1016/j.watres.2019.01.050.

[127] P. M. Brown and S. J. Beckerman, “Production of lithium metal grade lithium chloride from lithium-containing brine,” US4980136A, Dec. 25, 1990 Accessed: Jan. 26, 2022. [Online].Available:https://patents.google.com/patent/US4980136/en?oq=production+of+lithium+metal+grade+lithium+chloride+from+lithium+containing+brine

# 2 Chapter 2: Boron extraction from the salar de Hombre Muerto brines by alcohols


2.1 Introduction ..... 97

2.2 Material and methods ..... 98

2.2.1 Materials ..... 98

2.2.2 Methods ..... 101

2.2.2.1 Solvent extraction and stripping ..... 101

2.2.2.2 Analyses ..... 102

2.3 Results and discussions ..... 105

2.3.1 Boron speciation calculations ..... 105

2.3.2 Boron extraction by conventional solvents and DESs ..... 109

2.3.2.1 Influence of the diluent on boron extraction ..... 110

2.3.2.2 Influence of the extractant ..... 112

2.3.2.3 Influence of the pH ..... 115

2.3.2.4 Boron stripping ..... 121

2.3.3 Optimization of boron extraction and stripping conditions in the presence of 2-butyloctan-1-ol as extractant ..... 124

2.3.3.1 Boron extraction and impurities co-extraction ..... 124

2.3.3.2 Boron stripping ..... 127

2.3.4 Nature of the extracted complex ..... 129

2.3.5 Boron crystallization ..... 132

2.3.6 Flowsheet for boron extraction and valorization as borax ..... 134

2.4 Conclusion ..... 139

References ..... 141

## 2.1 Introduction

Our daily life is surrounded by boron-based compounds or materials such as detergents, fertilizers, glasses and ceramics. Nowadays, the huge demand of boron will be responsible for large boron extraction from boron-rich continental brines as those of the salar de Hombre Muerto in the northwestern Argentina. Moreover, boron extraction from brines contributes to reduce the impurities before lithium extraction from these sources [1]. It is therefore of great importance to investigate different routes to extract and valorize boron from brines.

This work distinguishes itself within the field due to its focus on a novel approach to boron extraction from brines. Unlike conventional methods reliant on solar evaporation for brine concentration before extraction, the study targets direct boron extraction from native brines. Most future lithium production plants are anticipated to adopt technologies that bypass solar evaporation (Direct Lithium Extraction), emphasizing the need to extract boron directly from these brines a facet rarely explored in prior studies. The aim is to identify a highly efficient and selective extraction solvent capable of recovering and maximizing the value of boron as pure boric acid or borax, without relying on solar evaporation. This introduces a new pathway for obtaining top-quality boric acid or borax directly from brines, offering a supplementary approach to the prevalent method of boron extraction. Additionally, while solvent extraction for boron retrieval from brine has encountered challenges, notably concerning alcohol solubility within the brine leading to increased effluent treatment and extractant consumption, a crucial breakthrough has been uncovered. The selected alcohol demonstrates notably lower solubility in brine compared to conventional boron extractants used in such processes, addressing a key limitation in this field. Moreover, the study breaks new ground by delving into the intricate physicochemistry of boron extraction by alcohols. Unlike previous research that often focused solely on the presence of boric acid in brines, the approach considers the complex boron speciation within the brine. This comprehensive analysis extends beyond boron to encompass the myriad of other elements present in the brine. The findings highlight the nuanced interplay between boron extraction, pH variations, and the co-extraction of elements like magnesium and calcium at different pH values. Consequently, this study contributes insights into the intricate physicochemical dynamics involved in boron extraction, elucidating its interactions with other impurities present in the brine.

These objectives are achieved in this chapter by selecting from the literature the most relevant aliphatic alcohols and alcohols-based deep eutectic solvents (DESs) to investigate

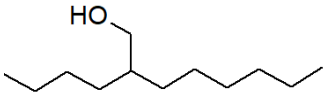
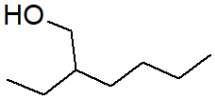
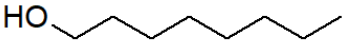
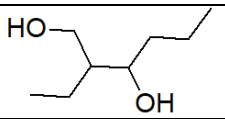
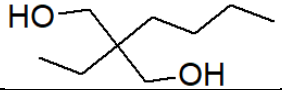
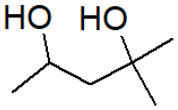
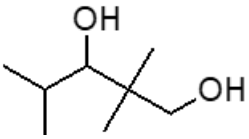
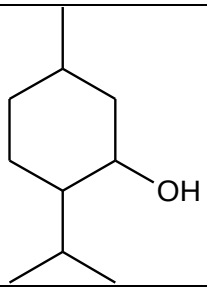
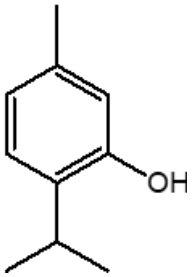
boron extraction from two native brines sourced from the salar de Hombre Muerto in Argentina, alongside a synthetic brine simulating these native compositions. These investigations delve into the influence of the nature of the diluent and alcohol, alcohol concentration, organic to aqueous phase volume ratios (O/A), pH, and temperature on boron extraction efficiency, selectivity of boron towards calcium, magnesium, sodium, lithium, and potassium, alcohol solubility in brines and water solubility in organic phases. Thereafter, the efficient boron extraction conditions are used to develop a continuous countercurrent extraction process. Boron stripping from the loaded organic phases is also studied by considering three stripping solutions including hydrochloric acid, sodium hydroxide and deionized water. Then, the optimal stripping conditions of boron are used to strip boron efficiently and valorize it as borax by crystallization. Finaly, a flowsheet gathering boron extraction, stripping and crystallization is proposed for efficient boron processing from the salar de Hombre Muerto brines.

## 2.2 Material and methods

### 2.2.1 Materials

Mono alcohols including octan-1-ol (Oc, purity=99%), 2-butyloctan-1-ol (BOc, purity=95%), 2-ethylhexan-1-ol (EH, purity=99.6%), diols including 2-methylpentane-2,4-diol (MPD, purity =99%), 2-ethylhexane-1,3-diol (EHD, purity=97%) 2-butyl-2-ethylpropane-1,3-diol (BEPD, purity=99%) and 2,2,4-triméthylpentane-1,3-diol (TMPD, purity=99%), and thymol (Thy, purity=98.5%) were purchased from Sigma-Aldrich (France) while menthol (Men, purity=98.9%) was purchased from VWR (France). Kerosene (Low odour) and *m*-xylene (purity=99%) were also provided by Sigma-Aldrich (France) while toluene (purity=100%) was supplied by VWR (France). Sulfonated kerosene (sulfur content = 0.69 mg $kg^{-1}$) was purchased from Maoming Taihong Petrochemical co., Ltd. The chemical structures and dynamic viscosities at 25 °C of the above-mentioned alcohols are reported in Table 2. 1.

**Table 2. 1:** Structures and dynamic viscosities of the selected alcohols at 25 °C (η=dynamic viscosity of pure alcohol).

| Alcohol | Number of carbon atoms in the alkyl chain | Structure | η (mPa s) |
|---|---|---|---|
| 2-butyloctan-1-ol (BOc) | 12 |  | 18 |
| 2-ethylhexan-1-ol (EH) | 8 |  | 7.5 |
| octan-1-ol (Oc) | 8 |  | 7.3 |
| 2-ethylhexane-1,3-diol (EHD) | 8 |  | 186.5 |
| 2-butyl-2-ethylpropane-1,3-diol (BEPD) | 9 |  | Solid |
| 2-methylpentane-2,4-diol (MPD) | 6 |  | 27.6 |
| 2,2,4-triméthylpentane-1,3-diol (TMPD) | 8 |  | Solid |
| Menthol (Men) | 10 |  | Solid |
| Thymol (Thy) | 10 |  | Solid |

The brines of the Salar de Hombre Muerto (Argentina) contain a large variety of ions including lithium, boron, potassium, magnesium, calcium, sodium, chloride, sulfate, strontium, and iron ([2], [3]). These brines are highly concentrated in monovalent and divalent elements as shown in Table 2.2. Investigations on the influence of the nature of alcohols and diluents on boron extraction were performed with a synthetic brine (SB) which the composition was similar

to the composition of a native brine denoted native brine 1 (NB1) because the native brine was not enough to perform all experiments. The similarity between SB and NB1 was confirmed by extraction experiments under the same extraction conditions, *i.e.* same concentration of extractant, phase volume ratio O/A, pH and temperature, which showed no significant difference in the extraction efficiency of boron between the native brine 1 (NB1) and the synthetic brine (SB). Afterwards, the influence of the nature of the brine on the extraction properties of the selected alcohol (2-butyloctan-1-ol) was investigated for two native brines of the Salar de Hombre Muerto (Argentina) referred as native brine 1 (NB1) and native brine 2 (NB2) as well as the synthetic brine (SB) mimicking NB1(Table 2.2).

Magnesium chloride ($MgCl_2$, purity=98%, Sigma-Aldrich), calcium chloride ($CaCl_2$, purity=90%, Sigma-Aldrich), boric acid ($H_3BO_3$, Sigma-Aldrich, purity=99.5%), lithium sulfate ($Li_2SO_4$, Sigma-Aldrich, purity=98.5%), sodium chloride (NaCl, VWR, purity=99.9%) and potassium chloride (KCl, VWR, purity=99.5%) were dissolved in deionized water produced with the Puranity TU water system (VWR, resistivity=18 MΩ.cm) to prepare the synthetic brine (SB) which mimics NB1. Iron and strontium were not accounted for preparing the synthetic brine as their concentrations were lower than 0.1 g $L^{-1}$. Hydrochloric acid (HCl, purity=37%, Sigma-Aldrich) and sodium hydroxide (NaOH, purity=99%, VWR) were used as received to adjust the pH of the synthetic brine.

**Table 2. 2:** Composition, pH, ionic strength (I) and density at room temperature (25±0.5 °C) of native brine 1 (NB1), native brine 2 (NB2) and synthetic brine (SB). The ionic strength was determined by considering the speciation calculated with the Phreeqc software (databases: Pitzer, Core10, Amm and Minteq.V4).

| Brine | pH | I | Density | Concentration (g $L^{-1}$) | | | | | | | | | |
|---|---|---|---|---|---|---|---|---|---|---|---|---|---|
| | | (mol $kg_w^{-1}$) | (g $cm^{-3}$) | Li | Ca | Mg | B | Na | Sr | K | Fe | $Cl^-$ | $SO_4^{2-}$ |
| NB1 | 6.9 | 3.6 | 1.2 | 1.27 | 0.68 | 3.09 | 1.62 | 103.24 | 0.079 | 14.21 | 0.001 | 182.85 | 11.15 |
| NB2 | 7.5 | 3.46 | 1.2 | 0.75 | 0.1 | 2.51 | 0.54 | 103.29 | 0 | 7.8 | 0 | 176.15 | 14.13 |
| SB | 5.5 | 3.6 | 1.2 | 1.27 | 0.68 | 3.09 | 1.62 | 103.24 | 0 | 14.21 | 0 | 182.25 | 8.78 |

## 2.2.2 Methods

### 2.2.2.1 Solvent extraction and stripping

The first investigations devoted to identify the efficient extraction solvent were carried out at 35 °C because the shaker could not control the temperature at 25 °C during the summer time (the room temperature in our lab ranged during our experiments between 24 °C and 30°C). However, the shaker could control accurately the temperature at 35 °C. Therefore, the temperature was accurately controlled at 35 °C during the extraction solvent experiments. These studies were performed by mixing 5 mL of the synthetic brine (SB) with volumes of organic phases ranging from 5 to 35 mL depending on the phase volume ratio O/A. The organic phases contained 1 mol $L^{-1}$ alcohols (2-butyloctan-1-ol (BOc), 2-ethylhexan-1-ol (EH), octan-1-ol (Oc), 2-ethylhexane-1,3-diol (EHD), 2-methylpentane-2,4-diol (MPD) or 2-butyl-2-ethylpropane-1,3-diol (BEPD)) diluted in kerosene, sulfonated kerosene or a mixture of kerosene and toluene or *m*-xylene. They also contained alcohols-based deep eutectic solvents (DESs) such as Men:MPD, Men:TMPD, Thy:MPD and Thy:TMPD, prepared following the method reported by Almustafa et al. [4] which consists in heating 2:1 molar ratio of each DES at 60 °C and then cool the mixture at room temperature before extraction experiments.

The organic and aqueous phases were contacted in centrifuge tubes (50 mL) during the extraction and the stripping experiments in a thermostated shaker (Gherardt Laboshake THL500/1) at 200 rpm for 4 hours and 2 hours, respectively, for organic phases containing conventional extraction solvents (alcohols diluted in kerosene, sulfonated kerosene or a mixture of kerosene and toluene or *m*-xylene). Conversely, extraction and stripping experiments with DESs required 1 hour shaking to reach the steady state. Indeed, preliminary experiments showed that the steady state was reached under these experimental conditions (Figure A. 1−A. 4 in appendix for 1 mol $L^{-1}$ 2-butyloctan-1-ol diluted in kerosene for the sake of illustration for conventional solvents). It is expected that more intensive mixing/shaking will make the equilibrium to be reached faster. However, we chose to work under reproducible experimental conditions, and in this sense, a lab shaker did not provide intensive mixing, but it allowed for high reproducibility. Afterwards, the biphasic mixtures were centrifugated at 3,000 rpm for 2 min by using a SIGMA 3-16L centrifuge to separate the organic and the aqueous phases. The aqueous droplets were removed from the organic phases by filtering with 0.20 µm minisart made of polypropylene (Sartorius, France) and the organic droplets were removed

from the aqueous phases by filtering with 0.20 µm minisart made of regenerated cellulose (Sartorius, France).

The pH values of the aqueous phases were adjusted by adding 0.5 mol $L^{-1}$ hydrochloric acid (HCl) or 2 mol $L^{-1}$ sodium hydroxide (NaOH). After extraction, the boron-loaded organic phase was stripped with hydrochloric acid (HCl), sodium hydroxide (NaOH) or deionized water at O/A=4 and 35 °C for boron-loaded conventional solvent, and O/A=1 and 25 °C for DESs .

Thereafter, 2-butyloctan-1-ol was selected for further investigations despite the low extraction efficiency (55%; extraction conditions: 1 mol $L^{-1}$ 2-butyloctan-1-ol diluted in kerosene, O/A=4, pH=5.5 and 35 °C) because 2-butyloctan-1-ol exhibited low solubility in the synthetic brine (SB) and it can be solubilized in kerosene without adding toluene. Batch solvent extraction experiments were carried out at 25 °C since no significant influence of the temperature on the extraction efficiency was observed at 25 °C, 35 °C, 40°C and 50 °C in preliminary experiments (Table A. 9 in appendix). During the extraction tests, synthetic or native brines were mixed with the organic phase at different phase volume ratios (O/A) in centrifuge tubes (50 mL). The organic phases contained 2-butyloctan-1-ol diluted in kerosene at different concentrations. Extraction of boron from the synthetic brine (SB) and stripping tests of boron were performed in 500 mL glass vessels under stirring during 2 hours for the extraction tests and 1 hour for the stripping tests at 700 rpm by using a three-blade propeller (higher stirring was necessary to ensure good mixing in 500 mL-glass vessels). Then, the organic-aqueous phases mixtures were settled in 500 mL separating funnels for 30 min. For these tests, the extraction solvent was composed of 2 mol $L^{-1}$ 2-butyloctan-1-ol diluted in kerosene and 0.1 mol $L^{-1}$ NaOH was used as stripping solution. All extraction and stripping experiments were carried out at 25 °C and O/A=4. The reproducibility of these experiments was checked by performing 10 times extraction and stripping tests in centrifuge tubes (see experimental conditions above) under the same experimental conditions. The same values for the extraction and the stripping efficiencies were obtained. The extraction and stripping equilibria were reached faster when the tests were performed in the glass vessels under stirring with a three-blade propeller at 700 rpm.

#### 2.2.2.2 Analyses

Exactly 1 mL of aqueous phase was sampled and diluted in 2% (vol.) nitric acid prepared by dilution of 65% nitric acid (Sigma-Aldrich) in deionized water (resistivity=18 MΩ.cm). Elemental analyses of the samples were performed with a microwave plasma-atomic emission

spectrometer (MP-AES model 4210, Agilent, France). The analyses were confirmed by inductively coupled plasma-optical emission spectroscopy (ICP-OES model 7400 Duo, Thermo Fisher Scientific, France). ICP standards containing 1,000 mg $L^{-1}$ boron, potassium, magnesium, sodium, calcium and lithium were purchased from Sigma-Aldrich. The samples were diluted 100 times and 1,000 times in 2% (vol.) nitric acid for calcium analyses and for the other elements, respectively. It was inferred by chromatographic analyses (Dionex ICS 900 ™ IonPac™ AS22) that chloride and sulfate ions were not significantly extracted during liquid-liquid extraction experiments, and therefore, their concentrations in the samples were the same as in brines. The matrix effect was avoided by adding appropriate concentrations of chloride, sulfate and sodium in the standards so that their concentrations matched with those found in the samples to analyze ([5], [6], [7], [8]). Chloride, sulfate and sodium concentrations in the matrices were set by using hydrochloric acid (purity=37%, Sigma-Aldrich), sulfuric acid (purity=96%, Sigma-Aldrich) and 26 g $L^{-1}$ sodium chloride, respectively. For MP-AES analyses, concentrations of lithium, boron, potassium, magnesium, calcium and sodium were determined at 670.784 nm, 249.677 nm, 766.491 nm, 518.360 nm, 393.366 nm and 568.820 nm, respectively. For ICP-OES analyses, the following wavelengths were used: 670.784 nm (lithium), 249.773 nm (boron), 769.896 nm (potassium), 279.553 nm (magnesium), 315.887 nm (calcium) and 589.592 nm (sodium). The method used for elemental analyses is detailed in the section “Development of elemental analysis method” in appendix A.

Mass-balances were checked by performing quantitative elemental analyses in the stripping solution after full back-extraction from the organic phase.

Distribution ratio of the element e ($D_e$), extraction efficiency of the element e ($E_e$ (%)), selectivity coefficient of the element $e_1$ towards the element $e_2$ ($S_{e_1/e_2}$) and stripping efficiency of boron ($SE_B$) were calculated as follows:

$$D_e = \frac{\overline{[e]}}{[e]} \tag{2. 1}$$

$$E_e(\%) = \frac{\overline{[e]} \times \overline{V}}{[e] \times V + \overline{[e]} \times \overline{V}} \times 100 \tag{2. 2}$$

where $[e]$ and $\overline{[e]}$ are the concentrations of the element $e$ in the aqueous phase and in the organic phase at equilibrium, respectively. $\overline{V}$ and $V$ denote the volume of the organic and the aqueous phases, respectively.

By combining Equations 2. 1 and 2. 2, the extraction efficiency can be rewritten as follows:

$$E_e(\%) = \frac{D_e \times \nu}{1 + D_e \times \nu} \times 100 \quad (2.\ 3)$$

where $\nu$=O/A is the phase volume ratio between the organic and the aqueous phases (O and A stand for the organic phase volume and the aqueous phase volume, respectively).

The selectivity coefficient for $e_1$ towards $e_2$ was calculated as follows:

$$S_{e_1/e_2} = \frac{D_{e_1}}{D_{e_2}} \quad (2.\ 4)$$

where $D_{e_1}$ and $D_{e_2}$ are the distribution ratios of element 1 and element 2, respectively.

The boron stripping efficiency ($SE_B$) was calculated as:

$$SE_B(\%) = \frac{[B]' \times V'}{\overline{[B]'} \times \overline{V}' + [B]' \times V'} \times 100 \quad (2.\ 5)$$

$[B]'$ and $\overline{[B]'}$ are the boron concentrations in the stripping solution and in the organic phase at equilibrium during the stripping step. $\overline{V}'$ and $V'$ represent the volume of the organic and the aqueous phases.

The standard deviation on the extraction and stripping efficiencies, and the error on the analytical method were estimated to be within 4% by repeating the experiments three times and by analyzing the synthetic brine 10 times, respectively.

Dynamic viscosities of the organic phases before and after extraction were determined at 25 °C and 35 °C by using a Stabinger viscometer™ (Anton Paar SVM™ 2001). The viscometer was calibrated with the viscosity standards APN26, APS3, APN415 and APN7.5 provided by Anton Paar. Each sample was analyzed twice. The viscometer cell was cleaned by rinsing with pure ethanol and dried with air after each viscosity measurement.

Water contents in organic phases after extraction were analyzed by using a volumetric Karl Fisher Titrator (Mettler Toledo, France) after calibration with a standard containing 1% water (Sigma-Aldrich). These analyses were performed with HYDRANAL Composite 5 and Methanol Rapid (Sigma-Aldrich).

The solubilities of the alcohols ($S_{alc}$) in the aqueous phase after extraction were determined by Total Organic Carbon analyses (Shimadzu TOC-VCSH), as follows:

$$S_{alc} = \frac{(TOC_S - TOC_D)}{X} \quad (2.\ 6)$$

where $TOC_S$ is the total organic carbon of the extraction solvent (alcohol + diluent), $TOC_D$ is the Total Organic Carbon of the diluent and X is the mass fraction of carbon in the alcohol.

Solubilities of DESs ($S_{DES}$) were determined by the ratio between total organic carbon of the DES ($TOC_{DES}$) and the mass fraction of carbon in DES ($X_{DES}$).

## 2.3 Results and discussions

### 2.3.1 Boron speciation calculations

Speciation in aqueous phases plays an important role in solvent extraction since it can influence (increase or decrease) the extraction efficiency and the selectivity of the extractant. Boron speciation is complex and many different species can exist in solution depending on pH and concentrations of boron and other elements in the aqueous solutions [9]. The presence of boric acid, borate anions and polyborate species, *i.e.* diborate, triborate, tetraborate and pentaborate anions, in aqueous solutions containing 5g $L^{-1}$ boron in pure water was reported in the literature ([10],[11], [12]).

In this work, speciation calculations in aqueous phases were performed on a PC under Windows 11 with the free software Phreeqc ver. 3.7 which is computer program written in the C and $C^{++}$ programming languages [13]. The distribution of the species in the aqueous phases was performed by using the two ion-association aqueous models (the Lawrence Livermore National Laboratory model and WATEQ4F), the Pitzer specific-ion-interaction aqueous model or the SIT (Specific ion Interaction Theory) aqueous model depending on the ionic strength of the aqueous phases. The selected aqueous model was used to calculate the activity of the species which is the thermodynamic property needed to determine the concentration of species within the aqueous phases. For this purpose, the aqueous model required concentration of elements, pH, temperature, density and redox of the aqueous phase as well as the equilibrium constants or reaction enthalpies of the chemical reactions which occur in the aqueous phases. Therefore, the selected equilibrium constants and reaction enthalpies data must be reliable and consistent to provide accurate calculations.

Boron speciation in the aqueous phases was calculated by using the Pitzer and Minteq.V4 databases. The thermodynamic constants and the corresponding chemical reactions included in the databases for speciation calculations are reported in Table 2. 3. Speciation diagrams were calculated with PhreePlot which is a charting and plotting extension of Phreeqc for creating commonly needed types of diagrams. Boron speciation calculations with Phreeqc were

validated with literature data of 0.1 mol $kg^{-1}$ boron speciation diagrams in pure water [9], and reported in Figure 2. 1. Moreover, the influence of boron concentration on the distribution of boron species as a function of pH was investigated with aqueous solutions containing 0.15 mol $L^{-1}$ and 1.5 mol $L^{-1}$ boron in pure water. As shown in Figure 2. 2, pH strongly influences boron speciation since at acidic pH boric acid is the only species which exists in the solutions while at alkaline pH borates and polyborates are more present. In addition, when boron concentration is ten time higher, *i.e.* concentration increased from 0.15 mol $L^{-1}$ to 1.5 mol $L^{-1}$, sharp increase in the concentration of triborate and tretaborate anions ($B_3O_3(OH)_4^-$, and $B_4O_5(OH)_4^{2-}$) is observed at pH=6-10. This is attributed to the interaction between boric acid molecules to form polyborate anions at higher boron concentration in water [14].

**Table 2. 3:** Chemical reactions and thermodynamic constants used for speciation calculations of boron with Phreeqc (databases: Pitzer and Minteq.V4).

| Chemical reaction | log (K) |
|---|---|
| $H_3BO_3 \rightleftarrows H_3BO_3$ | 0 |
| $H_3BO_3 + H_2O \rightleftarrows B(OH)_4^- + H^+$ | $-9.2$ |
| $H_3BO_3 \rightleftarrows H_2BO_3^- + H^+$ | $-9.2$ |
| $2H_3BO_3 \rightleftarrows H_5(BO_3)_2^- + H^+$ | $-9.3$ |
| $3H_3BO_3 \rightleftarrows H_8(BO_3)_3^- + H^+$ | $-7.3$ |
| $3H_3BO_3 \rightleftarrows B_3O_3(OH)_4^- + 2H_2O + H^+$ | $-7.5$ |
| $4H_3BO_3 \rightleftarrows B_4O_5(OH)_4^{2-} + 3H_2O + 2H^+$ | $-16.1$ |
| $Ca^{2+} + H_3BO_3 + H_2O \rightleftarrows CaB(OH)_4^+ + H^+$ | $-7.6$ |
| $Ca^{2+} + H_3BO_3 \rightleftarrows CaH_2BO_3^+ + H^+$ | $-7.5$ |
| $Mg^{2+} + H_3BO_3 + H_2O \rightleftarrows MgB(OH)_4^+ + H^+$ | $-7.8$ |
| $Mg^{2+} + H_3BO_3 \rightleftarrows MgH_2BO_3^+ + H^+$ | $-7.7$ |
| $Na^+ + H_3BO_3 \rightleftarrows NaH_2BO_3 + H^+$ | $-9$ |

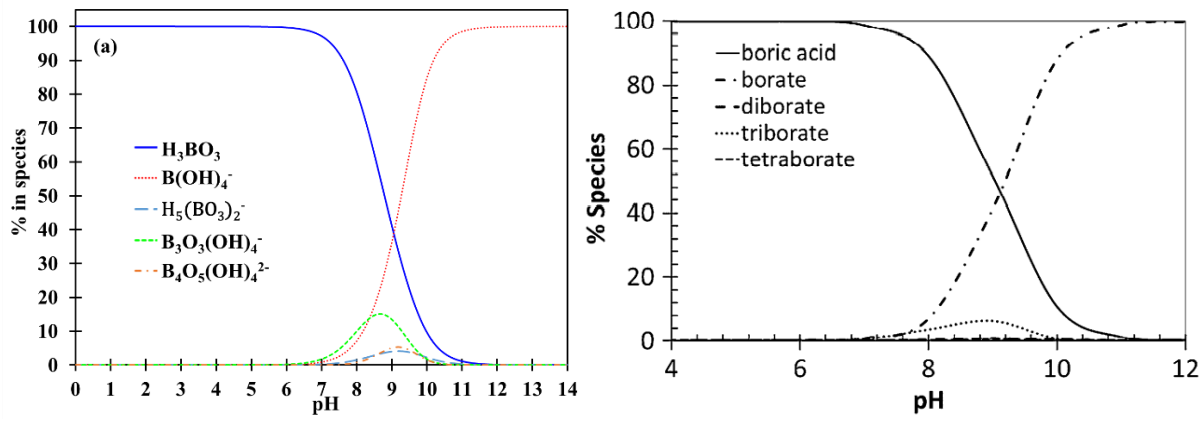



**Figure 2. 1:** Comparison of boron speciation in pure water (a) calculated by using the Phreeqc software with the Pitzer and Minteq.V4 databases and (b) reported in literature [9], [Boron] = 0.1 mol $kg^{-1}$) .

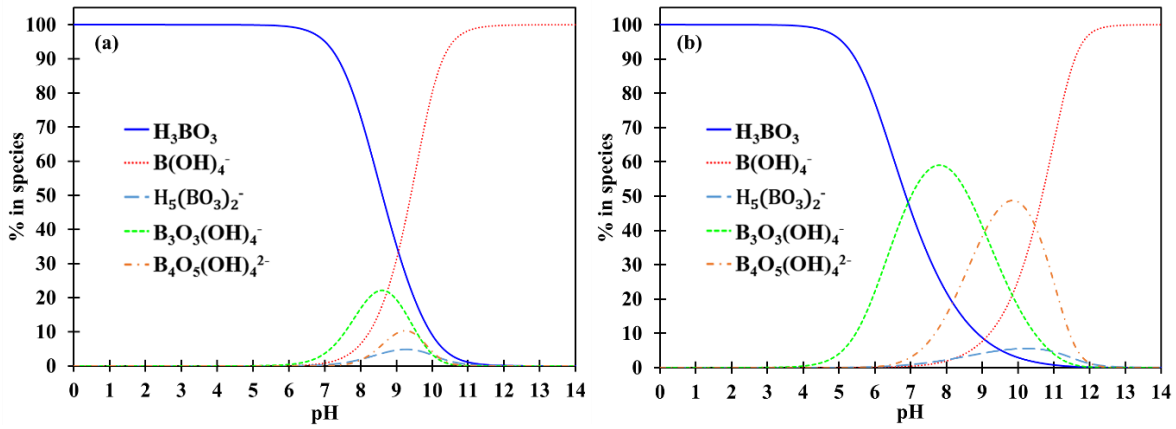



**Figure 2. 2:** Distribution of boron species as a function of pH for (a) 0.15 mol $L^{-1}$ boron and (b) 1.5 mol $L^{-1}$ boron in pure water. Speciation calculation performed by using the Phreeqc software with the Pitzer and Minteq.V4 databases.

The influence of the nature of the brine and pH on boron speciation in the brines of the salar de Hombre Muerto were investigated. As shown in Figure 2. 3, the speciation diagrams of boron as a function of pH in the brines reveal that the physicochemistry of boron speciation is intricate since 12 boron species exist in the brines in different concentrations depending on the pH. Boric acid, borate and polyborate anions as well as calcium, magnesium, and sodium borates are formed in the brines. Speciation diagrams of boron in the native brine 1 (NB1) and synthetic brine (SB) were similar since the composition of SB mimics NB1. Irrespective of the nature of the brine, no influence of pH on boron speciation at pH=1-5.5 is observed since boron exists only as boric acid in NB1 and NB2. However, at pH>5.5 the decrease in the concentration of boric acid is responsible for the increase in the concentration of borates and polyborates anions which react with sodium, calcium and magnesium to form sodium-boron, calcium-boron and magnesium-boron species, respectively. It is also important to point out that

the concentrations of polyborates species are higher in NB1 than NB2 because NB1 is the most boron concentrated brine (Table 2. 2). Calcium, potassium, lithium, magnesium and sodium speciation diagrams in the synthetic brine (SB) were also performed and reported in Figures A. 5−A. 9 (Pitzer, Core10, Amm and minteq.v4 databases were used).

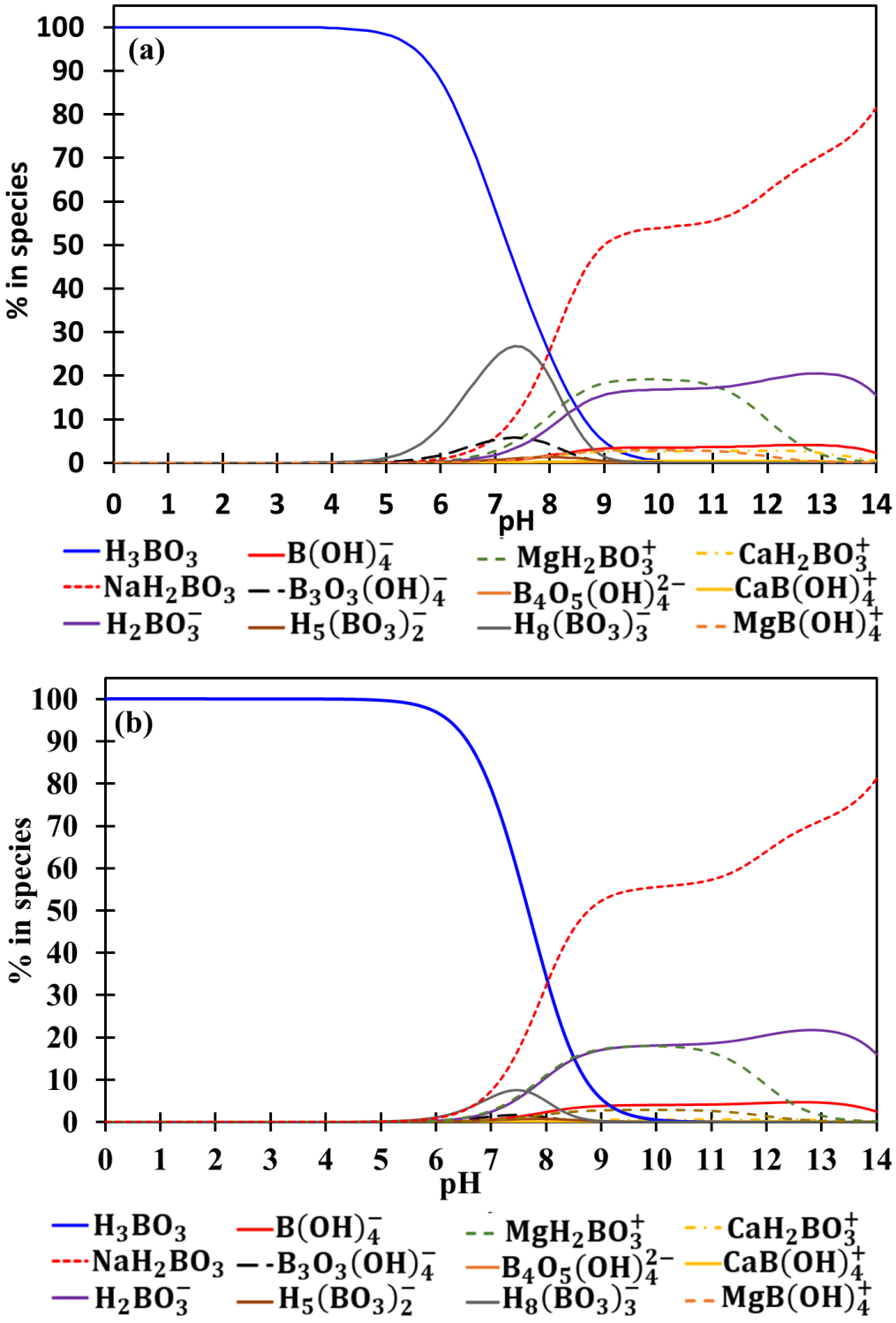


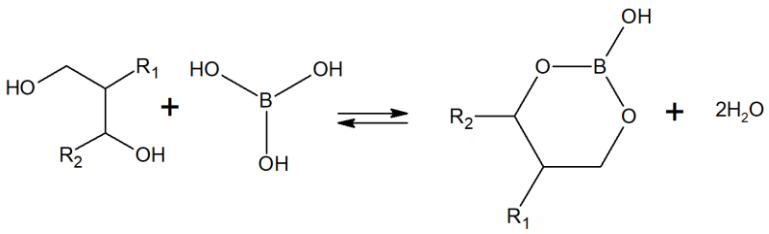

**Figure 2. 3:** Boron speciation vs. pH in (a) the synthetic brine or the native brine 1 and (b) the native brine 2.

## 2.3.2 Boron extraction by conventional solvents and DESs

Boron extraction from brine was investigated by using two types of extractants:

- **Conventional extraction solvents** composed of aliphatic mono alcohols or diols diluted in kerosene, sulfonated kerosene or a mixture of kerosene and toluene or *m*-xylene.
- **Unconventional extraction solvent**s composed of alcohols-based deep eutectic solvents (DESs) containing hydrogen bond donors (HBD) and hydrogen bond acceptors (HBA) that are diols and menthol or thymol, respectively. HBD and HBA are used as extractants and diluents, respectively.

Several authors ([15], [16], [17], [18], [19]) reported that boron is extracted as boric acid by alcohol-based conventional extraction solvents or DESs ([4], [20]) from low to high ionic strength aqueous solutions by an esterification reaction. For instance, Fan et al. [21] mentioned that the extraction of boric acid with 2-ethylhexane-1,3-diol occurs according to the following esterification reaction:




(2. 7)

where $R_1$ and $R_2$ are ethyl and propyl groups, respectively.

Conversely, Zhang et al. [22] assumed that an esterification cannot explain boron extraction by alcohols as the rate of esterification may be too slow during solvent extraction. Therefore, they expected that boron extraction under acidic conditions occurs through the following classical solvation equilibrium already reported in other studies ([16], [23], [24]):

$$B(OH)_3 + n\,\overline{R(OH)_m} \rightleftarrows \overline{B(OH)_3.nR(OH)_m} \qquad (2.\ 8)$$

where $\overline{R(OH)_m}$ is the alcohol (mono alcohol for m=1 and polyalcohol for m>1) in the organic phase and n is the number of alcohol molecules involved in the extraction.

From Equation 2. 8, the equations of the extraction constant ($K_{ex}$) and the distribution ratio of boron ($D_B$) are follows:

$$K_{ex} = \frac{\overline{[B(OH)_3.nR(OH)_m]}}{[B(OH)_3] \times \overline{[R(OH)_m]}^n} \quad (2.\ 9)$$

$$D_B = \frac{\overline{[B(OH)_3.nR(OH)_m]}}{[B(OH)_3]} \quad (2.\ 10)$$

By combining Equations 2. 9 and 2. 10, the extraction constant ($K_{ex}$) can be rewritten as follows:

$$K_{ex} = \frac{D_B}{\overline{[R(OH)_m]}^n} \quad (2.\ 11)$$

By taking the logarithm form of Equation 2. 11, the distribution ratio of boron ($D_B$) can be rewritten as follows:

$$\log(D_B) = \log(K_{ex}) + n \log(\overline{[R(OH)_m]}) \quad (2.\ 12)$$

The following equation obtained by combining Equations 2. 3 and 2. 12, shows that the extraction efficiency of boron depends on the temperature, the phase volume ratio O/A, the nature and the concentration of alcohol in the organic phase at the equilibrium:

$$\log\left(\frac{E_B}{100 - E_B}\right) = \log(K_{ex}(T)) + n \log(\overline{[R(OH)_m]}) + \mathrm{Log}(O/A) \quad (2.\ 13)$$

In order to select the most suitable extraction solvent for boron, extraction properties of the conventional solvents and alcohols-based deep eutectic solvents (DESs) were investigated by using the synthetic brine (SB) which the composition is reported in Table 2. 2. These investigations were conducted to explore the influence of the organic to aqueous phase volume ratios (O/A), the nature of the diluents and the extractants on boron extraction efficiency and impurities co-extraction. The effect of these factors on the viscosity of the loaded-organic phase, alcohol or DESs solubilities in the brine, water solubility in organic phases and the recyclability on the extraction solvents at constant temperature was also investigated in this work. Although pH does not directly affect the extraction efficiency as shown in Equation 2. 13, the influence of pH was also studied since boron speciation depends on pH (Figure 2. 3a), and can affect boron extraction efficiency and selectivity.

#### 2.3.2.1 Influence of the diluent on boron extraction

Preliminary experiments were carried out to investigate the solubility of the alcohols reported in Table 2. 1 in kerosene, sulfonated kerosene, toluene and *m*-xylene. All mono alcohols and diols are soluble in toluene and *m*-xylene at 1 mol $L^{-1}$ or 2 mol $L^{-1}$, showing the good solvation of these alcohols by these diluents. Conversely, diols (EHD, MPD and BEPD,

see full nomenclature and chemical formulas in Table 2. 1) are not soluble in kerosene or sulfonated kerosene at 1 mol $L^{-1}$. The much lower solubility of diols may be explained by the tendency of diols to form highly stable dimers, or even species with higher aggregation number. Aggregation of the alcohol molecules may reduce their solubility in low dielectric solvents such as kerosene and sulfonated kerosene. Finally, it was possible to solubilize 1 mol $L^{-1}$ diols in the mixture of 40% (wt) kerosene and 60% (wt) toluene as well as in the mixture of 40% (wt) kerosene and 60% (wt) *m*-xylene. Therefore, the extraction properties of EH, BOc, Oc, EHD, MPD and BEPD were compared in kerosene, sulfonated kerosene and kerosene modified with 60% (wt) toluene or *m*-xylene.

The extraction efficiencies of boron from the synthetic brine (SB) by 1 mol $L^{-1}$ alcohol diluted in kerosene, sulfonated kerosene and mixed diluents of kerosene with 60% (wt) toluene or 60% (wt) *m*-xylene are reported in Table 2. 4. There is no significant influence of the diluent on boron extraction when mono alcohols (BOc, EH and Oc) or diols (EHD, BEPD and MPD) were used as extractants. Likewise, the addition of toluene or *m*-xylene in the diluent does not significantly influence the water solubility in the extractant. Table 2. 4 shows that alcohols diluted in mixtures of kerosene and toluene or kerosene and *m*-xylene exhibit the lowest viscosities. The viscosity values remain the same before and after boron extraction indicating that the extracted boron does not influence the viscosity of the organic solvents. From these results, kerosene and the mixture 40% (wt) kerosene and 60% (wt) toluene were selected to investigate the influence of mono alcohols and diols, respectively, on boron extraction from the synthetic brine.

**Table 2. 4**: Effect of diluents on boron extraction efficiency ($E_B$), dynamic viscosity (η) and water solubility in the organic phase ($w_{H2O}$) after boron extraction by the extractant 1 mol $L^{-1}$ alcohol. Extraction conditions: O/A=1, pH=1 and 35 °C. ns: not soluble, *i.e.* solubility<1 mol $L^{-1}$.

| Alcohol | Diluents | | | | | | | | | | | |
|---|---|---|---|---|---|---|---|---|---|---|---|---|
| | Kerosene | | | Sulfonated kerosene | | | Kerosene and 60% (wt) toluene | | | Kerosene and 60% (wt) *m*-xylene | | |
| | $E_B$(%) | η (mPa s) | $w_{H2O}$ (%wt) | $E_B$ (%) | η (mPa s) | $w_{H2O}$ (%wt) | $E_B$ (%) | η (mPa s) | $w_{H2O}$ (%wt) | $E_B$ (%) | η (mPa s) | $w_{H2O}$ (%wt) |
| BOc | 22.2 | 2 | 0.1 | 23.5 | 1.7 | 0.1 | 22.2 | 0.8 | 0.2 | 21.7 | 0.9 | 0.1 |
| EH | 23.4 | 1.6 | 0.1 | 17.4 | 1.3 | 0.1 | 17.4 | 0.6 | 0.2 | 22.1 | 0.7 | 0.2 |
| Oc | 10.4 | 1.7 | 0.2 | 9.4 | 1.4 | 0.2 | 9.9 | 0.7 | 0.3 | 14.0 | 0.7 | 0.2 |
| EHD | ns | ns | ns | ns | ns | ns | 97.2 | 0.8 | 0.6 | 96.2 | 0.9 | 0.6 |
| BEPD | ns | ns | ns | ns | ns | ns | 93.7 | 1 | 0.7 | 93.6 | 1.1 | 0.7 |
| MPD | ns | ns | ns | ns | ns | ns | 89.7 | 0.7 | 0.7 | 88.8 | 0.7 | 0.6 |

Table 2. 5 shows that there is no significant influence of HBA, *i.e.* menthol or thymol, on boron extraction by TMPD or MPD. Despite the lowest viscosity and water solubility in the organic phase obtained with thymol-based DESs (Table 2. 5), menthol-based DESs were selected to investigate the influence of the nature of HBD on boron extraction because thymol is the most expensive HBA.

**Table 2. 5:** Effect of HBA on boron extraction efficiency ($E_B$), dynamic viscosity (η) and water solubility in the organic phase ($w_{H2O}$) after boron extraction by DESs. Extraction conditions: O/A=1, pH=5.5 and 25 °C.

| HBD (alcohol) | HBA | | | | | |
|---|---|---|---|---|---|---|
| | Menthol | | | Thymol | | |
| | $E_B$(%) | η (mPa s) | $w_{H2O}$ (%wt) | $E_B$(%) | η (mPa s) | $w_{H2O}$ (%wt) |
| TMPD | 100 | 124 | 2.6 | 100 | 45.5 | 2 |
| MPD | 98 | 68.4 | 3 | 97.3 | 32.7 | 2.6 |

### 2.3.2.2 Influence of the extractant

The nature of the extractant is particularly important in boron extraction process as the extractant controls the efficiency of the process and the purity of the final product. Figures 2. 4 and 2. 5 show the influence of O/A volume ratio on the extraction efficiency of boron by the different extractants diluted in kerosene (Figure 2. 4a) or a mixture of kerosene and 60% (wt) toluene (Figure 2. 4b) and diols-based DESs, respectively. The boron extraction efficiencies

by mono alcohols in kerosene follow the same order (*i.e.*, BOc ~ EH>Oc) which is not significantly affected by the O/A volume ratio (Figure 2. 4a). In contrast, only a slight influence of O/A volume ratio on boron extraction efficiencies is observed at O/A>1 when the diols were used as the extractant. The extraction efficiencies decrease, especially for low values of O/A volume ratios, according to the following orders: EHD>BEPD>MPD (Figure 2. 4 a) and TMPD>MPD (Figure 2. 5).

Regarding the mono alcohols, the highest extraction efficiency of BOc may be attributed to the highest hydrophobicity as the number of carbon atoms in BOc (12 carbon atoms) is greater than in Oc (8 carbon atoms). Among the mono alcohols, EH exhibits higher extraction efficiency than Oc despite the same number of carbon atoms, likely because of the presence of ramifications in the chemical structure of EH, which may contribute to improve the stability of the extracted complex.

DFT calculations reported in literature showed that the two hydroxyl groups in 1,3- diols may stabilize boron in the organic phase by forming a six-member ring species ([30], [33], [34], [25]). Therefore, the presence of two hydroxyl groups in diols increases the extraction efficiency. Similar complexation and similar stabilization effects are expected with TMPD, MPD, EHD and BEPD. The difference in boron extraction efficiency for this class of molecules is not significant and within the experimental error as 99%, 97.4% and 96.4% boron were extracted by EHD, BEPD and MPD at O/A volume ratio of 2, respectively (Figure 2. 4b), and 97.4% and 94.9% extraction efficiencies of boron were reached by Men:TMPD and Men:MPD at O/A=1, respectively (Figure 2. 5).

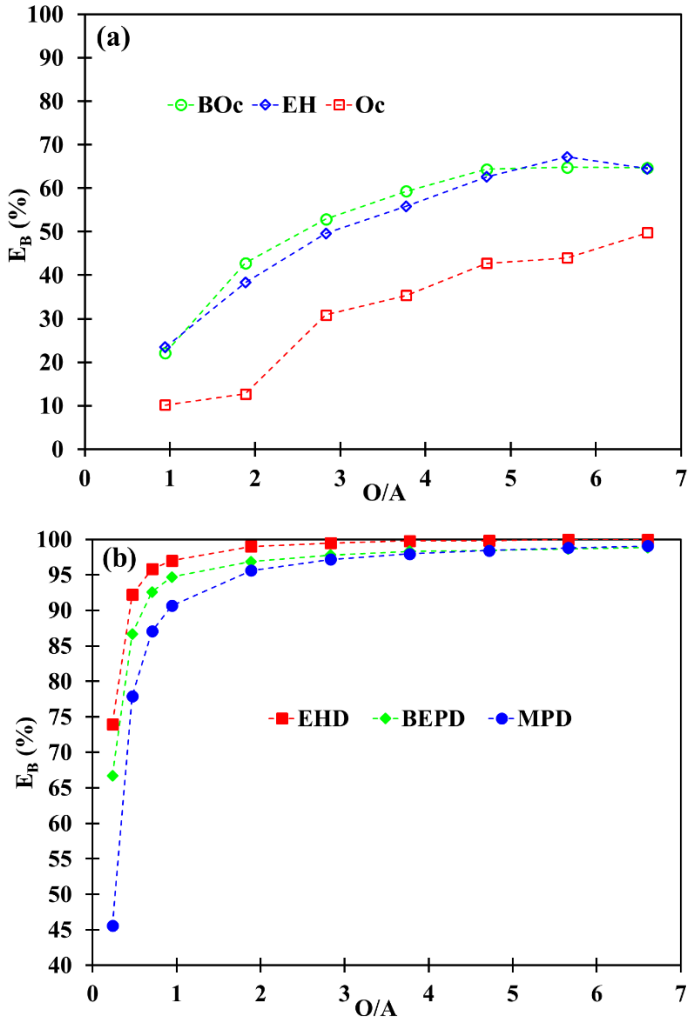



**Figure 2. 4:** Influence of O/A volume ratio on the extraction efficiencies of boron by 1 mol $L^{-1}$ (a) mono alcohols diluted in kerosene and (b) diols diluted in kerosene modified with toluene at pH=1 and 35 °C.

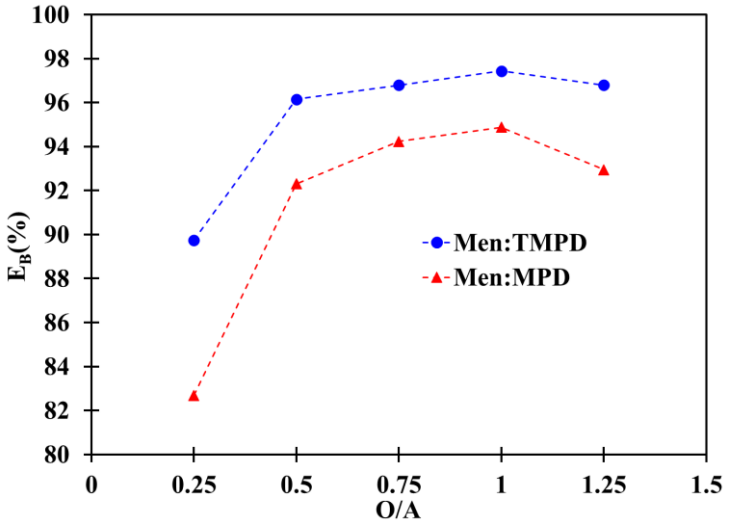



**Figure 2. 5:** Influence of O/A volume ratio on the extraction efficiencies of boron by diols-based DESs (Men:TMPD and Men:MPD) at pH=5.5 and 25 °C.

### 2.3.2.3 Influence of the pH

The extraction properties of the alcohols were studied as a function of pH at a constant phase ratio O/A=0.5 in DESs, O/A=2 in the mixed diluent of kerosene and toluene and at O/A=4 in kerosene so that the extraction efficiencies are high enough to test the influence of pH on extraction efficiency (>30%). Figures 2. 6 and 2. 7 show that the same trend is observed irrespective of the nature of the alcohols. The boron extraction efficiency is constant until pH~5.5. Above this pH, the extraction efficiency decreases more or less sharply depending on the nature of the alcohol. The values of the boron extraction efficiency in the plateau region (pH<5.5) depends on the nature of the extractant and follows the order: BOc~EH>Oc, when the alcohol is diluted in kerosene, EHD>BEPD>MPD when the alcohol is diluted in kerosene modified with toluene and TMPD>MPD for alcohols-containing DESs.

According to Equation 2. 13, the extraction efficiency of boron should not depend on the pH in the aqueous phase. However, Figures 2. 6 (a) and 2. 7 shows a significant decrease in extraction efficiency of boron by mono alcohols and diols-containing DESs when the pH of the aqueous phase is greater than 5.5. This phenomenon may be explained by (i) change in boron speciation, (ii) co-extraction of other elements or (iii) salting-out effect. There is no salting-out effect as the ionic strength in the aqueous solutions does not change significantly according to Phreeqc calculations (I=3.5−3.6 mol $kg^{-1}$). Likewise, the drop in extraction efficiency cannot be explained by co-extraction of impurities as no co-extraction of other elements occurs at pH greater than 5.5 when mono alcohols and diols -containing DESs are used as extractant. Therefore, the decrease of boron extraction efficiency can be explained by the decrease in concentration of the extractable boron species, *i.e.* $H_3BO_3$, when pH is greater than 5.5 (Figure 2. 8), and the formation of non-extractable anionic species of boron ($B(OH)_4^-$ , $H_5(BO_3)_2$, $B_3O_3(OH)_4^-$ , $H_2BO_3^-$, $H_8(BO_3)_3^-$ and $B_4O_5(OH)_4^{2-}$) and the formation of the non-extractable mixed complexes (ion-pairs) $NaH_2BO_3$, $MgH_2BO_3^+$, $CaH_2BO_3^+$, $CaH_2B(OH_4)^+$ and $MgH_2B(OH_4)^+$ (Figure 2. 3). The non-extractability of these mixed complexes by the mono alcohols and diols-containing DESs is supported by the absence of sodium, magnesium and calcium co-extraction along with boron.

Conversely, calcium and magnesium are coextracted at pH greater than 6 whereas no co-extraction of sodium, potassium and lithium occurs when diols diluted in the mixture of kerosene and toluene are used instead of mono alcohols and diols-based DESs (Figure 2. 9). Therefore, the mixed complex $NaH_2BO_3$ is not significantly extractable by diols diluted in the

mixture of kerosene and toluene while mono alcohols and diols-based DESs can extract it more efficiently. It is also of interest to point out that the drop of boron extraction efficiency at pH>5.5 is much less pronounced in the case of diols diluted in the mixture of kerosene and toluene than mono alcohols and diols-based DESs. This is attributed to the decrease in concentration of the extractable species, $H_3BO_3$, which is compensated by the formation of $CaH_2BO_3^+$ and $MgH_2BO_3^+$ (Figure 2. 8) that may be extracted by forming a neutral extractable species with chloride anions, *i.e.* $CaH_2BO_3Cl$ and $MgH_2BO_3Cl$. The extraction of these mixed species in the organic phase is supported by the drop of selectivity towards calcium and magnesium depicted in Figure 2. 9 at pH>6 where calcium and magnesium are co-extracted with boron at alkaline pH by diols diluted in the mixture of kerosene and toluene while no co-extraction occurs when mono alcohols and diols-based DESs are used as extractant.

Figure 2. 9 shows that calcium is the main species co-extracted at pH 8.3 by both BEPD and EHD with a selectivity ($S_{B/Ca}$) of 16.5 and 41.3, respectively, for boron towards calcium. At pH 8.3, MPD exhibits a high selectivity of boron toward magnesium ($S_{B/Mg}$=21.2). Hydrophobicity, branching at the vicinity of the hydroxyl functional group of the aliphatic alcohols and the number of hydroxyl groups influence the extraction efficiency and the selectivity.

Figures 2. 6, 2. 7 and 2. 9 show that the highest extraction efficiency and selectively of boron from the synthetic brine is obtained at pH 5.5 when 1 mol $L^{-1}$ BOc, EH or Oc is diluted in kerosene (O/A=4), 1 mol $L^{-1}$ EHD, BEPD or MPD is diluted in the mixture of kerosene and toluene (O/A=2) or diols-based DESs such as Men:TMPD and Men:MPD (O/A=1) are employed. Furthermore, it is interesting to highlight that pH 5.5 is closed to the natural pH of brines. Therefore, extraction at pH 5.5 reduces the use of huge amount of reagent to adjust the pH.

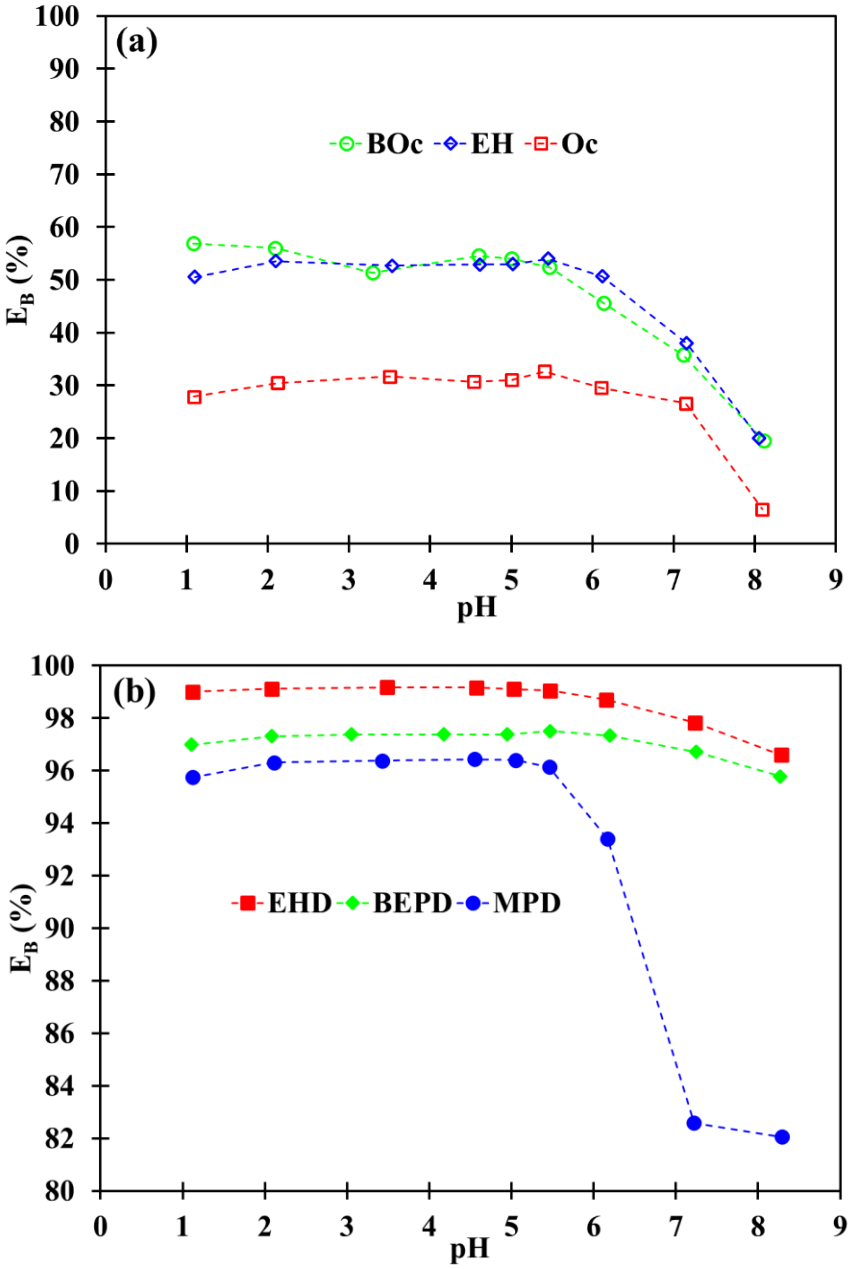



**Figure 2. 6:** Influence of the initial pH on boron extraction from the synthetic brine by (a) the mono alcohols BOc, EH and Oc diluted in kerosene (O/A=4) and (b) the diols EHD, BEPD and MPD diluted in kerosene modified with 60% (wt) toluene (O/A=2). Alcohol concentration=1 mol $L^{-1}$; 35 °C. No co-extraction of K, Li, Mg, Ca and Na was observed with mono alcohols.

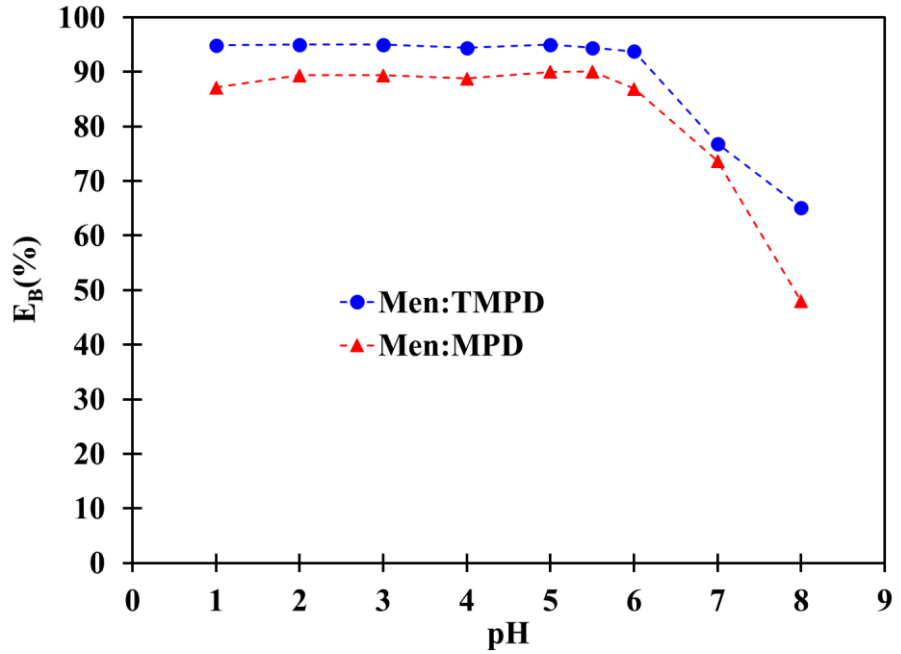



**Figure 2. 7:** Influence of the initial pH on boron extraction from the synthetic brine by diols-based DESs (Men:TMPD and Men:MPD) at O/A=0.5 and 25 °C. No co-extraction of K, Li, Mg, Ca and Na was observed.

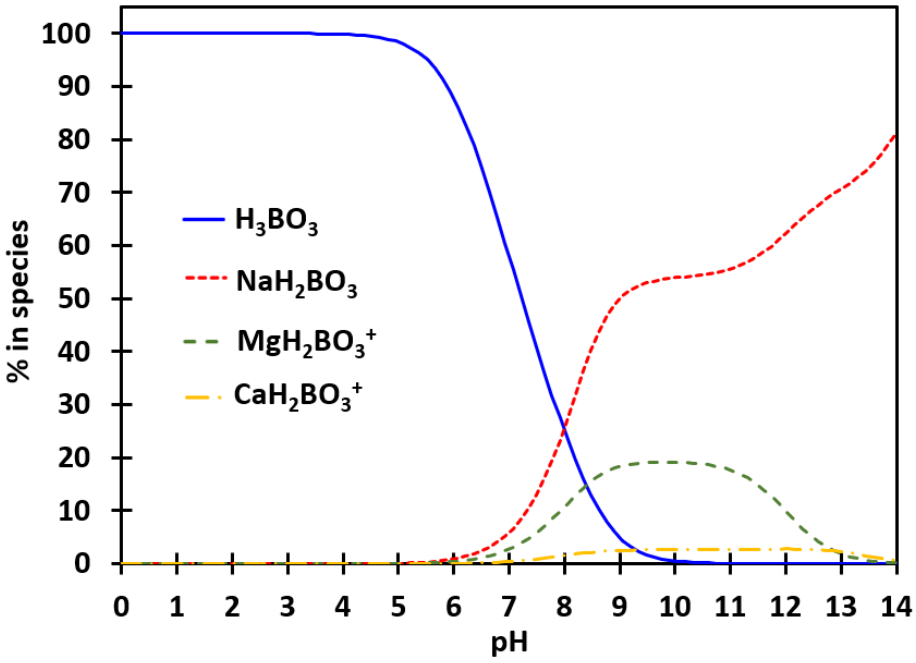



**Figure 2. 8:** Boron speciation in the synthetic brine as a function of initial pH (only the extractable boron species and the non-extractable species $NaH_2BO_3$ are reported).

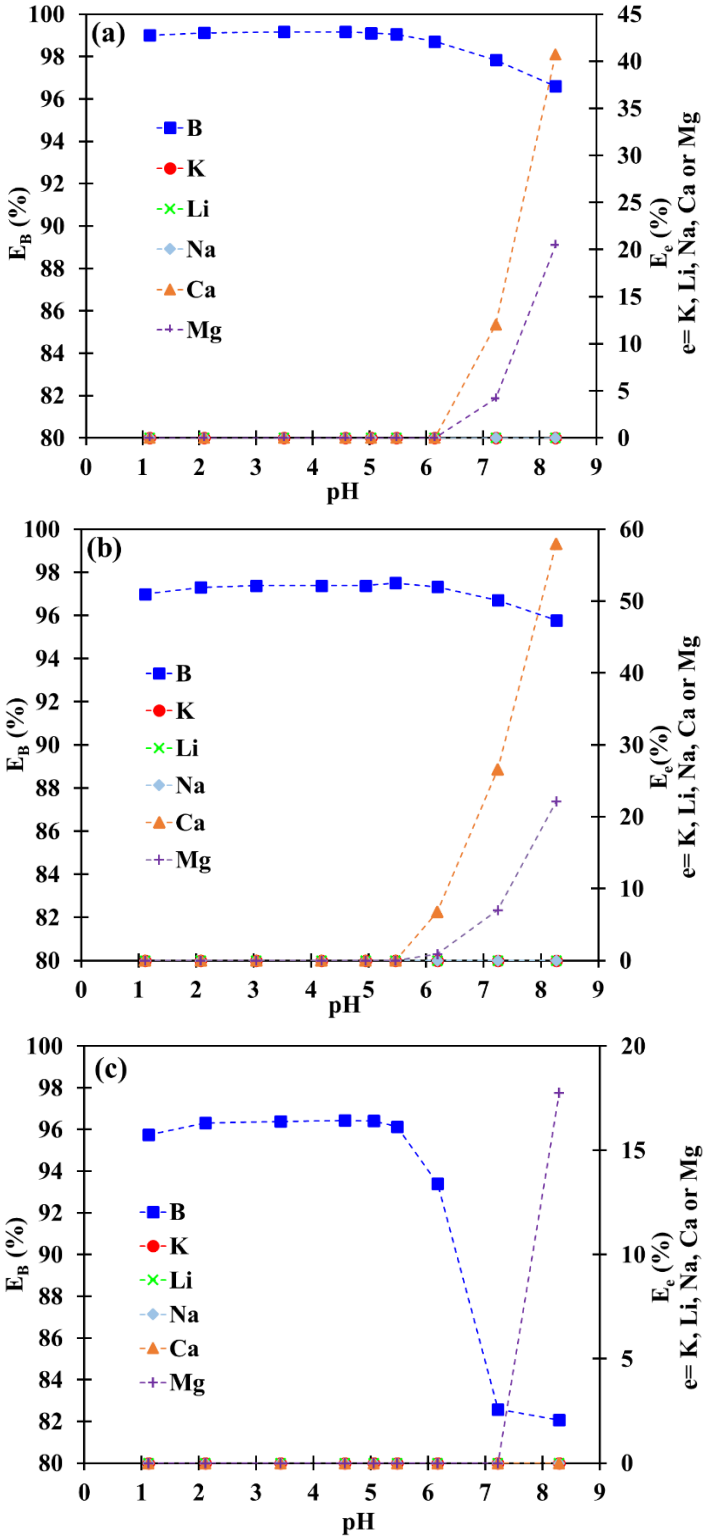



**Figure 2. 9:** Influence of the initial pH of the synthetic brine on the extraction of boron and other elements (K, Li, Mg, Ca and Na) by (a) EHD, (b) BEPD and (c) MPD diluted in kerosene modified with toluene ([alcohol]=1 mol $L^{-1}$, O/A=2 and 35 °C).

Tables 2. 6 and 2. 7 reports the extraction efficiencies of boron by the alcohols under the optimal extraction conditions, the dynamic viscosity of the organic phases after extraction, the

water solubility in the organic phases and the solubility of the alcohols in the brine deduced from the measurements of total organic carbon (TOC).

**Table 2. 6:** Extraction efficiencies of boron ($E_B$) by mono alcohols in kerosene and diols in the mixture of kerosene and toluene, dynamic viscosities (η) and water solubility ($w_{H2O}$) in the loaded organic phase, and solubility of the alcohols ($S_{alc}$) in the synthetic brine under the optimal extraction conditions.

| | Kerosene | | | | | Kerosene + 60% (wt) toluene | | | |
|---|---|---|---|---|---|---|---|---|---|
| Mono alcohols | $E_B$ (%) | η (mPa s) | $w_{H2O}$ (% wt) | $S_{alc}$ (mg $L^{-1}$) | Diols | $E_B$ (%) | η (mPa s) | $w_{H2O}$ (% wt) | $S_{alc}$ (mg $L^{-1}$) |
| BOc | 55 | 2 | 0.1 | 19 | EHD | 99 | 0.8 | 0.6 | 1,368 |
| EH | 55 | 1.6 | 0.2 | 40 | BEPD | 97 | 1 | 0.7 | 259 |
| Oc | 32 | 1.7 | 0.2 | 43 | MPD | 96 | 0.7 | 0.7 | 12,603 |

(O/A=2 and 4 for alcohols diluted in kerosene and toluene mixture and kerosene, respectively, pH=5.5, temperature=35 °C, [alcohol]=1 mol $L^{-1}$).

**Table 2. 7:** Extraction efficiencies of boron ($E_B$) by diol-based DESs (Men:TMPD and Men:MPD), dynamic viscosities after extraction (η) and water solubility ($w_{H2O}$) in the loaded organic phase, and solubility of DES ($S_{DES}$) in the synthetic brine under the optimal extraction conditions (O/A=0.5, and 25 °C).

| DES | $E_B$ (%) | η (mPa s) | $w_{H2O}$ (%wt) | $S_{DES}$ (mg $L^{-1}$) |
|---|---|---|---|---|
| Men:TMPD | 97.1 | 74.1 | 2.7 | 6,690 |
| Men:MPD | 93.1 | 43.9 | 3 | 7,606 |

The water solubility in the organic phases is higher with diols (0.7−3%) than with mono alcohols (~0.2%) (Tables 2. 6 and 2. 7). Therefore, the presence of two hydroxyl groups in the alcohol molecules favors water extraction to the organic phases, especially for diol-containing DESs. Conversely, diols promote the boron extraction and exhibit higher extraction efficiency than mono alcohols. However, the presence of two hydroxyl groups increases the hydrophilicity of the molecules, and therefore, increases the solubility of diols in the brine as shown by the higher values of $S_{alc}$ in Table 2. 6. It was difficult to determine the solubility of diols alone in DESs since menthol also dissolves along with alcohol in the brine. Then solubilities of DESs are reported in Table 2. 7. The hydrophilicity decreases when the number of carbon atoms in the alkyl chains of the alcohols increases as shown in Tables 2. 6 and 2. 7. Indeed, the solubility of mono alcohols in the brine ($S_{alc}$=19−43 mg $L^{-1}$) is significantly below

those reported by Garrett and Folkestad who acknowledged solubilities of not less than 200 mg $L^{-1}$ for equivolume mixture of kerosene and *iso*octanol ([26], [27]). However, the solubility of BEPD (259 mg $L^{-1}$) in the synthetic brine was greater than that of *iso*octanol diluted in kerosene (200 mg $L^{-1}$). For all investigated alcohols (mono alcohols and diols), the solubility in the synthetic brine follows the following order reflecting the effect of the number of carbon atoms in the alkyl chain (Table 2. 1): BOc (12 carbon atoms)<EH (8 carbon atoms)<Oc (8 carbon atoms); BEPD (9 carbon atoms)<<EHD (8 carbon atoms)<<MPD (6 carbon atoms) in the mixture of kerosene and toluene, and TMPD (8 carbon atoms)<<MPD (6 carbon atoms) in DESs.

The increase of the number of carbon atoms in the alkyl chains is responsible for an increase of the hydrophobicity. When the number of carbon atoms in the alkyl chains and hence the hydrophobicity of the molecule increases, the extraction efficiency also increases. Indeed, in the case of linear mono alcohols, the extraction efficiency of boron increases from 32% to 55% when the number of carbon atoms in the alkyl chains increases from 8 for Oc to 12 for BOc. There is no significant difference in hydrophobicity between Oc and EH as they have the same number of carbon atoms in the alkyl chains. However, the extraction efficiency of boron by EH is greater than by Oc. Therefore, it seems that ramification (branching) of the alkyl chains increases the extraction efficiency of boron. The ramification favors the extraction of boron by stabilizing the boric acid in the complex formed between boric acid and alcohol. Conversely, it is difficult to conclude for diols since there is no significant difference of boron extraction efficiencies when the ramification and the number of carbon atoms in the alkyl chains change.

#### 2.3.2.4 Boron stripping

Several authors reported that hydrochloric acid (HCl), sodium hydroxide (NaOH), sulfuric acid ($H_2SO_4$) and deionized water can be used to strip boron ([22], [28], [29]). In this study, stripping tests of boron contained in the loaded organic phases were performed with 0.2 mol $L^{-1}$ hydrochloric acid, 0.2 mol $L^{-1}$ sodium hydroxide, and deionized water (Figures 2. 10 and 2. 11).

Figures 2. 10 and 2. 11 show that the stripping efficiency of boron is greater from the extraction solvent containing mono alcohols than diols. This is a result of stronger interactions between boron and diols than between, boron and mono alcohols, as reflected by higher extraction efficiency by diols than mono alcohols. Sodium hydroxide is the best stripping

reagent irrespective of the extractants, since alkaline solution favors the formation of $B(OH)_4^-$ (Figure 2. 3a), which is not an extractable species [30]. Likewise, the stripping efficiency with hydrochloric acid is low as low pH in acidic solution of HCl favors the formation of $H_3BO_3$, which is highly extractable, and therefore remains in the organic phase. However, the stripping efficiency is not nil when HCl is used probably because of the affinity between boric acid and water molecules, and the competition between boric acid extraction and hydrochloric acid extraction by the alcohols, which destabilized boron-alcohol interactions. Xu et al. [17] reported that increasing the concentration of HCl from 0.5 mol $L^{-1}$ to 3 mol $L^{-1}$ reduces the stripping efficiency by about 12%. This is probably due to the salting-out effect. Indeed, the high salting-out effect is caused by the reduction of water activity and a decrease of the affinity between boric acid and water molecules.

It is of interest to point out that deionized water can strip boron even if the stripping efficiency is not high, especially in the systems where diols are used as extractants. Therefore, water may destabilize the boron species in the organic phase. It can be inferred that water-alcohol interactions are stringer than boric acid-alcohol interactions. Moreover, there is no significant difference between the stripping efficiency of boron by HCl and deionized water irrespective of the alcohol.

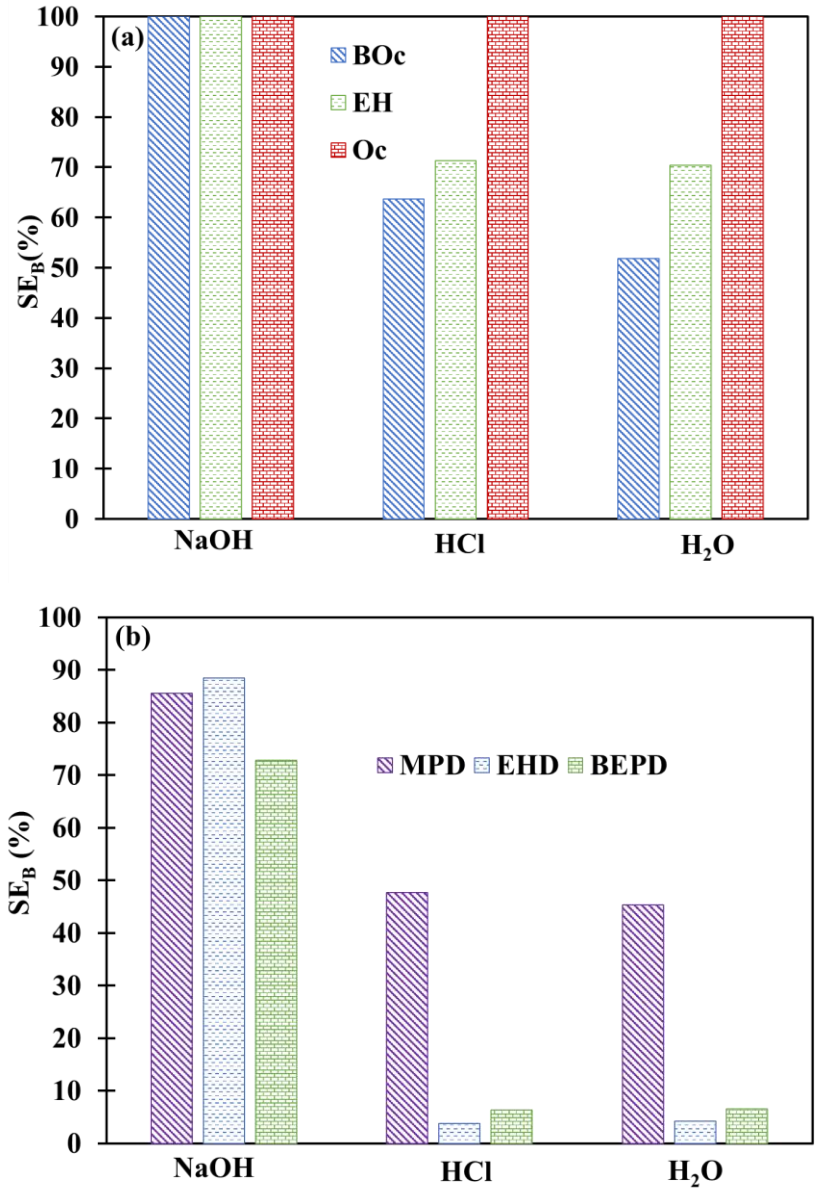



**Figure 2. 10:** Boron stripping at 35 °C from an organic phase composed of 1 mol $L^{-1}$ (a) mono alcohols in kerosene and (b) diols in kerosene and 60% (wt.) toluene. Stripping solutions: 0.2 mol $L^{-1}$ NaOH, 0.2 mol $L^{-1}$ HCl or deionized water at 35 °C. The loaded organic phase was obtained by contacting the synthetic brine with the fresh organic phase at (a) O/A=4 and (b) O/A=2.

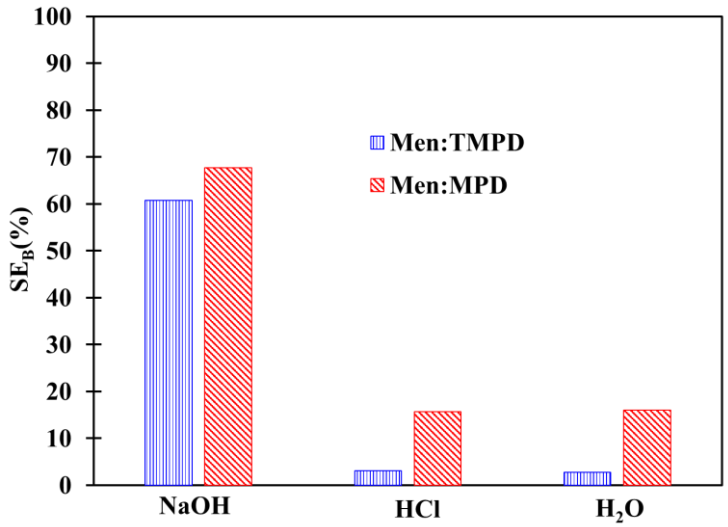



**Figure 2. 11:** Boron stripping at 25 °C from an organic phase composed of diol-based DESs (Men:TMPD and Men:MPD). Stripping solutions: 0.2 mol $L^{-1}$ NaOH, 0.2 mol $L^{-1}$ HCl or deionized water at 25 °C. The loaded organic phase was obtained by contacting the synthetic brine with the fresh organic phase at O/A=1.

### 2.3.3 Optimization of boron extraction and stripping conditions in the presence of 2-butyloctan-1-ol as extractant

The previous investigations on boron extraction by mono alcohols and diols show that diols, especially diols-containing DESs, provide the highest extraction efficiencies of boron (93.1−97.1%) despite the lowest phase volume ratio (O/A=0.5) (Tables 2. 6 and 2. 7). In contrast, DESs exhibit high solubility in brine (>6,000 mg $L^{-1}$) which is not recommended for industry applications since high solubility is responsible for high solvent loss and increase of effluent treatment cost. Likewise, diols diluted in the mixture of kerosene and toluene exhibit high solubility in the synthetic brine (259−12,603 mg $L^{-1}$). In addition, toluene is a serious drawback in industry since it is responsible for safety issues [31]. Therefore, 2-butyloctan-1-ol diluted in kerosene is selected for further investigations in order to identify the optimal boron extraction and stripping conditions.

#### 2.3.3.1 Boron extraction and impurities co-extraction

Figure 2. 12 shows the influence of the concentration of 2-butyloctan-1-ol in kerosene, the phase volume ratio (O/A) and the pH at equilibrium on boron extraction efficiency from the synthetic brine at 25 °C. An increase of 2-butyloctan-1-ol concentration is responsible for an increase of boron extraction efficiency. The curve in Figure 2. 12 (a) shows that the extraction efficiency reaches a plateau (%$E_B$=70%) when 2-butyloctan-1-ol concentration is greater than 2 mol $L^{-1}$. No co-extraction of lithium, calcium magnesium, sodium and potassium was

observed. Therefore, the other extration tests were performed with 2 mol $L^{-1}$ 2-butyloctan-1-ol in kerosene.

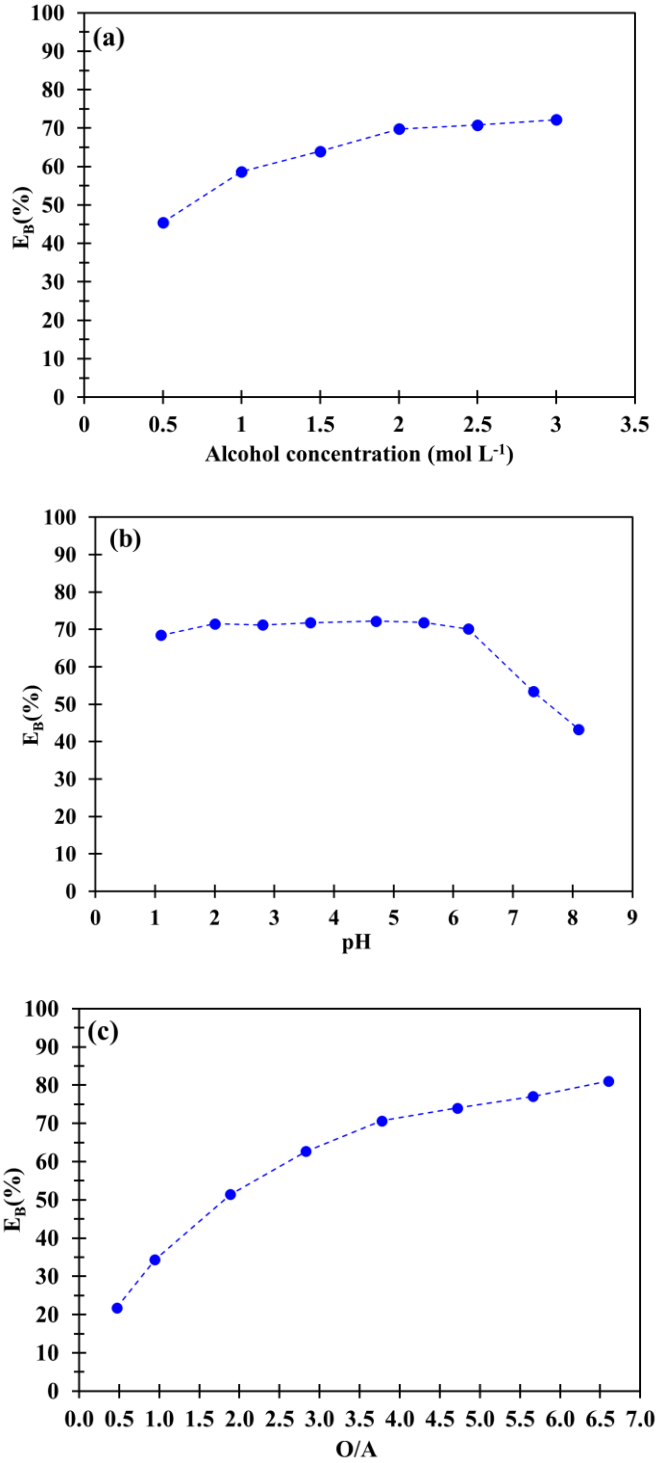



**Figure 2. 12:** Influence of (a) 2-butyloctan-1-ol concentration in kerosene (O/A=4, pH=1, 25 °C), (b) pH (O/A=4, extraction solvent: 2 mol $L^{-1}$ 2-butyloctan-1-ol, 25 °C) and (c) O/A (pH=1, extraction solvent: 2 mol $L^{-1}$ 2-butyloctan-1-ol in kerosene, 25 °C) on boron extraction efficiency from the synthetic brine (SB).

Boron extraction efficiency does not depend on pH when pH values are lower than 5.5 (%$E_B$=70, Figure 2. 12b). Above this value, an increase of pH is responsible for a sharp decrease of boron extraction efficiency. This significant decrease in the extraction effciency of boron can be explained by the change in boron speciation as a function of pH (Figure 2. 3a). This is explained in section 2.3.2.3. Indeed, the extractable species of boron, *i.e.* boric acid, is progressively converted into borate and forms mixed complexes with sodium, calcium and magnesium when pH increases.

Figure 2. 12(c) shows an increase of boron extraction efficiency when the phase volume ratio (O/A) increases as it is expected according to Equation 2. 3. Around 22% of boron is extracted at O/A=0.5, extraction reaches 70% at O/A=4, and even 81% at O/A=6.6 when the pH at equilibrium is the same and equal to 1. However, O/A=4 seems to be a good compromise to achieve high extraction efficiency even at moderate flowrate of the extraction solvent.

Figure 2. 13 compares the influence of the phase volume ratio (O/A) on boron extraction efficiency for the synthetic brine (SB) and the native brines (NB1 and NB2) under the previous optimal experimental conditions (extraction solvent: 2 mol $L^{-1}$ 2-butyloctan-1-ol in kerosene, pH=5.5 for SB, pH=6.9 for NB1, pH=7.5 for NB2, temperature=25 °C). Despite the difference in chemical composition of the brines, Figure 2. 13 shows that the extraction curves for the synthetic brine (SB) and the native brine 2 (NB2) are very similar. Surprisingly, the extraction curves obtained for SB and NB1 are different even though both brines have similar compositions.

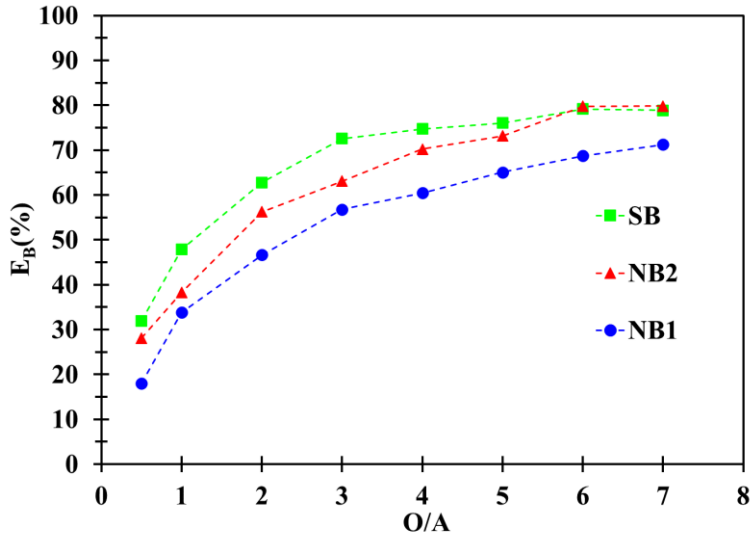



**Figure 2. 13:** Extraction of boron from the synthetic brine (SB) and the native brines (NB1 and NB2) at different phase volume ratios O/A (extraction solvent: 2 mol $L^{-1}$ 2-butyloctan-1-ol in kerosene, pH=5.5 for SB, pH=6.9 for NB1, pH=7.5 for NB2, 25 °C ).

This difference may be due to the water activity of the brines that are not necessarly the same, and/or the different values of pH between the two brines since pH influences the extraction efficiency at pH greater than 5.5 (Figure 2. 12b).

Under the optimal extraction conditions, *i.e.* 2 mol $L^{-1}$ 2-butyloctan-1-ol in kerosene, pH=5.5, O/A=4 and 25 °C, 10 extraction tests from SB were performed with 500 mL glass vessels. The average values of boron extraction efficiency was 66±3%.

This investigation shows a high selectivity of boron extraction from brines under the optimal conditions mentioned above which leads to provide high purity boron salt when boron is co-valorized in plants.

### 2.3.3.2 Boron stripping

Around 20 mL of boron-loaded organic phase was prepared for stripping tests by contacting 5 mL of the synthetic brine (SB) with 20 mL of extraction solvent under the optimal extraction conditions, *i.e.* 2 mol $L^{-1}$ 2-butyloctan-1-ol diluted in kerosene at O/A=4, pH 5.5 and 25 °C. Boron extraction experiments from SB were repeated 6 times and the average extraction efficiency was 72±1%. Boron concentration and water content in the organic phase after extraction were 0.024 mol $L^{-1}$ and 0.3 %wt, respectively.

Figure 2. 14 shows the effect of the nature of the stripping solution (0.2 mol $L^{-1}$ sodium hydroxyde (NaOH), 0.2 mol $L^{-1}$ hydrochloric acid (HCl) and deionized water) on the stripping efficiency at O/A=4 and 25 °C. The stripping efficiency of boron follows this order: NaOH (100%) >> HCl (54%) ≳ $H_2O$ (50%). The same stripping efficiency order was reported in section 2.3.2.4 where sodium hydroxide was the best stripping solution while hydrochloric acid and deionized water exhibited the lowest and similar stripping efficiencies of boron .

Figure 2. 15 shows that boron stripping efficiency increases when sodium hydroxide concentration increases. Full stripping is achieved with 0.1 mol $L^{-1}$ sodium hydroxide and no increase of stripping efficiency is observed above this concentration. After stripping with 0.1 mol $L^{-1}$ sodium hydroxide, the water content in the organic phase and the solubility of 2-butyloctan-1-ol in the stripping solution were 0.4 % (wt) and 181 mg $L^{-1}$, respectively. The solubility of 22-butyloctan-1-ol in the stripping solution (181 mg $L^{-1}$) is much lower than that reported by Garrett et al. [32] (2,000 mg $L^{-1}$). Such a low value of 2-butyloctan-1-ol solubility in the stripping solution avoids the use of activated carbon to reduce its concentration and avoid additional operating and capital costs for the effuent treatment.

In order to study the reproducibility of boron stripping from the loaded extraction solvent, 10 stripping tests were performed by using 500 mL glass vessels with 0.1 mol $L^{-1}$ sodium hydroxide at O/A=4 and 25 °C. The average value of boron stripping efficiency was 95±5%.

Finally, it should be highlighted that boron is fully strip in one stage from the loaded organic phase by 0. 1 mol $L^{-1}$ NaOH at O/A=4 and 25 °C. Furthermore, alcohol solubility is very low in the effluent, which avoid the implementation of expensive effluent treatment to remove organic matter from the stripping solution and allows the production of pure borax.

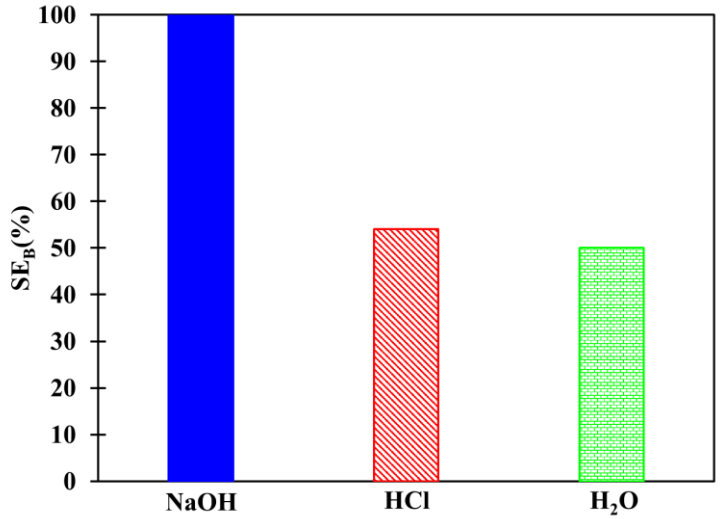



**Figure 2. 14:** Boron stripping efficiency when 0.2 mol $L^{-1}$ NaOH, 0.2 mol $L^{-1}$ HCl and deionized water are used as stripping solutions (O/A=4, 25 °C). The organic phase was previously loaded by contacting the extraction solvent (2 mol $L^{-1}$ 2-butyloctan-1-ol diluted in kerosene) with the synthetic brine (SB) at O/A=4, pH=5.5 and 25 °C.

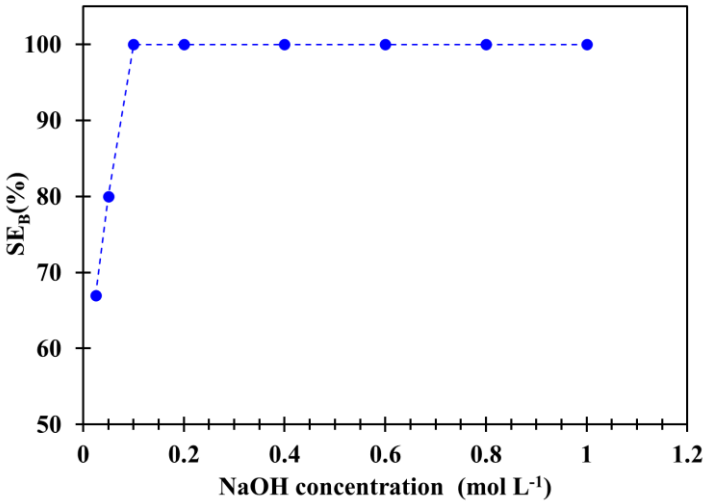
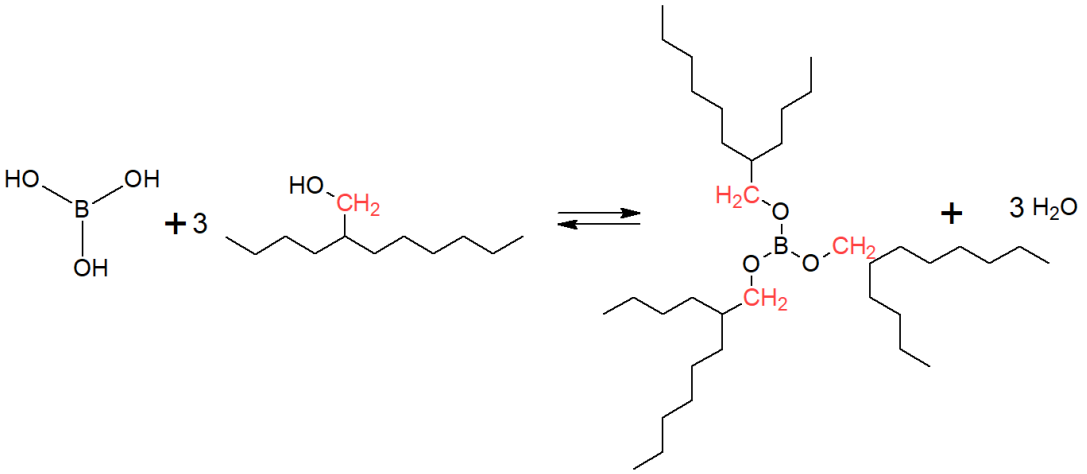



**Figure 2. 15:** Influence of sodium hydroxyde concentration on boron stripping efficiency (O/A=4, 25 °C). The organic phase was previously loaded by contacting the extraction solvent (2 mol $L^{-1}$ 2-butyloctan-1-ol diluted in kerosene) with the synthetic brine (SB) at O/A=4, pH=5.5 and 25 °C.

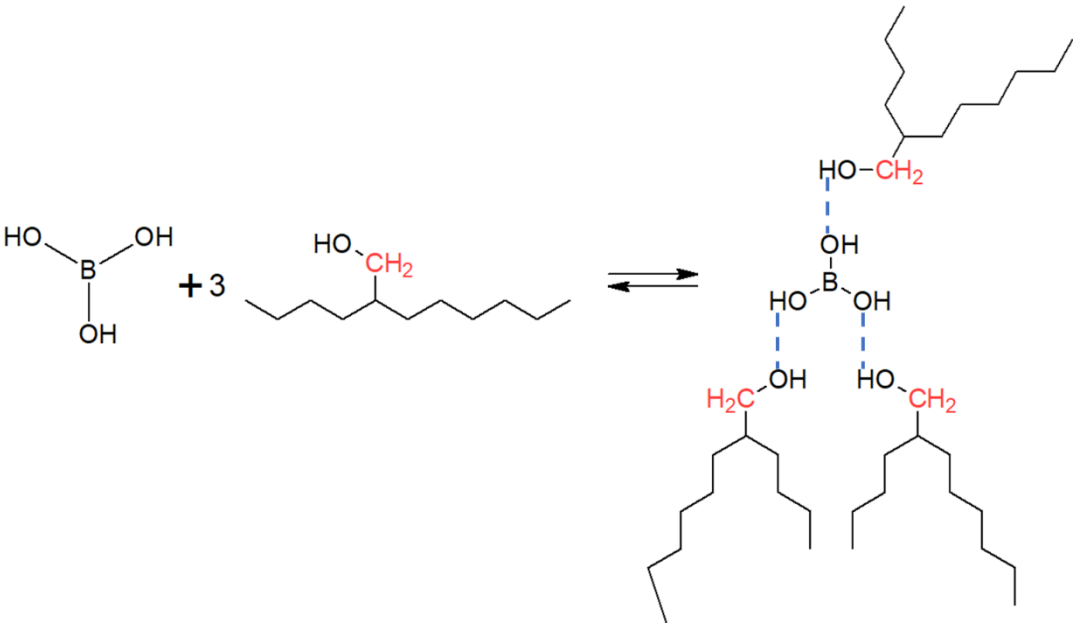
## 2.3.4 Nature of the extracted complex

The nature of the extracted complex strongly depends on the composition of the brine and the nature of the extractant ([36], [44]). Boric acid can be extracted by alcohols via (i) esterification, (ii) solvation or both solvation and esterification. Peng et al. [16] reported that boric acid was extracted via esterification by 2 mol $L^{-1}$ 2-butyloctan-1-ol in sulfonated kerosene from a very acidified boron-concentrated brine (2.6 g $L^{-1}$ boron). In that work, the extraction experiment was performed at phase volume ratio O/A=1, pH=1.3 and 20 °C. and the ester complex was identified by FTIR (Fourier Transform Infrared Spectroscopy) analysis.

Equations 2.14 and 2.15 illustrate boric acid extraction by 2-butyloctan-1-ol via esterification and solvation, respectively (one molecule of boric acid with 3 molecules of 2-butyloctan-1-ol are used for the sake of illustration).




(2. 14)




(2. 15)

In this research, boric acid extraction cannot be explained by esterification since boric acid is stripped by deionized water (Figure 2. 14). In case of esterification, boric acid should not be stripped by water alone because it would require more energy to break the single bonds between boric acid and the alcohol [33], while electrostatic interactions especially hydrogen bonds between boric acid and 2-butyloctan-1-ol molecules can be easily destabilized by water molecules. Therefore, it can be inferred that boric acid is extracted by solvation via hydrogen bonds. In order to support this assumption, $^{1}H$ NMR analysis of the organic phase was performed before and alter extraction (Figure 2. 16). Before boron extraction, the peaks of the proton corresponding to the hydroxyl function OH and the proton attributed to the $CH_2$ alkyl group bonded to OH (in red in Equations 2. 14 and 2. 15) are located at 4.85 ppm and 3.65 ppm, respectively.

After extraction, the peak attributed to the proton of the $CH_2$ group remains at the same chemical shift, and the proton of the OH function attributed to free boric acid and OH from the 2-butyloctan-1-ol are at 4.75 ppm.

It is expected that the esterification leads to upshield of the proton of the $CH_2$ group in red in Equations 2. 14 and 2. 15 due to bond formation between the oxygen of the hydroxyl group and boron. Therefore, the small peak observed at 3.9 ppm may be attributed to the chemical shift of the proton in the $CH_2$ group in red of the ester represented in Equation 2 15. Therefore, it seems that most of boron is extracted by hydrogen bonds. The surface integration of the peaks at 3.65 ppm and 3.9 ppm showed that 98% of boric acid was extracted by solvation and 2% by esterification. This result is supported by Balinski et al. [34] and Zhang et al. [22] who reported that boric acid extraction by mono alcohols mainly involves solvation but also esterification at lower extent. Therefore, when boric acid is extracted by 2-butyloctan-1-ol, Equation 2. 13 can be rewritten as follows:

$$\log(D) = \mathrm{n}\log\left(\overline{[\mathrm{R(OH)}]}\right) + \log(\mathrm{K}_{ex}) \qquad (2.\ 16)$$

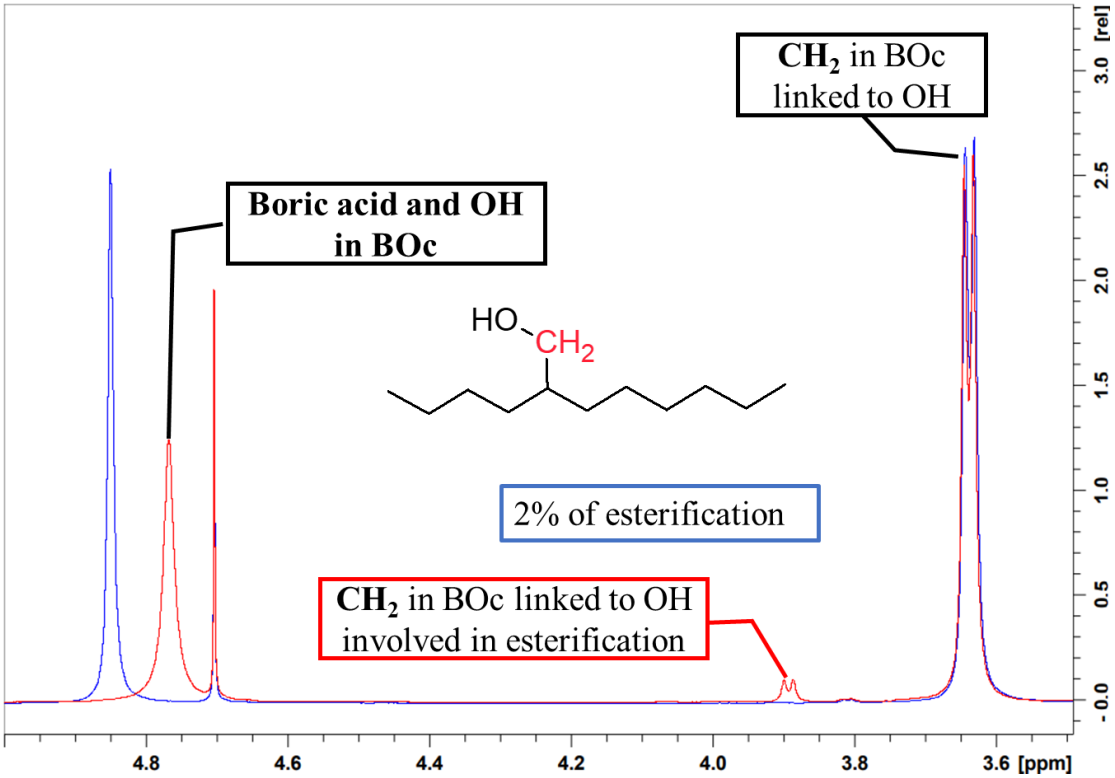



**Figure 2. 16:** Stacked $^{1}H$ NMR spectrum of the organic phase before extraction (blue spectrum) and after extraction (red spectrum).

Data from Figure 2. 12(a) were used to plot the logarithm of the distribution ratio of boron ($\log(D_B)$) as a function of the logarithm of the concentration of the free alcohol ($\overline{[R(OH)]}$) [Figure 2. 17]. Since boron concentration in the organic phase after extraction was very low and ranged between 0.017 mol $L^{-1}$ and 0.027 mol $L^{-1}$, it was assumed that there was no significant difference between the concentration of the free alcohol ($\overline{[R(OH)]}$) in the organic phase after extraction and the initial concentration of alcohol before extraction. As shown in Figure 2. 17, $\log(D_B)$ vs. $\log(\overline{[R(OH)]})$ is linear with a slope of n=0.65, indicating that the extraction involves one molecule of boric acid and 0.65 equivalent of 2-butyloctan-1-ol. Similar result was obtained by Balinski et al. [34]. The deviation of the stoichiometric coefficient (n=0.65) from the 1 can be attributed to the presence of several solvate complexes in the organic phase ([22], [34]). The solvate complexes can be boric acid-monomer of 2-butyloctan-1-ol and boric acid-polymers of 2-butyloctan-1-ol. Unfortunately, slope analysis method does not allow to identify these solvate complexes. Only a physicochemical model including all species involved in boron extraction could help to describe more accurately the physicochemistry of boron extraction.

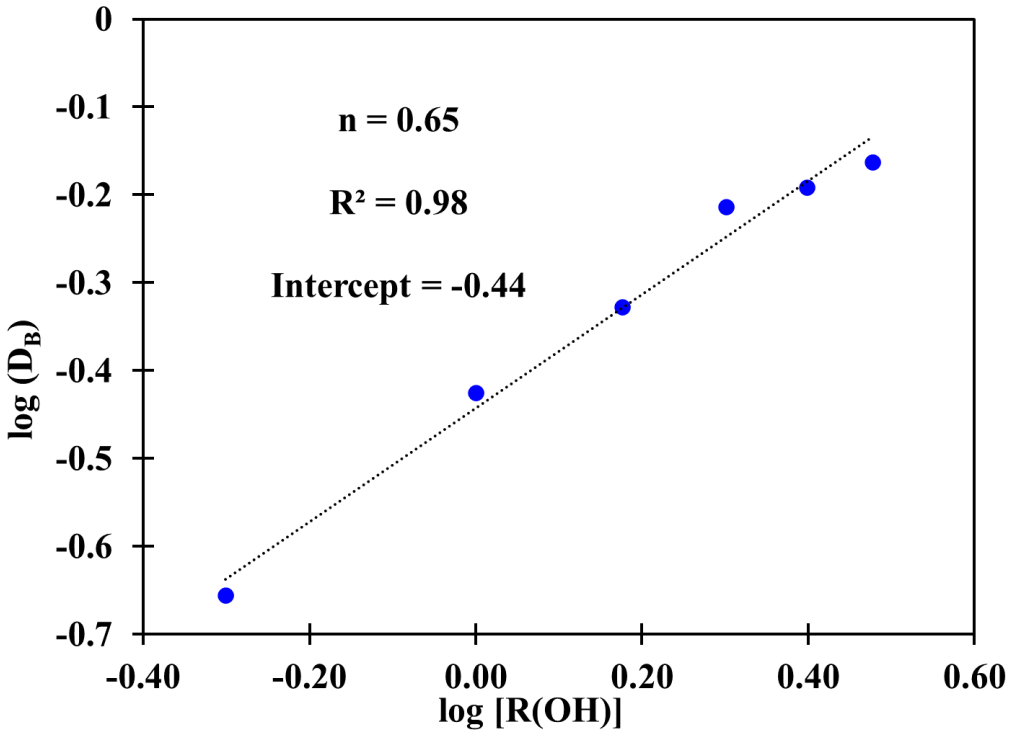



**Figure 2. 17:** log of the distribution ratio of boron as a function of log of the concentration of 2-butyloctan-1-ol in the organic phase after extraction ([2-butyloctan-1-ol]=0.5−3 mol $L^{-1}$, O/A=4, pH=1 and 25 °C).

## 2.3.5 Boron crystallization

Boron extraction from the synthetic brine and stripping tests were caried out in 500 ml glass vessels under the optimal extraction and stripping conditions (2 mol $L^{-}$2-butyloctan-1-ol diluted in kerosene, O/A=4, pH=5.5 and 25 °C for extraction, and 0.1 mol $L^{-1}$ NaOH, O/A=4 and 25 °C for stripping). Ten extraction and stripping experiments were conducted with 100 ml aqueous phases and 400 ml organic phases so that the volume of the stripping solution is enough for performing crystallization experiments. The extraction and stripping efficiencies of boron were 66±3% and 95±5%, respectively.

After stripping experiments, the stripping solution containing 0.9 g $L^{-1}$ boron and 2.3 g $L^{-1}$ sodium was crystallized by evaporation with a rotary evaporator (VWR, France). The stripping solution was heated at 45 °C under vacuum (ca.10 mbar, vacuum in the rotary evaporator obtained by using a diaphragm vacuum pump, LABOPORT N 820 G). After 24 hours, water was fully removed and the solid was washed with pure ethanol (VWR, France) and dried in oven at 100 °C for 30 min. Then, the solid was characterized by X-ray diffraction (XRD). As shown in Figure 2. 18, the solid is identified as teepleite ($Na_2B(OH)_4Cl$), which is obtained through reaction between sodium chloride and boric acid in aqueous phase [35]. The

formation of teepleite is attributed to the presence of chloride due to co-extraction and co-stripping of chloride during the extraction and the stripping steps (analysis of the stripping solution with an ionic chromatography evidences the presence of 484.4 mg $L^{-1}$ chloride in the stripping solution). This indicates that chloride was co-extracted with boric acid from the brine probably as hydrochloric acid by forming hydrogen bonds with the alcohol [36].

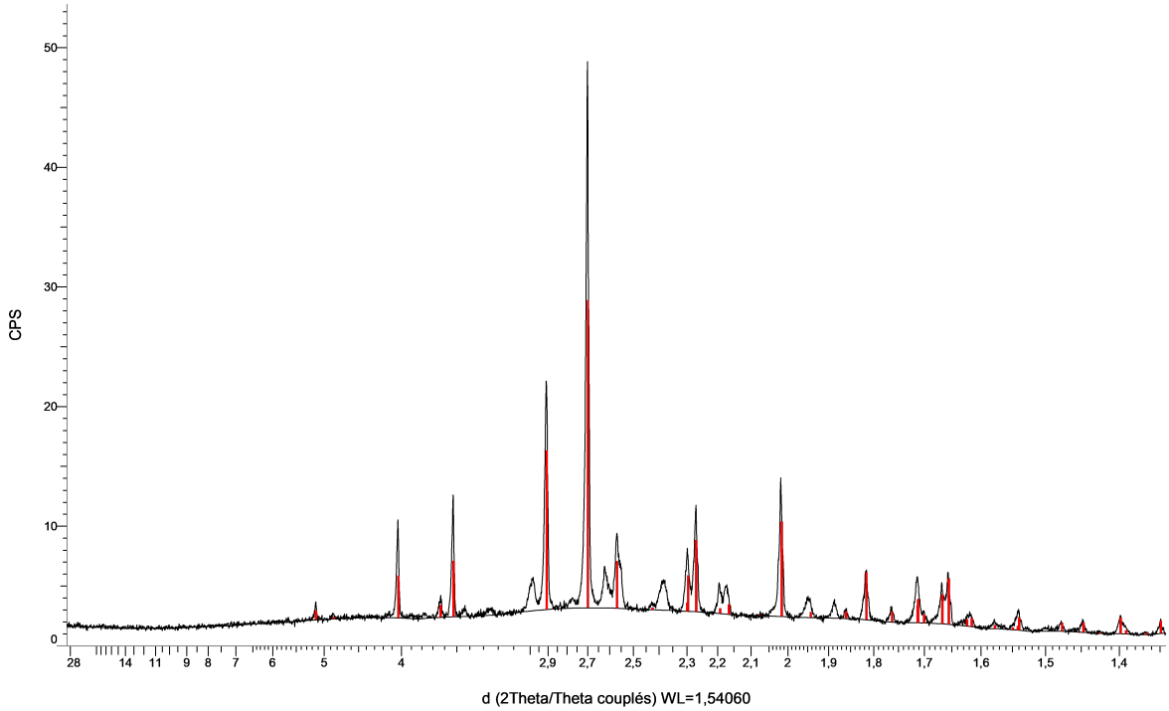



**Figure 2. 18:** X-ray diffraction (XRD) pattern of the crystallized solid (in black) and teepleite [35] (in red).

Teepleite cannot be valorized on the market while borax can be valorized. Therefore, the work hereafter was dedicated to find the experimental conditions to avoid teepleite formation and to favor borax crystallization. The stripping solution was first evaporated in the same condition as previously in order to reach 11.76 g $L^{-1}$ boron which was greatly higher than 5.8 g $L^{-1}$ (borax solubility in water at 20 °C is 51 g $L^{-1}$, which is equivalent to 5.8 g $L^{-1}$ boron [37], [38], [39]). The resulting solution was then crystallized selectively as borax by cooling at 20 °C during 8 hours. The solid was washed with pure ethanol (VWR, France) and dried in oven at 100 °C for 30 min. The crystallization efficiency reaches 54%. XRD analysis showed that the solid was a mixture of borax ($Na_2B_4O_7 \bullet 10H_2O$) and tincalconite ($B_2H_5NaO_6$) (Figure 2. 19). However, borax ($Na_2B_4O_7 \bullet 2H_2O$, purity=99%) was obtained by drying the solid at 100 °C for 24 hours.

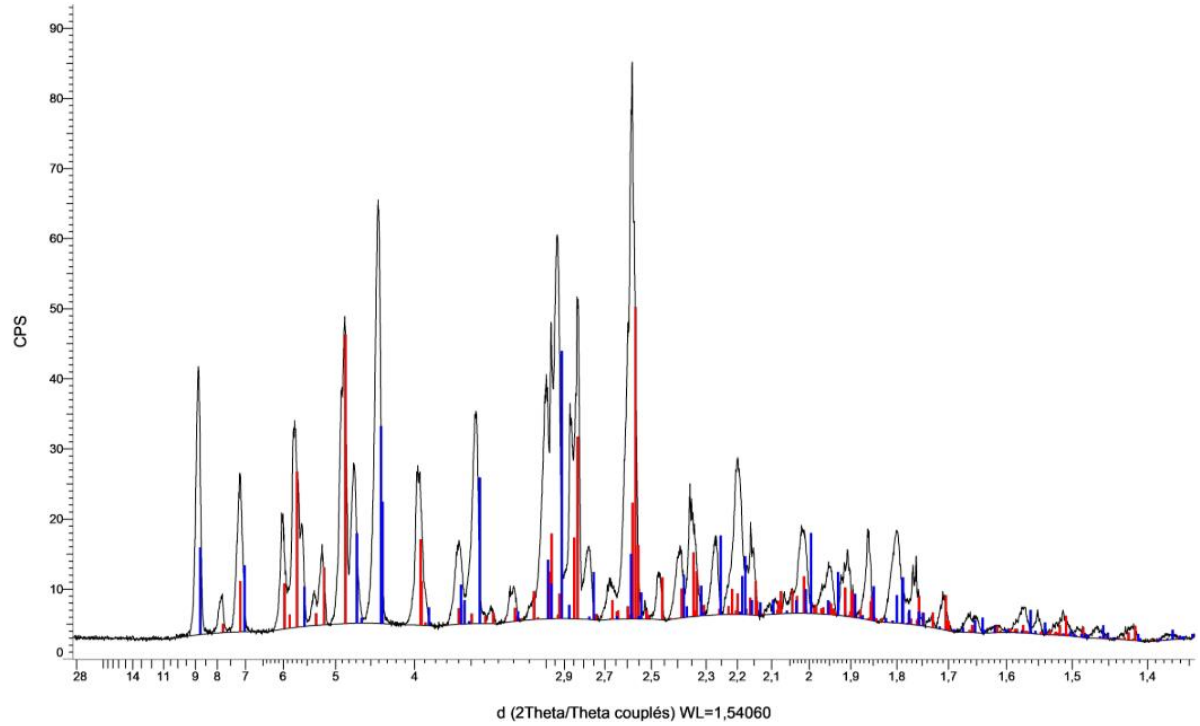



**Figure 2. 19:** X-ray diffraction (XRD) patterns of the crystallized solid (in black), borax (in red) and Tincalconite (in blue). The phases were identified by using the database of the X-ray diffractometer (EVA software).

## 2.3.6 Flowsheet for boron extraction and valorization as borax

The boron concentration in the boron-depleted brine was set at 25 mg $L^{-1}$ for McCabe-Thiele simulation since Brown et al. [40] reported that boron concentration in brines should be less than 25 mg $L^{-1}$ to guarantee the production of high-grade lithium carbonate for high performance lithium-ion batteries. The McCabe-Thiele method [41] was used with values of boron extraction efficiencies as a function of O/A (Figure 2. 13) to determine the number of mixers-settlers needed to extract boron from the different brines (SB, NB1 and NB2) under optimal experimental conditions. McCabe-Thiele diagrams showed that a phase volume ratio of O/A=6 is required to remove boron from SB and NB2 whereas O/A=9 is necessary to remove boron from NB1 (see Figure A. 10 in appendix).

Figure 2. 20 shows that four mixers-settlers are needed at O/A=4 to extract boron from SB and NB2 so that less than 25 mg $L^{-1}$ of boron remain in the effluent. The same number of mixers-settlers can be used to process the native brine 1 (NB1) provided that O/A=7. It is indeed necessary to increase O/A to extract boron efficiently from NB1 because the boron extraction efficiency from this brine is lower since the natural pH of NB1 (pH=6.9) is higher than the pH of SB (pH=5.5).

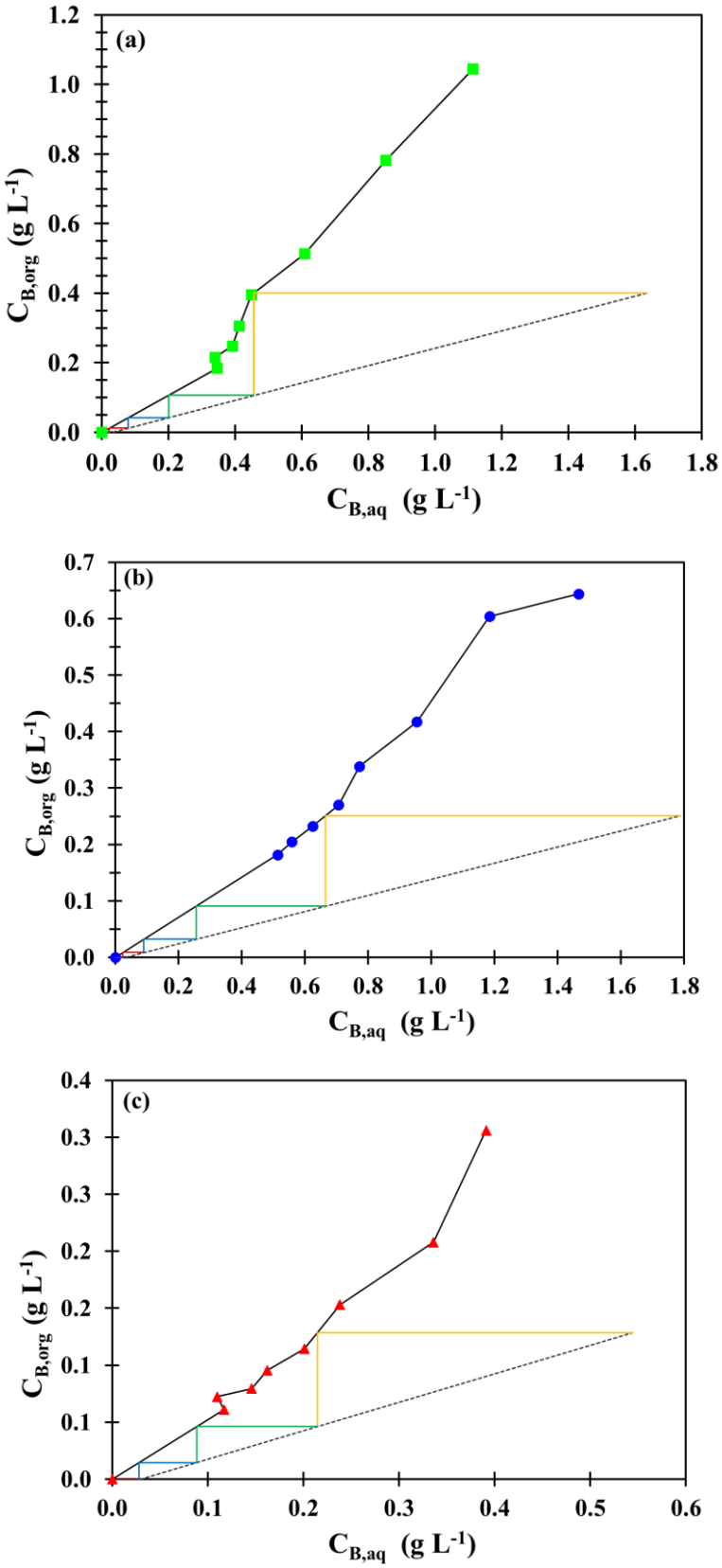
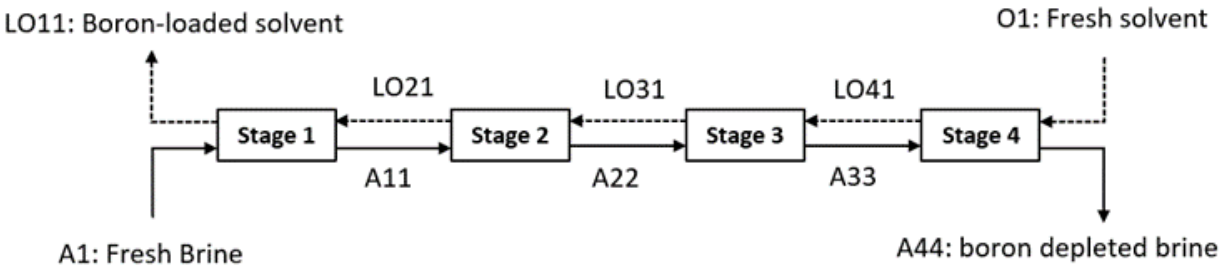



**Figure 2. 20:** McCabe-Thiele diagrams for boron extraction from (a) the synthetic brine (SB) with O/A=4, (b) the native brine 1 (NB1) for O/A=7 and (c) the native brine 2 (NB2) with O/A=4 ($C_{B,org}$ and $C_{B,aq}$ are boron concentration in the organic phase and in the aquous phase, respectively).

Under the same extraction conditions, no significant difference in the extraction efficiency of boron for both synthetic brine (SB) and native brine 1 (NB1) was observed. For instance, when boron is extracted from SB or NB1 with 2 mol $L^{-1}$ 2-butyloctan-1-ol diluted in kerosene at 25 °C, O/A=4 and pH=6.9, boron extraction efficiency reaches 60.5% (see extraction efficiency of boron under the extraction conditions mentioned above in Figure 2. 12 (b) for SB and in Figure 2. 13 for NB1). Therefore, simulation of countercurrent extraction of boron from the brines following the model reported in Figure 2. 21 was performed to determine boron extraction efficiency in each stage when 2 mol $L^{-1}$ 2-butyloctan-1-ol diluted in kerosene was contacted with only the synthetic brine (SB) at pH 5.5 or the native brine 2 (NB2) at pH 7.5 and O/A=4 (Table 2. 8).

**(a)**




**(b)**

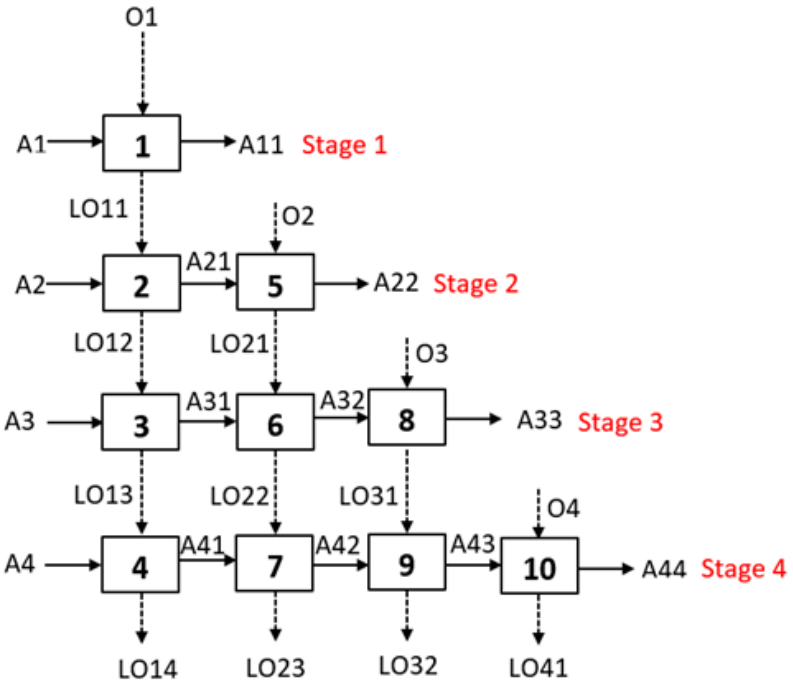



**Figure 2. 21:** Simulation model for countercurrent extraction of boron from synthetic (SB) and native brine 2 (NB2) using 2 mol $L^{-1}$ 2-butyloctan-1-ol diluted in kerosene (O/A=4; pH=5.5 and 7.5). LO: Loaded organic phase, A: Aqueous phase.

The simulation shows that the use of three stages leads to 92.4% and 78.6% of boron extraction efficiency and the addition of one more stage increases the extraction efficiency to 98.2% and 94.2% when the feed solution is the synthetic brine and the native brine 2, respectively. Therefore, the implementation of three mixers-settlers is enough to extract boron from the synthetic brine whereas 4 mixers-settlers are required to extract boron from the native brine 2.

**Table 2. 8:** Boron extraction efficiency in each stage of four-stage continuous countercurrent extraction for the synthetic brine (SB) and the native brine 2 (NB2) (Extractant=2 mol $L^{-1}$ 2-butyloctan-1-ol, Diluent=kerosene, O/A=4, 25 °C).

| Stage | $E_B$(%) | |
|---|---|---|
| | Synthetic brine (SB) | Native brine 2 (NB2) |
| 1 | 70 | 46.4 |
| 2 | 82.2 | 63.1 |
| 3 | 92.4 | 78.6 |
| 4 | 98.2 | 94.2 |

Under these conditions (2 mol $L^{-1}$ 2-butyloctan-1-ol diluted in kerosene contacted with the synthetic brine (SB) at pH 5.5 or the native brine 2 (NB2) at pH 7.5 and O/A=4), the solubility of 2-butyloctan-1-ol in SB was 18 mg $L^{-1}$ and the dynamic viscosity of the organic phase after extraction was very close to the viscosity before extraction, *i.e.* 4.4 mPa s. Furthermore, it is important to highlight that, under these experimental conditions, the solubility of 2-butyloctan-1-ol in the brine (18 mg $L^{-1}$) is much lower than that reported in literature ([32], [42]) (solubility between 100 mg $L^{-1}$ and 200 mg $L^{-1}$). Even if the initial concentration of boron was 1.60 g $L^{-1}$ and 0.54 g $L^{-1}$ in SB and NB2, respectively, it is interesting to point out that the residual concentration of boron in the brine was 25 mg $L^{-1}$ in the last stage, as expected. Boron extraction was highly selective since no co-extraction of lithium, magnesium, calcium, sodium and potassium was observed. Long-chain mono alcohols like heptanol, octanol, nonanol, and decanol have the capacity to extract hydrochloric acid or sulfuric acid by forming hydrogen bonds with the alcohol functional group. In this study, Table 2. 9 does not evidence significant sulfate extraction, likely due to the high pH value of the brine, as indicated by the negligible decrease in sulfate concentration after boron extraction. Conversely, Table 2. 9 exhibits a slight extraction of chloride anions through the formation of hydrogen bonds between HCl and the alcohol functional group. This is evidenced by the decrease in chloride concentration following boron extraction, accompanied by a pH increase from 5.5 to 6.8. It is worth noting that the chloride extraction observed here is less significant compared to the findings by Garrett et al. [32].

**Table 2. 9:** Composition, pH and density of the synthetic brine (SB) before extraction and after extraction (Extractant=2 mol $L^{-1}$ 2-butyloctan-1-ol, Diluent=kerosene, O/A=4, 25 °C).

| Synthetic brine | pH | Density | Concentration (g $L^{-1}$) | | | | | | | |
|---|---|---|---|---|---|---|---|---|---|---|
| | | (g $cm^{-3}$) | Li | Ca | Mg | B | Na | K | $Cl^-$ | $SO_4^{2-}$ |
| Before extraction | 5.5 | 1.2 | 1.27 | 0.68 | 3.09 | 1.62 | 103.24 | 14.21 | 182.25 | 8.78 |
| After extraction | 6.8 | 1.2 | 1.27 | 0.68 | 3.09 | 0.025 | 103.24 | 14.21 | 181.77 | 8.76 |

Finally, boron extraction by 2 mol $L^{-1}$ 2-butyloctan-1-ol in kerosene and crystallization as borax can be implemented following the flowsheet in Figure 2. 22.

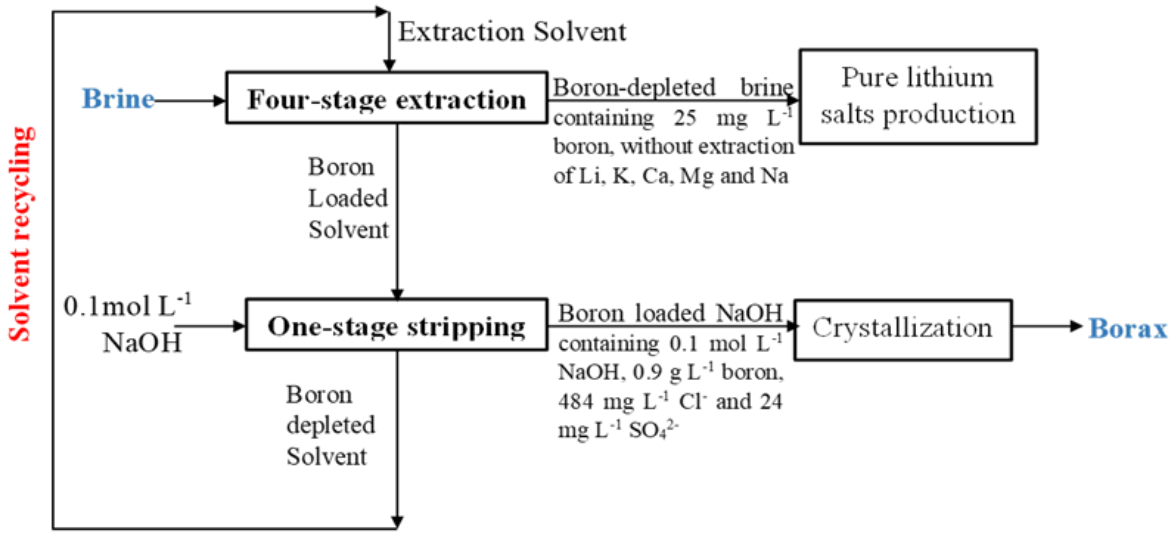



**Figure 2. 22**: Flowsheet for boron extraction from brine and valorization as borax.

## 2.4 Conclusion

Boron extraction from a synthetic brine, simulating the composition of native brine of the salar de Hombre Muerto, was investigated as a function of the phase volume ratio O/A, pH, temperature and alcohol concentration with conventional extraction solvents (mono alcohols diluted in kerosene and diols diluted in a mixture of kerosene 40% (wt) and toluene 60% (wt)) and diol-based DESs. Boron extraction efficiency did not depend on the temperature irrespective of the nature of the alcohol. Boron speciation in brine determined by using the software Pheeqc, combined with data on boron extraction, revealed that boron was extracted by alcohols as boric acid at acidic pH, without co-extraction of the other elements (potassium, calcium, sodium, lithium and magnesium). However, at alkaline pH, magnesium and calcium were co-extracted to the organic phase containing diols due to the decrease of boric acid content and the formation of ion-pairs of borate with these metal ions in the aqueous phase.

Preliminary investigations showed that among the selected extraction solvents, deep eutectic solvents (DESs) provided remarkable extraction efficiency towards boron (93.1−97.1%) with much less organic phase volume (O/A=0.5). However, despite the high performance of DESs and their composition in renewable components such as menthol and thymol, these DESs cannot be employed for industry applications since they are highly soluble in brine (solubility>6 g $L^{-1}$). Among the mono alcohols diluted in kerosene, 2-butyloctan-1-ol containing 12 carbon atoms and the 2-ethylhexan-1-ol containing 8 carbon atoms exhibited the best extraction efficiency of boron (55%) followed by octan-1-ol (8 carbon atoms) at O/A=4, pH=5.5 and 35 °C. This reveals that the hydrophobicity and the branching of the alcohol strongly impact the extraction efficiency. Among the diols diluted in the mixture of kerosene 40% (wt) and toluene 60% (wt), the best extraction efficiency of 99% was obtained with 1 mol $L^{-1}$ 2-ethylhexane-1,3-diol at pH=5.5, O/A=2 and 35 °C. Diols are better extractants than mono alcohols because the two hydroxyl functions favor boron extraction by forming a more stable complex compared to mono alcohols. Conversely, diols co-extracted calcium and magnesium at alkaline pH and exhibited solubilities greater than 259 mg $L^{-1}$ in the brine. Hence, 2-butyloctan-1-ol was preferred due to its solubility in non-aromatic diluents and its lower solubility in brine (18 mg $L^{-1}$) compared to 2-ethylhexane-1,3-diol.

A potential method for extracting boron from brines involves using a 2 mol $L^{-1}$ solution of 2-butyloctan-1-ol in kerosene as the extraction solvent. Unlike industrial processes described in chapter 1 (section 1.2.3.5), this extractant has low solubility in brine (18 mg $L^{-1}$) and

stripping solution (181 mg $L^{-1}$), allowing easy removal using activated carbon adsorption. It shows good boron extraction efficiency, especially in countercurrent continuous mode, and demonstrates high selectivity for boron towards lithium, calcium, magnesium, potassium, and sodium. Importantly, this method enables direct boron extraction from low or high boron-concentrated native brines without needing to acidify and concentrate the brines via evaporation. In one instance, using four stages, it removed 94.2% and 98.2% of boron from salar de Hombre Muerto (Argentina) brines without adjusting their pH, at an O/A ratio of 4 and 7, respectively. Boron was fully recovered from the loaded organic phase using a stripping solution containing 0.1 mol $L^{-1}$ NaOH, allowing subsequent boron crystallization as high-purity borax (purity=99%). This boron extraction process can precede direct lithium extraction (DLE) or the classic solar evaporation method, as depicted in Figure 2. 22, allowing co-valorization of boron with lithium. This co-production of lithium salts alongside boron products like borax reduces waste generation, offering environmental benefits.

Traditionally, boron was extracted from brines using commercial alcohols like Isooctanol, 2-ethylhexan-1-ol, or 2-chloro-4 (1,1,3,3)-tetramethylbutyl-6-methylol-phenol. However, these alcohols had high solubility in both brine and stripping solutions. Therefore, finding efficient and appropriate molecules for boron recovery from native brines is crucial. This study highlights that an extraction solvent comprising 2 mol $L^{-1}$ 2-butyloctan-1-ol diluted in kerosene exhibits efficient extraction, selectivity, and stripping properties for boron. Its low solubility in both brine and the stripping solution is a significant advantage. However, researchers have also suggested that using highly hydrophobic alcohols might further minimize solubility in these solutions. They showed that the length of aliphatic alcohols, the number of alcohol functional groups, and the branching of alkyl groups significantly impact solubility ([43], [44]).

Nuclear magnetic resonance analyses showed that boron was extracted by 2 mol $L^{-1}$ 2-butyloctan-1-ol diluted in kerosene mainly via solvation. Nethertheless, FTIR, and DFT calculations may be employed for better understanding of the nature of the extracted complex. Then, slop analysis method showed that the extracted complex involved one molecule of boric acid and 0.6 equivalent molecule of 2-butyloctan-1-ol. A robust methode like physicochemical modeling could be needed to confirm this result. Additionally, preliminary crystallization experiment showed relative high crystallisation efficiency of boron (54%). However, further investigations are required to crystallize boron efficienciently.

# References


[1] P. M. Brown and S. J. Beckerman, “Production of lithium metal grade lithium chloride from lithium-containing brine,” US4980136A, Dec. 25, 1990 Accessed: Jan. 26, 2022. [Online].Available:https://patents.google.com/patent/US4980136/en?oq=production+of+lithium+metal+grade+lithium+chloride+from+lithium+containing+brine

[2] C. H. Díaz Nieto, N. A. Palacios, K. Verbeeck, A. Prévoteau, K. Rabaey, and V. Flexer, “Membrane electrolysis for the removal of Mg2+ and Ca2+ from lithium rich brines,” *Water Res.*, vol. 154, pp. 117–124, May 2019, doi: 10.1016/j.watres.2019.01.050.

[3] C. H. Díaz Nieto, K. Rabaey, and V. Flexer, “Membrane electrolysis for the removal of Na+ from brines for the subsequent recovery of lithium salts,” *Sep. Purif. Technol.*, vol. 252, p. 117410, Dec. 2020, doi: 10.1016/j.seppur.2020.117410.

[4] G. Almustafa, R. Sulaiman, M. Kumar, I. Adeyemi, H. A. Arafat, and I. AlNashef, “Boron extraction from aqueous medium using novel hydrophobic deep eutectic solvents,” *Chem. Eng. J.*, vol. 395, p. 125173, Sep. 2020, doi: 10.1016/j.cej.2020.125173.

[5] S. Barth, “Comparison of NTIMS and ICP-OES methods for the determination of boron concentrations in natural fresh and saline waters,” *Fresenius J. Anal. Chem.*, vol. 358, no. 7, pp. 854–855, Jul. 1997, doi: 10.1007/s002160050522.

[6] M. Kühn, C. Niewöhner, M. Isenbeck-Schröter, and H. D. Schulz, “Determination of major and minor constituents in anoxic thermal brines of deep sandstone aquifers in Northern Germany,” *Water Res.*, vol. 32, no. 2, pp. 265–274, Feb. 1998, doi: 10.1016/S0043-1354(97)00252-2.

[7] H. Tao, Y. Xiao-ping, G. Ya-fei, L. Ming-li, D. Ji, and D. Tian-long, “Determination of Lithium in High Salinity Samples by Inductively Coupled Plasma Optical Emission Spectrometry (ICP-OES),” *Spectrosc. Spectr. Anal.*, vol. 40, no. 4, pp. 1214–1220, Apr. 2020, doi: 10.3964/j.issn.1000-0593(2020)04-1214-07.

[8] Z. Chen-ling, J. Na, L. Jia, L. Bing-bing, and H. Mei, “Investigation of Lithium Analysis in Geothermal Water by Inductively Coupled Plasma Optical Emission Spectrometry,” *Spectrosc. Spectr. Anal.*, vol. 41, no. 12, pp. 3876–3880, Dec. 2021, doi: 10.3964/j.issn.1000-0593(2021)12-3876-05.

[9] A. Graff, E. Barrez, P. Baranek, M. Bachet, and P. Bénézeth, “Complexation of Nickel Ions by Boric Acid or (Poly)borates,” *J. Solut. Chem.*, vol. 46, no. 1, pp. 25–43, Jan. 2017, doi: 10.1007/s10953-016-0555-x.

[10] S. Sarri, P. Misaelides, D. Zamboulis, and J. Warchoł, “Boron removal from aqueous solutions by a polyethylenimine-epichlorohydrin resin,” *J. Serbian Chem. Soc.*, vol. 83, no. 2, pp. 251–264, 2018.

[11] T. Zhang, D. Li, and L. Meng, “Recent progresses on the boron species in aqueous solution: structure, phase equilibria, metastable zone width (MZW) and thermodynamic model,” *Rev. Inorg. Chem.*, vol. 41, no. 1, pp. 49–60, Mar. 2021, doi: 10.1515/revic-2020-0012.

[12] R. E. Mesmer, C. F. B. Jr, and F. H. Sweeton, “Acidity measurements at elevated temperatures. VI. Boric acid equilibriums,” ACS Publications. Accessed: Nov. 11, 2022. [Online]. Available: https://pubs.acs.org/doi/pdf/10.1021/ic50109a023

[13] D. L. Parkhurst and C. A. J. Appelo, “Description of input and examples for PHREEQC version 3: a computer program for speciation, batch-reaction, one-dimensional transport, and inverse geochemical calculations,” U.S. Geological Survey, Reston, VA, USGS Numbered Series 6-A43, 2013. doi: 10.3133/tm6A43.

[14] V. Kochkodan, N. B. Darwish, and N. Hilal, “Chapter 2 - The Chemistry of Boron in Water,” in *Boron Separation Processes*, N. Kabay, M. Bryjak, and N. Hilal, Eds., Amsterdam: Elsevier, 2015, pp. 35–63. doi: 10.1016/B978-0-444-63454-2.00002-2.

[15] P. Ayers, A. W. L. Dudeney, and F. Kahraman, “Solvent extraction of boron with 2-ethyl-1,3-hexanediol and 2-chloro-4-(1,1,3,3-tetramethylbutyl)-6-methylol-phenol,” *J. Inorg. Nucl. Chem.*, vol. 43, no. 9, pp. 2097–2100, Jan. 1981, doi: 10.1016/0022-1902(81)80556-8.

[16] X. Peng *et al.*, “Recovery of boric acid from salt lake brines by solvent extraction with 2-butyl-1-n-octanol,” *Hydrometallurgy*, vol. 177, pp. 161–167, May 2018, doi: 10.1016/j.hydromet.2018.03.013.

[17] Z. Xu *et al.*, “Recovery of boron from brines with high magnesium content by solvent extraction using aliphatic alcohol,” *RSC Adv.*, vol. 11, no. 26, pp. 16096–16105, Apr. 2021, doi: 10.1039/D1RA01906F.

[18] N. Bachelier and J.-F. Verchere, “Formation of neutral complexes of boric acid with 1,3-diols in organic solvents and in aqueous solution,” *Polyhedron*, vol. 14, no. 13, pp. 2009–2017, Jul. 1995, doi: 10.1016/0277-5387(94)00451-J.

[19] R. R. Grinstead, “Removal of Boron and Calcium from Magnesium Chloride Brines by Solvent Extraction,” *Prod. RD*, vol. 11, no. 4, pp. 454–460, Dec. 1972, doi: 10.1021/i360044a020.

[20] G. Almustafa *et al.*, “Liquification of 2,2,4-trimethyl-1,3-pentanediol into hydrophobic eutectic mixtures: A multi-criteria design for eco-efficient boron recovery,” *Chem. Eng. J.*, vol. 426, p. 131342, Dec. 2021, doi: 10.1016/j.cej.2021.131342.

[21] X. Fan, X. Yu, Y. Guo, and T. Deng, “Recovery of Boron from Underground Brine by Continuous Centrifugal Extraction with 2-Ethyl-1,3-hexanediol (EHD) and Its Mechanism,” *J. Chem.*, vol. 2018, p. e7530837, Oct. 2018, doi: 10.1155/2018/7530837.

[22] R. Zhang *et al.*, “Extraction of boron from salt lake brine using 2-ethylhexanol,” *Hydrometallurgy*, vol. 160, pp. 129–136, Mar. 2016, doi: 10.1016/j.hydromet.2016.01.001.

[23] J. Lü, J. Liu, Y. Sun, and C. Li, “Kinetics of Forward Extraction of Boric Acid from Salt Lake Brine by 2-Ethyl-1,3-hexanediol in Toluene Using Single Drop Technique,” *Chin. J. Chem. Eng.*, vol. 22, no. 5, pp. 496–502, May 2014, doi: 10.1016/S1004-9541(14)60059-8.

[24] J. Guo, Y. Yang, X. Gao, and J. Yu, “Boron extraction from lithium-rich brine using mixed alcohols,” *Hydrometallurgy*, vol. 197, p. 105477, Nov. 2020, doi: 10.1016/j.hydromet.2020.105477.

[25] J. Guo, Y. Yang, X. Gao, and J. Yu, “Boron extraction from lithium-rich brine using mixed alcohols,” *Hydrometallurgy*, vol. 197, p. 105477, Nov. 2020, doi: 10.1016/j.hydromet.2020.105477.

[26] D. E. Garrett, *Handbook of Lithium and Natural Calcium Chloride*. Elsevier, 2004.

[27] F. Folkestad, K. Loiten, G. Mejdell, and A. Torvund, “Method of removing boric acid and boric acid salts from aqueous magnesium chloride solutions,” US3855392A, Dec. 17, 1974 Accessed: Apr. 15, 2023. [Online]. Available: https://patents.google.com/patent/US3855392A/en

[28] H. Hoşgoren, S. Tural, F. Kahraman, M. Toğrul, and M. Karakaplan, “Solvent extraction of boron with l,2-dihydroxy-4-oxadodecane (dhd) in n-amyl alcohol,” *Solvent Extr. Ion Exch.*, vol. 15, no. 2, pp. 249–257, Mar. 1997, doi: 10.1080/07366299708934477.

[29] J. R. Kumar, C.-J. Kim, H.-S. Yoon, D.-J. Kang, and J.-Y. Lee, “Recovery of Boron and Separation of Lithium from Uyuni Salar Brine using 2, 2, 4-Trimethyl-1, 3-Pentanediol (TPD),” *Korean J. Met. Mater.*, vol. 53, no. 8, pp. 578–583, Aug. 2015, doi: 10.3365/KJMM.2015.53.8.578.

[30] X. Peng, D. Shi, Y. Zhang, L. Zhang, L. Ji, and L. Li, “Recovery of boron from unacidified salt lake brine by solvent extraction with 2,2,4-trimethyl-1,3-pentanediol,” *J. Mol. Liq.*, vol. 326, p. 115301, Mar. 2021, doi: 10.1016/j.molliq.2021.115301.

[31] “ICSC 0078-Toluene.” Accessed: Jul. 17, 2023. [Online]. Available: https://www.ilo.org/dyn/icsc/showcard.display?p_lang=fr&p_card_id=0078&p_version=2

[32] D. E. Garrett, “Part 1 - Lithium,” in *Handbook of Lithium and Natural Calcium Chloride*, D. E. Garrett, Ed., Oxford: Academic Press, 2004, pp. 1–235. doi: 10.1016/B978-012276152-2/50037-2.

[33] H. Li, H. Li, Q. Dai, H. Li, and J.-L. Brédas, “Hydrolytic Stability of Boronate Ester-Linked Covalent Organic Frameworks,” *Adv. Theory Simul.*, vol. 1, no. 2, p. 1700015, 2018, doi: 10.1002/adts.201700015.

[34] A. Balinski, V. Recksiek, and N. Kelly, “Solvent Extraction of Boric Acid: Comparison of Five Different Monohydric Alcohols and Equilibrium Modeling with Numerical Methods,” *Processes*, vol. 9, no. 2, Art. no. 2, Feb. 2021, doi: 10.3390/pr9020398.

[35] C. Shuguang, L. Jun, and L. Bing, “Thermochemistry of teepleite,” *Thermochim. Acta*, vol. 376, no. 2, pp. 169–174, Sep. 2001, doi: 10.1016/S0040-6031(01)00562-7.

[36] A. G. Kasikov and A. M. Petrova, “Extraction of sulfuric and hydrochloric acids with macromolecular aliphatic alcohols of varied structure,” *Russ. J. Appl. Chem.*, vol. 81, no. 12, pp. 2079–2083, Dec. 2008, doi: 10.1134/S1070427208120069.

[37] W. C. Blasdale and C. M. Slansky, “The Solubility Curves of Boric Acid and the Borates of Sodium,” *J. Am. Chem. Soc.*, vol. 61, no. 4, pp. 917–920, Apr. 1939, doi: 10.1021/ja01873a043.

[38] “Borax Decahydrate | Multifunctional boric oxide source | U.S. Borax.” Accessed: May 27, 2024. [Online]. Available: https://www.borax.com/products/borax-decahydrate

[39] “ICSC 0567 - Tetraborate de sodium, decahydrate.” Accessed: May 27, 2024. [Online]. Available:https://chemicalsafety.ilo.org/dyn/icsc/showcard.display?p_lang=fr&p_card_id=0567

[40] P. M. Brown and S. J. Beckerman, “Production of lithium metal grade lithium chloride from lithium-containing brine,” US4980136A, Dec. 25, 1990 Accessed: Jan. 26, 2022. [Online].Available:https://patents.google.com/patent/US4980136/en?oq=production+of+lithium+metal+grade+lithium+chloride+from+lithium+containing+brine

[41] W. L. McCabe, J. C. Smith, and P. Harriott, *Unit operations of chemical engineering*. McGraw-Hill, 1993. Accessed: May 09, 2024. [Online]. Available: https://thuvienso.hoasen.edu.vn/handle/123456789/8475

[42] D. E. Garrett, “Chapter 8 - Processing,” in *Borates*, D. E. Garrett, Ed., San Diego: Academic Press, 1998, pp. 333–400. doi: 10.1016/B978-012276060-0/50009-7.

[43] M. Karakaplan, S. Tural, B. Tural, Y. Turgut, and H. Hoşgören, “The Solvent Extraction of Boron with Synthesized Aliphatic 1,3-Diols: Stripping and Extraction Behavior of Boron by 2,2,5-Trimethyl-1,3-hexanediol,” *Solvent Extr. Ion Exch.*, vol. 22, no. 6, pp. 897–911, Dec. 2004, doi: 10.1081/SEI-200037400.

[44] M. Karakaplan, S. Tural, M. Sunkür, and H. Hoşgören*, “Effect of 1,3-Diol Structure on the Distribution of Boron Between CHCl3 and Aqueous Phase,” *Sep. Sci. Technol.*, vol. 38, no. 8, pp. 1721–1732, Jan. 2003, doi: 10.1081/SS-120019405.

# 3 Chapter 3: Production of high-grade borax and lithium carbonate by combining solvent extraction, precipitation and electrodialysis operations


3.1 Introduction ..... 147

3.2 Materials and methods ..... 147

3.2.1 Boron extraction and stripping ..... 147

3.2.2 Brine processing by electrodialysis ..... 148

3.2.2.1 Electrodialysis cells ..... 148

3.2.2.2 Data analysis ..... 152

3.2.3 Analyses ..... 153

3.2.4 Speciation calculations ..... 154

3.3 Results and discussion ..... 154

3.3.1 Boron extraction ..... 154

3.3.2 Stage I of the electrodialysis ..... 155

3.3.2.1 Magnesium and calcium removal ..... 155

3.3.2.2 Magnesium hydroxide production ..... 161

3.3.3 Stage II of the electrodialysis ..... 163

3.3.3.1 Sodium recovery ..... 163

3.3.3.2 Sodium carbonate production ..... 166

3.3.4 Stage III of the electrodialysis ..... 171

3.3.4.1 Lithium recovery ..... 171

3.3.4.2 Lithium carbonate production ..... 172

3.3.5 Flowsheet of the overall process ..... 175

3.4 Conclusion ..... 177

References ..... 179

## 3.1 Introduction

Electrodialysis (ED) is a membrane technology employed to separate ions through ion-exchange membrane from one solution to another one under an electrical field ([1], [2], [3]). ED has been used for decades for desalination of seawater ([4], [5], [6]), production of drinking water and salts [7]. Nowadays, electrodialysis appears as a relevant technology in hydrometallurgy that could be employed in many applications including direct lithium extraction from brines ([8], [9], [10], [11]). However, the numerous impurities within lithium-rich continental brines as those of the salar de Hombre Muerto make lithium recovery very intricate. Indeed, boron, magnesium, calcium, sodium and potassium impurities should be removed before lithium extraction. A three-stage electrodialysis process has been developed by Torres et al. [12] allowing selective extraction and co-valorization of magnesium, calcium and sodium with lithium. Magnesium and calcium were recovered as magnesium hydroxide and calcium hydroxide, respectively, while sodium was extracted as sodium carbonate. In last, lithium was produced as lithium carbonate with a purity of 97.5% whereas it is generally expected at least 99.5% for battery grade lithium carbonate [13].

This chapter investigates the impact of boron extraction on the performance of the electrodialysis process, particularly on the quality of lithium carbonate with the aim to co-valorize boron as borax besides magnesium, calcium and sodium from salar de Hombre Muerte brine. In this chapter, it was decided to use 2 mol $L^{-1}$ 2-butyloctan-1-ol diluted in kerosene to extract boron prior to electrodialysis in accordance with the results presented in the previous chapters. After performing boron extraction, magnesium and calcium were removed by electrodialysis, and sodium was recovered as sodium carbonate by combining electrodialysis and precipitation using carbon dioxide. Finally, lithium was recovered as lithium carbonate in the last stage of the electrodialysis process.

## 3.2 Materials and methods

### 3.2.1 Boron extraction and stripping

Boron extraction and stripping experiments were performed under the optimal extraction and stripping conditions reported in chapter 2, *i.e.* 2 mol $L^{-1}$ 2-butyloctan-1-ol diluted in kerosene, pH=7.5, O/A=4 and 25 °C for the extraction and 0.1 mol $L^{-1}$ sodium hydroxide, O/A=4 and 25 °C for the stripping. Therefore, 4 L of the extraction solvent were mixed with 1 L of native brine from the salar de Hombre Muerto which the composition is reported in Table 3. 1. Boron was stripped from the loaded organic phase with 1 L of 0.1 mol $L^{-1}$ sodium

hydroxide. Both extraction and stripping operations were performed by mixing the organic and aqueous phases in 10 L-glass vessel using two propellers composed of four blades each. The first propeller was fixed in the middle of the aqueous phase and the second propeller was in the middle of the organic phase so that the steady state was reached after 5 min stirring at 216 rpm (see the configuration of the extraction and stripping setup in Figure B. 1 in appendix B, and the data of extraction and stripping equilibrium tests in Table B. 1 in appendix B). After extraction or stripping, the organic-aqueous phases mixtures were settled for 5 min to separate the organic phase and the aqueous phase. Then, the boron-loaded organic phase obtained after boron extraction was employed for the stripping test, while the boron-depleted brine was further processed by electrodialysis. After boron stripping, the boron-free organic phase was used to perform the next extraction experiment, while the boron in the stripping solution was crystallized as borax according to experimental conditions reported in chapter 2-section 2.3.5. The extraction and stripping efficiencies of boron ($E_B$(%) and $SE_B$(%), respectively) were calculated as follows:

$$E_B(\%) = \frac{[B]_0 - [B]}{[B]_0} \times 100 \quad (3.\ 1)$$

$$SE_B(\%) = \frac{[B]'}{[B]_0 - [B]} \times 100 \quad (3.\ 2)$$

where $[B]_0$ and $[B]$ are the concentrations of boron in the brine before boron extraction and after boron extraction, respectively. $[B]'$ is boron concentration in the stripping solution at equilibrium.

**Table 3. 1:** Composition, total dissolved solid (TDS) and pH of the brine from the salar de Hombre Muerto.

| Concentrations (mg $L^{-1}$) | | | | | | | | pH | TDS ($g\ L^{-1}$) |
|---|---|---|---|---|---|---|---|---|---|
| B | K | Li | Mg | Na | Ca | $Cl^-$ | $SO_4^{2-}$ | | |
| 507.6 | 6,812 | 578 | 2,315.9 | 91,732.5 | 119.1 | 176,144.5 | 14,129.7 | 7.5 | 304.5 |

## 3.2.2 Brine processing by electrodialysis

### 3.2.2.1 Electrodialysis cells

A non-pretreated brine, *i.e.* brine without boron extraction, and a boron-depleted brine, *i.e.* brine after boron extraction, were processed by electrodialysis in three stages (Figure 3. 1). In

stage I, calcium and magnesium were removed. Then, the outlet of the cathodic compartment of stage I fed the middle compartment of stage II where sodium was recovered as sodium carbonate. Finally, the outlet of the middle compartment of stage II fed the middle compartment of stage III in which lithium was converted into lithium carbonate. All electrodialysis experiments were carried out in batch mode at room temperature 22±2 °C. The electrodialysis cells were designed and made in house based on previous works reported in literature ([14], [15]). The cells were composed of three compartments made of acrylic frames. The frames were bolted together between two rectangular acrylic plates. Each compartment was separated by cation exchange membrane (CEM) (CMI-7000S, Membrane International Inc., USA) or anion exchange membrane (AEM) (AMI-7001CR, Membrane International Inc., USA). Membrane specifications are given in Table B. 2 in appendix B. The anodic, middle and cathodic compartments were connected each to Schott-bottle. The aqueous solutions in the anodic, middle and cathodic compartments were constantly recirculated through the cell compartments using a peristaltic pump (flow rate=18 L $h^{-1}$, PC28 APEMA, Argentina). Recirculation also ensured stirring of the solutions. The anode used was a titanium (Ti) mesh electrode coated with an iridium-based mixed metal oxide ($IrO_2/TiO_2$; 65/35%, Magneto Special Anodes), with a centrally attached, perpendicular current collector. The cathode was a stainless-steel wire mesh with a stainless-steel current collector. The distance between the electrodes was 23 mm. Between the surface of the electrodes and the membranes, two plastic meshes were placed to avoid direct contact between the electrodes and the membranes. Experiments were run in galvanostatic mode using a DC/CC regulated power supply (V&A instrument, China). The current densities were reported with respect to the projected geometric surface of the membrane in contact with the solutions. The cell voltage was monitored directly from the digital screen in the power supply. After each experiment, the electrodialysis cells and the membranes were rinsed with de-ionized water. When not in use, the membranes were kept in artificial brine.

In stage I, the volume of each compartment and the surface area of the membrane in contact with the solutions were 200 mL and 0.01 $m^2$, respectively. The anodic and middle compartments were separated by a cation exchange membrane (CEM), and the middle and cathodic compartments were separated by an anion exchange membrane (AEM). The anodic compartment and the middle compartments were connected each to Schott-bottle containing 0.05 mol $L^{-1}$ nitric acid ($HNO_3$) and 0.01 mol $L^{-1}$ hydrochloric acid (HCl), respectively. While the cathodic compartment was connected to a Schott-bottle that was employed as a decanter

and contained the non-pretreated brine or the brine depleted of boron. The volume of anolyte, catholyte or brine was 1 L. Magnesium and calcium removal lasted 5 hours. The recovered precipitates were centrifuged at 3,200 rpm for 15 min (LC-15 Lugimac, Argentina), washed with deionized water, and dried in a laboratory oven at 100 °C for 24 hours.

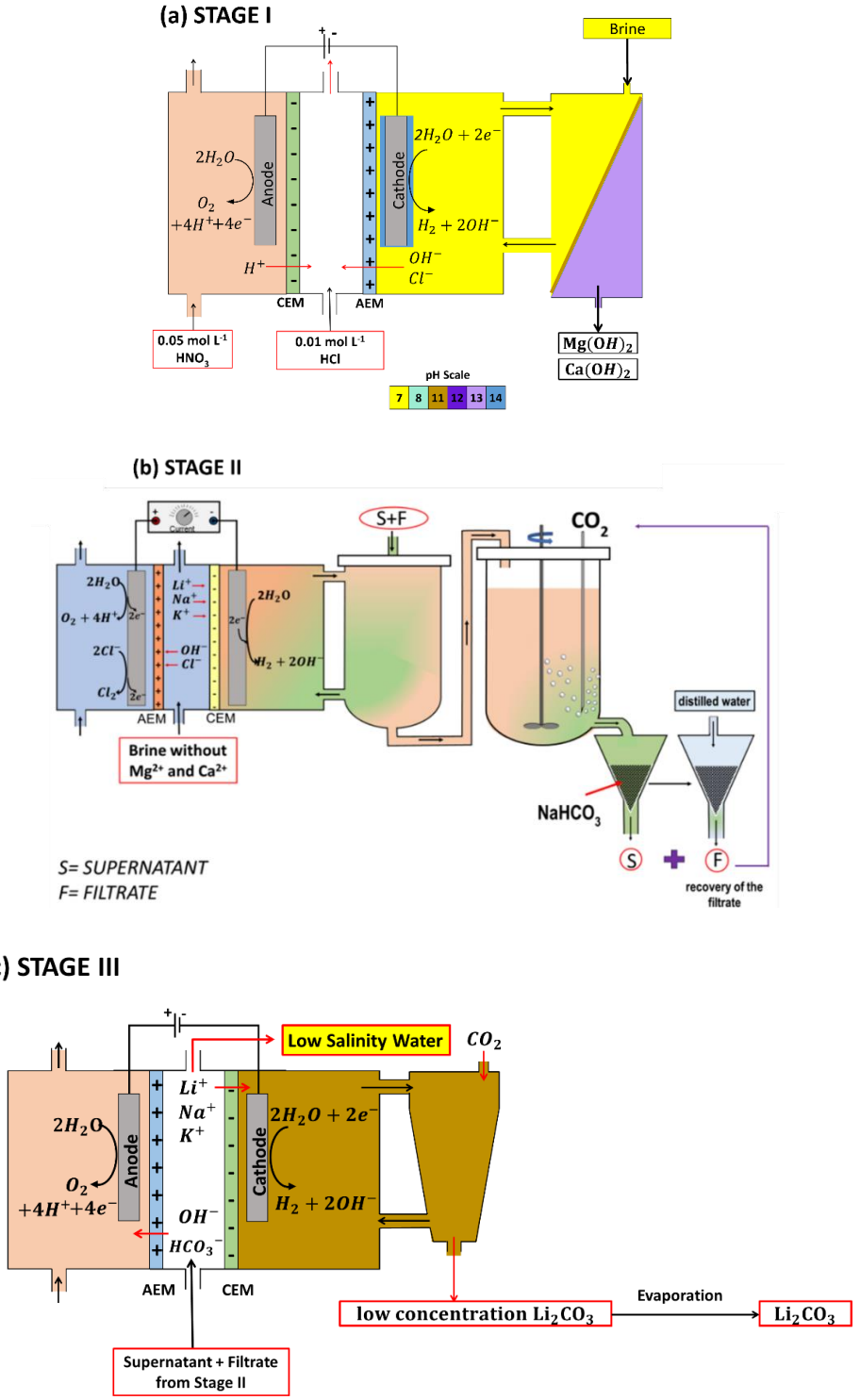



**Figure 3. 1:** (a) Stage I, (b) Stage II and (c) Stage III implemented during the electrodialysis experiments.

Particularly, in stages II and III, the total volume for each compartment and the surface area of the membrane in contact with the solutions were 100 mL and 0.005 $m^2$, respectively. Additionally, the anodic and middle compartments were separated by an anion exchange membrane (AEM), and the middle and cathodic compartments were separated by a cation exchange membrane (CEM). The electro-membrane experiments in stages II and III were focused on the transfer of cations from the middle to the cathodic compartment and anions transfer from the middle compartment to the anodic compartment. Therefore, chloride transfer into the anodic compartment and water oxidation can be responsible for chlorine and $O_2$ gas formation at pH below 7 [16]. For safety reasons, the anodic compartment was connected to Schott-bottle containing 2 L of 0.5 mol $L^{-1}$ sodium carbonate ($Na_2CO_3$), which buffered the solution at pH=11 and allowed to disproportionate $Cl_2$ into $Cl^-$ and $ClO^-$[16].

In stage II, the cathodic and middle compartments were connected each to Schott-bottle containing 250 mL of 0.1 mol $L^{-1}$ sodium bicarbonate ($NaHCO_3$) and 500 mL of stage I outlet (brine without calcium and magnesium), respectively. High volume ratio between the solution in the middle compartment and the catholyte allowed to efficiently concentrate cations in the catholyte. The electro-membrane experiments were performed up to 30 V, since high drop of ion concentration in the middle compartment is responsible for the increase of the cell voltage due to the increase of the cell resistance [17].

In order to respect the chemical stability of the membranes, three consecutive batch electrodialysis experiments were carried out with the non-pretreated brine or the boron-depleted brine. Each experiment was manually stopped when the pH of catholyte reached about 14. Then, the aqueous solutions in the three compartments were transferred separately in Schott-bottles to avoid water transfer between the compartments by osmosis. The cations-loaded catholyte was transferred in an external Schott-bottle working as decanter where carbon dioxide ($CO_2$) was bubbled until pH=7.7−8 in order to precipitate sodium as sodium bicarbonate ($NaHCO_3$). Thereafter, the precipitate was recovered by vacuum filtration, washed with deionized water at 0 °C to prevent the redissolution of the solid, and dried in a laboratory oven at 100 °C for 24 hours. After filtration, the mixture of catholyte depleted of sodium (supernatant) and water obtained from solid wash (filtrate) was returned to the cell as well as the anolyte and the brine previously transferred in the bottles to perform the second electrodialysis experiment. Therefore, three electrodialysis-precipitation experiments were performed with the non-pretreated brine and the boron-depleted brine.

In stage III, the cathodic and the middle compartments were connected each to Schott-bottle containing 150 mL of 0.1 mol $L^{-1}$ lithium carbonate ($Li_2CO_3$) and 200 mL of the catholyte obtained after the last precipitation in stage II (sodium-depleted catholyte), respectively. Unfortunately, the low volume ratio between the solution in the middle compartment and the catholyte (1.3) and water migration from the middle compartment to both catholyte and anolyte were a limitation for cations concentration in the catholyte. The electrodialysis experiment was performed for 11 hours until the voltage reached 30 V. Then, the catholyte was transferred into a Schott-bottle to perform $CO_2$ bubbling for 1h30 min until the pH reached 9.4. No precipitate was observed as the solubility of $Li_2CO_3$ was not reached in the catholyte due to the low concentration of lithium. Therefore, $Li_2CO_3$ was crystallized by evaporation at 90 °C. Evaporation was stopped when the catholyte volume was reduced by four. Then, the solid was washed with deionized water at 100 °C to avoid the redissolution and dried in a laboratory oven at 100 °C for 24 hours.

### 3.2.2.2 Data analysis

- The circulated charge per liter of brine (C $L^{-1}$) was calculated as follows:

$$\text{Charge} = \frac{i \times t}{V} \tag{3. 3}$$

where i (in A) and *t* (in s) are the applied constant current and the electrodialysis time, respectively. V is the volume of the brine employed for the electrodialysis experiment.

- The normalized concentration ($C/C_0$) referred to the ratio between the concentration of an element at time *t* in the electrodialysis compartment (C) and the initial concentration ($C_0$) of the element in the same compartment.

- The electrochemical energy consumption per volume of treated brine (Wh $L^{-1}$) was calculated as follows:

$$E = \int_0^t \frac{E_{source} \times i \times dt}{V_0} \tag{3. 4}$$

where $E_{source}$ (V) is the voltage drop in the electrodialysis cell. And $V_0$ is the initial brine volume.

- The separation coefficient ($F_{M_1-M_2}$) referred to the ratio of concentrations in the middle compartment of coexisting cations at time *t* divided by the ratio of the initial concentrations. The separation coefficient was calculated as follows:

$$F_{M_1-M_2} = \frac{\left(C_{M_1}/C_{M_2}\right)_t}{\left(C_{M_1}/C_{M_2}\right)_0} \quad (3.5)$$

where $C_{M_1}$ and $C_{M_2}$ are the concentrations of cation $M_1$ and $M_2$, respectively. If $F_{M_1-Li} > 1$ then lithium passes through the CEM preferentially. Conversely, if $F_{M_1-Li} < 1$ then the coexisting cation passes preferentially through the CEM.

### 3.2.3 Analyses

The aqueous solutions were sampled for chemical analyses. Magnesium and calcium concentrations were determined by complexometric titrations with EDTA (Anedra, p.a.). Eriochrome Black T (Anedra, p.a.) and Murexide (Anedra, p.a.) were used as complexometric indicators to determine the endpoint. Concentrations of magnesium and calcium obtained by titration were confirmed by microwave plasma-atomic emission spectrometer analyses (MP-AES model 4210, Agilent, France). The samples were diluted 100 times for calcium analysis and 1000 times for magnesium analysis as well as lithium, boron, potassium and sodium analyses with the microwave plasma-atomic emission spectrometer previously mentioned. ICP Standards (VWR) containing 1,000 mg $L^{-1}$ boron, lithium, magnesium, potassium, calcium or sodium were used to plot the calibrations curves. Concentrations of lithium, boron, potassium, magnesium, calcium and sodium were determined at 670.784 nm, 249.677 nm, 766.491 nm, 518.360 nm, 393.366 nm and 568.820 nm, respectively (see more detailed of the elemental analysis method in appendix A). Concentrations of $Cl^-$ and $SO_4^{2-}$ were determined by chromatographic analyses (Dionex ICS 900 ™ IonPac™ AS22). The pH was registered with a pH-meter (Hanna), and by universal pH test paper strips. The repeatability of the experiments was checked by repeating the experiments twice, and the relative error was below 4%.

All the solids were ground before XRD analysis. The bulk mineralogy of the suspended particle matter (SPM) was determined by X-ray diffraction using a D8 Discover Bruker diffractometer with an X-ray tube emitting Cu-Kα1 radiation (λ=1.5406 Å). X-ray diffraction patterns were recorded at 40 kV and 40 mA on powder samples under ambient conditions and within a range of 2θ (2.5°−65°), a step size of 0.035°, and a 3-s collection time wih a LynxEye detector.

### 3.2.4 Speciation calculations

Speciation calculations in aqueous phase were performed with the software Phreeqc ver. 3.7 [18]. Speciation diagrams were plotted with PhreePlot which is a charting and plotting extension of Phreeqc. All the details on the method employed for speciation calculations are reported in chapter 2-section 2.3.1.

## 3.3 Results and discussion

### 3.3.1 Boron extraction

Eight batch extractions of boron were performed to recover 90% of boron from the brine of the salar de Hombre Muerto (Table B. 3 in appendix B). The brine composition before and after extraction is depicted in Table 3. 2. There is no significant difference between potassium, sodium or lithium concentrations before and after boron extraction (Table 3. 2). However, significant decrease in magnesium and calcium concentrations are observed after boron extraction. Magnesium and calcium concentrations decrease by 11.3% and 23%, respectively (Table 3. 2). This can be attributed to (i) co-extraction or (ii) precipitation. Magnesium and calcium cannot be co-extracted with boron since 2-butyloctan-1-ol does not extract calcium and magnesium under these experimental conditions (see boron extraction by 2-butyloctan-1-ol in chapter 2). Conversely, magnesium and calcium can be precipitated under alkaline conditions as magnesium hydroxide ($Mg(OH)_2$) and calcium hydroxide ($Ca(OH)_2$), respectively [16]. Hence, the alkalinity of the brine after boron extraction (pH=8.8) is responsible for magnesium and calcium precipitation. The slight increase in brine pH after boron extraction is attributed to the co-extraction of hydrochloric acid evidenced by the decrease of chloride concentration in the brine (Table 3. 2). Afterwards, the brine was filtered to remove the colloidal suspension formed due to magnesium hydroxide precipitation [19]. After filtration, the boron-depleted brine was utilized to investigate magnesium and calcium removal by electrodialysis.

**Table 3. 2:** Composition and pH of the brine of the salar de Hombre Muerto (1) before and (2) after boron extraction.

| | Concentrations (mg $L^{-1}$) | | | | | | | | pH |
|---|---|---|---|---|---|---|---|---|---|
| Brine | B | K | Li | Mg | Na | Ca | $Cl^-$ | $SO_4^{2-}$ | |
| (1) | 507.6 | 6,812 | 578 | 2,315.9 | 91,732.5 | 119.1 | 176,144.5 | 14,129.7 | 7.5 |
| (2) | **50.8** | 6685 | 546 | 2054.9 | 88,802.0 | 91.6 | 155,422.3 | 12,733.1 | 8.8 |

## 3.3.2 Stage I of the electrodialysis

### 3.3.2.1 Magnesium and calcium removal

Exactly 1 L of the non-pretreated brine or the boron-depleted brine were processed in the cathodic compartment of the electrodialysis cell at 215 A $m^{-2}$ for 5 hours (corresponding to 38,700 C circulated charge per liter of treated brine) to remove calcium and magnesium (data of pH, current, voltage, and boron, magnesium and calcium concentrations as a function of the electrodialysis time for each brine are gathered in Tables B. 4 and B. 5 in appendix B). In the anodic compartment, water is oxidized to oxygen (Equation 3. 6). Concomitantly, in the cathodic compartment, water is reduced to hydrogen with simultaneous production of $OH^-$ (Equation 3. 7).

$$2H_2O \rightarrow O_2 + 4H^+ + 4e^- \quad (3.\ 6)$$

$$2H_2O + 2e^- \rightarrow H_2 + 2OH^- \quad (3.\ 7)$$

As shown in Figure 3. 2, the pH of the non-pretreated brine or the boron-depleted brine increases as a function of electrodialysis time since water reduction in the cathodic compartment generates $OH^-$ anions (Equation 3. 7). Figure 3. 2 shows that the same trend is observed for both non-pretreated brine and boron-depleted brine. However, the pH of boron-depleted brine increases rapidly compared to that of the non-pretreated brine. For instance, at 180 min the pH of boron-depleted brine reached 12, while 260 min was required to reach pH=12 in the non-pretreated brine (Figure 3. 2). Then, the presence of boron in the brine increases the electrodialysis time. Sharp and slight increases of pH are observed at different time depending on the nature of the brine (Figure 3. 2). The sharp increases of pH observed at the early stage of the experiment are attributed to the slight precipitation phenomena while the slight increases of pH can be explained by important precipitation of solid. Indeed, the $OH^-$ anions produced in the cathodic compartment are highly or slightly consumed by the cationic species in solution to form precipitates. Therefore, low consumption of $OH^-$ was responsible for high increases of pH, while high consumption of $OH^-$ remained the brines pH roughly constant. $K^+$, $Mg^{2+}$, $Ca^{2+}$, $Na^+$ and $Li^+$ cations can precipitate as KOH, $Mg(OH)_2$ $Ca(OH)_2$, NaOH and LiOH, respectively, under alkaline conditions. However, Table 3. 3 indicates that $Ca(OH)_2$ and $Mg(OH)_2$ exhibit the lowest solubility in water [16]. Then, it can be inferred that the precipitates are $Ca(OH)_2$ and $Mg(OH)_2$. According to the values of solubility products of magnesium hydroxide ($pK_{SP,Mg(OH)2}$=11.25) and calcium hydroxide ($pK_{SP,Ca(OH)2}$=5.3), $Mg(OH)_2$ is less soluble than $Ca(OH)_2$ and thus, $Mg(OH)_2$ precipitates before $Ca(OH)_2$. This

difference in precipitation between $Ca(OH)_2$ and $Mg(OH)_2$ is observed in Figure B. 2 in appendix B.

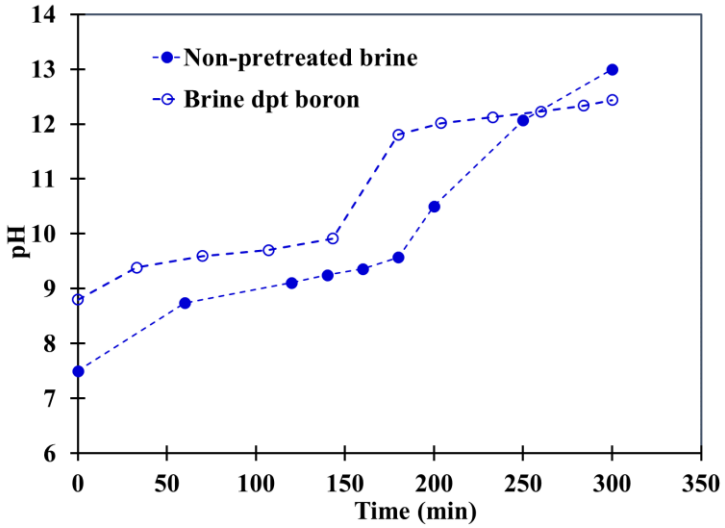



**Figure 3. 2:** pH of the non-pretreated brine and the boron-depleted brine as a function of the electrodialysis time (dpt denotes depleted).

**Table 3. 3:** Solubility at 25 °C or 20 °C of salts that could precipitate in the cathodic compartment (* solubility at 20 °C) [16].

| Salt | Solubility (g $L^{-1}$) |
|---|---|
| KOH | 1,207.5 |
| NaOH | 1,000 |
| LiOH | 124.9 |
| $Ca(OH)_2$ | 1.2* |
| $Mg(OH)_2$ | $6.9\times10^{-3}$* |

Figures 3 .3 (a) and (b) show magnesium and calcium concentrations as a function of pH, respectively, in both non-pretreated brine and boron-depleted brine as a function of pH. A significant decrease in magnesium concentration is observed at pH=8.7−9.9 in the brines (Figure 3. 3 (a)). Full precipitation of magnesium was achieved at pH=10.5 in the non-pretreated brine. Conversely the pH had to be increased up to 11.5 to totally remove magnesium by precipitation when electrodialysis experiments were conducted in the boron-depleted brine. Similar results were reported by Nieto et al. [20] for the non-pretreated brine. Figures B. 3 and B. 4 in appendix B show that several species of magnesium or calcium exist in the non-pretreated brine and the boron-depleted brine. The precipitation of magnesium at lower pH in the non-pretreated brine than in the boron-depleted brine can be attributed to the difference in concentrations regarding $MgOH^+$, $MgH_2BO_3^+$ and $MgB(OH)_4^+$ (Figure 3. 4). Indeed, $Mg^{2+}$ forms $MgOH^+$ with $OH^-$ in solution according to Equation 3. 8. $MgH_2BO_3^+$ and $MgB(OH)_4^+$

are formed according to the reactions reported in Equations 3. 10 and 3. 12. The difference of behavior observed between the non-pretreated brine and the boron-depleted brine cannot be explained by the precipitation of $Mg(OH)_2$ from $MgOH^+$ (Equation 3. 9) since no significant difference is observed between $MgOH^+$ speciation vs pH in the non-pretreated brine and the brine depleted of boron.

$MgH_2BO_3^+$ and $MgB(OH)_4^+$ concentrations are higher in the non-pretreated brine (Figure 3. 4). Then, it can be inferred that magnesium precipitates at lower pH in the presence of chloride due to the formation of solids such as $MgH_2BO_3Cl$ and $MgB(OH)_4Cl$ from $MgH_2BO_3^+$ and $MgB(OH)_4^+$, respectively, according to Equations 3. 11 and 3. 13. This assumption is supported by the presence of boron and chloride anions in the precipitate (Table B. 6 in appendix B). Hence, boron favors magnesium precipitation in the non-pretreated brine but contributes to increase the electrodialysis time and decrease the purity of the magnesium precipitate.

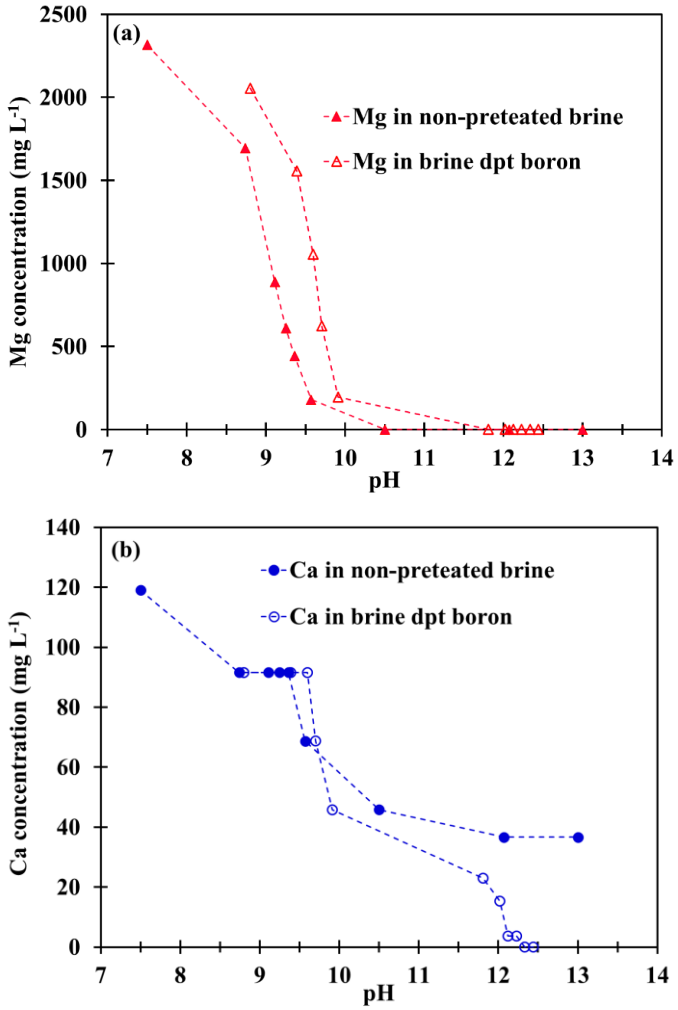



**Figure 3. 3:** (a) Magnesium and (b) calcium concentrations in the brines as a function of the pH during the electrodialysis (dpt denotes depleted).

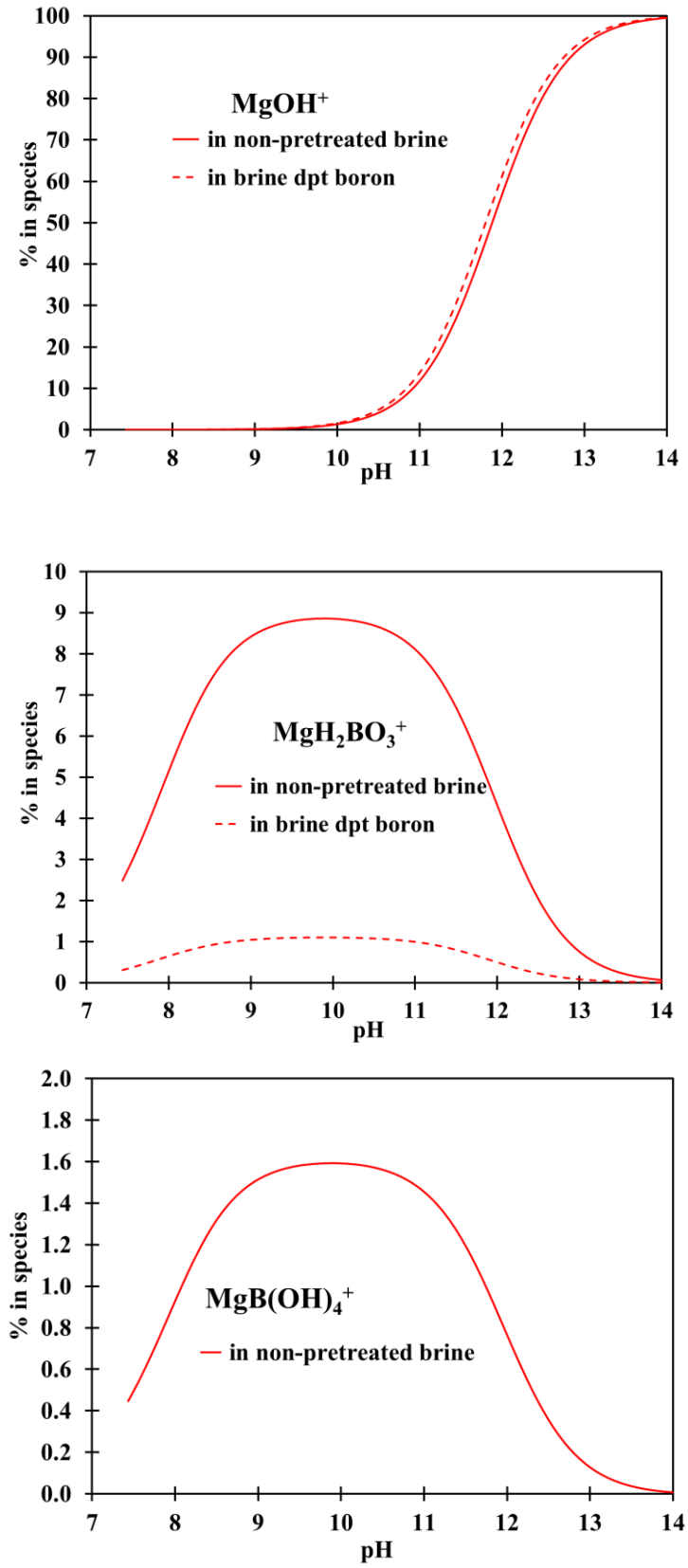



**Figure 3. 4:** Magnesium speciation vs pH in the non-pretreated brine and brine depleted of boron. Only $MgOH^+$, $MgH_2BO_3^+$ and $MgB(OH)_4^+$ species were reported in these Figures (dpt denotes depleted).

$$Mg^{2+} + OH^- \rightleftarrows MgOH^+ \quad (3.\ 8)\ [16]$$

$$MgOH^+ + OH^- \rightleftarrows Mg(OH)_{2(S)} \quad (3.\ 9)\ [16]$$

$$Mg^{2+} + H_3BO_3 \rightleftarrows MgH_2BO_3^+ + H^+ \quad (3.\ 10)\ [21]$$

$$MgH_2BO_3^+ + Cl^- \rightleftarrows MgH_2BO_3Cl_{(S)} \quad (3.\ 11)$$

$$\mathbf{Mg^{2+} + H_3BO_3 + H_2O \rightleftarrows MgB(OH)_4^+ + H^+} \quad (3.\ 12)\ ([22], [23])$$

$$MgB(OH)_4^+ + Cl^- \rightleftarrows MgB(OH)_4Cl_{(S)} \quad (3.\ 13)$$

Figure 3. 3 (b) shows that boron can contribute to decrease calcium concentration only at pH=7.5−8.8. This can be attributed to the precipitation of $CaH_2BO_3Cl$ and $CaB(OH)_4Cl$ species (Equations 3. 17 and 3. 19). These species are obtained through the formation of boron-calcium species such as $CaH_2BO_3^+$ and $CaB(OH)_4^+$ species (Figure 3. 5), which are formed according to Equations 3. 16 and 3. 18. The decrease of calcium concentration in the brines is also attributed to the formation of $CaOH^+$ (Equation 3. 14) which precipitates as $Ca(OH)_2$ according to Equation 3. 15. There is no influence of pH on calcium precipitation at pH=8.8−9.6 and 91.6 mg $L^{-1}$ Ca was found in the brines (Figure 3. 3 (b)). However, calcium precipitation is more pronounced at pH above 9.6 in the depleted-boron brine than in the non-pretreated brine. Low calcium precipitation could be explained by the formation of the highly soluble boron-calcium species $CaH_2BO_3Cl$ and $CaB(OH)_4Cl$ under very alkaline solution. The residual calcium concentration in the non-pretreated brine (36.6 mg $L^{-1}$) was removed by putting the brine in contact with ambient carbon dioxide for 24 hours. It is important to point out that boron extraction from brine could contribute to achieve selective precipitation of magnesium and calcium since magnesium hydroxide can be precipitated at pH=8.8−9.6, and calcium hydroxide can be precipitated by increasing the pH between 9.6 and 12.3.

$$Ca^{2+} + OH^- \rightleftarrows CaOH^+ \quad (3.\ 14)\ [16]$$

$$CaOH^+ + OH^- \rightleftarrows Ca(OH)_{2(S)} \quad (3.\ 15)\ [16]$$

$$Ca^{2+} + H_3BO_3 \rightleftarrows CaH_2BO_3^+ + H^+ \quad (3.\ 16)\ [21]$$

$$CaH_2BO_3^+ + Cl^- \rightleftarrows CaH_2BO_3Cl_{(S)} \quad (3.\ 17)$$

$$Ca^{2+} + H_3BO_3 + H_2O \rightleftarrows CaB(OH)_4^+ + H^+ \quad (3.\ 18)\ [22]$$

$$CaB(OH)_4^+ + Cl^- \rightleftarrows CaB(OH)_4Cl_{(S)} \quad (3.\ 19)$$

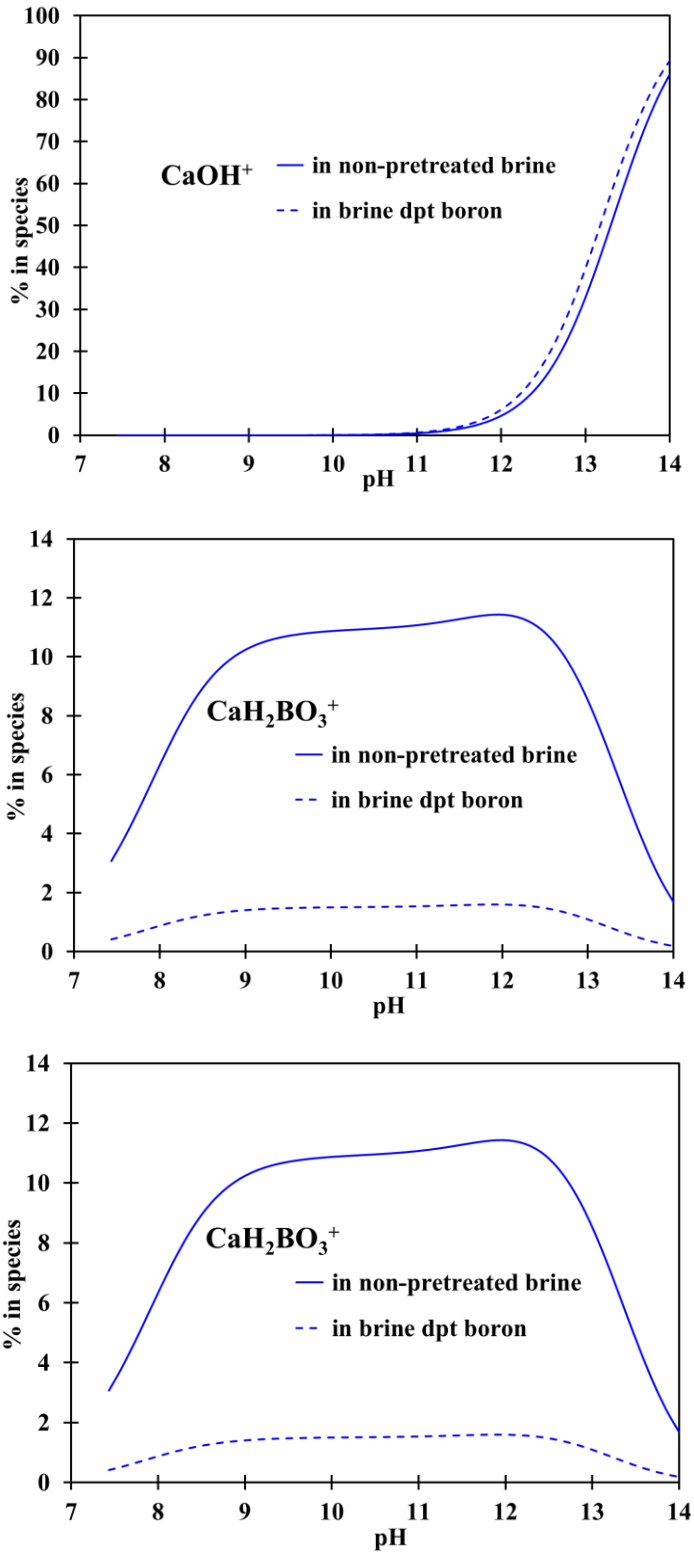



**Figure 3. 5:** Ca speciation vs pH in the non-pretreated brine and the brine depleted of boron. Only $CaOH^+$, $CaH_2BO_3^+$ and $CaB(OH)_4^+$ species were reported in these Figures. dpt denotes depleted.

Table 3. 4 gathers boron, potassium, lithium, magnesium, sodium, calcium, chloride and sulfate concentrations in the brines before and after stage I. The concentrations of potassium, lithium, sodium, chloride and sulfate increase slightly after the experiment for both non-pretreated brine and boron-depleted brine. This is explained by the migration of water molecules from the cathodic compartment to the middle comportment by electroosmosis ([24], [25], [26], [27], [28]) and water reduction into $OH^-$ and $H_2$ (Equation 3. 7).

The energy consumptions were 0.062 kWh and 0.052 kWh per liter of non-pretreated brine and boron-depleted brine, respectively. This indicates that boron extraction before the electrodialysis decreases the energy consumption by 17%.

**Table 3. 4:** Composition and pH of (1) non-pretreated brine, (2) non-pretreated brine in the cathodic compartment after magnesium and calcium removal, (3) boron-depleted brine, and (4) boron-depleted brine in the cathodic compartment after magnesium and calcium removal.

| | Concentration (mg $L^{-1}$) | | | | | | | | pH |
|---|---|---|---|---|---|---|---|---|---|
| Brine | B | K | Li | Mg | Na | Ca | $Cl^-$ | $SO_4^{2-}$ | |
| (1) | 507.6 | 6,812 | 578 | 2,315.9 | 91,732.5 | 119.1 | 176,144.5 | 14,129.7 | 7.5 |
| (2) | 446.7 | 8,800 | 715 | **0** | 110,633.5 | **0** | 185,799.9 | 16,365.5 | 13 |
| (3) | 50.8 | 6,685 | 546 | 2,054.9 | 88,802 | 91.6 | 155,422.3 | 12,733.1 | 8.8 |
| (4) | 50.8 | 7,427.5 | 560 | **0** | 89,315 | **0** | 151,974.7 | 13,283.8 | 12.4 |

### 3.3.2.2 Magnesium hydroxide production

After precipitation, the solid was removed from the brines by centrifugation and filtration under vacuum. Thereafter, it was harvested and dried at 100 °C for 24 hours in oven. The weight of the solid obtained from the electro-membrane experiment carried out with the non-pretreated brine or the boron-depleted brine was higher than that calculated by considering the total amount of magnesium and calcium initially present in the brine (26.4 g vs 5.8 g for 1 liter of non-pretreated brine and 21.7 g vs 5.1 g for 1 liter of boron-depleted brine). Elemental analysis of the solids after redissolution in nitric acid showed traces of potassium, boron, calcium and lithium, and large amount of sodium and chloride (Table B. 6 in appendix B). This is attributed to the colloidal nature of $Mg(OH)_2$ which behaves like a sponge entrapping large quantities of species such as sodium and chloride. The colloidal precipitate is also responsible for filtration issues due to coagulation and flocculation phenomena ([19], [29], [30]). The highest weight of solid measured after processing the non-pretreated brine (26.4 g for the non-pretreated brine vs. 21.3 g for the boron-depleted brine) indicates that the presence of boron increases impurities co-precipitation in the solid. Elemental and XRD analyses evidenced that

the solid produced from the boron-depleted brine was composed of 73% sodium chloride and 16.4% magnesium hydroxide (Figure 3. 6). Unfortunately, calcium hydroxide diffractogram was not identified in the solid because of the very low initial concentration of calcium within the brine compared to that reported by Nieto et al. [20]. The purity of $Mg(OH)_2$ in the solid was not high enough to envisage magnesium valorization in industry. Therefore, the solid was washed with deionized water at room temperature to remove NaCl impurities. Then, the solid was dried and characterized by XRD spectroscopy. Figure 3 .7 shows that the solid is mainly composed of $Mg(OH)_2$ with purity of 71.2% determined by elemental analyses. This indicates that additional work must be done to improve the solid washing or by using other purification strategy.

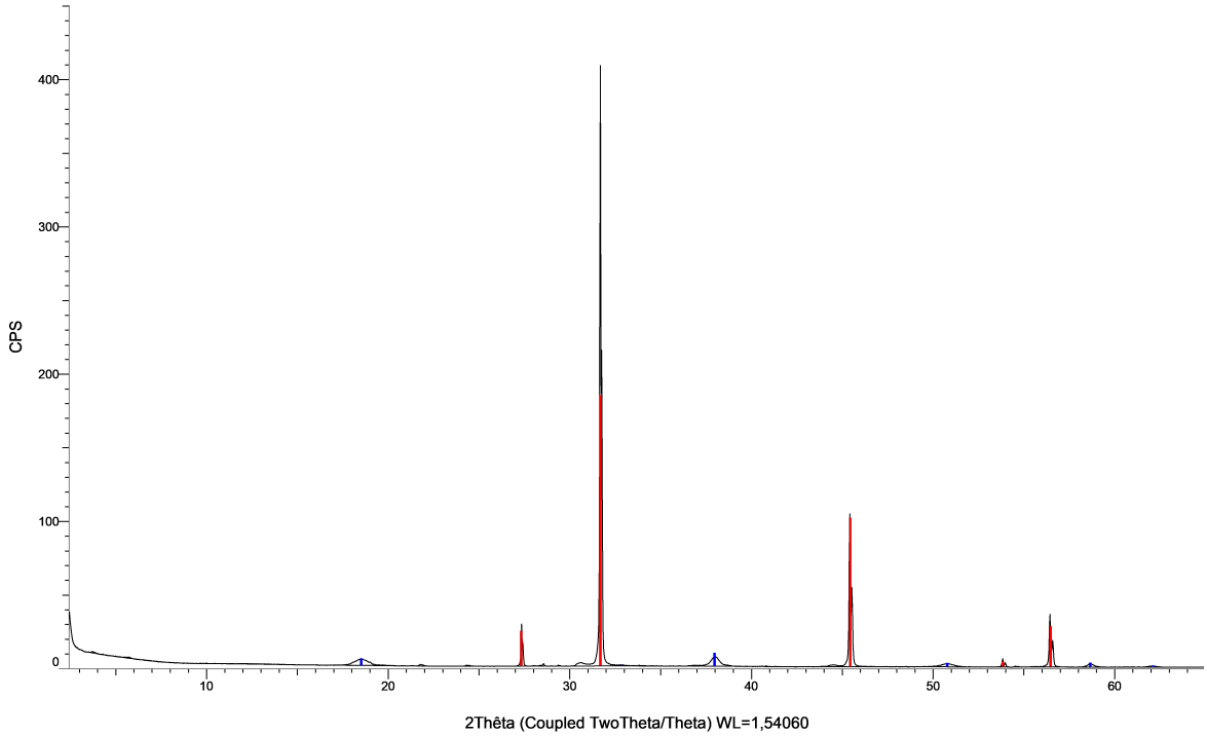



**Figure 3. 6:** XRD pattern of the solid obtained after magnesium and calcium removal (in black). Reference XRD patterns of NaCl (in red) and $Mg(OH)_2$ (in blue).

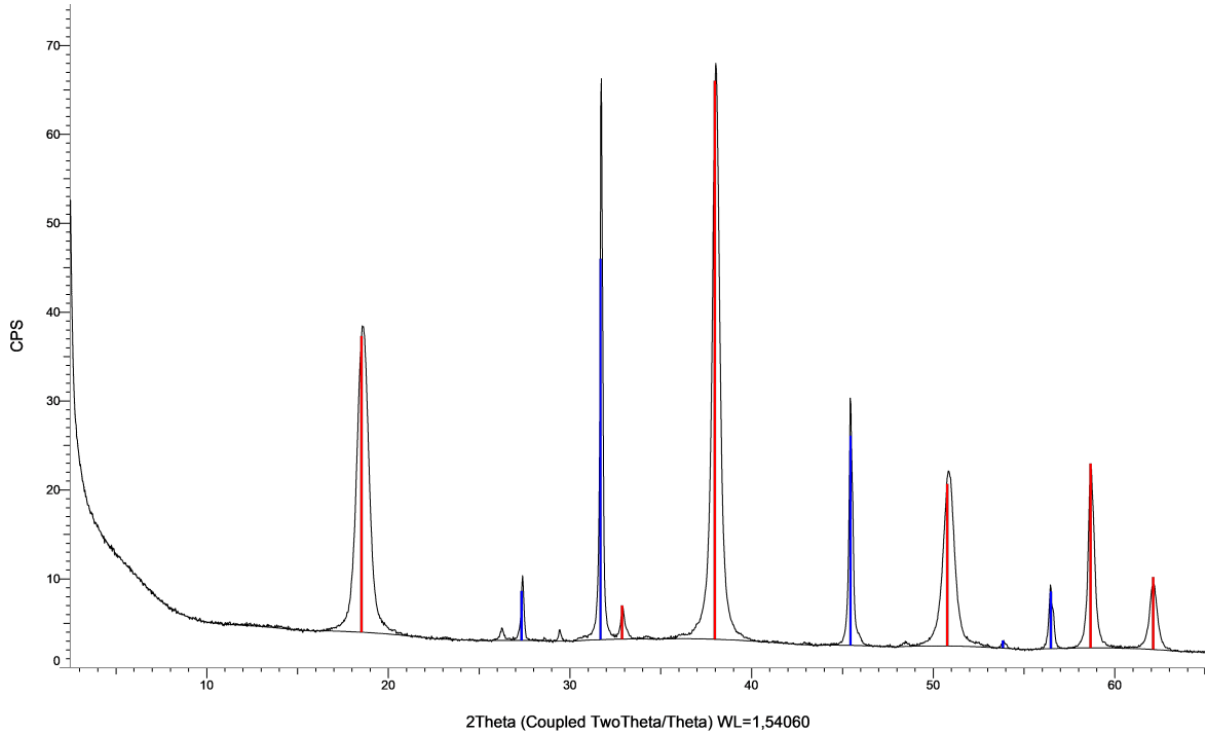



**Figure 3. 7:** XRD pattern of the solid obtained after washing (in black). Reference patterns of $Mg(OH)_2$ (in red) and NaCl (in blue).

## 3.3.3 Stage II of the electrodialysis

### 3.3.3.1 Sodium recovery

In stage II of the electrodialysis (Figure 3. 1(b)), the middle compartment of the cell was fed with the brines after magnesium and calcium removal, *i.e.* the non-pretreated brine or the boron-depleted brine leaving stage I (see brines composition before and after stage II in Table 3. 5). The anodic and the cathodic compartments were connected to aqueous solutions containing 0.5 mol $L^{-1}$ $Na_2CO_3$ (pH=11.4) and 0.1 mol $L^{-1}$ $NaHCO_3$ (pH=9.4), respectively. The electro-membrane experiments were carried out at 150 A $m^{-2}$. Water reduction in the cathodic compartment was responsible for the increase of the catholyte pH and its oxidation in the anodic compartment decreased the anolyte pH, as expected (Equations 3. 6 and 3. 7). Three consecutive electrodialysis experiments were performed for each brine until the voltage and the current reached 30 V and ~ 0 A, respectively, (see pH in the three compartments of the electrodialysis cell, voltage, current and concentrations of sodium, potassium and lithium in the middle compartment after each experiment for the non-pretreated brine and the brine depleted of boron in Tables B. 7 and B. 8 in appendix B).

**Table 3. 5:** Composition and pH of (1) the non-pretreated brine before stage II, (2) the non-pretreated brine in the middle compartment after stage II, (3) the boron-depleted brine before stage II, and (4) the boron-depleted brine in the middle compartment after stage II.

| Brine | Concentration (mg $L^{-1}$) | | | | | | pH |
|---|---|---|---|---|---|---|---|
| | B | K | Li | Na | $Cl^-$ | $SO_4^{2-}$ | |
| (1) | 446.7 | 8,800 | 715 | 110,633.5 | 185,799.9 | 16,365.5 | 13 |
| (2) | 1,218.2 | **0** | **491.5** | **19,675** | 594 | 9,413.1 | 12.4 |
| (3) | 50.8 | 7427.5 | 560 | 89,315 | 151,974.7 | 13,283.8 | 12.4 |
| (4) | 62.0 | **0** | **6.8** | **251** | 42.6 | 86.7 | 11.8 |

Figures B. 5 and B. 6 in appendix B indicate that sodium, lithium and potassium exist mainly in the brines as $Na^+$, $Li^+$ and $K^+$ at the natural pH of those processed brines (Table 3. 5). During the electrodialysis, these cations and the anions ($Cl^-$ and $SO_4^{2-}$) migrate from the middle compartment to the cathodic and anodic the compartments, respectively. Therefore, their concentration in the middle compartment is significantly reduced. Figure 3. 8 shows the normalized concentrations ($C/C_0$) of sodium, lithium and potassium in the brines as a function of the circulated charge per liter of brine. Sodium, lithium and potassium concentrations decrease with the extent of the electrodialysis irrespective of the nature of the brine because $Na^+$, $Li^+$ and $K^+$ cations are transferred from the middle compartment to the cathodic compartment. However, lithium concentration increases at 190,000 C $L^{-1}$ in the brines. This is attributed to the reduction of water volume *via* electroosmosis as previously mentioned.

At the end of the electrodialysis, potassium was removed from the brines while a certain amount of sodium and lithium still remained in the middle compartment (Table 3. 5). Furthermore, concentrations of sodium and lithium were higher in the non-pretreated brine than in the boron-depleted brine (Table 3. 5). Therefore, the low value of current observed at the end of the electrodialysis (~ 0 A) can be explained by an error in the experimental measurement. Indeed, the current must not be nil when cations still remain in the middle compartment. For further investigations, it is therefore suggested to perform real time conductivity and ideally concentration measurement during the electrodialysis correlating with the current. As reported by Nieto et al. [31], the residual concentrations of lithium and sodium can be removed by extending the experiment above 491,490 C $L^{-1}$ and 576,630 C $L^{-1}$ for the boron-depleted brine and the non-pretreated brine, respectively. This evidences that more energy is needed to remove these residual concentrations.

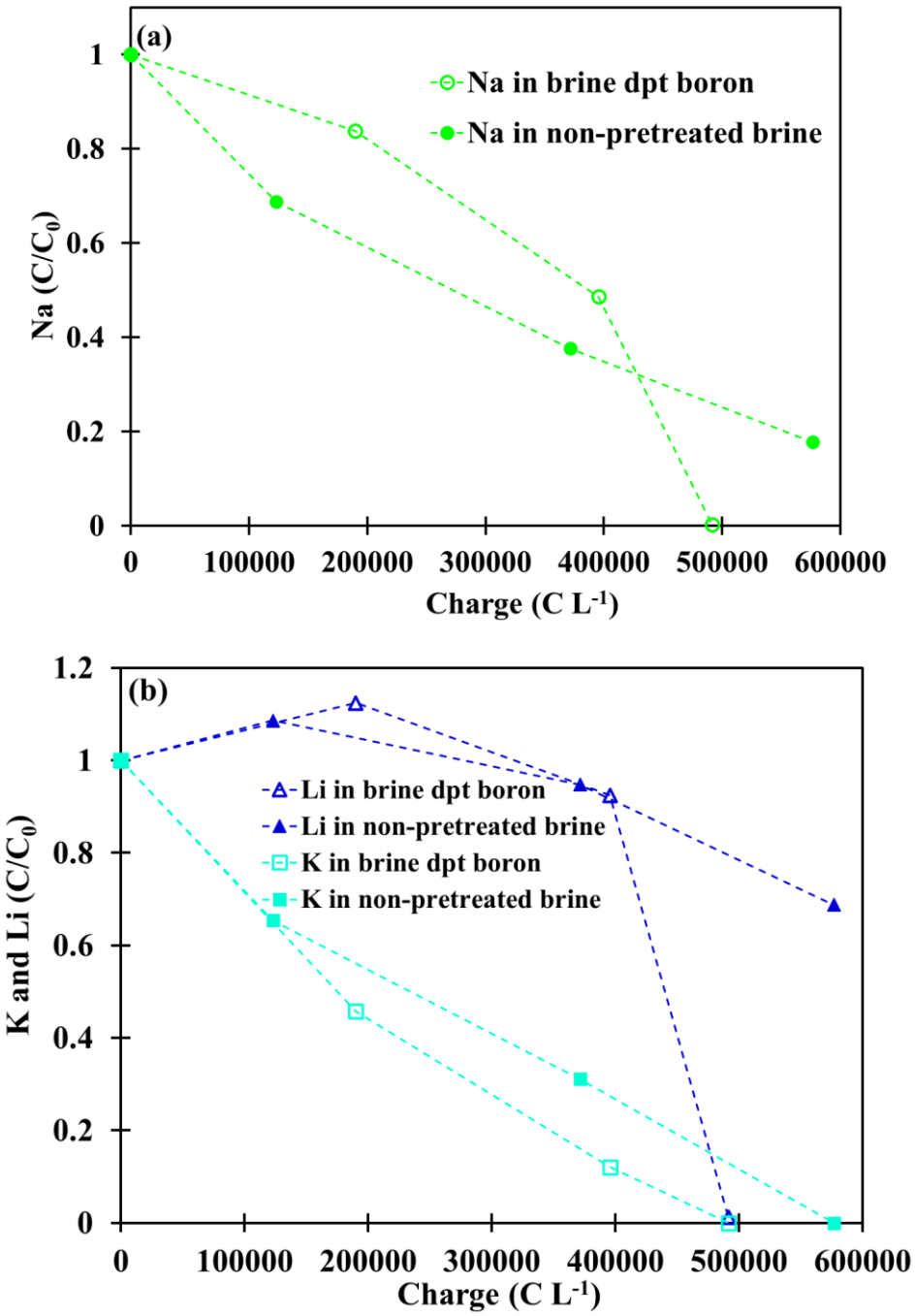



**Figure 3. 8:** Normalized concentrations of (a) sodium, and (b) lithium and potassium in the middle compartment as a function of the circulated charge per liter of brine for the non-pretreated brine and the boron-depleted brine depleted (dpt denotes depleted).

Tables 3. 6 (a) and (b) show the separation coefficient between different cations for the non-pretreated brine and the boron-depleted brine, respectively, as a function of the extent of the electrodialysis. Irrespective of the nature of the brine, $F_{Na-K}$ and $F_{Li-K}$ values are greater than 1. Therefore, $K^+$ migration through the CEM is more important than $Na^+$ and $Li^+$. Additionally, $Na^+$ transfer through the CEM occurs preferentially compared to $Li^+$ since $F_{Na-Li}$ values are lower than 1. Hence, it can be inferred that cations migrate from the middle compartment to

the cathodic compartment through the CEM following this order: $K^+ > Na^+ > Li^+$. This migration order is supported by hydration free energy of cations which the order is the opposite of that of the separation coefficient : $K^+ < Na^+ < Li^+$ [32]. Similar results were reported by Nieto et al. [31].

**Table 3. 6:** Separation coefficients of $K^+$, $Na^+$ and $Li^+$ as a function of the circulated charge per liter of brine (a) for the non-pretreated brine and (b) the boron-depleted brine.

**(a)**

| $F_{Na-K}$ | $F_{Na-Li}$ | $F_{Li-K}$ | Charge (C $L^{-1}$) |
|---|---|---|---|
| 1 | 1 | 1 | 0 |
| 1.1 | 0.6 | 1.7 | 123,030 |
| 1.2 | 0.4 | 3.0 | 371,430 |
| - | 0.3 | - | 576,630 |

**(b)**

| $F_{Na-K}$ | $F_{Na-Li}$ | $F_{Li-K}$ | Charge (C $L^{-1}$) |
|---|---|---|---|
| 1 | 1 | 1 | 0 |
| 1.8 | 0.7 | 2.5 | 189,900 |
| 4.0 | 0.5 | 7.6 | 395,460 |
| - | 0.2 | - | 491,490 |

After stage II, the total dissolved solid amounts (TDS) in the boron-depleted brine and the non-pretreated brine were 0.7 g $L^{-1}$ and 48.2 g $L^{-1}$, respectively. This result indicates that boron extraction favors the recovery of anions and cations. In addition, It is interesting to highlight that the energy consumption is reduced by 15% in stage II by removing boron from the brine since the energy consumptions during electrodialysis for the boron-depleted brine is 0.53 kWh $L^{-1}$ whereas it is 0.62 kWh $L^{-1}$ for the non-pretreated brine.

### 3.3.3.2 Sodium carbonate production

After each electrodialysis experiment, $CO_2$ was bubbled at 2 L $min^{-1}$ for 7 hours in the catholyte containing the transferred $K^+$, $Na^+$ and $Li^+$ cations in order to precipitate sodium as sodium bicarbonate ($NaHCO_3$) or sodium carbonate ($Na_2CO_3$). Therefore, three precipitation experiments were performed with catholyte obtained from the non-pretreated brine or the boron-depleted brine. Since the precipitation experiments were the same, only data of the first precipitation experiment with the catholyte obtained from the boron-depleted brine were reported in this chapter. This catholyte was composed of 58,252 mg $L^{-1}$ sodium, 289 mg $L^{-1}$ lithium, 11,088 mg $L^{-1}$ potassium and 8.5 g $L^{-1}$ carbonate anions ($CO_3^{2-}$) before the $CO_2$

bubbling. At the beginning of the precipitation experiment the temperature increased from 25 °C to 43 °C after 30 min of $CO_2$ bubbling. This energy could be recovered in industrial plants. As the catholyte was alkaline (pH=13.4), $CO_2$ bubbling was responsible for the decrease of pH in the cathodic compartment (Figure 3. 10). This is explained by the reaction between $CO_2$ and $OH^-$ to form bicarbonate anions (Equation 3. 20). In the presence of water, $CO_2$ is also converted into carbonate or carbonic acid (Equations 3. 21 and 3. 22).

$$CO_2 + OH^- \rightleftarrows HCO_3^- \quad (3.\ 20)$$

$$CO_2 + H_2O \rightleftarrows CO_3^{2-} + 2H^+ \quad (3.\ 21)$$

$$CO_2 + H_2O \rightleftarrows H_2CO_3 \quad (3.\ 22)$$

Figure 3. 9 indicates that bicarbonate ($HCO_3^-$) content is higher at pH=7−9, while carbonate ($CO_3^{2-}$) is the only species in solution at pH above 11. These bicarbonate and carbonate anions can precipitate $K^+$, $Na^+$ and $Li^+$ cations according to Equations 3. 23−3. 27 [16]. Therefore, $CO_2$ bubbling should be performed until pH=7−9 in order to precipitate sodium as sodium bicarbonate ($NaHCO_3$) and prevent the precipitation of lithium carbonate and potassium carbonate at pH above 11 since lithium carbonate exhibits the lowest solubility in water (Table 3. 7).

$$2\,Na^+ + CO_3^{2-} \rightleftarrows Na_2CO_{3(S)} \quad (3.\ 23)$$

$$Na^+ + HCO_3^- \rightleftarrows NaHCO_{3(S)} \quad (3.\ 24)$$

$$K^+ + CO_3^{2-} \rightleftarrows K_2CO_{3(S)} \quad (3.\ 25)$$

$$K^+ + HCO_3^- \rightleftarrows KHCO_{3(S)} \quad (3.\ 26)$$

$$Li^+ + CO_3^{2-} \rightleftarrows Li_2CO_{3(S)} \quad (3.\ 27)$$

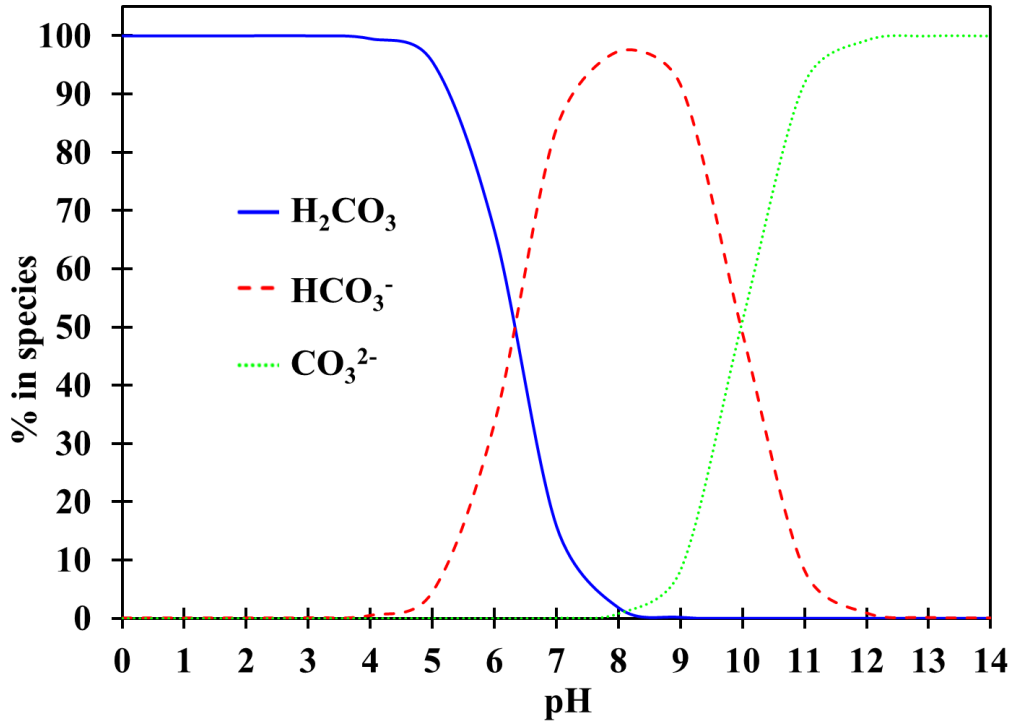



**Figure 3. 9:** Carbonate speciation in pure water as a function of pH. 0.1 mol $L^{-1}$ carbonate was used for speciation calculations.

**Table 3. 7:** Solubility of the salts at 25 °C in pure water [16].

| Salt | Solubility (g $L^{-1}$) |
|---|---|
| $K_2CO_3$ | 1114.2 |
| $KHCO_3$ | 362.4 |
| $Na_2CO_3$ | 307.2 |
| $NaHCO_3$ | 102.8 |
| $Li_2CO_3$ | 13.0 |

Figure 3. 11 evidences that bicarbonate and sodium bicarbonate are the only species of carbonate in the catholyte at pH=7.7. Lithium carbonate, sodium carbonate, potassium carbonate and potassium bicarbonate species are not reported in Figure 3. 11 because of the lack of their thermodynamic data in the databases Pitzer and Minteq.V4 [18]. Nevertheless, these speciation diagrams provided consistent experimental condition to selectively precipitate sodium. Therefore, $CO_2$ was bubbled until the pH of the catholyte reached 7.7 (Figure 3. 10). As shown in Figure 3. 10, sodium concentration decreases slightly until pH=9.8 and exhibits sharp decrease at pH=9.8−7.7. The difference of behavior regarding sodium precipitation as a function of pH is attributed to carbonate anions speciation. Indeed, the increase in carbonate concentration from 8.5 g $L^{-1}$ to 69.5 g $L^{-1}$ during the $CO_2$ bubbling is responsible for huge

amount of bicarbonate production (see Figure 3. 10 for the increase in carbonate concentration and Figure 3. 11 for the increase in the concentration of bicarbonate). Hence, the produced bicarbonate anions precipitate significantly sodium as sodium bicarbonate at pH=9.8−7.7 (Figure 3. 10). Lithium and potassium concentrations in the catholyte decreased at pH=13.4−9.8 during $CO_2$ bubbling. Conversely, their concentrations increase at pH below 9.8 (Figure 3. 10). This can be explained by the formation of lithium carbonate, potassium carbonate and potassium bicarbonate species which can precipitate when their solubilities are reached in some pH regions (see the solubility of these salts at 25 °C in Table 3. 7).

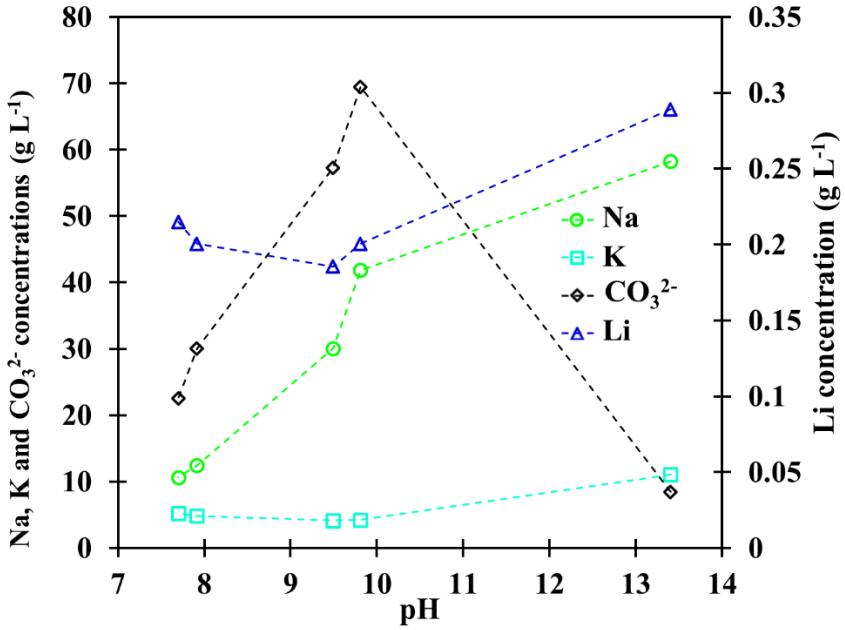



**Figure 3. 10:** Sodium, lithium, potassium and carbonate anions ($CO_3^{2-}$) concentrations in the catholyte during $CO_2$ bubbling as a function of pH.

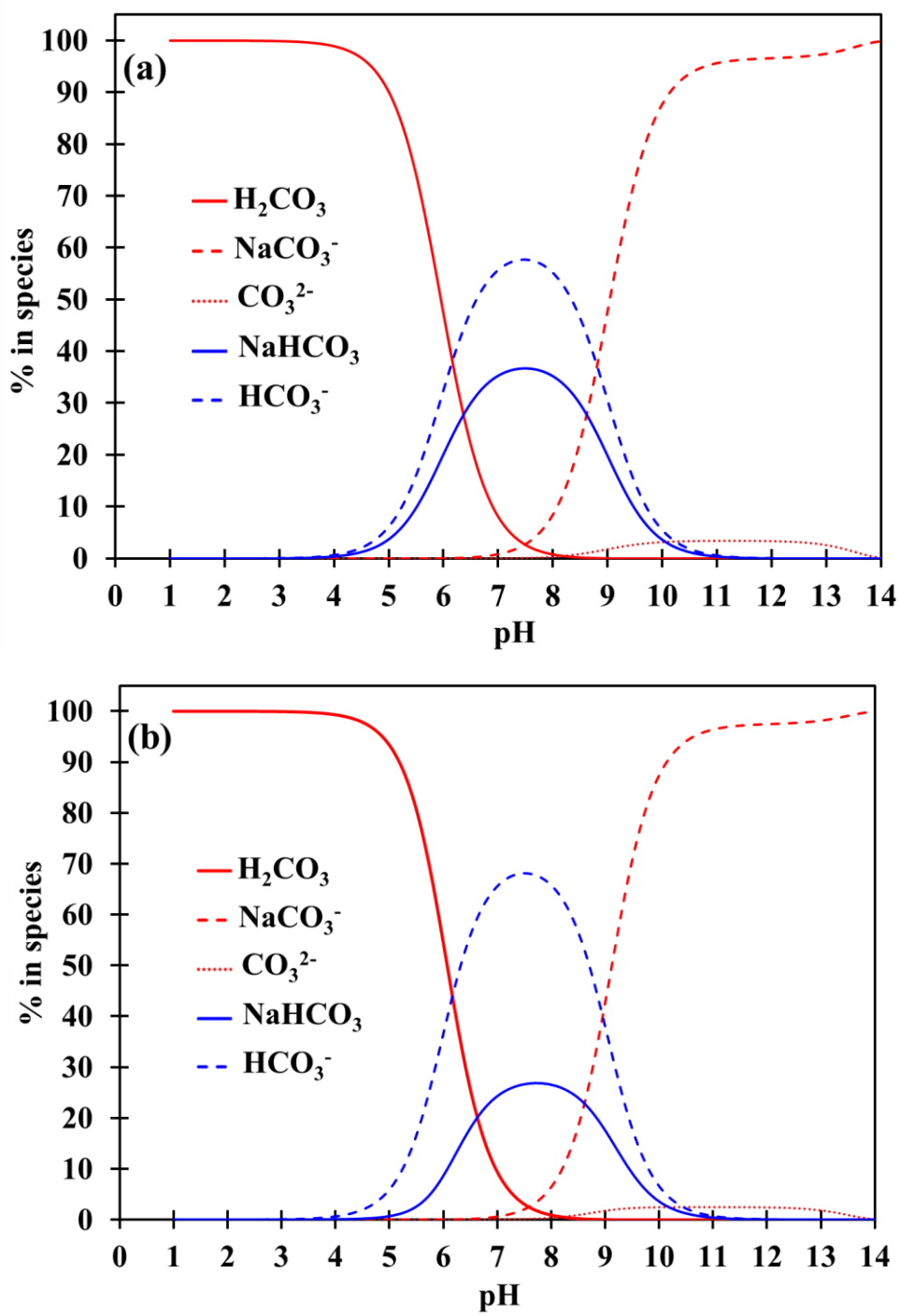



**Figure 3. 11:** Carbonate speciation as a function of pH (a) before $CO_2$ bubbling and (b) at the maximum concentration of carbonate (69.5 g $L^{-1}$) obtained during $CO_2$ bubbling.

After the three precipitation experiments for the catholyte obtained from the boron-depleted brine, the solids were recovered by filtration under vacuum and heated at 110 °C for 24 hours to convert $NaHCO_3$ into $Na_2CO_3$ [33]. This convertion of $NaHCO_3$ into $Na_2CO_3$ can be an opportunity of $CO_2$ recycling in the process (Equation 3. 28).

$$NaHCO_{3(s)} \rightarrow Na_2CO_{3(s)} + CO_{2(g)} + H_2O_{(g)} \quad (3.\ 28)$$

Afterwards, 82.7 g of solid were harvested. Elemental analyses showed that the solid was composed of 41.2% sodium ($Na_2CO_3$ purity=95%), 0.4% potassium and 0.1% lithium. Therefore, the solid was washed with deionized water at 0 °C to minimize redissolution of $Na_2CO_3$ and remove the impurities. The washed solid was dried as previously. XRD analysis showed that the solid was only composed of $Na_2CO_3$ (Figure 3. 12). The purity of $Na_2CO_3$ (99.99%) was confirmed by elemental analyses.

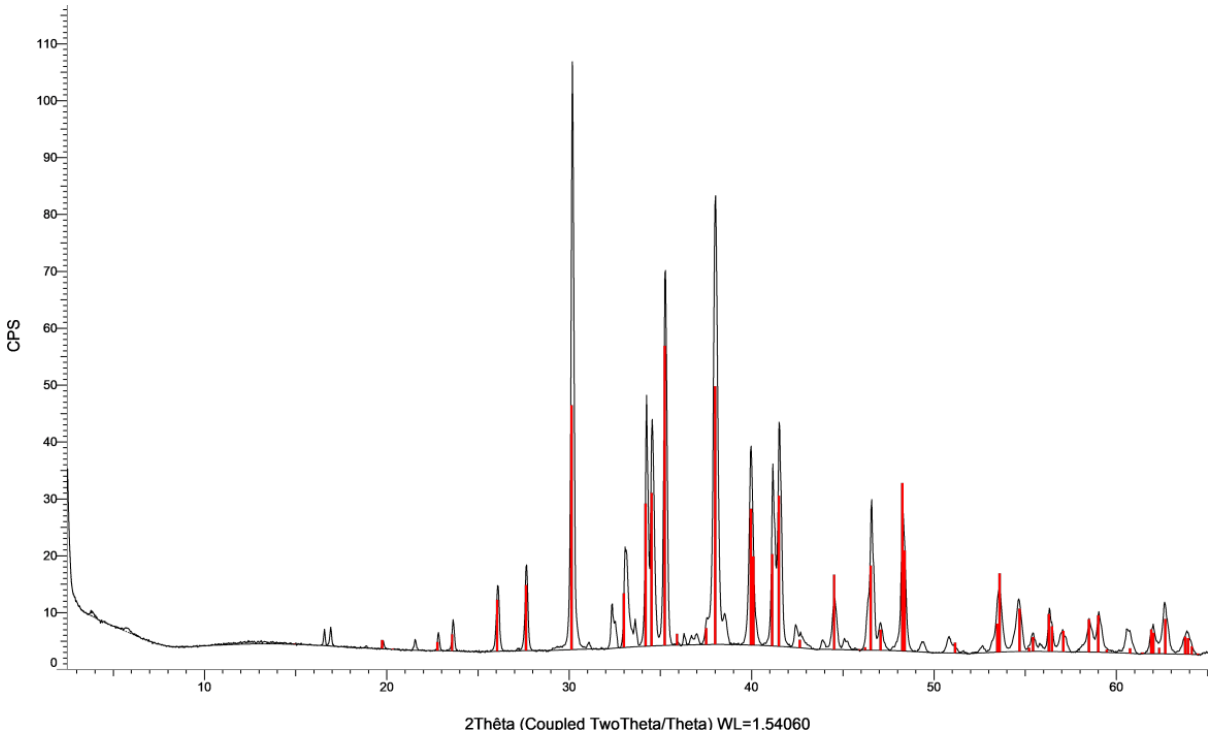



**Figure 3. 12:** XRD pattern of the solid after washing (in black). Reference XRD patterns of sodium carbonate in red. The solid was obtained by precipitation of the catholyte in stage II.

## 3.3.4 Stage III of the electrodialysis

### 3.3.4.1 Lithium recovery

Boron was not detected in the catholytes obtained in the stage II for both non-pretreated brine and boron-depleted brine. Therefore, lithium extraction from the catholyte obtained after sodium precipitation in stage II for only boron-depleted brine was performed by implementing stage III of the electrodialysis process. The solution contained 986 mg $L^{-1}$ lithium, 8,332 mg $L^{-1}$ potassium and 27,602 mg $L^{-1}$ sodium and fed the middle compartment of the electro-membrane cell (Figure 3. 1 (c)). The cathodic and the anodic compartment were fed by 0.1 mol $L^{-1}$ $Li_2CO_3$ and 0 .5 mol $L^{-1}$ $Na_2CO_3$, respectively. The experiment was performed at 150 A $m^{-2}$ for 11 hours. Table 3. 8 reports the evolution of pH in the three compartments of the electro-

membrane cell, voltage, current and, concentrations of lithium, sodium and potassium in the middle compartment as a function of the electrodialysis extent. During the experiment, the pH in the cathodic compartment increases due to water reduction (Equation 3. 7) and the pH in the anodic compartment decreases because of water oxidation (Equation 3. 6). At the end of the electrodialysis sodium, lithium and potassium were removed from the middle compartment to the cathodic compartment (Table 3. 8). The separation coefficients of the cations were similar to those in stage II and cations migrate through the CEM as follows: $K^+ > Na^+ > Li^+$. The higher concentrations in sodium and potassium, and the more preferential migration of sodium and potassium than lithium is a disadvantage for efficient lithium recovery. Torres et al. reported that low ratio [Na]/[Li] improves the lithium recovery by electrodialysis [17].

**Table 3. 8:** Evolution of pH in the three compartments of stage III, voltage, current and, concentrations of lithium, sodium and potassium in the middle compartment as a function of the electrodialysis extent.

| Time (min) | Charge (C $L^{-1}$) | pH middle | pH of anolyte | pH of catholyte | Na (mg $L^{-1}$) | Li (mg $L^{1}$) | K (mg $L^{-1}$) | Current (A) | Voltage (V) |
|---|---|---|---|---|---|---|---|---|---|
| 0 | 0 | 8.4 | 11.1 | 10.1 | 27,602 | 986 | 8,332 | 0.75 | 4.4 |
| 249 | 56,025 | 8.9 | 10.2 | 12.9 | 20,614 | 838 | 3,420 | 0.75 | 4.4 |
| 434 | 97,650 | 9.4 | 10.0 | 12.9 | 10,287.5 | 605 | 627.5 | 0.75 | 4.7 |
| 691 | 155,475 | 10.5 | 9.9 | 13.0 | **0** | **0** | **0** | 0 | 30 |

### 3.3.4.2 Lithium carbonate production

Sodium, lithium and potassium concentrations in the catholyte at the end of stage III (25,375 mg $L^{-1}$ sodium, 870 mg $L^{-1}$ lithium and 3,589 mg $L^{-1}$ potassium) were lower than those of the middle compartment before the experiment (Table 3. 8). This is attributed to the increase in the volume of the catholyte due to electroosmosis as previously discussed. $CO_2$ was bubbled in the catholyte at 2.5 L $min^{-1}$ and 25 °C for 1h30 until the pH reached 10 so that carbonate concentration was high enough to precipitate lithium as lithium carbonate (Figure 3. 9). No precipitation was observed because lithium concentration (870 mg $L^{-1}$) was much lower than 2.4 g $L^{-1}$ (solubility of lithium carbonate at 25 °C=13 g $L^{-1}$ which is equivalent to 2.4 g $L^{-1}$ lithium). Therefore, lithium concentration must be increased beyond 2.4 g $L^{-1}$. The catholyte was evaporated at 90 °C under stirring until the volume was reduced by four. Table 3. 9 gathers the concentrations of lithium, potassium and sodium during the evaporation step. At the end of

the evaporation, lithium, potassium and sodium concentrations should be 3,424 mg $L^{-1}$, 13,120 mg $L^{-1}$, and 114,016 mg $L^{-1}$, respectively. However, Table 3. 9 indicates that sodium and lithium concentrations significantly decrease. Indeed, during evaporation lithium carbonate and sodium carbonate crystallized since $Li_2CO_3$ and $Na_2CO_3$ solubilities at 90 °C reaches 8.1 g $L^{-1}$ and 447 g $L^{-1}$, respectively, which are equivalent to 1.5 g $L^{-1}$ lithium and 192.3 g $L^{-1}$ sodium ([16], [34]). The crystals were recovered by filtration and the solid was dried at 100 °C for 24 hours. XRD analysis of the solid showed the presence of $Li_2CO_3$ and $Na_2CO_3$ (Figure 3. 13). The purity of the lithium carbonate reached 65% , which is too low for battery applications since lithium carbonate battery-grade ranges between 99.5% and 99.95% [8].

The crystallized solid was washed with deionized water at 90 °C to minimize the redissolution of $Li_2CO_3$ and remove $Na_2CO_3$ impurities. The washed solid was dried as previously described. Figure 3. 14 evidences that there is no significant difference between the diffractograms of the washed solid and lithium carbonate. Elemental analyses of the solid indicated that lithium carbonate purity was 99.9%.

**Table 3. 9:** Composition of catholyte (1) before evaporation, (2) when the volume of catholyte was reduced by 2 and (3) when the volume of the catholyte was reduced by 4.

| | Concentration of element (mg $L^{-1}$) | | |
|---|---|---|---|
| Catholyte | K | Li | Na |
| (1) | 3,280 | 856 | 28,505 |
| (2) | 6,194 | 1,533 | 53,013 |
| (3) | 12,946 | 1,866 | 103,398 |

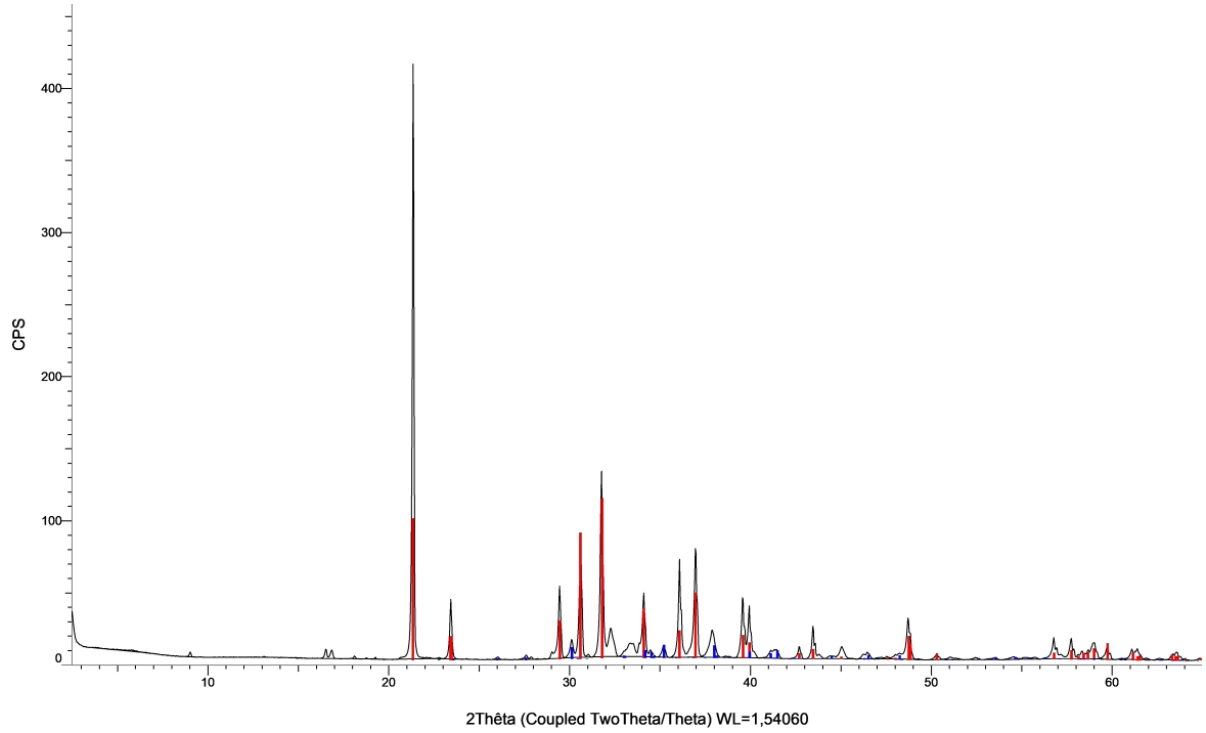



**Figure 3. 13:** XRD pattern of the crystallized solid from the catholyte of stage III (in black), and reference XRD patterns of lithium carbonate (in red) and sodium carbonate (in blue).

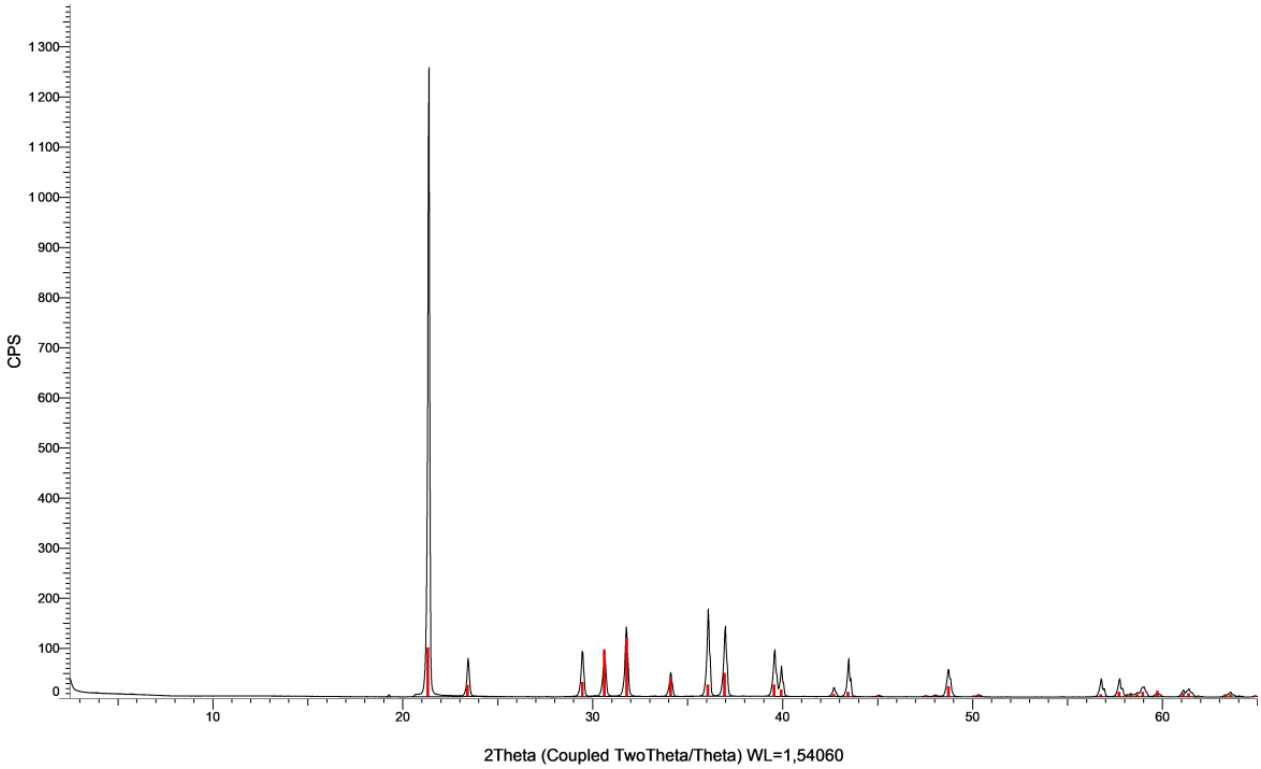



**Figure 3. 14:** XRD pattern of the washed solid (in black) and reference XRD patterns of lithium carbonate (in red). The solid was obtained by crystallization of the catholyte in stage III.

### 3.3.5 Flowsheet of the overall process

The flowsheet in Figure 3. 15 gathers the main operations involved in boron extraction, magnesium and sodium co-valorization and battery-grade lithium carbonate production. It is important to point out that the produced low salinity water can be employed in the process for solids washing and the electrodialysis operations.

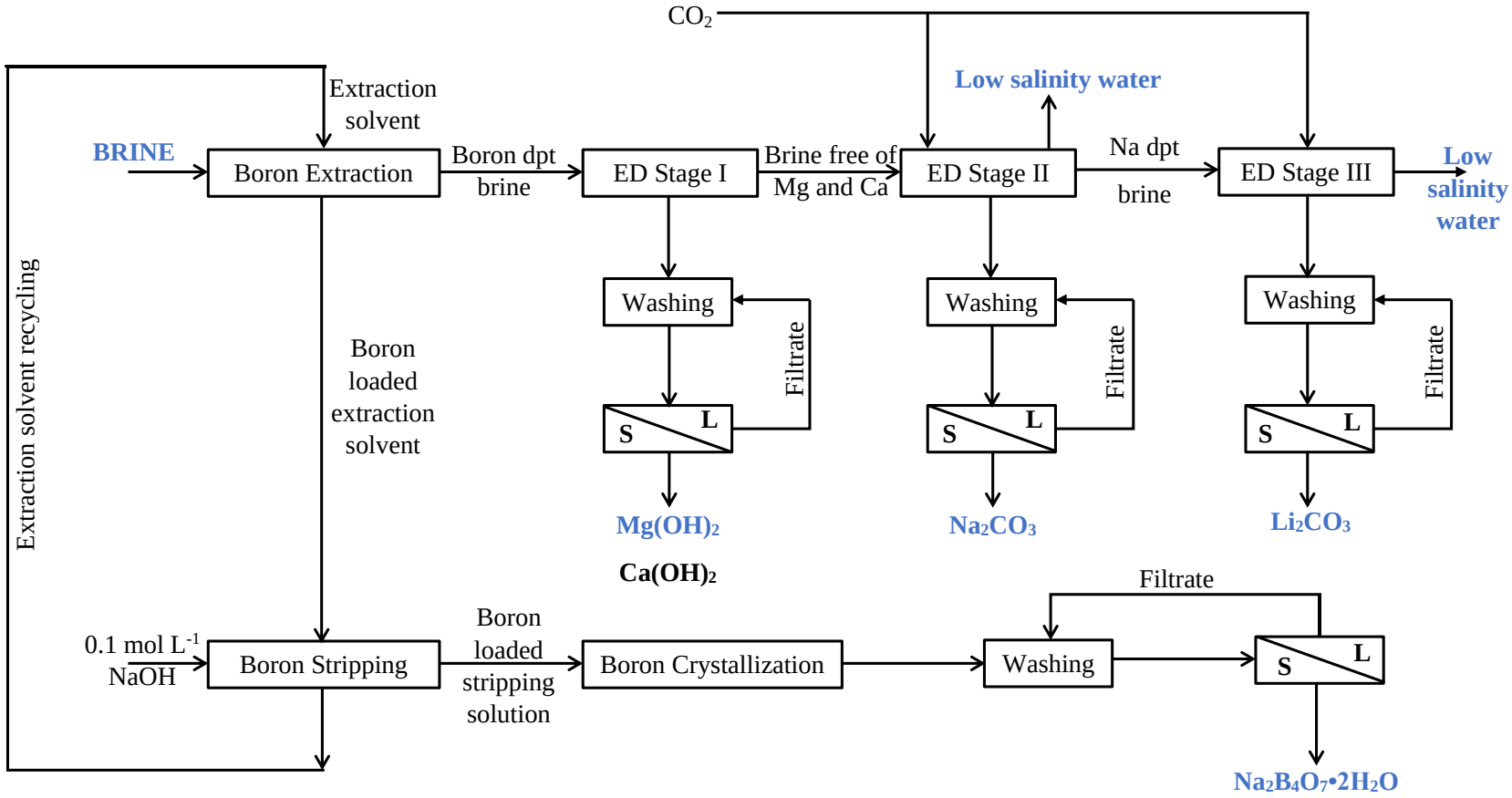



**Figure 3. 15:** Flowsheet of the overall process for borax, magnesium hydroxide, sodium carbonate and battery-grade lithium carbonate production from the salar de Hombre brine (dpt denotes depleted. )

## 3.4 Conclusion

Electrodialysis is a selective technology suitable to extracting lithium from low salinity lithium-rich brines. Therefore, the brines from the salar de Hombre Muerto, which contain high concentrations of boron, magnesium, calcium, potassium and sodium, require several pretreatment steps before direct lithium extraction by electrodialysis. Torres et al. [12] have proposed an electrodialysis process relying on three stages which allows the co-valorization of other brine components and lithium as lithium carbonate. In this chapter boron was extracted from the brine by using 2 mol $L^{-1}$ 2-butyloctan-1-ol diluted in kerosene before performing the electrodialysis process developed in Jujuy, Argentina. The results presented in this chapter were used to investigate the influence of boron extraction on the performances of the electrodialysis process in terms of energy consumption and purity of the produced salts.

Boron extraction efficiency reached 90% by performing 8 batch extractions with l L of brine and 4 L of the extraction solvent at pH=7.5 at 25 °C. Afterwards, the non-pretreated brine and the boron-depleted brine were employed in the three stages of the electrodialysis process. This study showed that boron extraction before the electrodialysis experiments contribute to:

- Decrease the impurities in stage I by 18% and reduce the amount of water needed to wash $Mg(OH)_2$ obtained from the boron-depleted brine.
- Reduce the electrodialysis time in stage I from 300 min for the non-pretreated brine to 233 min for the boron-depleted brine. Then, the energy consumption was reduced by 17%. This was explained by the formation of neutral species of boron-magnesium and boron-calcium that keep magnesium and calcium in solution and then, increase the energy consumption required to remove magnesium and calcium.
- Decrease the energy consumption was reduced by 15% in stage II since 5,461 min was required to recover sodium, potassium and lithium from the boron-depleted brine instead of 6,407 min for the non-pretreated brine.

Overall, magnesium hydroxide (purity=71.2%), sodium carbonate (purity= 99.99%) and lithium carbonate (purity=99.9%) were produced from the boron-depleted brine by combining stages I, II and III of the electrodialysis process. After stage II, the TDS was decreased by 99.8% since the TDS in the brine from the salar de Hombre Muerto was initially 304.5 g $L^{-1}$ and it reached 0.7 g $L^{-1}$ at the end of stage II. Then, the produced low salinity water can be employed for solids washing and the electrodialysis operations. This research highlights the critical importance of boron extraction for lithium carbonate production by electrodialysis because

boron removal contributes to reducing the operating cost *via* significant decrease of the impurities in the produced salts and the energy consumption by 32%. This work also addresses the intricate physicochemistry of magnesium, calcium, sodium and lithium speciation in alkaline solutions or carbonate-rich solutions. Unlike the conventional lithium extraction processes, this work points out the relevance of the co-valorization of boron, magnesium and sodium impurities in lithium plants, which reduces the waste production in this industry. The large amount of sodium in the brines entails huge energy consumption to remove sodium which can increase the operating costs. However, the co-produced sodium carbonate may make this process economically beneficial. The high content of sodium in brine is also responsible for the reduction of the efficiency of lithium extraction in stage III since sodium migrates more preferentially than lithium. Therefore, more selective membranes towards lithium should be employed and developed to avoid this issue and reduce the impurity in the produced lithium carbonate. Further investigations are needed to:

- Improve the purity of $Mg(OH)_2$ obtained in stage I by using efficient washing like counter-current washing.
- Increase lithium concentration in the cathodic compartment of stage III which will allow to precipitate lithium carbonate solely by $CO_2$ bubbling instead of evaporation. This could be achieved by increasing the ratio between the volume of aqueous phase employed in the middle compartment and the catholyte.

# References


[1] T. A. Davis and D. A. Glassner, “Electrodialysis,” in *Handbook of Downstream Processing*, E. Goldberg, Ed., Dordrecht: Springer Netherlands, 1997, pp. 140–166. doi: 10.1007/978-94-009-1563-3_6.

[2] W. S. W. Ho and K. K. Sirkar, Eds., *Membrane Handbook*. Boston, MA: Springer US, 1992. doi: 10.1007/978-1-4615-3548-5.

[3] M. S. Mintz, “ELECTRODIALYSIS—PRINCIPLES OF PROCESS DESIGN,” *Ind. Eng. Chem.*, vol. 55, no. 6, pp. 18–28, Jun. 1963, doi: 10.1021/ie50642a003.

[4] B. Pilat, “Practice of water desalination by electrodialysis,” *Desalination*, vol. 139, no. 1, pp. 385–392, Sep. 2001, doi: 10.1016/S0011-9164(01)00338-1.

[5] M. Reig *et al.*, “Concentration of NaCl from seawater reverse osmosis brines for the chlor-alkali industry by electrodialysis,” *Desalination*, vol. 342, pp. 107–117, Jun. 2014, doi: 10.1016/j.desal.2013.12.021.

[6] L. K. Wang, J. P. Chen, Y.-T. Hung, and N. K. Shammas, Eds., *Membrane and Desalination Technologies*. Totowa, NJ: Humana Press, 2011. doi: 10.1007/978-1-59745-278-6.

[7] H. Strathmann, “Electrodialysis, a mature technology with a multitude of new applications,” *Desalination*, vol. 264, no. 3, pp. 268–288, Dec. 2010, doi: 10.1016/j.desal.2010.04.069.

[8] O. Murphy and M. N. Haji, “A review of technologies for direct lithium extraction from low Li+ concentration aqueous solutions,” *Front. Chem. Eng.*, vol. 4, Nov. 2022, doi: 10.3389/fceng.2022.1008680.

[9] J. Farahbakhsh *et al.*, “Direct lithium extraction: A new paradigm for lithium production and resource utilization,” *Desalination*, vol. 575, p. 117249, Apr. 2024, doi: 10.1016/j.desal.2023.117249.

[10] A. Khalil, S. Mohammed, R. Hashaikeh, and N. Hilal, “Lithium recovery from brine: Recent developments and challenges,” *Desalination*, vol. 528, p. 115611, Apr. 2022, doi: 10.1016/j.desal.2022.115611.

[11] S. Gmar and A. Chagnes, “Recent advances on electrodialysis for the recovery of lithium from primary and secondary resources,” *Hydrometallurgy*, vol. 189, p. 105124, Nov. 2019, doi: 10.1016/j.hydromet.2019.105124.

[12] W. R. Torres, C. H. Díaz Nieto, A. Prévoteau, K. Rabaey, and V. Flexer, “Lithium carbonate recovery from brines using membrane electrolysis,” *J. Membr. Sci.*, vol. 615, p. 118416, Dec. 2020, doi: 10.1016/j.memsci.2020.118416.

[13] V. T. Luong, D. J. Kang, J. W. An, M. J. Kim, and T. Tran, “Factors affecting the extraction of lithium from lepidolite,” *Hydrometallurgy*, vol. 134–135, pp. 54–61, Mar. 2013, doi: 10.1016/j.hydromet.2013.01.015.

[14] S. Maes, W.-Q. Zhuang, K. Rabaey, L. Alvarez-Cohen, and T. Hennebel, “Concomitant Leaching and Electrochemical Extraction of Rare Earth Elements from Monazite,” *Environ. Sci. Technol.*, vol. 51, no. 3, pp. 1654–1661, Feb. 2017, doi: 10.1021/acs.est.6b03675.

[15] J. Desloover, A. Abate Woldeyohannis, W. Verstraete, N. Boon, and K. Rabaey, “Electrochemical Resource Recovery from Digestate to Prevent Ammonia Toxicity during Anaerobic Digestion,” *Environ. Sci. Technol.*, vol. 46, no. 21, pp. 12209–12216, Nov. 2012, doi: 10.1021/es3028154.

[16] D. W. H. Rankin, “CRC handbook of chemistry and physics, 89th edition, edited by David R. Lide,” *Crystallogr. Rev.*, vol. 15, no. 3, pp. 223–224, Jul. 2009, doi: 10.1080/08893110902764125.

[17] W. R. Torres, N. C. Zeballos, and V. Flexer, “Effect of [Na+]/[Li+] concentration ratios in brines on lithium carbonate production through membrane electrolysis,” *Faraday Discuss.*, vol. 247, no. 0, pp. 101–124, Oct. 2023, doi: 10.1039/D3FD00051F.

[18] D. L. Parkhurst and C. A. J. Appelo, “Description of input and examples for PHREEQC version 3: a computer program for speciation, batch-reaction, one-dimensional transport, and inverse geochemical calculations,” U.S. Geological Survey, Reston, VA, USGS Numbered Series 6-A43, 2013. doi: 10.3133/tm6A43.

[19] Q. Yuan, Z. Lu, P. Zhang, X. Luo, X. Ren, and T. D. Golden, “Study of the synthesis and crystallization kinetics of magnesium hydroxide,” *Mater. Chem. Phys.*, vol. 162, pp. 734–742, Jul. 2015, doi: 10.1016/j.matchemphys.2015.06.048.

[20] C. H. Díaz Nieto, N. A. Palacios, K. Verbeeck, A. Prévoteau, K. Rabaey, and V. Flexer, “Membrane electrolysis for the removal of Mg2+ and Ca2+ from lithium rich brines,” *Water Res.*, vol. 154, pp. 117–124, May 2019, doi: 10.1016/j.watres.2019.01.050.

[21] E. J. Reardon, “Dissociation constants for alkali earth and sodium borate ion pairs from 10 to 50°C,” *Chem. Geol.*, vol. 18, no. 4, pp. 309–325, Dec. 1976, doi: 10.1016/0009-2541(76)90013-9.

[22] K. Sasaki, K. Toshiyuki, K. Ideta, J. Miyawaki, and T. Hirajima, “Interfacial effects of MgO in hydroxylated calcined dolomite on the co-precipitation of borates with

hydroxyapatite," *Colloids Surf. Physicochem. Eng. Asp.*, vol. 504, pp. 1–10, Sep. 2016, doi: 10.1016/j.colsurfa.2016.05.044.

[23] Y. Xiong, L. Kirkes, and T. Westfall, "Experimental Determination of Solubilities of Brucite [Mg(OH)2(cr)] in Na2SO4 Solutions with Borate to High Ionic Strengths: Interactions of MgB(OH)4+with Na2SO4," *J. Solut. Chem.*, vol. 47, no. 4, pp. 595–610, Apr. 2018, doi: 10.1007/s10953-018-0742-z.

[24] M. Iwata, T. Tanaka, and M. S. Jami, "Application of Electroosmosis for Sludge Dewatering—A Review," *Dry. Technol.*, vol. 31, no. 2, pp. 170–184, Jan. 2013, doi: 10.1080/07373937.2012.691592.

[25] D. Wiley and G. F. Weihs, "Electro-osmosis, Overview of," in *Encyclopedia of Membranes*, E. Drioli and L. Giorno, Eds., Berlin, Heidelberg: Springer, 2016, pp. 1–3. doi: 10.1007/978-3-642-40872-4_2079-2.

[26] V. I. Zabolotskii, K. V. Protasov, and M. V. Sharafan, "Sodium chloride concentration by electrodialysis with hybrid organic-inorganic ion-exchange membranes: An investigation of the process," *Russ. J. Electrochem.*, vol. 46, no. 9, pp. 979–986, Sep. 2010, doi: 10.1134/S1023193510090028.

[27] N. Lakshminarayanaiah, "Electroosmosis in Ion-Exchange Membranes," *J. Electrochem. Soc.*, vol. 116, no. 3, p. 338, Mar. 1969, doi: 10.1149/1.2411842.

[28] A. H. Galama, M. Saakes, H. Bruning, H. H. M. Rijnaarts, and J. W. Post, "Seawater predesalination with electrodialysis," *Desalination*, vol. 342, pp. 61–69, Jun. 2014, doi: 10.1016/j.desal.2013.07.012.

[29] L. Semerjian and G. M. Ayoub, "High-pH–magnesium coagulation–flocculation in wastewater treatment," *Adv. Environ. Res.*, vol. 7, no. 2, pp. 389–403, Jan. 2003, doi: 10.1016/S1093-0191(02)00009-6.

[30] X. Huang *et al.*, "Removal of petroleum sulfonate from aqueous solutions using freshly generated magnesium hydroxide," *J. Hazard. Mater.*, vol. 219–220, pp. 82–88, Jun. 2012, doi: 10.1016/j.jhazmat.2012.03.059.

[31] C. H. Díaz Nieto, K. Rabaey, and V. Flexer, "Membrane electrolysis for the removal of Na+ from brines for the subsequent recovery of lithium salts," *Sep. Purif. Technol.*, vol. 252, p. 117410, Dec. 2020, doi: 10.1016/j.seppur.2020.117410.

[32] B. Tansel, "Significance of thermodynamic and physical characteristics on permeation of ions during membrane separation: Hydrated radius, hydration free energy and viscous effects," *Sep. Purif. Technol.*, vol. 86, pp. 119–126, Feb. 2012, doi: 10.1016/j.seppur.2011.10.033.

[33] M. Mahmoudkhani and D. W. Keith, “Low-energy sodium hydroxide recovery for CO2 capture from atmospheric air—Thermodynamic analysis,” *Int. J. Greenh. Gas Control*, vol. 3, no. 4, pp. 376–384, Jul. 2009, doi: 10.1016/j.ijggc.2009.02.003.

[34] W. Cheng, Z. Li, and F. Cheng, “Solubility of Li2CO3 in Na–K–Li–Cl brines from 20 to 90°C,” *J. Chem. Thermodyn.*, vol. 67, pp. 74–82, Dec. 2013, doi: 10.1016/j.jct.2013.07.024.

# General conclusion

Battery-grade lithium carbonate production from lithium-rich continental brines as those from the salar de Hombre Muerto requires to remove the other brine components such as boron, magnesium, calcium, potassium and sodium. The conventional processes employ high amount of chemicals to remove these compounds that generates large quantity of non-valorized salts responsible for environmental concerns. In addition, these processes are time consuming and responsible for water loss *via* solar evaporation. Sustainable and efficient lithium carbonate production requires direct lithium extraction (DLE) from brines and co-valorization of the other salts. Among the DLE technologies reported in literature, electrodialysis can be employed to selectively extract lithium from brines. Torres et al. [1] proposed an electrodialysis process allowing to produce lithium carbonate, and co-valorize magnesium, calcium and sodium from brines. However, boron was not extracted and was responsible for the production of low grade salts. This PhD work proposes to perform solvent extraction of boron prior to electrodialysis and precipitation in order to co-valorize boron and lithium as pure borax and battery-grade lithium carbonate, respectively, while producing also other byproducts such as magnesium hydroxide and sodium carbonate for further co-valorization.

First mono alcohols (2-butyloctan-1-ol, 2-ethylhexan-1-ol and octan-1-ol) diluted in kerosene or sulfonated kerosene as well as diols (2-ethylhexane-1,3-diol, 2-methylpentane-2,4-diol and 2-butyl-2-ethylpropane-1,3-diol) diluted in kerosene modified with 60% (wt) toluene or *m*-xylene and diol-based DESs were employed for boron extraction from brine of the salar de Hombre Muerto. This extraction solvent was selected after exploring the influence of the diluent, the nature of the extractant, the phase volume ratio (O/A) and the temperature on boron extraction efficiency, boron selectivity toward magnesium, calcium, sodium, potassium and lithium, and the solubility of the extractant in the brine. It was found that:

- The nature of the diluent did not influence boron extraction irrespective of the extractant.
- Alcohols containing high number of carbon atoms and ramifications favored boron extraction *via* the formation of stable complex with boron.
- Diol-based extraction solvents exhibited the highest extraction efficiency of boron due to the presence of two hydroxyl functions compared to mono alcohols. Conversely, they showed high solubility in the brine (solubility > 250 mg $L^{-1}$). The diols-containing DESs and conventional extraction solvents containing diols showed the same extraction efficiencies of boron despite the lower phase volume ratio (O/A=0.5) employed for

DESs. However, DESs were more soluble in the brine than the conventional extraction solvents containing diols (solubility of DESs>6 g $L^{-1}$).

- Mono alcohols, particularly 2-butyloctan-1-ol, exhibited the lowest solubility (18 mg $L^{-1}$). Therefore, 2-butyloctan-1-ol was employed to identify the optimal extraction conditions of boron.
- 2 mol $L^{-1}$ 2-butyloctan-1-ol diluted in kerosene extracted 94.2% boron in four-stage countercurrent extraction at O/A=4, pH=7.5 and 25 °C. Furthermore, no significant influence of the temperature on boron extraction was observed.
- Boron was extracted as boric acid by 2-butyloctan-1-ol. This result was evidenced by investigating the influence of pH on boron extraction combined with boron speciation in the brine.
- Among the stripping solutions, 0.1 mol $L^{-1}$ NaOH fully stripped boron in one stage at O/A=4 and 25 °C. Then, the boron-loaded stripping solution was crystallized at 20 °C to produce high purity borax ($Na_2B_4O_7 \bullet 2H_2O$, purity=99%).

Thereafter, the identified optimal extraction conditions of boron were implemented in batch mode alongside the electrodialysis process previously mentioned in order to investigate the influence of boron extraction on the performances of the process. The main findings from this work are:

- More than 90% boron was extracted from native brine of the salar de Hombre Muerto by 2 mol $L^{-1}$ 2-butyloctan-1-ol diluted in kerosene at O/A=4, pH=7.5 and 25 °C. This extraction solvent enables to extract boron from low or high boron concentrated brines.
- Magnesium and calcium impurities were removed in stage I of the electrodialysis. The recovered salt was composed of 71.2% $Mg(OH)_2$.
- High migration efficiency of sodium (99.9%) was reached in stage II while the purity of sodium carbonate obtained by precipitation with carbon dioxide was 99.99%.
- In stage III of the electrodialysis, lithium was valorized as battery-grade lithium carbonate (purity of the produced lithium carbonate=99.9%).
- The energy consumption of the electrodialysis process was decreased by 32% when boron was extracted before the electrodialysis experiments.

The novelty of this PhD work relies on the following points:

- Presently, boron and lithium are extracted from brines concentrated by solar evaporation. The next generations of lithium production plants will implement direct

lithium extraction technologies, which generally do not require solar evaporation. Therefore, boron should be directly extracted from brines and not from brines after solar evaporation. Only few papers addressed boron extraction from native brines before solar evaporation. This work was devoted to find efficient and selective extraction solvent to recover and valorize boron as pure borax from native brines without solar evaporation. Hence, it introduces an avenue for producing high-grade borax directly from brines, offering a complementary approach to the predominant method of boron extraction from brines.

- Research in literature investigated the extraction properties of boron from low salinity synthetic brines, or acidified brines or brines after solar evaporation without investigating the co-extraction of the other cations present in the brines. This work investigates the extraction of boron from high salinity native brines and synthetic brine representative to native brine of the salar de Hombre Muerto (Argentina). It is particularly important to take into account the other cations present in the brines during extraction experiments since the boron salts produced from brines must be very pure and lithium co-extraction with boron extraction has to be avoided.
- One limitation of using solvent extraction to extract boron from brines is the high solubility of alcohols in the brines, leading to increase effluent treatment and extractant consumption. Surprisingly, few papers in the literature provide solubility data of boron extractants from brines. This study reveals that the selected alcohol exhibits significantly lower solubility in the brine compared to more conventional boron extractants.
- Few studies delve into the physicochemistry of boron extraction by alcohols, typically considering only the presence of boric acid in the brine. However, boron speciation within brines is intricate, and the brines composition extend beyond boron to encompass various other elements. In this research, boron speciation calculations were employed alongside analysis of other ions within the brines. This allowed to elucidate the variance in boron extraction concerning pH and revealed the concurrent extraction of magnesium and calcium by diols at elevated pH levels. Consequently, this work offers valuable insights into the complex physicochemistry governing boron extraction alongside other impurities.
- A breakthrough on direct lithium extraction by electrodialysis was achieved in this work through the investigations on magnesium, calcium, sodium, potassium, lithium

and carbonate anions speciation in the brines using the free software Phreeqc. This enables better understanding of the physicochemistry of these species in alkaline solutions and allows to identify the efficient conditions to precipitate selectively sodium and lithium.

- The sustainability of this process was highlighted by the valorization of boron, magnesium and sodium with lithium, the reduction of the energy consumption and the reduction of water consumption *via* water recycling.

Despite the numerous breakthroughs previously mentioned in boron and lithium extractions in this research, it is suggested to:

- Investigate the extraction equilibria involved in boron extraction by 2-bytul-1-octanol by developing a physicochemical modeling in order to describe more accurately the nature of the extracted complex.
- Remove boron in four mixers-settlers as reported in chapter 2-section 2.3.6 in order to significantly reduce the impurities in the byproducts of stage I and decrease the energy consumption of the electrodialysis process.
- Precipitate magnesium and calcium separately by pH control in stage I of the electrodialysis.
- Reduce the energy consumption in stage II because it could be a limitation in industrial scale.
- Improve lithium recovery by reducing the amount of sodium impurity in stage III.

# References

[1] W. R. Torres, C. H. Díaz Nieto, A. Prévoteau, K. Rabaey, and V. Flexer, “Lithium carbonate recovery from brines using membrane electrolysis,” *Journal of Membrane Science*, vol. 615, p. 118416, Dec. 2020, doi: 10.1016/j.memsci.2020.118416.

# Summary of the thesis in French

# Titre : Développement d'un procédé d'extraction directe de bore à partir des saumures du salar de Hombre Muerto (Argentine) dans le cadre de la production de carbonate de lithium de haute pureté pour l'industrie des batteries.

## Contexte

Actuellement, la demande en minéraux est en forte croissance à cause du développement des nouvelles technologie pour la transition énergétique. La plupart des minéraux sont extraits à partir des minerais tandis que les minéraux de lithium sont à la fois extraits à partir des minerais et des saumures. Par conséquent, les saumures sont des ressources alternatives pour assurer une bonne partie de la production de lithium pour des applications industrielles à long terme. Les saumures contiennent plusieurs minéraux dont les compositions diffèrent en fonction du gisement. On distingue deux types de saumures: les saumures souterraines (les saumures géothermales et des gisements de pétrole) et les saumures continentales (lacs salés et salar). Les saumures issues des salars sont principalement localisées en Amérique du Sud notamment en Argentine, Bolivie et Chili, à haute altitude dans des régions à faibles pluviométrie.

La saumure du salar de Hombre Muerto, dans le Nord-Ouest de l'Argentine, contient des réserves importantes en lithium, potassium, calcium, sodium, magnésium, bore, chlorure et sulfate. L'extraction du lithium à partir de cette saumure est un défi majeur à cause de la forte teneur des autres constituants. De nos jours, les procédés d'extraction de lithium à partir des saumures sont essentiellement basés sur des opérations d'évaporation solaire et de précipitation chimique [1]. Le temps nécessaire à la production de carbonate de lithium est très long car il s'étend entre un et deux ans. De plus, ces procédés conventionnels sont responsables de perte énorme en eau durant l'évaporation solaire et consomment d'énorme quantité de produits chimiques pour l'élimination de autres constituants des saumures qui en plus ne sont pas valorisées. En effet, ces constituants sont extraites sous forme de sels et stockées dans des décharges engendrant de potentiels impacts environnementaux. Dans le contexte de l'économie circulaire, cette technologie n'est pas assez efficace et durable. De nouvelles techniques d'extraction directe de lithium basées sur l'extraction liquide-liquide, l'extraction solide-liquide ou des technologies membranaires sont en cours d'étude pour assurer une extraction durable et efficace du lithium. Parmi ces technologies, l'électrodialyse est rapporté comme étant une technologie pertinente pour l'extraction du lithium [2]. Diaz Nieto et al. ([3], [4], [5]) ont

récemment développé un procédé qui combine l'électrodialyse et une précipitation successive sur trois étapes permettant de séparer le magnésium, le calcium, le sodium et le lithium respectivement sous forme d'hydroxyde de magnésium, d'hydroxyde de calcium, de carbonate de sodium et de carbonate de lithium. Cependant, le carbonate de lithium produit n'est pas suffisamment pure puisque sa pureté ne dépasse pas 97,5%. Il est donc nécessaire d'améliorer l'efficacité de ce procédé pour pouvoir atteindre des puretés compatibles avec celles requises par l'industrie des batteries lithium-ion (>99,5%) [6]. Parmi les constituants de la saumures, l'élimination du bore est particulièrement importante puisqu'il cause des problèmes de filtration après l'étape de précipitation et participe à la production de carbonate de lithium de faible pureté non utilisable pour la production de batteries lithium-ion. En effet, la teneur en bore dans les saumures doit être inférieure à 25 mg $L^{-1}$ pour assurer la production de carbonate de lithium de qualité batterie [7]. De plus, la co-extraction du bore contenue dans les saumures pourrait contribuer à répondre à la demande en bore dans les industries fortement consommatrices telles que les industries de production de verres, céramiques, engrais et détergents [8], mais aussi dans les autres secteurs tels que le nucléaire [9], l'acier [10], la pharmacie [11], la catalyse [12], le textile [13], le stockage de l'hydrogène [14], le béton [15] et le domaine militaire [16].

Plusieurs technologies telles que l'adsorption [17], la précipitation [18], l'électrodialyse [19], les résines échangeuses d'ions [20], l'extraction liquide-liquide ([21], [22], [23], [24]) et l'osmose inverse [25] ont été testées pour l'extraction du bore à partir des saumures ou d'autres solutions aqueuses. L'extraction liquide-liquide est une opération unitaire mature qui est déjà mise en œuvre dans les procédés hydrométallurgiques ([26], [27]). Dans les usines actuelles de production de lithium, les alcools sont communément utilisés comme extractant pour l'extraction liquide-liquide du bore à partir de saumures concentrées par évaporation solaire, malgré leur forte solubilité dans les saumures qui génère d'importants couts [28].

Cette thèse s'est focalisée sur le développement d'un procédé d'extraction directe du bore à partir des saumures natives du salar de Hombre Muerto avec pour objectif la co-valorisation du bore sous forme d'acide borique ou de borax et la production de carbonate de lithium de haute qualité pour la production des batteries lithium-ion. Pour atteindre cet objectif, une combinaison d'opérations d'extraction liquide-liquide, d'électrodialyse et de précipitation a été réalisée pour extraire le bore, séparer les autres constituant du lithium et produire du carbonate de lithium. Contrairement aux méthodes traditionnelles qui sont basées sur la concentration des saumures par évaporation solaire avant l'élimination du bore et la cristallisation de chlorure de lithium puis sa conversion en carbonate de lithium, cette recherche se focalise sur une extraction

du bore puis du lithium directement à partir de la saumure sans évaporation solaire préalable. Cette approche permet d'anticiper l'évolution des usines de production de lithium, qui vont probablement s'affranchir de l'évaporation solaire, soulignant ainsi la nécessité de mettre en œuvre l'extraction directe du bore à partir des saumures qui est un aspect rarement exploré dans les études précédentes rapportées dans la littérature.

Pour accomplir ces objectifs, le chapitre 1 présente une revue complète de la littérature sur le bore et le lithium, couvrant leur sources, réserves ou ressources, de même que la production, la demande, les procédés de traitement et les applications industrielles. Le chapitre 2 se focalise sur l'étude de l'extraction du bore à partir des saumures en utilisant des solvants eutectiques profonds et six alcools tels que le 2-butyloctan-1-ol (BOc), 2-ethylhexan-1-ol (EH), octan-1-ol (Oc), 2-ethylhexane-1,3-diol (EHD), 2-methylpentane-2,4-diol (MPD) et le 2-butyl-2-ethylpropane-1,3-diol (BEPD) dilués dans du kérosène, kérosène sulfoné, un mélange de kérosène et de toluène ou de xylène. Ces investigations se focalisent sur la compréhension de l'influence des facteurs tels que la nature du diluent et de l'alcool, la concentration de l'alcool, le rapport volumique entre la phase organique et la phase aqueuse (O/A), le pH et la température sur le rendement d'extraction du bore, la sélectivité du bore vis-à-vis du calcium, magnésium, sodium, lithium et du potassium, la solubilité de l'alcool dans les saumures, la solubilité de l'eau dans la phase organique et le recyclage des alcools mentionnés précédemment. Par la suite, les conditions optimales conduisant à une extraction efficace et sélective du bore ont été utilisées pour tester le schéma de procédé en continue et à contre-courant. Finalement, le chapitre 3 aborde l'intégration de l'opération d'extraction liquide-liquide du bore développée dans le chapitre 2 à des opérations d'électrodialyse constituées de trois étapes permettant de produire du carbonate de lithium, de co-valoriser le bore et d'éliminer le calcium, le magnésium et le sodium. Suite à cette étude, un schéma de procédé combinant des opérations d'extraction liquide-liquide, d'électrodialyse et de précipitation a été proposé pour la valorisation de co-produits et la production de carbonate de lithium de qualité batterie.

# Résultats et discussion

## Extraction liquide-liquide du bore

Les expériences d'extraction du bore ont été réalisées sur deux saumures natives, *i.e.* saumure native 1 (SN1) et saumure native 2 (SN2), et une saumure synthétique (SS) dont la composition est similaire à la saumures native 1. Le pH, la densité, la force ionique et la composition de ces trois saumures sont rassemblés dans le tableau ci-dessous.

**Tableau:** Composition, pH, force ionique (I) et densité à température ambiante de la saumure native 1 (SN1), la saumure native 2 (SN2) et la saumure synthétique (SS). La force ionique a été déterminée en considérant les calculs de spéciation réalisés avec le logiciel Phreeqc (base de données: Pitzer, Core10, Amm and Minteq.V4).

| Saumure | pH | I (mol $kg_w^{-1}$) | densité (g $cm^{-3}$) | Concentration (g $L^{-1}$) | | | | | | | | | |
|---|---|---|---|---|---|---|---|---|---|---|---|---|---|
| | | | | Li | Ca | Mg | B | Na | Sr | K | Fe | $Cl^-$ | $SO_4^{2-}$ |
| SN1 | 6.9 | 3.6 | 1.2 | 1.27 | 0.68 | 3.09 | 1.62 | 103.24 | 0.079 | 14.21 | 0.001 | 182.85 | 11.15 |
| SN2 | 7.5 | 3.46 | 1.2 | 0.75 | 0.1 | 2.51 | 0.54 | 103.29 | 0 | 7.8 | 0 | 176.15 | 14.13 |
| SS | 5.5 | 3.6 | 1.2 | 1.27 | 0.68 | 3.09 | 1.62 | 103.24 | 0 | 14.21 | 0 | 182.25 | 8.78 |

Pour identifier le meilleur système d'extraction du bore, des études préliminaires ont été réalisées avec les solvants d'extraction communément utilisés dans la littérature. Les propriétés d'extraction de trois mono alcools (2-butyloctan-1-ol (BOc), 2-ethylhexan-1-ol (EH) et octan-1-ol (Oc)) dilués à 1 mol $L^{-1}$ dans du kérosène, et trois di-alcools (2-ethylhexane-1,3-diol (EHD), 2-methylpentane-2,4-diol (MPD) et 2-butyl-2-ethylpropane-1,3-diol (BEPD)) dilués 1 mol $L^{-1}$ dans un mélange de kérosène 40% (wt) et de toluène 60% (wt) ont été étudiées. Aussi, des solvants non conventionnels tels que les solvants eutectiques profonds à base d'alcool qui regroupent le Men:MPD, Men:TMPD, Thy:MPD et le Thy:TMPD ont été utilisés pour l'extraction du bore à partir de la saumure synthétique. Les expériences d'extraction liquide-liquide et de désextraction ont été réalisées en mettant en contact la phase organique et la phase aqueuse dans des tubes de centrifugation de 50 mL dans un agitateur mécanique thermostaté (Gherardt Laboshake THL500/1) sous agitation à 200 tours $min^{-1}$ respectivement pendant 4 heures et 2 heures, pour les solvants classiques et 1 heure pour les solvants non conventionnels.

Les solvants eutectiques profonds ont montré un rendement d'extraction remarquable pour le bore (93,1−97,1%) avec moins de volume de phase organique (O/A=0.5). Cependant, malgré cette haute performance et leur composition en produits renouvelables tels que le menthol et le thymol, ces solvants eutectiques profonds ne peuvent pas être utilisés pour des applications industrielles puisqu'ils sont très solubles dans la saumure (solubilité>6 g $L^{-1}$). Parmi les mono alcools dilués dans le kérosène, le 2-butyloctan-1-ol contenant 12 atomes de carbone et le 2-ethylhexan-1-ol contenant 8 atomes de carbone ont montré un meilleur rendement d'extraction pour le bore avec O/A=4, à pH=5.5 et 35 °C. Cela révèle que l'hydrophobicité et les ramifications de d'alcool influencent fortement le rendement d'extraction. Parmi les di-alcools dilués dans le mélange de kérosène 40% (wt) et toluène 60% (wt), le meilleur rendement d'extraction (99%) a été obtenu par le 2-ethylhexane-1,3-diol à 1 mol $L^{-1}$, à pH=5.5, O/A=2 et

35 °C. Les diols sont meilleurs que les mono alcools à cause de la présence des deux fonctions hydroxyles qui favorisent l'extraction du bore en formant un complexe plus stable comparé aux mono alcools. A l'inverse, les diols ont montré une co-extraction du calcium et du magnésium à des pH alcalins, en plus ces alcools ont montré une solubilité supérieure à 259 mg $L^{-1}$ dans la saumure. Par conséquent, le 2-butyloctan-1-ol a été choisi à cause de sa solubilité dans les diluants non-aromatiques et de sa faible solubilité dans la saumure comparé au 2-ethylhexane-1,3-diol.

A partir de la saumure synthétique, un rendement d'extraction du bore de 70% a été obtenu avec 2-butyloctan-1-ol dilué à 2 mol $L^{-1}$ dans du kérosène, O/A=4, à pH=5.5 et 35 °C. Ce système d'extraction a été utilisé pour extraire en une seule étape 60,5% de bore à partir de la saumure native 1 (SN1) avec un rapport des volumes des phases O/A=4, à pH=6,9 et à 25 °C. Tandis que 46,4% de bore est extrait à partir de la saumure native 2 (SN2) avec O/A=4, à pH=7.5 et à 25 °C. La méthode de McCabe-Thiele [29] a été utilisée pour déterminer le nombre d'étage qu'il faut pour extraire le bore en continue de telle sorte que la concentration résiduelle du bore dans les saumures soit inférieure à 25 mg $L^{-1}$. Les résultats ont montrés que 4 mélangeurs-décanteurs permettent d'extraire 98,2% et 94,2% de bore, respectivement à partir de la saumure synthétique (SS) ou la saumure native 1 (SN1) et la saumure native 2 (SN2) sans ajustement de pH avec O/A=4 pour SS ou SN2 et O/A=7 pour SN1. Ces résultats ont été confirmés par une simulation de l'extraction du bore en continue et à contre-courant.

Une étude de l'influence de la température sur l'extraction du bore a montré que le rendement d'extraction du bore n'est pas dépendant de la température. Des calculs de spéciation du bore dans la saumure effectué à l'aide du logiciel Pheeqc [30], combiné avec des données d'extraction du bore en fonction du pH ont montré que le bore est extrait par les alcools sous forme d'acide borique en milieu acide sans co-extraction des autres éléments tels que le potassium, le calcium, le sodium, le lithium et le magnésium. Des analyses par résonance magnétique nucléaire (RMN) de la phase organique avant et après l'extraction du bore par le 2-butyloctan-1-ol dilué à 2 mol $L^{-1}$ dans le kérosène ont prouvé que le bore est principalement extrait par solvatation au lieu d'une esterification [31].

Parmi les solutions de désextraction utilisées, *i.e.* l'hydroxyde de sodium (NaOH) à 0,2 mol $L^{-1}$, l'acide chloridrique (HCl) à 0,2 mol $L^{-1}$ et l'eau déminéralisée, NaOH montre un meilleur rendement de désextraction du bore (100%) suivi de HCl (54%) et de $H_2O$ (50%). L'étude de l'effet de la concentration de NaOH sur le rendement de désextraction du bore a

montré que seulement une concentration de 0.1 mol $L^{-1}$ de NaOH était nécessaire pour obtenir une désextraction totale du bore en une étape à partir de la phase organique chargée. La solution de désextraction chargée en bore a été ensuite évaporée pour atteindre une concentration en bore de 11.8 g $L^{-1}$, ensuite le bore a été cristallisé sous forme de borax par refroidissement à 20 °C pendant 8 heures. Le rendement de cristallisation était de 54%. Une analyse par diffraction des rayons X (DRX) a montré que le solide formé est composé de borax ($Na_2B_4O_7•10H_2O$) et de tincalconite ($B_2H_5NaO_6$). Le solide a ensuite été chauffé à 100 °C pendant 24 heures pour obtenir uniquement du borax ($Na_2B_4O_7•2H_2O$) dont la pureté est de 99%.

## Production de borax, de carbonate de lithium de qualité batterie et co-valorisation des impuretés en combinant des opérations d'extraction liquide-liquide, d'électrodialyse et de précipitation.

Dans un premier temps, 90% du bore a été extrait à l'aide de 8 extractions en batch à partir de la saumure native 2 (SN2) avec 2-butyloctan-1-ol dilué à 2 mol $L^{-1}$ dans du kérosène, O/A=4, à pH=7,5 et à température ambiante. Cela a été rendu possible en mettant en contact 1 litre de la phase aqueuse et 4 litres de la phase organique sous agitation à 216 tours $min^{-1}$ pendant 5 min en utilisant un système d'agitation à deux hélices. Après l'extraction, le bore a été désextrait à partir de la phase organique chargée en bore avec de l'hydroxyde de sodium à 0,1 mol $L^{-1}$. Après la désextraction, le bore a été cristallisé sous forme de borax comme mentionné précédemment.

Ensuite, la saumure dépourvue de bore a servi à l'étude de l'influence de l'extraction du bore sur les performances du procédé d'électrodialyse développé par le laboratoire CIDMEJu en Argentine. Ce procédé d'électrodialyse était composé de trois étapes qui contiennent chacune une cellule électrochimique. Chaque cellule est composée de trois compartiments, *i.e.* compartiment anodique, cathodique et le compartiment du milieu. L'anode était faite d'une électrode à maille en titane (Ti) recouverte d'un oxyde métallique mixte à base d'iridium (IrO2/TiO2 ; 65/35%, Magneto Special Anodes), avec un collecteur de courant perpendiculaire fixé au centre. La cathode était un treillis métallique en acier inoxydable avec un collecteur de courant en acier inoxydable. Dans le compartiment anodique, les molécules d'eau étaient oxydées pour produire des protons $H^+$ et de l'oxygène, tandis que les molécules d'eau étaient réduites dans le compartiment cathodique pour produire des hydroxydes ($OH^-$) et de l'hydrogène. Toutes les expériences d'électrodialyse ont été réalisées en batch et à température ambiante. Le magnésium et le calcium ont été éliminés de la saumure dans la première étape de l'électrodialyse avec une densité de courant constante (215 A $m^{-2}$). Ensuite, le sodium a été

précipité de la saumure dans la deuxième étape de l'électrodialyse sous forme de carbonate de sodium à l'aide de dioxyde de carbone ($CO_2$) avec 150 A $m^{-2}$. Enfin, le lithium a été précipité dans la troisième étape sous forme de carbonate de lithium à l'aide de $CO_2$ avec 150 A $m^{-2}$.

L'extraction du bore avant les expériences d'électrodialyse a permis de réduire les impuretés dans le solide obtenu dans l'étape I et la consommation énergétique, respectivement de 18% et 17%. Aussi, la production d'hydroxyde de magnésium de haute pureté a été obtenu (pureté=71,2%). Dans l'étape II, alors qu'une excellente pureté de carbonate de sodium (pureté=99,99%) a été produite, l'extraction du bore a été un avantage à la réduction de la charge totale dissoute dans la saumure et la consommation énergétique, respectivement de 99,8% et 15%. Dans l'étape III de l'électrodialyse, du carbonate de lithium de qualité batterie (pureté=99,9%) a été obtenu.

Le schéma de procédé ci-dessous présente les opérations qui ont été utilisées pour l'extraction du bore, la co-valorisation du magnésium et du sodium, de mème que la production de carbonate de lithium de qualité batterie. Il est très important de souligner que l'eau à faible teneur en sels peut être utilisées pour le lavage des solides et pour les besoins en eau des opérations d'électrodialyse.

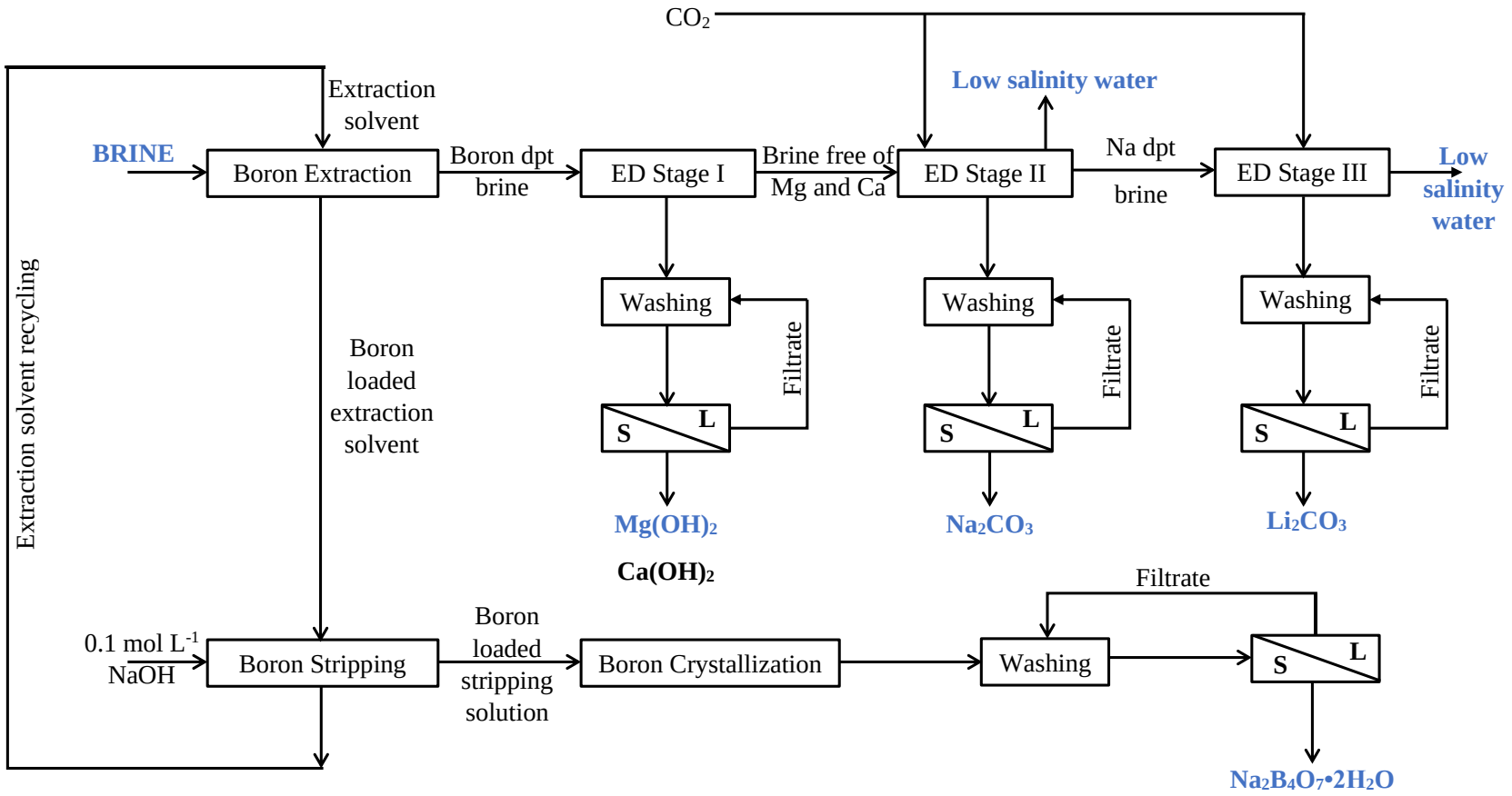



**Figure:** Schéma du procédé global de production de borax, d'hydroxyde de magnésium, de carbonate de sodium et de carbonate de lithium de qualité batterie.

# Conclusion

Les nombreux constituants dans les saumures continentales comme celles du salar de Hombre Muerto rendent l'extraction du lithium très complexe. Les procédés conventionnels d'extraction de lithium à partir des saumures ne sont pas assez efficaces pour une extraction durable du lithium à long terme à cause de la perte énorme en eau et de la production énorme de déchets solides. C'est dans ce contexte que s'inscrit cette thèse qui a pour but de développer un procédé d'extraction directe du bore et du lithium à partir des saumures du salar de Hombre Muerto afin de co-valoriser le bore sous forme de borax, de produire du carbonate de lithium de haute pureté pour l'industrie des batteries et de co-valoriser les autres constituants dans l'objectif de produire efficacement le lithium et de réduire drastiquement l'impact environnemental.

Parmi les solvants eutectiques profonds, les mono alcools et les diols sélectionnés à partir de la littératures pour l'étude de l'extraction du bore, 2-butyloctan-1-ol dilué à 2 mol $L^{-1}$ dans du kérosène a permis d'extraire efficacement et sélectivement le bore avec une solubilité très faible ( 18 mg $L^{-1}$). Ce système d'extraction a été utilisé pour extraire le bore à partir d'une saumure native. La saumure dépourvue de bore a servi dans un procédé d'électrodialyse à trois étapes pour produire de l'hydroxyde de magnésium, du carbonate de sodium et du carbonate de lithium, respectivement dans les étapes I, II et III. L'extraction du bore avant le procédé d'électrodialyse a permis de réduire la quantité des impuretés dans le solide obtenu dans l'étape I de 18%. Elle a aussi permis de réduire la consommation énergétique totale du procédé de 32%. A la fin de l'étape III, de l'eau à très faible teneur en sel a été obtenue, pouvant servir à répondre au besoin en eau du procédé d'électrodialyse. L'implémentation du procédé d'extraction liquide-liquide à côté du procédé d'électrodialyse permet de produire du borax ($Na_2B_4O_7 \cdot 2H_2O$, pureté=99%), de l'hydroxyde de magnésium ($Mg(OH)_2$, pureté=71,2%), du carbonate de sodium ($Na_2CO_3$, pureté=99,99%) et du carbonate de lithium de haute pureté pouvant servir à la production des batteries lithium-ion ($Li_2CO_3$, pureté=99,9%).

Cette recherche se distingue dans le domaine sur plusieurs points :

- Contrairement aux procédés conventionnels, cette recherche étudie l'extraction directe du bore et du lithium à partir des saumures natives en évitant l'étape d'évaporation solaire et l'utilisation de produits chimiques pour la précipitation des impuretés de lithium.

- Dans ce travail, la sélectivité des alcools pour le bore et leur solubilité dans la saumure ont été étudiées, ce qui est rarement rapporté dans la littérature.
- Cette étude s'est également penché sur la physicochimie complexe de l'extraction du bore, de sa spéciation dans les saumures de même que la physicochimie de la spéciation du lithium, un aspect rarement étudié dans la littérature.
- Une étude qui combine des opérations d'extraction liquide-liquide, d'électrodialyse et de précipitation a été réalisée pour produire des sels de haute pureté de borax, d'hydroxyde de magnésium, de carbonate de sodium et de carbonate de lithium.

Malgré les nombreuses avancées qui ont été apportées par cette thèse dans ce domaine, certains verrous restent à lever notamment :

- Une investigation sur les équilibres d'extractions impliquées lors de l'extraction du bore par le 2-butyloctan-1-ol à l'aide d'une modélisation physicochimique, qui permettra de décrire avec plus de précision la nature du complexe extrait.
- L'élimination du bore dans 4 mélangeurs-décanteurs avant le procédé d'électrodialyse. Cela permettra de réduire considérablement les impuretés dans les sous-produits de l'étape I et la consommation énergétique du procédé d'électrodialyse.
- Précipiter le magnésium et le calcium séparément à l'aide d'un contrôle de pH dans l'étape I de l'électrodialyse
- Réduire la consommation énergétique dans l'étape II car il pourrait représenter un frein à l'implémentation du procédé d'électrodialyse en industrie.

# References


[1] F. Meng, J. McNeice, S. S. Zadeh, and A. Ghahreman, “Review of Lithium Production and Recovery from Minerals, Brines, and Lithium-Ion Batteries,” *Mineral Processing and Extractive Metallurgy Review*, vol. 42, no. 2, pp. 123–141, Feb. 2021, doi: 10.1080/08827508.2019.1668387.

[2] S. Gmar and A. Chagnes, “Recent advances on electrodialysis for the recovery of lithium from primary and secondary resources,” *Hydrometallurgy*, vol. 189, p. 105124, Nov. 2019, doi: 10.1016/j.hydromet.2019.105124.

[3] C. H. Díaz Nieto, K. Rabaey, and V. Flexer, “Membrane electrolysis for the removal of Na+ from brines for the subsequent recovery of lithium salts,” *Separation and Purification Technology*, vol. 252, p. 117410, Dec. 2020, doi: 10.1016/j.seppur.2020.117410.

[4] C. H. Díaz Nieto, N. A. Palacios, K. Verbeeck, A. Prévoteau, K. Rabaey, and V. Flexer, “Membrane electrolysis for the removal of Mg2+ and Ca2+ from lithium rich brines,” *Water Research*, vol. 154, pp. 117–124, May 2019, doi: 10.1016/j.watres.2019.01.050.

[5] W. R. Torres, C. H. Díaz Nieto, A. Prévoteau, K. Rabaey, and V. Flexer, “Lithium carbonate recovery from brines using membrane electrolysis,” *Journal of Membrane Science*, vol. 615, p. 118416, Dec. 2020, doi: 10.1016/j.memsci.2020.118416.

[6] V. T. Luong, D. J. Kang, J. W. An, M. J. Kim, and T. Tran, “Factors affecting the extraction of lithium from lepidolite,” *Hydrometallurgy*, vol. 134–135, pp. 54–61, Mar. 2013, doi: 10.1016/j.hydromet.2013.01.015.

[7] J. Guo, Y. Yang, X. Gao, and J. Yu, “Boron extraction from lithium-rich brine using mixed alcohols,” *Hydrometallurgy*, vol. 197, p. 105477, Nov. 2020, doi: 10.1016/j.hydromet.2020.105477.

[8] T. Turkbay, J. Bongono, T. Alix, B. Laratte, and B. Elevli, “Prior knowledge of the data on the production capacity of boron facilities in Turkey,” *Cleaner Engineering and Technology*, vol. 10, p. 100539, Oct. 2022, doi: 10.1016/j.clet.2022.100539.

[9] M. M. Nasseri, “Comparison of HfB2 and ZrB2 behaviors for using in nuclear industry,” *Annals of Nuclear Energy*, vol. 114, pp. 603–606, Apr. 2018, doi: 10.1016/j.anucene.2017.12.060.

[10] J. Eichler and C. Lesniak, “Boron nitride (BN) and BN composites for high-temperature applications,” *Journal of the European Ceramic Society*, vol. 28, no. 5, pp. 1105–1109, Jan. 2008, doi: 10.1016/j.jeurceramsoc.2007.09.005.

[11] F. Ali, N. S Hosmane, and Y. Zhu, “Boron Chemistry for Medical Applications,” *Molecules*, vol. 25, no. 4, Art. no. 4, Jan. 2020, doi: 10.3390/molecules25040828.

[12] “Borophene and Boron-Based Nanosheets: Recent Advances in Synthesis Strategies and Applications in the Field of Environment and Energy - Chand - 2021 - Advanced Materials Interfaces - Wiley Online Library.” Accessed: Jan. 25, 2023. [Online]. Available: https://onlinelibrary-wiley-com.bases-doc.univ-lorraine.fr/doi/full/10.1002/admi.202100045

[13] A. Mergen, M. H. Demirhan, and M. Bilen, “Processing of boric acid from borax by a wet chemical method,” *Advanced Powder Technology*, vol. 14, no. 3, pp. 279–293, Jan. 2003, doi: 10.1163/15685520360685947.

[14] G. Moussa, R. Moury, U. B. Demirci, T. Şener, and P. Miele, “Boron-based hydrides for chemical hydrogen storage,” *International Journal of Energy Research*, vol. 37, no. 8, pp. 825–842, 2013, doi: 10.1002/er.3027.

[15] M. H. Kharita, S. Yousef, and M. AlNassar, “Review on the addition of boron compounds to radiation shielding concrete,” *Progress in Nuclear Energy*, vol. 53, no. 2, pp. 207–211, Mar. 2011, doi: 10.1016/j.pnucene.2010.09.012.

[16] M. M. Harussani, S. M. Sapuan, G. Nadeem, T. Rafin, and W. Kirubaanand, “Recent applications of carbon-based composites in defence industry: A review,” *Defence Technology*, vol. 18, no. 8, pp. 1281–1300, Aug. 2022, doi: 10.1016/j.dt.2022.03.006.

[17] Z. Guan, J. Lv, P. Bai, and X. Guo, “Boron removal from aqueous solutions by adsorption — A review,” *Desalination*, vol. 383, pp. 29–37, Apr. 2016, doi: 10.1016/j.desal.2015.12.026.

[18] Y.-J. Shih, C.-H. Liu, W.-C. Lan, and Y.-H. Huang, “A novel chemical oxo-precipitation (COP) process for efficient remediation of boron wastewater at room temperature,” *Chemosphere*, vol. 111, pp. 232–237, Sep. 2014, doi: 10.1016/j.chemosphere.2014.03.121.

[19] L. Melnik, O. Vysotskaja, and B. Kornilovich, “Boron behavior during desalination of sea and underground water by electrodialysis,” *Desalination*, vol. 124, no. 1, pp. 125–130, Nov. 1999, doi: 10.1016/S0011-9164(99)00096-X.

[20] M. Gazi and N. Bicak, “Selective boron extraction by polymer supported 2-hydroxylethylamino propylene glycol functions,” *Reactive and Functional Polymers*, vol. 67, no. 10, pp. 936–942, Oct. 2007, doi: 10.1016/j.reactfunctpolym.2007.05.019.

[21] N. Bicak, M. Gazi, and B. F. Senkal, “Polymer supported amino bis-(cis-propan 2,3 diol) functions for removal of trace boron from water,” *Reactive and Functional Polymers*, vol. 65, no. 1, pp. 143–148, Nov. 2005, doi: 10.1016/j.reactfunctpolym.2005.01.010.

[22] M. D. Joshi, G. Chalumot, Y. Kim, and J. L. Anderson, “Synthesis of glucaminium-based ionic liquids and their application in the removal of boron from water,” *Chem. Commun.*, vol. 48, no. 10, pp. 1410–1412, Jan. 2012, doi: 10.1039/C1CC14327A.

[23] M. Karakaplan, S. Tural, B. Tural, Y. Turgut, and H. Hoşgören, “The Solvent Extraction of Boron with Synthesized Aliphatic 1,3-Diols: Stripping and Extraction Behavior of Boron by 2,2,5-Trimethyl-1,3-hexanediol,” *Solvent Extraction and Ion Exchange*, vol. 22, no. 6, pp. 897–911, Dec. 2004, doi: 10.1081/SEI-200037400.

[24] W. L. A. Brooks, C. C. Deng, and B. S. Sumerlin, “Structure–Reactivity Relationships in Boronic Acid–Diol Complexation,” *ACS Omega*, vol. 3, no. 12, pp. 17863–17870, Dec. 2018, doi: 10.1021/acsomega.8b02999.

[25] A. Farhat, F. Ahmad, N. Hilal, and H. A. Arafat, “Boron removal in new generation reverse osmosis (RO) membranes using two-pass RO without pH adjustment,” *Desalination*, vol. 310, pp. 50–59, Feb. 2013, doi: 10.1016/j.desal.2012.10.003.

[26] G. M. Ritcey, “Solvent extraction in hydrometallurgy: Present and future,” *Tsinghua Science and Technology*, vol. 11, no. 2, pp. 137–152, Apr. 2006, doi: 10.1016/S1007-0214(06)70168-7.

[27] A. Chagnes, Ed., *Advances in Hydrometallurgy*. MDPI - Multidisciplinary Digital Publishing Institute, 2020. doi: 10.3390/books978-3-03928-940-0.

[28] D. E. Garrett, “Part 1 - Lithium,” in *Handbook of Lithium and Natural Calcium Chloride*, D. E. Garrett, Ed., Oxford: Academic Press, 2004, pp. 1–235. doi: 10.1016/B978-012276152-2/50037-2.

[29] W. L. McCabe, J. C. Smith, and P. Harriott, *Unit operations of chemical engineering*. McGraw-Hill, 1993. Accessed: May 09, 2024. [Online]. Available: https://thuvienso.hoasen.edu.vn/handle/123456789/8475

[30] D. L. Parkhurst and C. A. J. Appelo, “Description of input and examples for PHREEQC version 3: a computer program for speciation, batch-reaction, one-dimensional transport, and inverse geochemical calculations,” U.S. Geological Survey, Reston, VA, USGS Numbered Series 6-A43, 2013. doi: 10.3133/tm6A43.

[31] X. Fan, X. Yu, Y. Guo, and T. Deng, “Recovery of Boron from Underground Brine by Continuous Centrifugal Extraction with 2-Ethyl-1,3-hexanediol (EHD) and Its

Mechanism," *Journal of Chemistry*, vol. 2018, p. e7530837, Oct. 2018, doi: 10.1155/2018/7530837.

# Appendices

# Appendix A

## Development of elemental analysis method

Elemental analyses of the brines by microwave plasma-atomic emission spectrometer (MP-AES) or inductively coupled plasma-optical emission spectroscopy (ICP-OES) were challenging due the high concentration of sodium (103 g $L^{-1}$), chloride (182 g $L^{-1}$) and sulfate (11 g $L^{-1}$). For MP-AES analyses, concentrations of lithium, boron, potassium, magnesium, calcium and sodium were determined at 670.784 nm, 249.677 nm, 766.491 nm, 518.360 nm, 393.366 nm and 568.820 nm, respectively. For ICP-OES analyses, the following wavelengths were used: 670.784 nm (lithium), 249.773 nm (boron), 769.896 nm (potassium), 279.553 nm (magnesium), 315.887 nm (calcium) and 589.592 nm (sodium).

Exactly 1 mL of the brine was sampled and diluted in 2% (vol.) nitric acid prepared by diluting concentrated nitric acid (purity=65%, Sigma-Aldrich) in deionized water. First, sodium concentration in the samples was determined by diluting the samples 1,000 times. Chromatographic analyses evidenced that chloride and sulfate anions were not significantly extracted during boron extraction experiments. Therefore, to avoid the well-known matrix effect ([1], [2], [3], [4]), sodium was analyzed with a standardization curve made of five solutions containing different concentration of sodium as well as 182 mg $L^{-1}$ chloride and 11 mg $L^{-1}$ sulfate (Table A. 1). Sodium concentration in the standards was obtained by using ICP standard containing only 1000 mg $L^{-1}$ sodium (Sigma-Aldrich). Conversely, chloride and sulfate concentrations in the standards were obtained with hydrochloric acid (purity=37%, Sigma-Aldrich) and sulfuric acid (purity=96%, Sigma-Aldrich), respectively. The standards were also composed of 2% (vol.) nitric acid as the analyzed samples. Table A. 2 gathers the volumes of sodium standard, hydrochloric acid (HCl), sulfuric acid ($H_2SO_4$) and nitric acid ($HNO_3$) used to prepare the standards required to plot the standardization curves with respect to the concentration of sodium and anions (Table A. 1). Each standard was prepared in 100 mL volumetric flask. Therefore, the volume needed to reach 100 mL in the standards was completed with deionized water.

**Table A. 1:** Sodium, sulfate and chloride concentrations in the standards used to plot the standardization curves for sodium analysis.

| | Concentration in each standard (mg $L^{-1}$) | | | | |
|---|---|---|---|---|---|
| Na and anions | **0/Blank** | **1** | **2** | **3** | **4** |
| Na | 0 | 50 | 75 | 100 | 150 |
| $SO_4^{2-}$ | 11 | 11 | 11 | 11 | 11 |
| $Cl^-$ | 182 | 182 | 182 | 182 | 182 |

**Table A. 2:** Volumes of sodium standard (1,000 mg $L^{-1}$), hydrochloric acid (purity=37%), sulfuric acid (purity=96%) and nitric acid (purity=65%) used to prepare each standard in 100mL volumetric flask.

| | Volume of the aqueous solution in each standard (mL) | | | | |
|---|---|---|---|---|---|
| Aqueous solution | **0/Blank** | **1** | **2** | **3** | **4** |
| Na | 0 | 5 | 7.5 | 10 | 15 |
| $HNO_3$ | 2 | 2 | 2 | 2 | 2 |
| $H_2SO_4$ | 0.00065 | 0.00065 | 0.00065 | 0.00065 | 0.00065 |
| HCl | 0.040 | 0.040 | 0.040 | 0.040 | 0.040 |
| Total volume of the standard (ml) | 100 | 100 | 100 | 100 | 100 |

Sodium analysis in the samples indicated that there was no significant difference between sodium concentration in the brines before and after boron extraction. Therefore, boron, potassium, lithium and magnesium were then analyzed by diluting the samples 1000 times. Moreover, the matrix effect was prevented by performing the elemental analysis with standardization curves made of six solutions containing different concentrations of each element, 103 mg $L^{-1}$ sodium, 182 mg $L^{-1}$ chloride and 11 mg $L^{-1}$ sulfate (Table A. 3). Boron, potassium, magnesium and lithium concentrations in the standards were obtained by using ICP standard containing only 1,000 mg $L^{-1}$ boron, potassium, magnesium and lithium (Sigma-Aldrich), respectively. Conversely, chloride, sulfate and sodium concentrations in the standards were obtained with hydrochloric acid (purity=37%, Sigma-Aldrich), sulfuric acid (purity=96%, Sigma-Aldrich) and 26 g $L^{-1}$ sodium chloride, respectively. Concentration of 26 g $L^{-1}$ sodium chloride was obtained by dissolution of 2.6 g sodium chloride (purity=99.9%) in 100mL deionized water. The standards were also composed of 2% (vol.) nitric acid as the analyzed samples. Table A. 4 gathers the volumes of hydrochloric acid (HCl), sulfuric acid ($H_2SO_4$), nitric acid ($HNO_3$), and boron, potassium, lithium and magnesium standards used to prepare the standards required to plot the standardization curves with respect to their concentrations (Table A. 3). Each standard was prepared in 100 mL volumetric flask.

Therefore, the volume needed to reach 100 mL in the standards was completed with deionized water.

**Table A. 3:** Sodium, sulfate, chloride, boron, potassium, magnesium and lithium concentrations in the standards used to plot the standardization curves for boron, potassium, magnesium and lithium analyses.

| | Concentration in each standard (mg $L^{-1}$) | | | | | |
|---|---|---|---|---|---|---|
| Element/ anion | **0/Blank** | **1** | **2** | **3** | **4** | **5** |
| **Na** | 103 | 103 | 103 | 103 | 103 | 103 |
| **Cl-** | 182 | 182 | 182 | 182 | 182 | 182 |
| **$SO_4^{2-}$** | 11 | 11 | 11 | 11 | 11 | 11 |
| K | 0 | 5 | 10 | 15 | 20 | 30 |
| Mg | 0 | 1 | 2 | 3 | 4 | 5 |
| B | 0 | 0.1 | 0.5 | 1 | 1.5 | 3 |
| Li | 0 | 0.25 | 0.5 | 1 | 1.5 | 2 |

**Table A. 4:** Volume of 26 g $L^{-1}$ NaCl, HCl (purity=37%), $H_2SO_4$ (purity=96%), $HNO_3$ (purity=65%), K, Mg, B and Li standards (1,000 mg $L^{-1}$) used to prepare each standard in 100mL volumetric flask.

| | Volume of the aqueous solution in each standard (mL) | | | | | |
|---|---|---|---|---|---|---|
| Aqueous solution | **0/Blank** | **1** | **2** | **3** | **4** | **5** |
| **NaCl** | 1 | 1 | 1 | 1 | 1 | 1 |
| **HCl** | 0.005 | 0.005 | 0.005 | 0.005 | 0.005 | 0.005 |
| **$H_2SO_4$** | 0.00064 | 0.00064 | 0.00064 | 0.00064 | 0.00064 | 0.00064 |
| **$HNO_3$** | 2 | 2 | 2 | 2 | 2 | 2 |
| K | 0 | 0.5 | 1 | 1.5 | 2 | 3 |
| Mg | 0 | 0.1 | 0.2 | 0.3 | 0.4 | 0.5 |
| B | 0 | 0.01 | 0.05 | 0.1 | 0.15 | 0.3 |
| Li | 0 | 0.025 | 0.05 | 0.1 | 0.15 | 0.2 |
| Total volume of the standard (ml) | 100 | 100 | 100 | 100 | 100 | 100 |

Finally, the samples were diluted 100 times for calcium analyses. Therefore, the matrix effect was avoided by performing the elemental analysis with standardization curves made of five solutions containing different concentration of calcium, 1,032 mg $L^{-1}$ sodium, 1,822 mg $L^{-1}$ chloride and 110 mg $L^{-1}$ sulfate (Table A. 5). Calcium concentration in the standards was obtained by using ICP standard containing only 1,000 mg $L^{-1}$ calcium (Sigma-Aldrich). Conversely, chloride, sulfate and sodium concentrations in the standards were obtained with hydrochloric acid (purity=37%, Sigma-Aldrich), sulfuric acid (purity=96%, Sigma-Aldrich) and 26 g $L^{-1}$ sodium chloride, respectively. Concentration of 26 g $L^{-1}$ sodium was obtained by

dissolution of 2.6 g sodium chloride (purity=99.9%) in 100mL deionized water. The standards were also composed of 2% (vol.) nitric acid as the analyzed samples. Table A. 6 gathers the volumes of hydrochloric acid (HCl), sulfuric acid ($H_2SO_4$), nitric acid ($HNO_3$) and calcium standard used to prepare the standards required to plot the standardization curves with respect to their concentration (Table A. 5). Each standard was prepared in 100 mL volumetric flask. Therefore, the volume need to reach 100 mL in the standards was completed with deionized water.

**Table A. 5:** Sodium, sulfate, chloride and calcium concentrations in the standards used to plot the standardization curves for calcium analysis.

| | Concentration in each standard (mg $L^{-1}$) | | | | |
|---|---|---|---|---|---|
| Element/ anion | **0/Blank** | **1** | **2** | **3** | **4** |
| **Na** | 1032 | 1032 | 1032 | 1032 | 1032 |
| **Cl-** | 1828 | 1828 | 1828 | 1828 | 1828 |
| **$SO_4^{2-}$** | 111 | 111 | 111 | 111 | 111 |
| Ca | 0 | 2.5 | 5 | 7.5 | 10 |

**Table A. 6:** Volume of 26 g $L^{-1}$ NaCl, HCl (purity=37%), $H_2SO_4$ (purity=96%), $HNO_3$ (purity=65%) and calcium standard (1,000 mg $L^{-1}$) used to prepare each standard in 100mL volumetric flask.

| | Volume of the aqueous solution in each standard (mL) | | | | |
|---|---|---|---|---|---|
| Aqueous solution | **0/Blank** | **1** | **2** | **3** | **4** |
| **NaCl** | 10 | 10 | 10 | 10 | 10 |
| **HCl** | 0.051 | 0.051 | 0.051 | 0.051 | 0.051 |
| **$H_2SO_4$** | 0.00645 | 0.00645 | 0.00645 | 0.00645 | 0.00645 |
| **$HNO_3$** | 2 | 2 | 2 | 2 | 2 |
| Ca | 0 | 0.25 | 0.5 | 0.75 | 1 |
| Total volume of the standard (ml) | 100 | 100 | 100 | 100 | 100 |

Boron, potassium, magnesium, lithium and calcium concentrations were determined in the stripping solutions by using the standardization curves previously mentioned. However, as boron was stripped by deionized water, 0.2 mol $L^{-1}$ hydrochloric acid or 0.1−1 mol $L^{-1}$ sodium hydroxide (NaOH), sodium, chloride and sulfate concentrations in the stripping solutions were then adjusted to their content in the previously mentioned matrices before boron, potassium, magnesium, lithium and calcium analyses. First, 1 ml of the boron-loaded stripping solutions was sampled and diluted 10 times in 10 mL solution containing 10.3 g $L^{-1}$ sodium, 18.2 g $L^{-1}$ chloride and 1.1 g $L^{-1}$ sulfate (Table A. 7). Chloride, sulfate and sodium concentrations in the

these solutions were obtained with hydrochloric acid (purity=37%, Sigma-Aldrich), sulfuric acid (purity=96%, Sigma-Aldrich) and 262.7 g $L^{-1}$ sodium chloride, respectively. Concentration of 262.7 g $L^{-1}$ sodium chloride was obtained by dissolution of 26.27 g sodium chloride (purity=99.9%) in 100mL deionized water. Table A. 7 gathers the volumes of sample, NaCl, HCl and $H_2SO_4$ used to obtain 10.3 g $L^{-1}$ sodium, 18.2 g $L^{-1}$ chloride and 1.1 g $L^{-1}$ sulfate in 10 mL tubes for each type of stripping solution. Given that the samples were already diluted 10 times, these solutions were thereafter diluted 10 times for calcium analysis and 100 times for boron, potassium, magnesium and lithium analyses.

**Table A. 7:** Volume of sample, 262.7 g $L^{-1}$ NaCl, HCl (purity=37%) and $H_2SO_4$ (purity=96%) used to obtain the concentrations of sodium, chloride and sulfate in the matrices for each type of stripping solution.

| | Volume of aqueous solution for each type stripping solution (mL) | | | | | | | |
|---|---|---|---|---|---|---|---|---|
| Aqueous solution | $H_2O$ | 0.2 mol $L^{-1}$ HCl | 0.1 mol $L^{-1}$ NaOH | 0.2 mol $L^{-1}$ NaOH | 0.4 mol $L^{-1}$ NaOH | 0.6 mol $L^{-1}$ NaOH | 0.8 mol $L^{-1}$ NaOH | 1 mol $L^{-1}$ NaOH |
| Sample | 1 | 1 | 1 | 1 | 1 | 1 | 1 | 1 |
| NaCl | 1 | 1 | 0.978 | 0.955 | 0.911 | 0.866 | 0.822 | 0.777 |
| HCl | 0.051 | 0.036 | 0.058 | 0.066 | 0.081 | 0.096 | 0.112 | 0.127 |
| $H_2SO_4$ | 0.006 | 0.006 | 0.006 | 0.006 | 0.006 | 0.006 | 0.006 | 0.006 |
| Total volume of the solution (ml) | 10 | 10 | 10 | 10 | 10 | 10 | 10 | 10 |

Depending on the analyzed element, the error on the analytical method was estimated to be within 2−7% by analyzing the synthetic brine 10 times. Table A. 8 gathers the concentrations of lithium, boron, potassium, magnesium, calcium and sodium for each analysis, the standard deviations and the analytical error for each element. The analytical error for boron was only within 4%.

**Table A. 8:** Concentrations of B, K, Li, Mg, Na and Ca for 10 analyses of the synthetic brine, the standard deviations and the analytical error.

| Analysis | B ($g\ L^{-1}$) | K ($g\ L^{-1}$) | Li ($g\ L^{-1}$) | Mg ($g\ L^{-1}$) | Na ($g\ L^{-1}$) | Ca ($g\ L^{-1}$) |
|---|---|---|---|---|---|---|
| 1 | 1.586 | 15.873 | 1.348 | 3.205 | 110.231 | 0.536 |
| 2 | 1.693 | 15.924 | 1.35 | 3.22 | 110.195 | 0.527 |
| 3 | 1.649 | 15.392 | 1.324 | 3.129 | 108.136 | 0.524 |
| 4 | 1.623 | 15.533 | 1.343 | 3.192 | 109.278 | 0.525 |
| 5 | 1.677 | 15.334 | 1.312 | 3.143 | 109.948 | 0.525 |
| 6 | 1.718 | 15.286 | 1.323 | 3.16 | 111.432 | 0.523 |
| 7 | 1.673 | 15.398 | 1.308 | 3.15 | 109.252 | 0.52 |
| 8 | 1.646 | 14.478 | 1.243 | 3.05 | 111.253 | 0.521 |
| 9 | 1.668 | 14.459 | 1.247 | 3.015 | 107.647 | 0.511 |
| 10 | 1.662 | 14.64 | 1.255 | 3.034 | 109.251 | 0.517 |
| Average | 1.66 | 15.23 | 1.31 | 3.13 | 109.66 | 0.523 |
| Standard deviation | 0.03 | 0.51 | 0.04 | 0.07 | 1.15 | 0.01 |
| 2*Standard deviation | 0.07 | 1.01 | 0.08 | 0.14 | 2.30 | 0.01 |
| Error (2 *Standard deviation /Average) | 0.04 | 0.07 | 0.06 | 0.04 | 0.02 | 0.02 |

## References


[1] S. Barth, "Comparison of NTIMS and ICP-OES methods for the determination of boron concentrations in natural fresh and saline waters," *Fresenius J Anal Chem*, vol. 358, no. 7, pp. 854–855, Jul. 1997, doi: 10.1007/s002160050522.

[2] M. Kühn, C. Niewöhner, M. Isenbeck-Schröter, and H. D. Schulz, "Determination of major and minor constituents in anoxic thermal brines of deep sandstone aquifers in Northern Germany," *Water Research*, vol. 32, no. 2, pp. 265–274, Feb. 1998, doi: 10.1016/S0043-1354(97)00252-2.

[3] H. Tao, Y. Xiao-ping, G. Ya-fei, L. Ming-li, D. Ji, and D. Tian-long, "Determination of Lithium in High Salinity Samples by Inductively Coupled Plasma Optical Emission Spectrometry (ICP-OES)," *Spectrosc. Spectr. Anal.*, vol. 40, no. 4, pp. 1214–1220, Apr. 2020, doi: 10.3964/j.issn.1000-0593(2020)04-1214-07.

[4] Z. Chen-ling, J. Na, L. Jia, L. Bing-bing, and H. Mei, "Investigation of Lithium Analysis in Geothermal Water by Inductively Coupled Plasma Optical Emission Spectrometry," *Spectrosc. Spectr. Anal.*, vol. 41, no. 12, pp. 3876–3880, Dec. 2021, doi: 10.3964/j.issn.1000-0593(2021)12-3876-05.

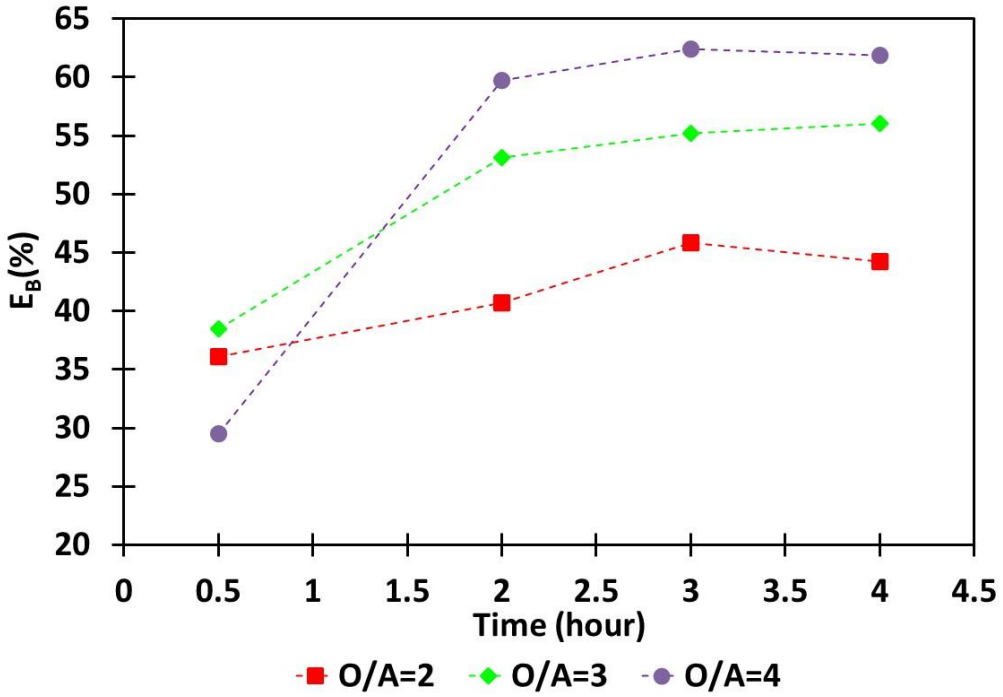



**Figure A. 1:** Extraction efficiency of boron from the synthetic brine (SB) as a function of time at different phase volume ratios. Extraction solvent: 1 mol $L^{-1}$ BOc in kerosene; pH=1; temperature=35 °C (no co-extraction of K, Li, Mg, Na and Ca was observed).

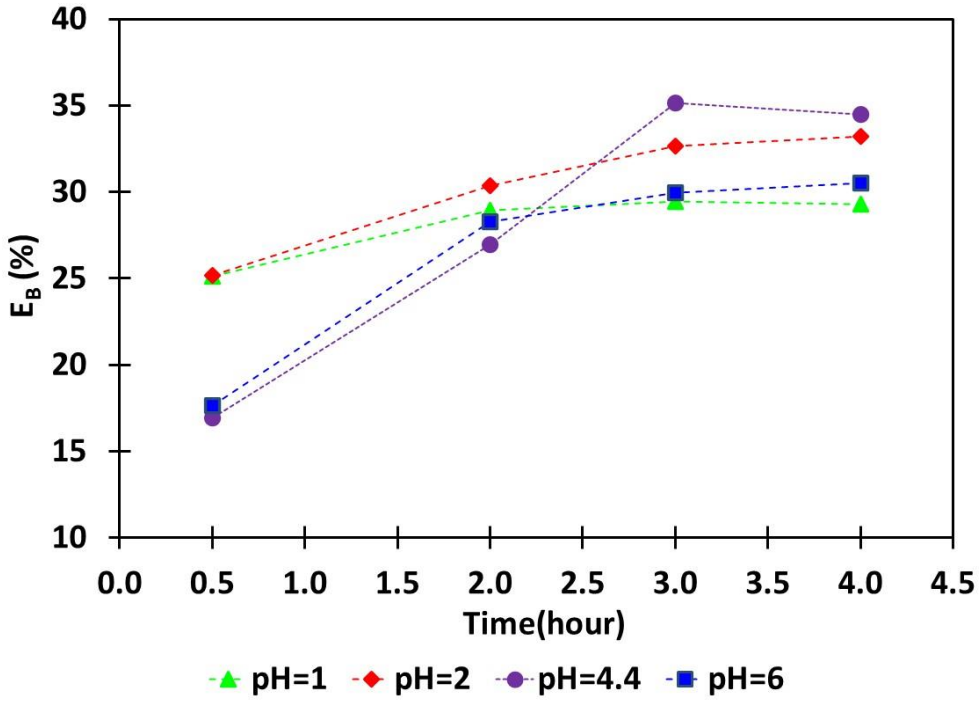



**Figure A. 2:** Extraction efficiency of boron from the synthetic brine (SB) as a function of time at different pH of the synthetic solution. Extraction solvent: 1 mol $L^{-1}$ BOc in kerosene; O/A=1; temperature=35 °C (no co-extraction of K, Li, Mg, Na and Ca was observed).

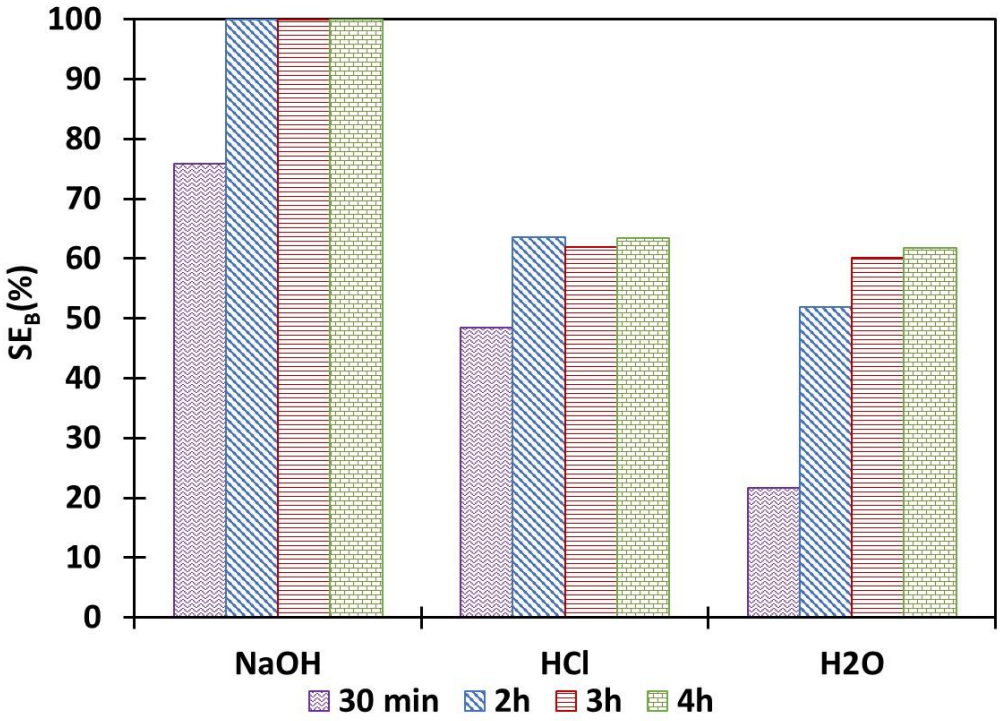



**Figure A. 3:** Influence of time on the stripping efficiency of boron from an extraction solvent containing 1 mol $L^{-1}$ BOc in kerosene previously loaded with 0.25 g $L^{-1}$ boron by contacting the extraction solvent with the synthetic brine (SB) at O/A=4 (temperature=35 °C and pH=5.5). Stripping solutions: 0.2 mol $L^{-1}$ NaOH, 0.2 mol $L^{-1}$ HCl or deionized water; O/A=4; temperature=35 °C.

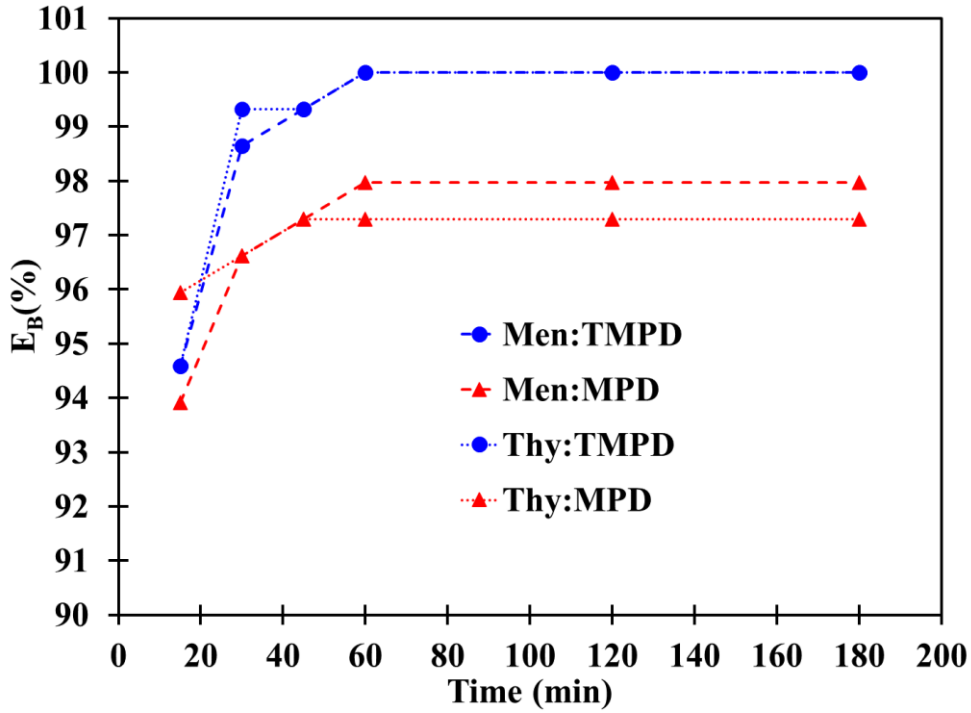



**Figure A. 4:** Extraction efficiency of boron from the synthetic brine (SB) as a function of time for different DES (no co-extraction of K, Li, Mg, Na and Ca was observed). Extraction conditions: O/A=1, pH=5.5 and 25 °C.

**Table A. 9:** Influence of the temperature on the extraction efficiency of boron (extraction solvent: 2 mol $L^{-1}$ 2-butyloctan-1-ol, O/A=4, pH=5.5).

| Temperature (°C) | $E_B$(%) |
|---|---|
| 25 | 71.9 |
| 35 | 70.7 |
| 40 | 70.7 |
| 50 | 70.9 |

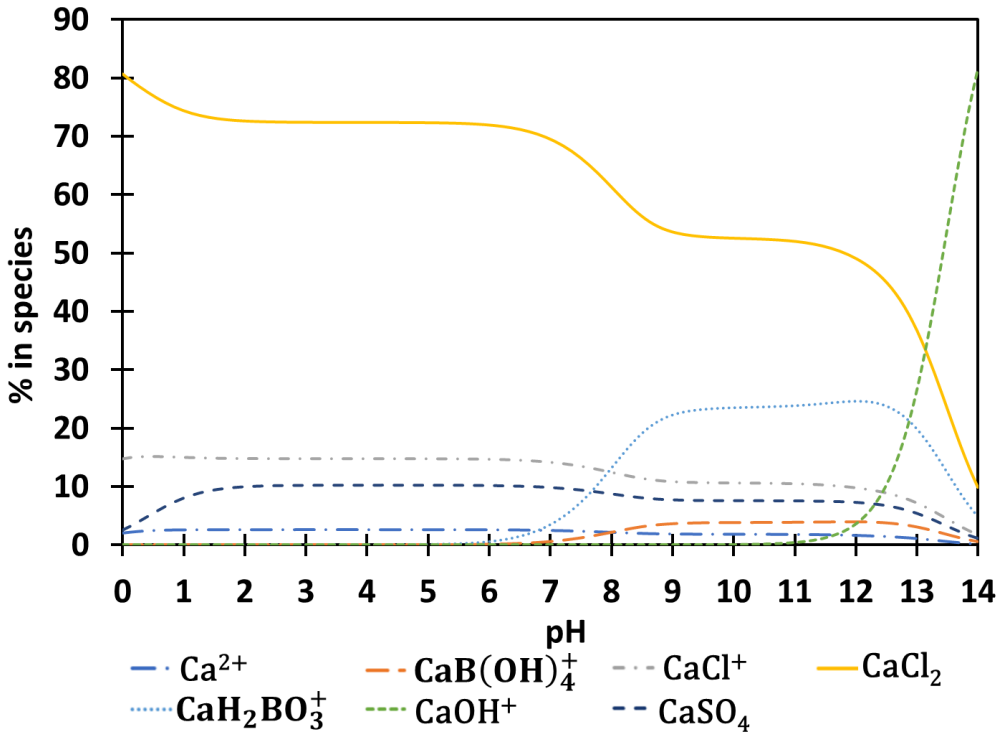



**Figure A. 5:** Calcium speciation in the synthetic brine vs. pH.

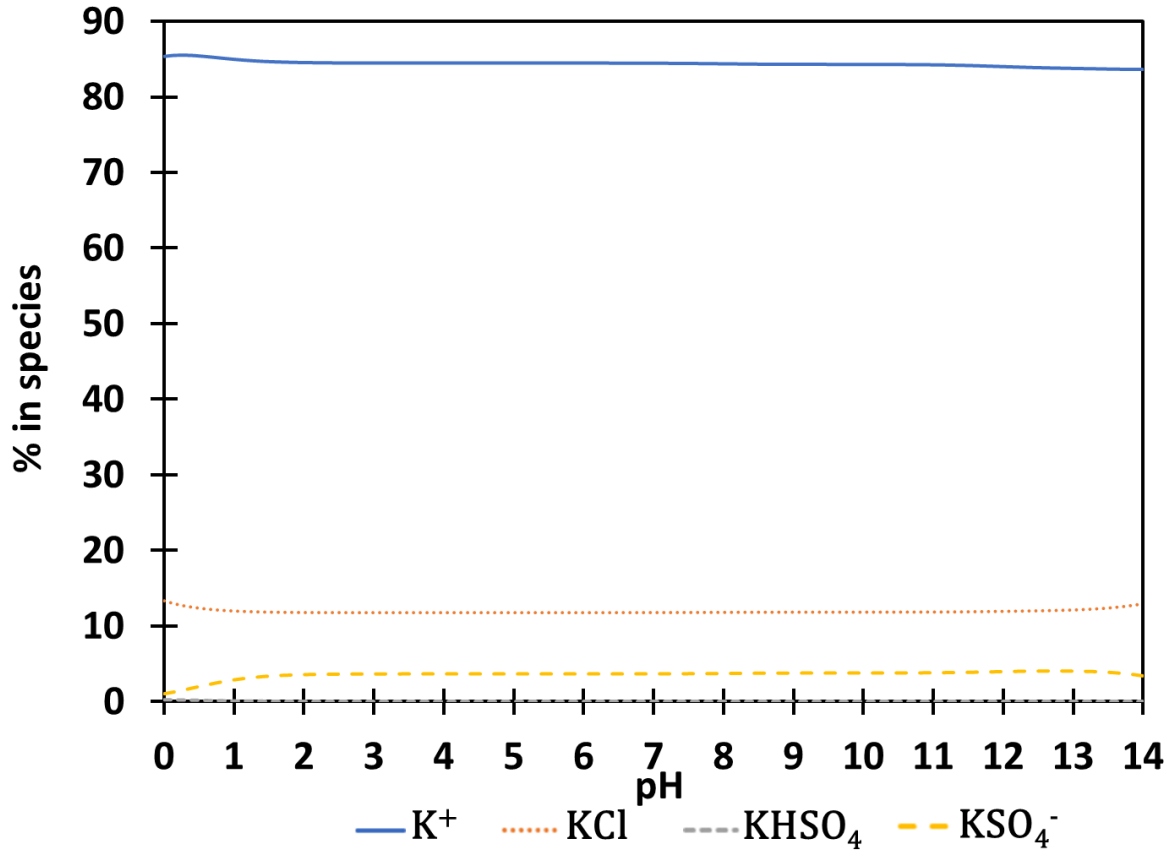



**Figure A. 6:** Potassium speciation in the synthetic brine vs. pH.

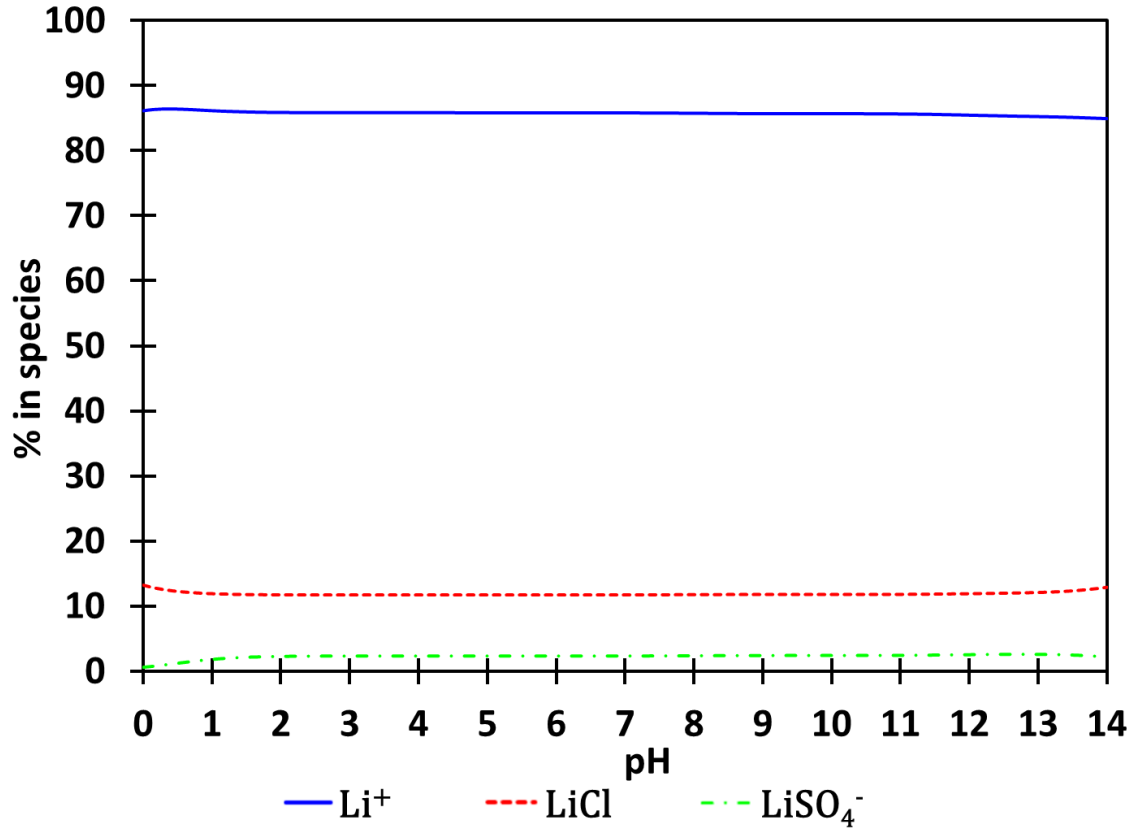



**Figure A. 7:** Lithium speciation in the synthetic brine vs. pH.

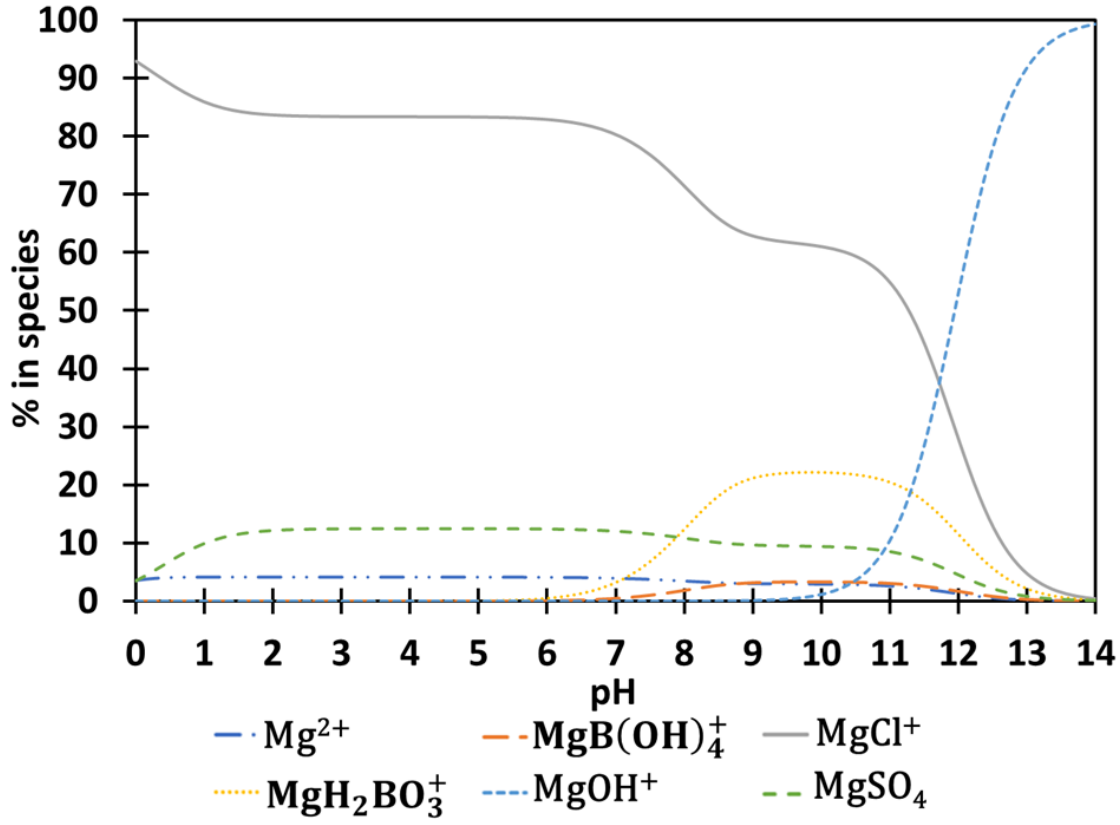



**Figure A. 8:** Magnesium speciation in the synthetic brine vs. pH.

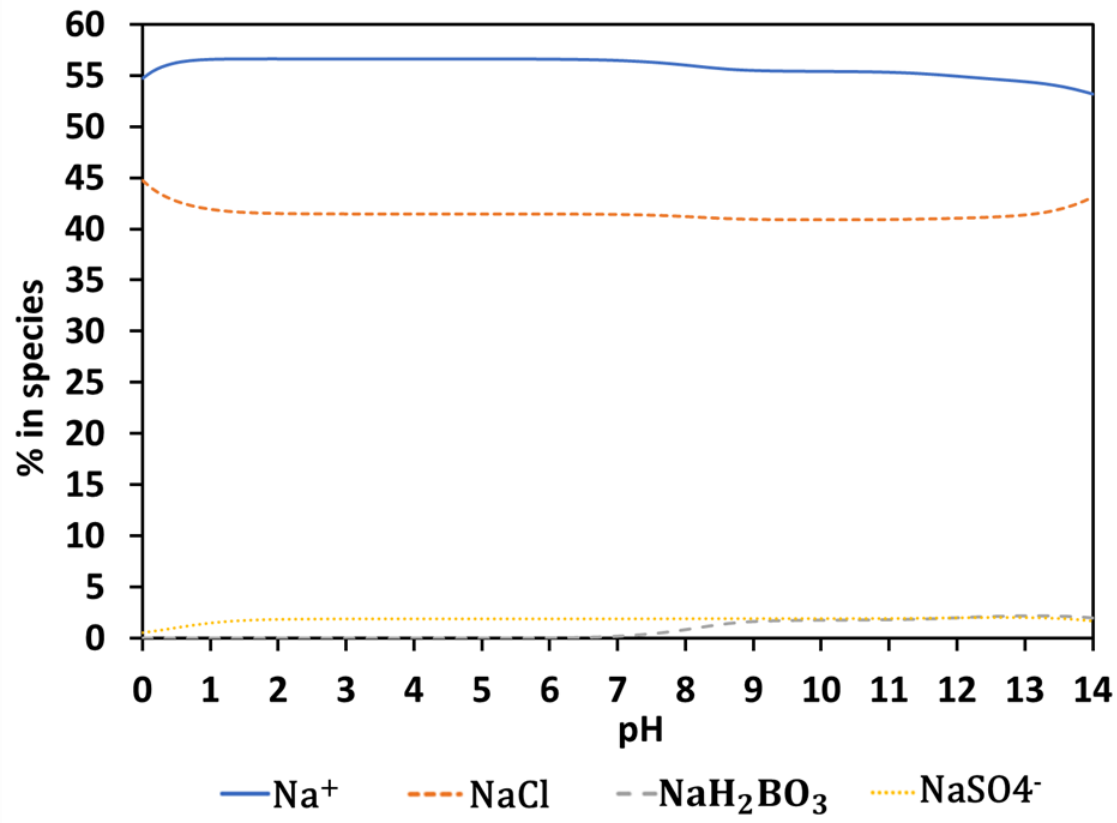
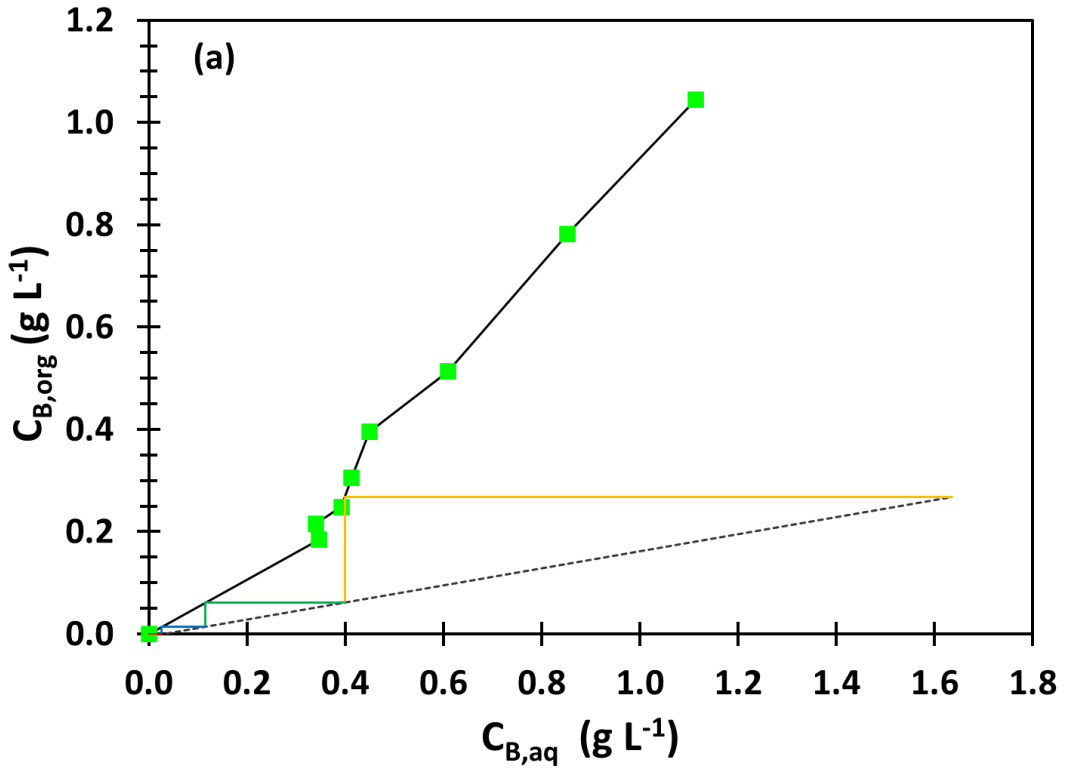
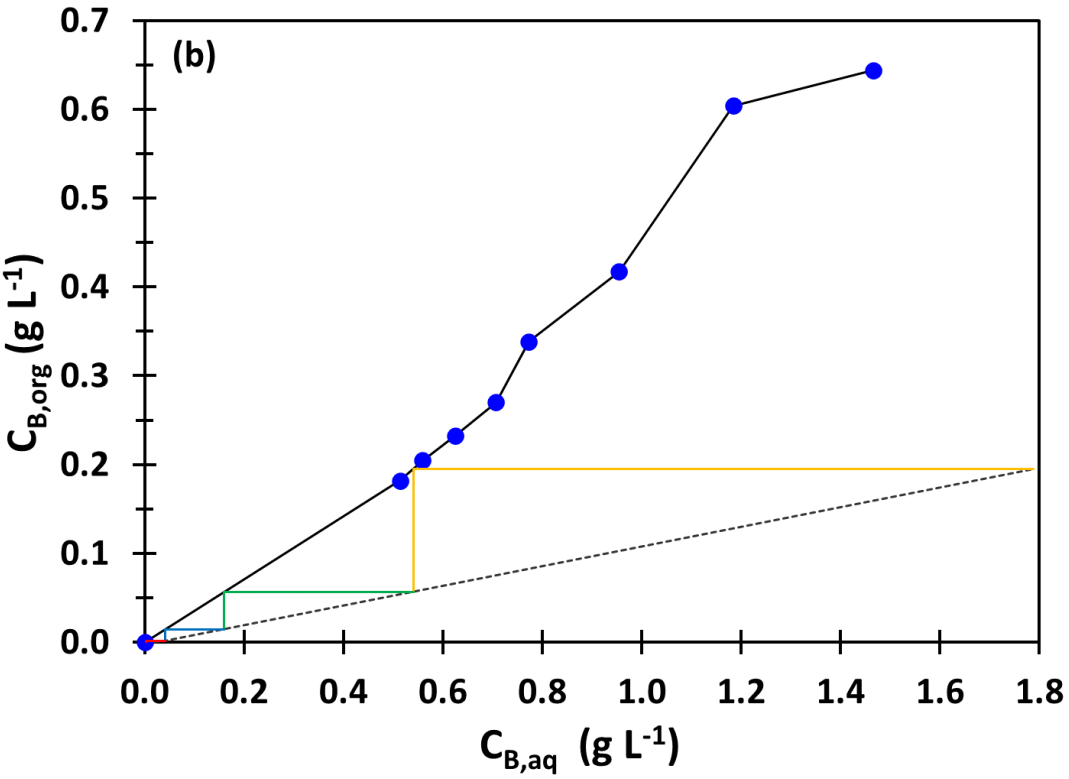



**Figure A. 9:** Sodium speciation in the synthetic brine vs. pH.


(a)
1.2
1.0
0.8
0.6
0.4
0.2
0.0
$C_{B,org}$ (g $L^{-1}$)
0.0
0.2
0.4
0.6
0.8
1.0
1.2
1.4
1.6
1.8
$C_{B,aq}$ (g $L^{-1}$)


(b)
0.7
0.6
0.5
0.4
0.3
0.2
0.1
0.0
$C_{B,org}$ (g $L^{-1}$)
0.0
0.2
0.4
0.6
0.8
1.0
1.2
1.4
1.6
1.8
$C_{B,aq}$ (g $L^{-1}$)

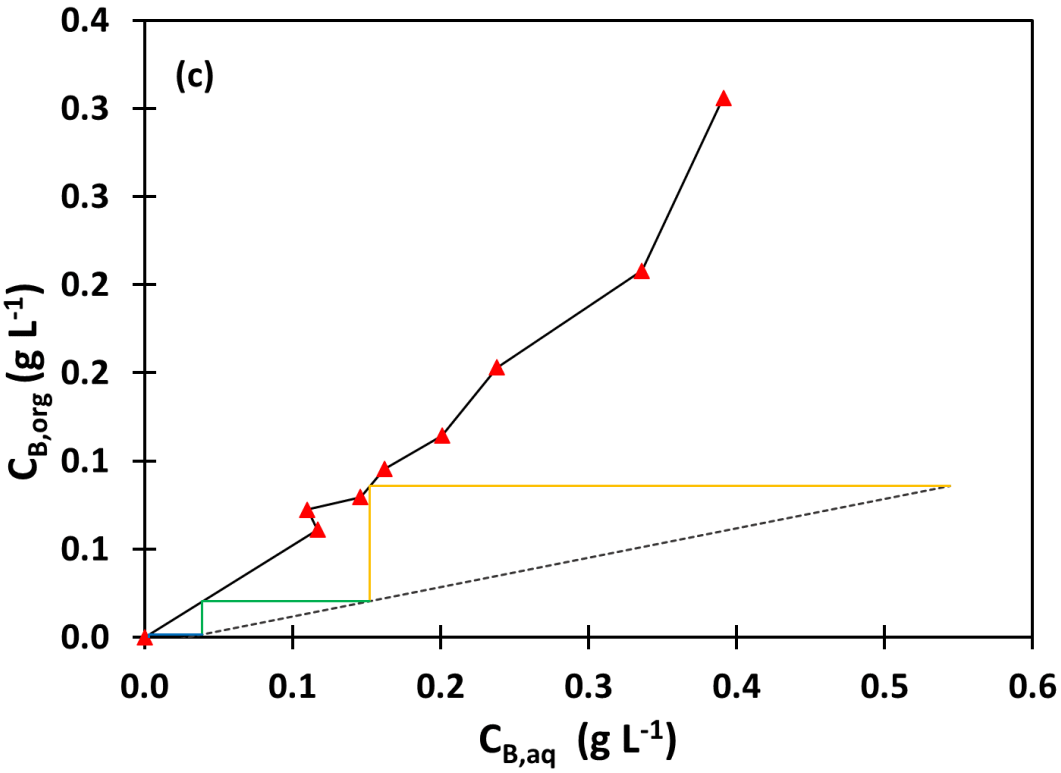



**Figure A. 10:** McCabe-Thiele diagrams for boron removal from (a) the synthetic brine (SB) at O/A=6, (b) the native brine 1 (NB1) at O/A=9 and (c) the native brine 2 (NB2) at O/A=6 ($C_{B,org}$ and $C_{B,aq}$ are boron concentration in the organic phase and in the aquous phase, respectively).

# Appendix B

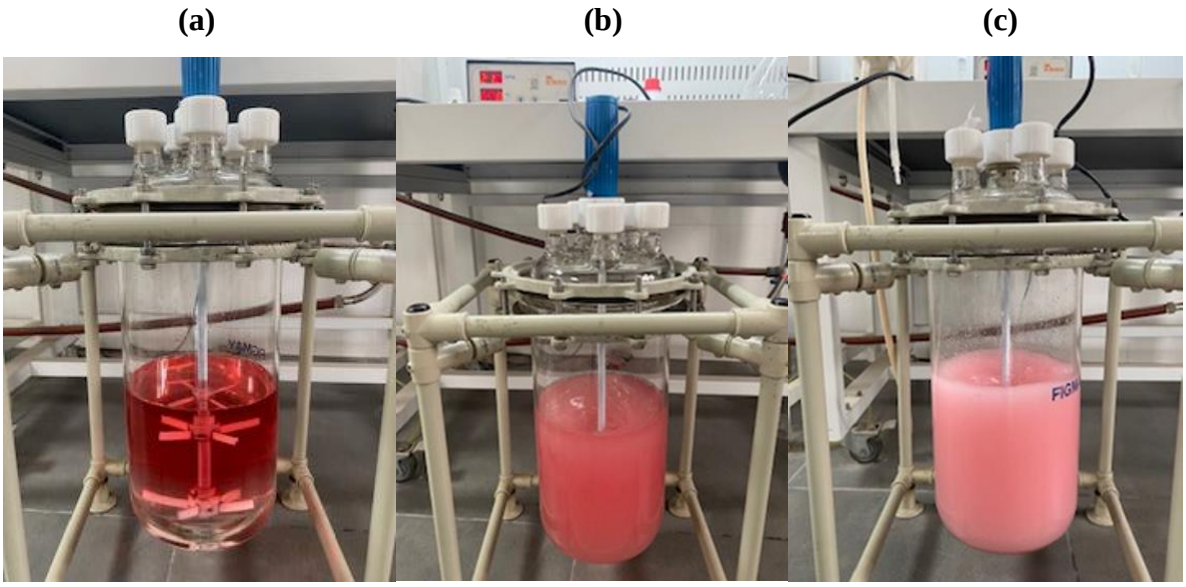



**Figure B. 1:** Setup of experiments (a) before boron extraction, (b) during boron extraction and (c) during boron stripping.

**Table B. 1:** Concentration of boron as a function of time in the brine after extraction and in the stripping solution after stripping. Extraction conditions: 2 mol $L^{-1}$ 2-butyloctan-1-ol in kerosene, pH=7.5, O/A=4 and 25 °C. Stripping conditions: 0.1 mol $L^{-1}$ NaOH, O/A=4 and 25 °C.

| | Boron concentration (mg $L^{-1}$) | |
|---|---|---|
| Time (min) | Extraction | Stripping |
| 0 | 507.6 | 0 |
| 5 | 274.1 | 244 |
| 10 | 274.1 | 244 |
| 15 | 274.1 | 244 |
| 30 | 274.1 | 244 |
| 45 | 274.1 | 244 |
| 60 | 274.1 | 244 |

**Table B. 2:** Technical specifications of ion exchange membranes. Data provided by the manufacturer (Membranes International Inc., https://ionexchangemembranes.com/).

| Specification | AMI-7001CR | CMI-7000S |
|---|---|---|
| Functional group | Quaternary Ammonium | Sulphonic acid |
| Standard Thickness | 0.450 ± 0.025 | 0.450 ± 0.025 |
| Electrical Resistance ($Ohm.cm^2$) 0.5 mol/L NaCl | < 40 | < 30 |
| Maximum Current Density ($Ampere/m^2$) | < 500 | < 500 |
| Permselectivity (%) 0.1 mol KCl/kg / 0.5 mol KCl/kg | 90 | 94 |
| Total Exchange Capacity (meq/g) | 1.3 ± 0.1 | 1.6 ± 0.1 |
| Water Permeability ($ml/hr/ft^2$) @5psi | < 3 | < 3 |
| Thermal Stability (°C) | 90 | 90 |

**Table B. 3:** Boron extraction efficiencies from the salar de Hombre Muerto brine as a function of the extraction step. Extraction conditions: 2 mol $L^{-1}$ 2-butyloctan-1-ol in kerosene, pH=7.5, O/A=4 and 25 °C.

| Extraction step | Extraction efficiency of boron (%) |
|---|---|
| 1 | 46 |
| 2 | 64 |
| 3 | 68 |
| 4 | 70 |
| 5 | 76 |
| 6 | 80 |
| 7 | 82 |
| 8 | 90 |

**Table B. 4:** Evolution of pH, current, voltage, and concentrations of boron, calcium and magnesium in the non-pretreated brine in the cathodic compartment during the electrodialysis in stage I.

| | Non-pretreated brine | | | | | |
|---|---|---|---|---|---|---|
| Electrodialysis time (min) | pH | [B] (mg $L^{-1}$) | Current (A) | Voltage (V) | [Ca] (mg $L^{-1}$) | [Mg] (mg $L^{-1}$) |
| 0 | 7.5 | 507.6 | 2.15 | 16.7 | 119.1 | 2315.9 |
| 60 | 8.7 | 487.3 | 2.15 | 7.3 | 91.6 | 1693.9 |
| 120 | 9.1 | 406.1 | 2.15 | 6.6 | 91.6 | 888.6 |
| 140 | 9.3 | 406.1 | 2.15 | 6.4 | 91.6 | 610.9 |
| 160 | 9.4 | 385.8 | 2.15 | 6.3 | 91.6 | 444.3 |
| 180 | 9.6 | 385.8 | 2.15 | 6.2 | 68.7 | 180.5 |
| 200 | 10.5 | 446.7 | 2.15 | 6.2 | 45.8 | 0.0 |
| 250 | 12.1 | 446.7 | 2.15 | 6 | 36.6 | 0.0 |
| 300 | 13.0 | 446.7 | 2.15 | 5.8 | 36.6 | 0.0 |

**Table B. 5:** Evolution of pH, current, voltage, and concentrations of boron, calcium and magnesium in the boron-depleted brine in the cathodic compartment during the electrodialysis in stage I.

| | Boron-depleted brine | | | | | |
|---|---|---|---|---|---|---|
| Electrodialysis time (min) | pH | [B] (mg $L^{-1}$) | Current (A) | Voltage (V) | [Ca] (mg $L^{-1}$) | [Mg] (mg $L^{-1}$) |
| 0 | 8.8 | 50.8 | 2.15 | 16.7 | 91.6 | 2054.9 |
| 33 | 9.4 | 50.8 | 2.15 | 8.2 | 91.6 | 1555.1 |
| 70 | 9.6 | 50.8 | 2.15 | 7.1 | 91.6 | 1055.2 |
| 107 | 9.7 | 50.8 | 2.15 | 6.8 | 68.7 | 624.8 |
| 143 | 9.9 | 50.8 | 2.15 | 6.4 | 45.8 | 194.4 |
| 180 | 11.8 | 50.8 | 2.15 | 6.3 | 22.9 | 0.0 |
| 204 | 12.0 | 50.8 | 2.15 | 6.2 | 15.3 | 0.0 |
| 233 | 12.1 | 50.8 | 2.15 | 6.2 | 3.7 | 0.0 |
| 260 | 12.2 | 50.8 | 2.15 | 6.1 | 3.7 | 0.0 |
| 284 | 12.3 | 50.8 | 2.15 | 6.1 | 0 | 0 |
| 300 | 12.4 | 50.8 | 2.15 | 6 | 0 | 0 |

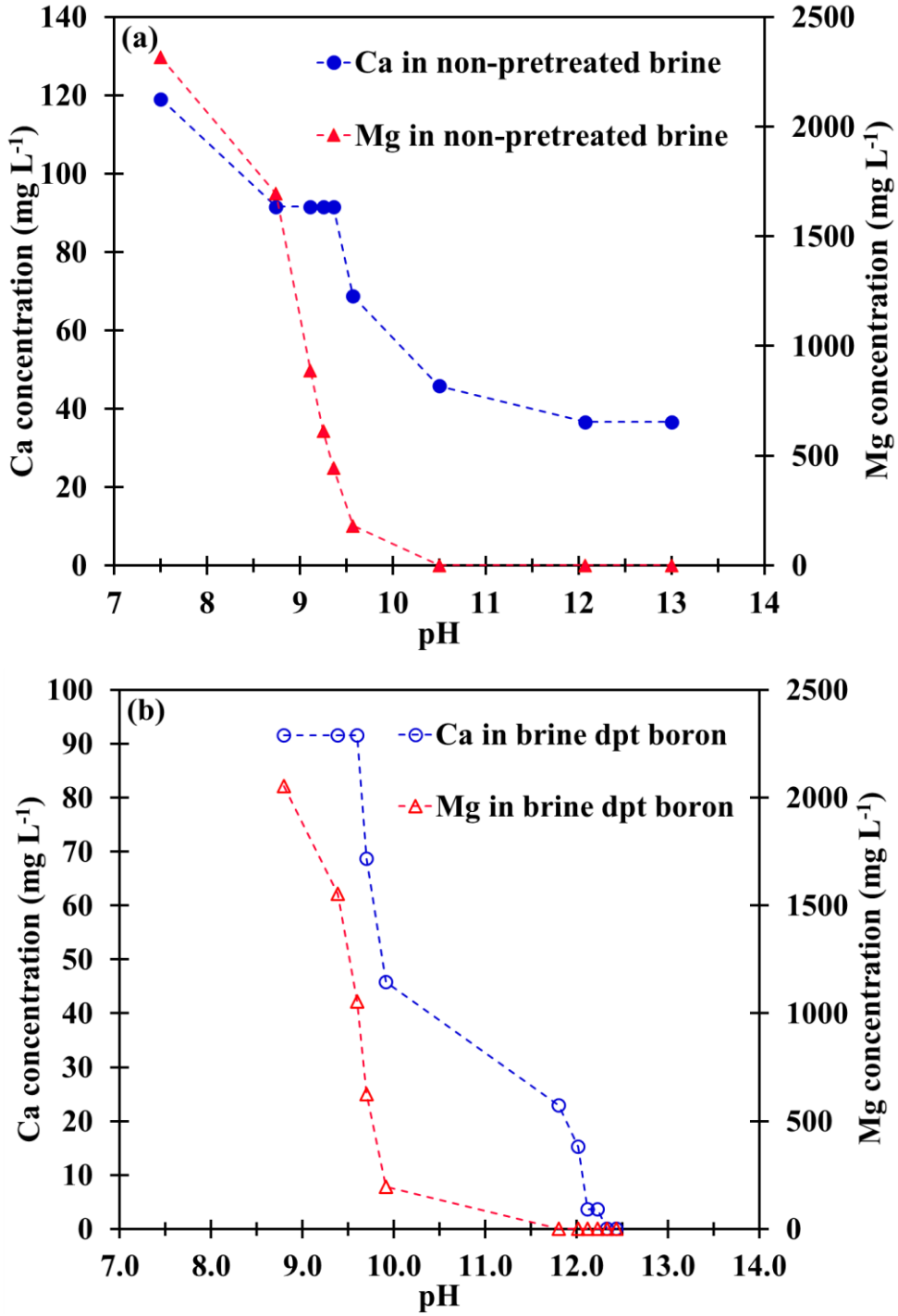



**Figure B. 2:** Calcium and magnesium concentrations vs. pH during electrodialysis in (a) the non-pretreated brine and (b) the boron-depleted brine.

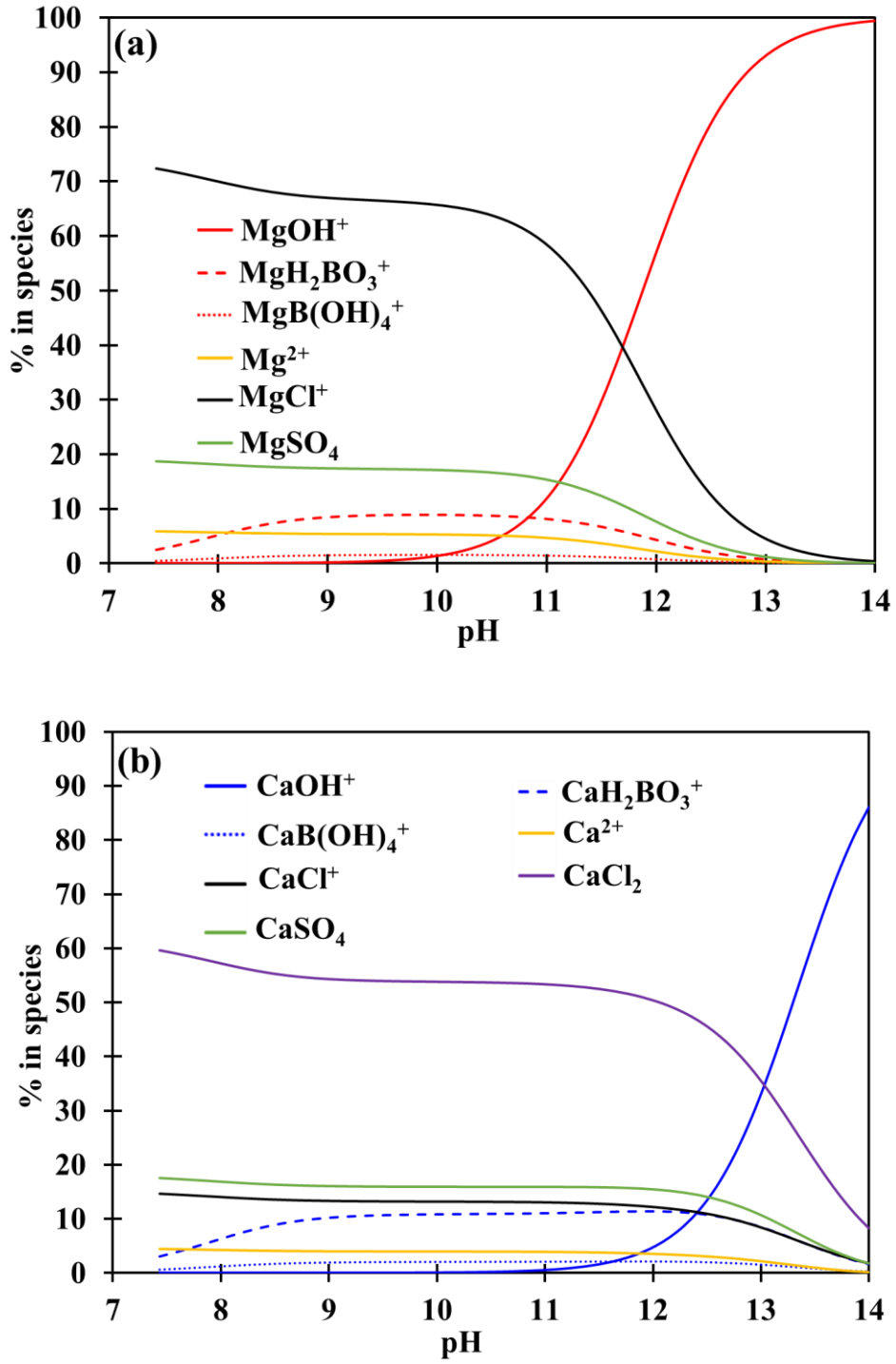



**Figure B. 3:** Speciation of (a) magnesium and (b) calcium vs. pH in the non-pretreated brine before stage I of the electrodialysis process.

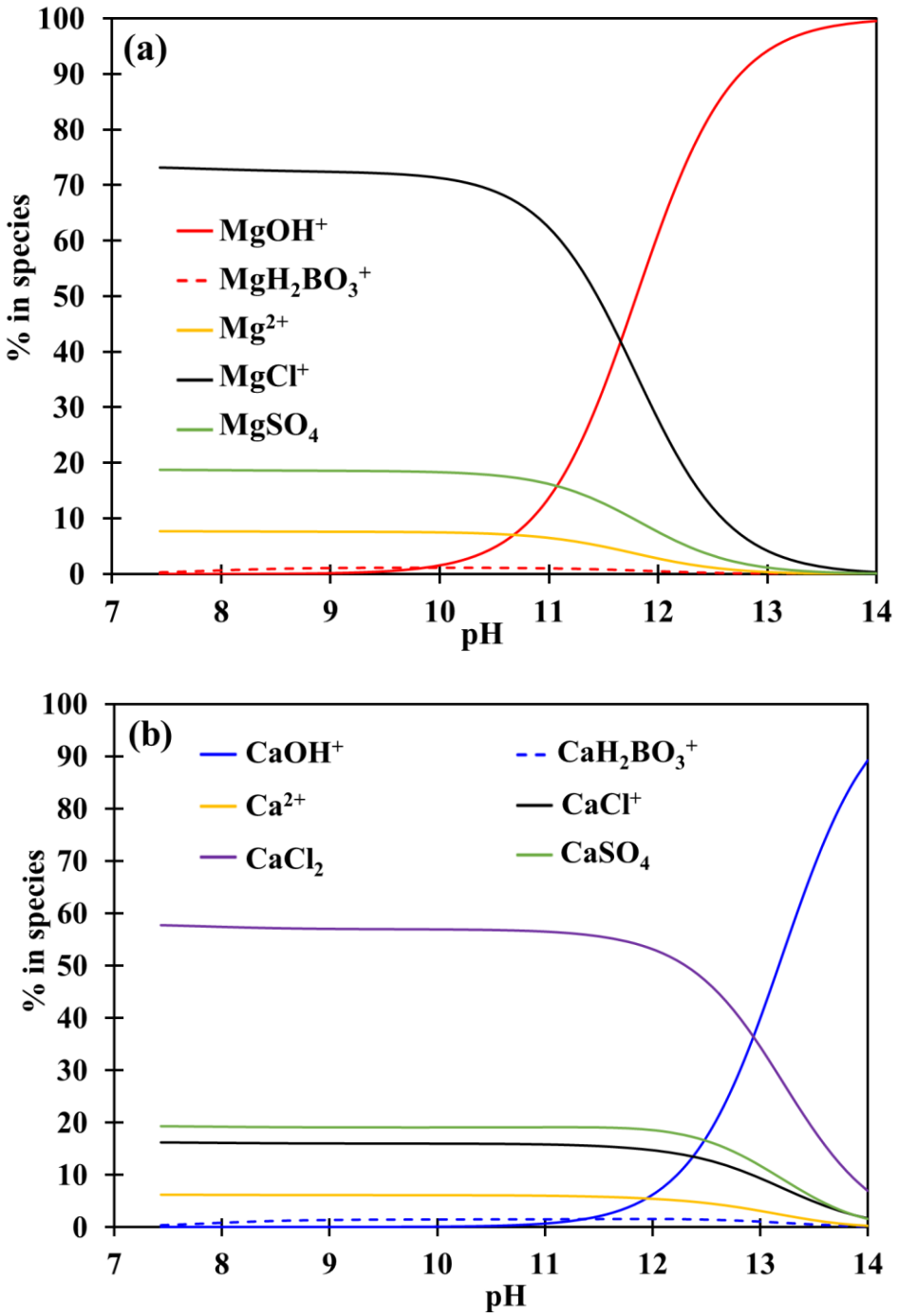



**Figure B. 4:** Speciation of (a) magnesium and (b) calcium vs pH in the boron-depleted brine before stage I of the electrodialysis process.

**Table B. 6:** Composition of the solid obtained for (1) the non-pretreated brine and (2) the boron-depleted brine after magnesium and calcium precipitations in stage I of the electrodialysis process.

| | Mass fraction (%) | | | | | | | |
|---|---|---|---|---|---|---|---|---|
| Solid | B | K | Li | Mg | Na | Ca | $Cl^-$ | $SO_4^{2-}$ |
| (1) | 0.3 | 1.7 | 0.2 | 5.6 | 28.8 | 0.4 | 44.6 | 3.8 |
| (2) | 0.2 | 1.6 | 0.2 | 6.9 | 28.8 | 0.4 | 43.9 | 3.9 |

**Table B. 7:** pH in the three compartments, current, voltage, and concentrations of sodium, lithium and potassium in the middle compartment at the end of each electrodialysis experiment in stage II for the non-pretreated brine.

| Experiment | Time (min) | pH of brine | pH of anolyte | pH of catholyte | Na (mg $L^{-1}$) | Li (mg $L^{-1}$) | K (mg $L^{-1}$) | Current (A) | Voltage (V) |
|---|---|---|---|---|---|---|---|---|---|
| 0 | 0 | 13.1 | 11.4 | 9.4 | 110633.5 | 715 | 8800 | 0.75 | 3.9 |
| 1 | 1367 | 13.1 | 9.4 | 13.8 | 76082 | 776.7 | 5752.5 | 0.75 | 3.9 |
| 2 | 4127 | 13.3 | 9.2 | 13.7 | 41621.5 | 677.6 | 2735.5 | 0.75 | 3.9 |
| 3 | 6407 | 13.4 | 9.2 | 13.5 | 19675 | 491.5 | 0 | 0 | 30 |

**Table B. 8:** Values of pH in the three compartments, current, voltage, and concentrations of sodium, lithium and potassium in the middle compartment at the end of each electrodialysis experiment in stage II for the boron-depleted brine.

| Experiment | Time (min) | pH of brine | pH anolyte | pH of catholyte | Na (mg $L^{-1}$) | Li (mg $L^{-1}$) | K (mg $L^{-1}$) | Current (A) | Voltage (V) |
|---|---|---|---|---|---|---|---|---|---|
| 0 | 0 | 12.4 | 11.4 | 9.4 | 89315 | 560 | 7427.5 | 0.75 | 3.9 |
| 1 | 2110 | 13.0 | 8.1 | 13.4 | 74820 | 629.5 | 3394 | 0.75 | 3.9 |
| 2 | 4394 | 13.5 | 11.6 | 13.6 | 43441 | 517.6 | 898.5 | 0.75 | 3.9 |
| 3 | 5461 | 11.8 | 12.8 | 13.6 | 251 | 6.8 | 0 | 0 | 30 |

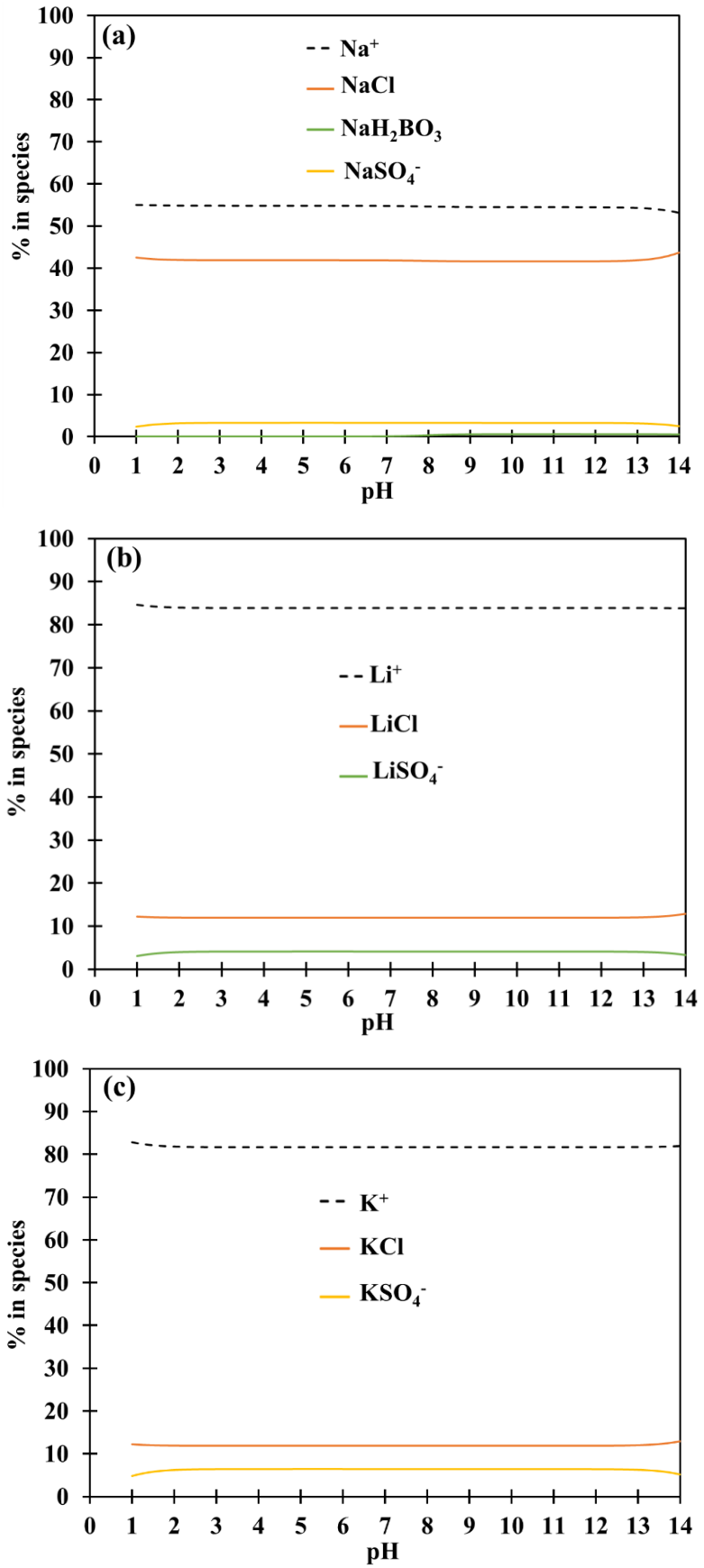



**Figure B. 5:** Speciation of (a) sodium, (b) lithium and (c) potassium vs pH in the non-pretreated brine before stage II of the electrodialysis process.

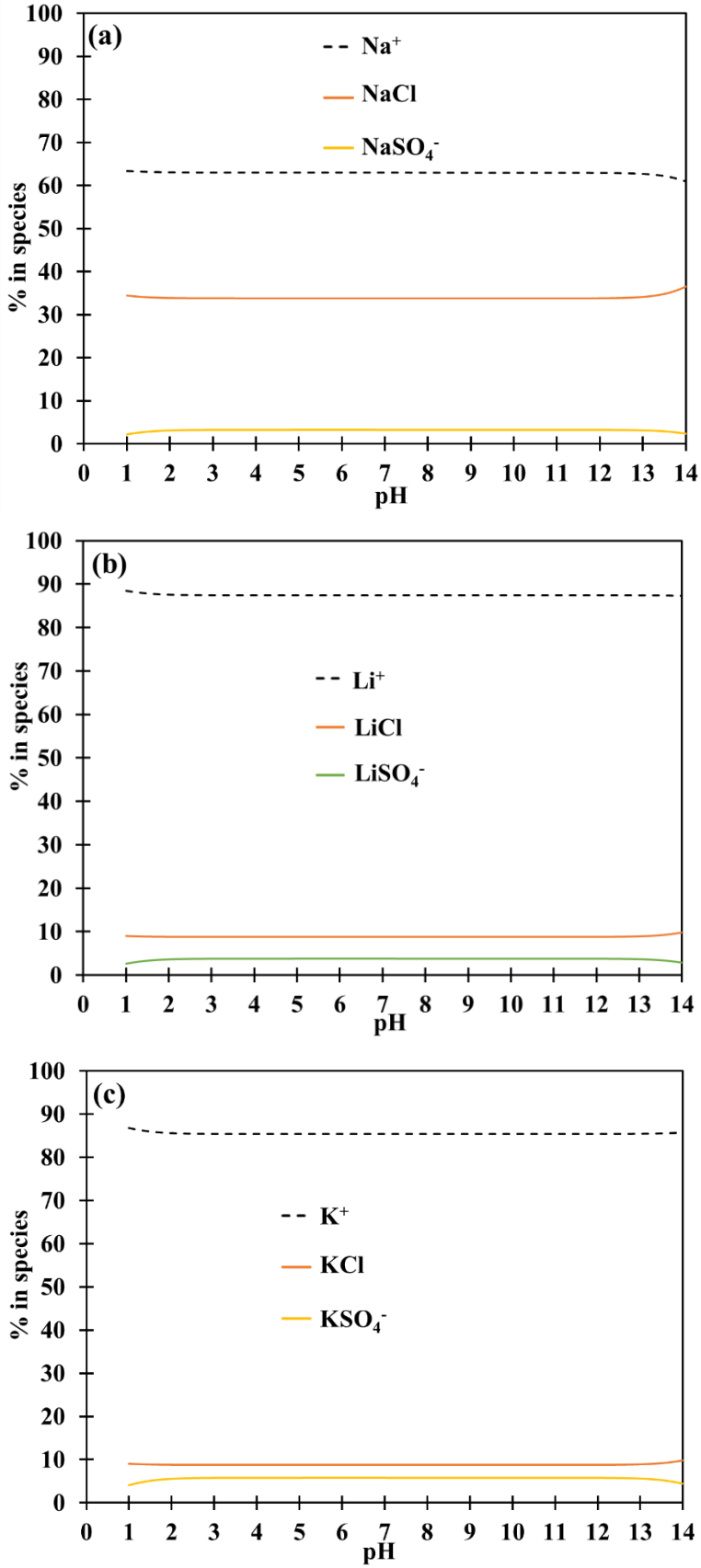



**Figure B. 6:** Speciation of (a) sodium, (b) lithium and (c) potassium vs pH in the boron-depleted brine before stage II of the electrodialysis process.